SURFACE PROPERTIES OF ASTEROIDS

by

CLARK R. CHAPMAN

A. B., Harvard College
(1967)

S.M., Massachusetts Institute of Technology
(1968)

SUBMITTED IN

PARTIAL FULFILLMENT OF THE REQUIREMENTS FOR THE

DEGREE OF DOCTOR OF PHILOSOPHY

at the

MASSACHUSETTS INSTITUTE OF TECHNOLOGY

February, 1972

Signature of Author.....Clark R. Chapman.....
Department of Earth and Planetary Sciences, October 11, 1971

Certified by.....Thomas D. McCord.....
Thesis Supervisor

Accepted by.....Theodore R. Madden.....
Chairman, Departmental Committee on Graduate Students

SURFACE PROPERTIES OF ASTEROIDS

by

Clark R. Chapman

Submitted to the Department of Earth and Planetary Sciences
on October 11, 1971
in partial fulfillment of the requirement
for the degree of
Doctor of Philosophy

Abstract

Reflectivities of 31 asteroids were measured in 24 filters (0.3 to 1.1 microns) using a double-beam photometer. Reflection spectra range from reddish to gray or slightly bluish in trend; there are many different curve shapes. Common types are: (1) reddish curves with 10% absorption bands near 0.95 microns or beyond 1.0 microns; (2) flat reflectivities in the visible and near-IR with sharp decreases in the UV; (3) flat reflectivities even into the UV. At least 14 different curve types are recognized.

A sample of 102 asteroids with reliably known colors is derived from the reflectivities and from a critical review of the literature. Several correlations of colors and spectral curve types with orbital and physical parameters for asteroids were examined: (1) There is a correlation with extreme semi-major axis a; asteroids with large aphelia have flat reflectivities into the UV while those with small perihelia are mostly reddish. (2). There is no strong correlation with proper eccentricity e or with proper inclination i. (3) Curve types show evidence for clustering on an a vs e plot, with 0.95 micron bands occurring mainly for Mars-approaching asteroids. (4) The Flora group asteroids are red, but most families and jet streams have members of different colors. (5) Color is not correlated with rotation period, but is weakly correlated with light-curve amplitude. (6) Color is strongly correlated with asteroid diameter. No large asteroids are reddish, no small ones bluish. If this correlation extends to albedo, as is probable, then there is a greater excess of large asteroids than shows in size-frequency relations based on absolute magnitude.

Some red asteroids become redder with phase angle (and absorption bands strengthen) while some gray asteroids become bluer with phase. Therefore the application of lunar-like color-phase corrections is not justified. Several asteroids show probable color variations with rotation, especially 6 Hebe.

Cratering theory applied to asteroids shows that the largest ones must retain regoliths; the smallest ones cannot. The chief factors are the population index of the impacting debris, which may be higher than is usually assumed, and the small-size cut-off of asteroidal particles.

Many asteroids have silicate surface compositions. Most reddish asteroids probably contain hypersthene pyroxene; some may contain predominant olivine. Such asteroids may resemble L type chondrites and CC3 type chondrites, respectively. A re-analysis of 4 Vesta confirms that it is eucritic with predominate pigeonite, but probably more calcium-rich than believed; no other asteroids yet observed resemble it. Some asteroid reflectivities resemble terrestrial basalts and suggest howarditic composition, although no bands can be measured. Asteroids with flat reflectivities into the UV must contain a large percentage of powdered opaques, probably iron-nickel, carbon, or magnetite. These surface compositions and the distributions of the asteroid colors as a function of a and size seem consistent with Mason's models for meteorite parent bodies and with Larimer and Anders' predictions for compositional variation of chondrite parent bodies. A weak band near 0.65 microns and other minor reflectivity features are not yet identified.

There is little evidence that hypervelocity impact shock or vitrification affect reflectivities. 324 Bamberga has been reported to have an extremely low albedo, which must be due to powdered opaques; yet it shows a significant 0.65 micron band. Since Bamberga is the fourth largest known asteroid and closely approaches Mars, it is a possible source for meteorites and should be studied further.

This reconnaissance study demonstrates the need for further reflectivity studies of asteroids. Supporting laboratory reflectivity measurements of meteorites and improved comparison-star calibrations are desirable.

Thesis Supervisor: Thomas B. McCord

Title: Associate Professor of Planetary Physics

ACKNOWLEDGEMENTS

I wish to thank Prof. Thomas McCord, who suggested this observational study, for his continuing enthusiams and assistance during the project. As my thesis advisor, his advice was always helpful, both during the observational phase and the writing phase of the work.

I also appreciate Dr. Torrence Johnson's willingness to listen to my ideas and make suggestions on an almost daily basis. His advice during the data reduction stage was especially helpful.

Among all the students associated with the M.I.T. Planetary Astronomy Laboratory who helped me from time to time, I wish to single out J. Kunin and J. Elias who provided programming advice and assistance. In addition, J. Elias kindly finished his new stellar calibrations in time to be used for the asteroid reductions. I also benefitted from discussions with M. Gaffey and M. Charette.

Though many persons helped me as observing assistants in the dome, most time was spent by A. Lazarewicz, T. Johnson, and -- especially -- Larry Lebofsky, who saw more clear skies during his nights helping me than during all the other nights of the year together, but remained cheerful nevertheless.

During my years in the Dept. of Earth and Planetary Sciences, I have benefited greatly from valuable interaction with many of the professors; I wish to mention specifically Profs. R. Hide, I. Shapiro, and G. Simmons. During the later stages of this project, I had useful conversations also with Profs. R. Burns, J. Lewis, and T. McGetchin.

I wish to thank Dr. P. Herget for providing ephemerides, Dr. J. Arnold for sending a card deck of asteroid orbital elements, and Drs. D. Matson and J. Williams for useful conversations and for providing data before publication. I also acknowledge helpful conversations with Drs. J. Adams, G. Hunt, and J. Salisbury concerning the interpretation of spectral reflectivities. Finally Dr. Edward Anders' help and encouragement in this work were especially valuable; without belittling the help of anyone else, Dr. Anders certainly packs more useful information into each minute of spoken conversation than anyone else I know.

My wife Jennalyn not only typed the entire manuscript, including tables, but provided professional bibliographic assistance at no extra charge. Her encouragement, patience, and determination were instrumental to the completion of this work.

The facilities of Hale Observatories, Kitt Peak National Observatory, and the erstwhile Division of Geological Sciences at Caltech were used. Partial financial support was provided by NASA grants NGR-22-009-473 and NGR-22-009-583.

TABLE OF CONTENTS

LIST OF FIGURES

LIST OF TABLES

PREFACE

"Perhaps the major unsolved problem in the field of meteoritics is that of the identification within the solar system of the present sources of meteorites of the various classes."

Wetherill (1969)

"One of the great challenges in meteoritics is to trace each class of meteorites to its parent body in the sky."

Anders and Mellick (1969)

The study of asteroids is a topic in Planetary Science with important implications for cosmochemistry, the origin of the solar system, solar system processes, and celestial dynamics. The study of asteroids, and of their surface properties in particular, has made great advances in recent years. The great promise of these studies was dramatized at the recent I.A.U. Colloquium on physical studies of minor planets held in Tucson earlier this year.

There are recently completed theses by J. Veverka on polarization studies, D. Matson on thermal flux measurements, and J. Williams on the evolution of asteroid orbits. Meanwhile Gehrels' group continues their exacting photometric work, meteoriticists are making great strides, achievements are being made in understanding the crystallographic bases of remote mineralogy, and astronomical instrumentation is becoming rapidly more sophisticated. Recent interest in possible asteroid space missions has spurred even more asteroid research. This thesis is a review of asteroid spectrophotometry to date, a report on a new reconnaissance study of the spectral reflectivities of 31 asteroids, and a discussion of the physical texture and possible mineralogy of asteroid surfaces. An attempt has been

made to relate the results to meteoritics, although I do not pretend detailed knowledge of that broad field.

For a topic which touches so many diverse fields, it is perhaps useful to say what my approach is, and what it is not. This is a thesis in observational astronomy; it is concerned with the synthesis and interpretation of observations. Much of the thesis is reconnaissance work in a new field: asteroid spectrophotometry. Hence, in order to guide further research, I have called attention to many possible correlations of potential importance. I do not intend, however, to suggest that all of these tentative results are in any sense conclusive. I try to distinguish between firm conclusions and tentative suggestions.

The thesis is not mainly a detailed examination of asteroid mineralogy; I have carried the mineralogical interpretation only so far as the data warrant. I have been concerned with the design of an observing program, with observational techniques, and with methods of data reduction, but the thesis is not concerned heavily with instrumentation since the instrumentation already existed. I have not investigated the orbital dynamics of asteroids and asteroidal fragments, since so many others have studied that subject, but I occasionally use their results. I have tried to develop some cratering theory when it is directly applicable to problems that have arisen in the more central parts of the thesis.

Note concerning the appendices and negativism

It is my personal conviction that there are both positive and negative results from the increasing pressures for brevity in modern scientific publication. Journal articles become artificial constructions which, like the proofs of mathematical theorems, bear little relationship to the actual

train of logic used in the scientific experiment. Experimental and theoretical details, even when fundamental to the validity of the work, become subordinated to a presentation and discussion of the results, or omitted altogether. It often becomes impossible to judge the merits of a piece of research from the publication alone, apart from the personal reputation of the author, and face-to-face or telephone discussions with the author, and other conventions of "the invisible college".

It may or may not be satisfactory, from the academic point-of-view, to let doctoral dissertations tend in the direction of journal articles. Perhaps professors can better judge a student through talking and working with him than by picking over details laboriously described in written prose. But I believe it is bad for the intellectual and historical development of science not to keep permanent records of how science is actually done, and I believe that Ph.D. theses are good vehicles for perpetuating a more complete and accurate record of the methodologies of science in the last third of the twentieth century. I find it a joy to read articles published in the 19th century or the first third of the present century, and to be able to follow the complete logic of early scientists. It is easy to see where they went right and where they went wrong. The future historian of science will not be able to do the same with our journal articles, which give little information on how the science was done. Perhaps theses can remain a more accurate and complete resevoir of scientific methodology.

For these reasons I have appended, in more detail than my adviser thought warranted, some details concerning the planning of the observing program, its execution, problems encountered, methods of data reduction, and presentation and description of the raw data. Many statements made

in the thesis find their support in the appendix. Also, useful methodological and procedural achievements are described in the appendices which should be of interest to a few readers. However, at the request of my advisor, no references have been made to Appendices II - VII in the body of the text of this thesis. These appendices will be omitted from any mass reproductions of this thesis. Interested readers are referred to the Table of Contents and then to the archival copy of the thesis.

Another unfortunate aspect of modern scientific prose style is the increasing tendency for authors to minimize their errors, their doubts, and their qualifications, if they are convinced themselves of the correctness of their results (as they almost always are). Thus even the slightest evidence of hesitancy or negativism in an author's wording is automatically assumed to imply that his results are no good. I reject this convention as a mutilation of the meaning of straightforward language. I do not follow that convention in this thesis.

Problems are admitted and discussed whenever they arise. Potential problems are described even when I doubt that they significantly affect the results. All sources of error are discussed, even when it is impossible to assign numbers to their magnitude. I am quite confident of the overall validity of my results and I believe my observations represent the epitome of the state-of-the-art. I urge readers to take what I say at face value, and not to surmise hidden implications. But I would rather that people underinterpret my data than overinterpret it.

Use of the terms "color" and "spectral reflectivity" in this thesis

The observed property of asteroids with which I am most concerned in this thesis is called spectral reflectivity. It can be defined as the albedo of a surface as a function of wavelength, scaled so as to be relatively independent of absolute differences in overall albedo between two different surfaces. In this thesis, reflectivities are scaled to unity at 0.57 microns. Thus we are referring to a wavelength-dependent reflective property of a surface that is independent of the spectral characteristics of either the illuminating source or the sensor.

In common usage, the word "color" refers to several concepts related to spectral reflectivity as perceived by human observers. Most scientific investigations of color refer to a characteristic of a surface which can be derived uniquely from the spectral reflectivity of the surface, as observed by some kind of standard human observer when the surface is illuminated by a standard lamp. In astronomy, color indices are ratios of brightnesses (or differences in magnitude) of an object observed in two different specified filters as recorded with standard sensors. Colors so defined are a grossly incomplete description of spectral reflectivity, because of the inherent limitation of color receptors in the human eye or the lack of spectral resolution in the astronomical filters. While a given spectral reflectivity implies a unique color (observed in the standard mode), no color or color index implies a unique spectral reflectivity (cf. Wyszecki and Stiles, 1967).

In this thesis, I use the terms in a somewhat different sense. Spectral reflectivity refers both to the intrinsic property of a surface described above, and to its relatively precise measurement, in the case of the asteroids, in about 24 narrow-bandwidth filters in the range 0.3

to 1.1 microns. The term color refers to the broader characteristics of the spectral reflectivity as measured above, and to broad-band measurements (such as UBV photometric color indices) which provide only partial information on spectral reflectivity. I refer to color in terms of broad trends in spectral reflectivity, especially in a relative sense. Spectral reflectivities which rise by factors of 2 to 3 from 0.3 to 1.1 microns will be called "red", and those which are relatively flat will be called "blue".

It should be borne in mind that, as illuminated by the sun and perceived by the human eye, all asteroids studied would appear quite gray. Few asteroids approach the "reddness" of the lunar maria, none is nearly so "red" as Mars. The bluest asteroids are very nearly the color of the sun or the bluest spots on the moon. I am discussing color characteristics in this thesis which differ in very subtle ways by the standards of everyday human experience.

CHAPTER I

INTRODUCTION

The asteroids may be the real Rosetta Stones of the Solar System. There is a good chance that asteroid surfaces differ fundamentally from the surface of the moon. The lunar surface has been superficially fragmented and redistributed by constant bombardment from space debris, and more fundamentally altered since the formation of the moon by volcanic processes extending at least a billion years toward the present. The space weathering of asteroid surfaces, however, is continually eating into the asteroids, exposing fresh material not deeply blanketed by debris. And it is more likely that asteroids have been relatively unmodified chemically, thermally, and mineralogically since early in the history of the solar system. Museum meteorite collections may well be vast samplings of asteroid surfaces, but we desperately need to know from which asteroids they may have come.

A. METHODS FOR STUDYING ASTEROID SURFACES

Astronomical approaches to the study of asteroid surfaces must rely almost entirely on analysis of emitted or reflected radiation from point sources. Aside from the inexact direct diameter measurements which have been done for a few asteroids and yield very approximate albedos (Dollfus, 1971), there are five major approaches to studying asteroid surfaces: photometry, colorimetry, polarimetry, radar reflection, and thermal IR flux measurements. Although some of the approaches yield difinitive determinations of some asteroidal characteristics, more frequently they yield ambiguous answers, even when the results of several approaches are

synthesized. Nevertheless it is often possible to study differences between asteroids in one or more of the observables, and the correlation of these data with other parameters (e.g. orbital elements) can often be very instructive. I will use this approach later in this thesis.

Photometry is the measurement of brightness of asteroids as a function of time, including phase angle. The absolute magnitude B(1,0) depends on albdeo and diameter. The phase law yields some information on the microstructure of the surface and reflective properties of the surface materials. The light-curve yields information on the fragmentation and spottedness of asteroids; also the rotation and orientation of spin axis have some bearing on asteroidal regolith development.

Colorimetry is the study of the intensity of reflected light as a function of wavelength and how these colors vary with phase angle and rotational phase. Colors depend on the chemical, physical, and mineralogical composition of the surface and the structure of the surface (e.g. particle size distributions). Polarimetry, also as a function of phase angle and rotation, yields data dependent on albedo, particle size, opaqueness, and composition. Studies of the thermal flux from asteroids yield, within the constraints of plausible models, estimates of albedo and diameter, and potentially some information on the thermal properties of the surface. Analysis of radar echoes yields information on spin, diameter, surface roughness at radar wavelengths, and bulk surface properties.

In addition to purely astronomical methods for studying asteroid surfaces, I can mention again the study of meteorites which may be pieces of some asteroids. Also, much can be hypothesized about the nature of asteroid surfaces from theoretical and laboratory investigations. Two approaches yet to come are astronomical measurements from observatories in

space (expanding accessible wavelengths and angular resolution) and close-up measurements from spacecraft (fly-bys, landings, and return of samples).

B. ASTEROID SURFACES: A SUMMARY OF WHAT IS KNOWN

Though much is surmised, little is understood about asteroid surface properties. Until recently, there was even a lack of observational data relevant to asteroid surfaces, but that situation is rapidly changing, as demonstrated at the recent I.A.U. symposium on the physical properties of asteroids held in Tucson in March 1971. The symposium proceedings "Physical Studies of Minor Planets" (T. Gehrels, editor) will appear as a NASA SP book by the end of the year. Gehrels' recent review article (1970) is the best alternate source.

Good UBV colors are known for several dozen asteroids, plus some color information on several dozen more (see Chaps. II and V). Color-phase relationships have been measured for a few asteroids and a color-rotation relation has been observed for one. Prior to the present asteroid project, good spectral reflectivity curves existed only for Vesta (McCord et al, 1970). Absolute magnitudes are known for most numbered asteroids, but phase effects have been studied for less than two dozen (Taylor, 1971) and opposition surges for only three (Taylor et al, 1971). Rotation periods are known for several dozen asteroids (Gehrels, 1970; Yang, Zhang, and Li, 1965) but there is only preliminary information on the orientation of the spin axes (Vesely, 1971) and the degree to which spottedness accounts for light-curves (Lacis and Fix, 1971). As a result of Veverka's (1970) recent thesis, there are good measurements of asteroid polarizations as a function of phase angle for about half a dozen asteroids.

Matson (1971; also his thesis just now being completed) has obtained thermal flux measurements for about a dozen asteroids. Only Icarus has been extensively studied by radar (Pettengill et al, 1969; Goldstein, 1969) although some of the major asteroids may be within reach (Goldstein, 1971).

As a result of these observations, we know that there are differences among asteroids in color and albedo, although most tend to be quite dark and slightly reddish. Although nobody has studied asteroid regolith development in detail, the polarization measurements suggest that some of the larger asteroids are dusty. A major mineral component on Vesta is probably pigeonite (McCord et al, 1970; see also Chap. VII). The processes by which meteoritic matter may be transported from parts of the asteroid belt to earth have been studied, but there are no definitive conclusions. There have been repeated indications that asteroid colors may show some correlation with distance from the sun, but the data have been questionable. In summary, little is known about asteroid surfaces but much new data has recently been obtained.

C. MOTIVATION FOR THE SPECTRAL REFLECTIVITY OBSERVATIONAL PROGRAM

We are currently in a stage of asteroid studies where reconnaissance work is needed -- collecting data from a moderately large statistical sample of asteroids. During the last two decades Gehrels and his associates have done the necessary photometric reconnaissance. The recent theses by Veverka and Matson (as augmented by studies by Gehrels' group and Allen (1971), respectively) have served this purpose for both polarization and thermal IR investigations. The related and supporting studies of asteroid orbits by Williams (1971) and of meteoritic implications for parent bodies by Anders (1971) and numerous other workers, have been greatly advanced

recently. Except for the possibility of obtaining asteroid diameters from stellar occultations, there is little immediate prospect for extending direct measurement of asteroid diameters or radar studies to numerous asteroids. The clear remaining need for asteroid reconnaissance studies has been in the direction of asteroid colorimetry or spectrophotometry.

Standard UBV photometry has been done for quite a few asteroids, but such wide-band work does not yield a very complete determination of the spectral reflectivity and is not very diagnostic. Watson's (1938) thesis was an early attempt to decipher asteroid mineralogy from color indices, but after three decades of work particularly by Russian astronomers, the latest results of Hapke (1971) are not much more definitive. The initial spectral reflectivities obtained for Vesta in two dozen narrowband filters, on the other-hand, were most promising and diagnostic of composition. Two additional developments now make a spectral reflectivity reconnaissance study of asteroids feasible:

(1) Advances in instrumentation and associated digital electronics have recently made efficient, multicolor, photoelectric pulse-counting programs possible for asteroids. The major problems with the new equipment and methodology have been worked out in the course of several years application to the moon, planets, and brighter planetary satellites. Much of this development has been done in the M.I.T. Planetary Astronomy Laboratory under Prof. T. McCord's guidance.

(2) Theoretical and laboratory investigations of the spectral transmittance properties of mineral crystals (Burns, 1965, and other workers) and extensive laboratory measurements of the reflectance properties of minerals, rocks, and powders (Adams and Filice, 1967; Hunt and Salisbury,

1970 a, 1970 b; Hunt *et al*, 1971, 1970) have now been carried out extensively. Sufficient understanding of the implications for remote-sensing has been achieved, partly through experience with the moon (McCord and Johnson, 1970), so that observations of solar system objects can be interpreted in terms of mineralogy and other surface properties with far less ambiguity than previously was the case.

For these reasons, the time seemed ripe for doing a thesis on reconnaissance studies of asteroid spectral reflectivities. This program is described in the next two chapters. The results are then correlated with other known or recently-determined properties of the asteroids in an attempt to formulate a consistent, though admittedly still hazy, picture of asteroid surface properties. Finally, now that the reconnaissance is completed, priorities for future more detailed work (both spectrophotometric and otherwise) can be sketched -- see the final chapter. I begin by reviewing early work on asteroid colors in the next chapter.

CHAPTER II

REVIEW OF SPECTROPHOTOMETRIC STUDIES OF ASTEROIDS*

A. INTRODUCTION

It was long assumed by astronomers that asteroids were grey reflectors of the solar spectrum and asteroids were used from time to time as solar-type comparison stars. In the classic article on asteroid spectrophotometry, Bobrovnikoff (1929) first questioned this premise and attempted to measure the characteristics of asteroid spectra. He compared microphotometric tracings of photographic spectra of asteroids with spectra of G-type stars. He concluded that (1) he was observing reflection spectra with no emission features; (2) that Ceres and Vesta lack any major absorptions in the visible like those of Jupiter, (3) that most asteroids have relatively low reflectivity in the UV and violet, (4) that there are differences between asteroid spectra, and (5) that several asteroids show color variations with rotation.

Although Watson (1938) regarded some of Bobrovnikoff's conclusions as uncertain due to insufficient standardization of the spectra, comparison with work done to the present demonstrates that the reliability of Bobrovnikoff's results was not surpassed until the advent of photoelectric UBV photometry. He concluded that 2 Pallas was unusually bright in the UV; also relatively bright in the UV were 1 Ceres, and 4 Vesta. Found

---

* Preliminary drafts for parts of this chapter served as the basis for part of the review article, currently in press, by Chapman et al (1971 b), bearing the same title.

to be very dark in the UV were 7 Iris and 12 Victoria, while 9 Metis was moderately dark. Weaker spectra also showed a relatively dark UV for 3 Juno, 8 Flora, 28 Bellona and 40 Harmonia. Another weak spectrum showed that 79 Eurynome was relatively bright in the UV -- the only case where Bobrovnikoff's result is at variance with more recent photoelectric work.

Of particular interst are Bobrovnikoff's conclusions regarding the variation of asteroid spectra with rotation. Not only did he discover Vesta's color variation with rotation, subsequently confirmed by Gehrels (1967) and Johnson and Kunin (Chapman et al, 1971b), but he actually deduced an approximately correct value for Vesta's rotation period from its color variations alone! It is most intriguing that two of his spectra for 6 Hebe show dramatic differences; one suggests Hebe is very dark in the UV while the other suggests it is bright. My own data indicate variability in the spectral reflectivity for Hebe and Matson's thermal IR measurements show dramatic differences (see Chap. VI).

Bobrovnikoff attempted to relate his asteroid spectra to possible compositions. He compared his spectra with comets and with reflectivities of meteoritic-type material, although he reached no definitive conclusions. All subsequent investigators have been interested in the compositional implications of asteroid color indices.

B. PHOTOGRAPHIC PHOTOMETRY

Microphotometric tracings of spectra taken of three asteroids by Johnson (1939) yielded the incorrect result that these asteroids were substantially bluer than the sun. Recht (1934) reached a similar erroneous conclusion from a more extensive study of the color indices of 34 asteroids obtained from magnitude measurements on normal photographic and

panchromatic plates. Recht's measurements have been criticized by several subsequent writers (Watson, 1938, Groeneveld and Kuiper, 1954). Not only do they show a large scatter due to the fact that the measurements of the two colors were often made from plates taken on different nights and for other reasons, but there is a strong correlation between the color index derived by Recht and the apparent magnitude of the asteroid -- indicative of a spurious systematic error in the photometry. I have tried to correct Recht's color indices for the systematic error, but the corrected indices still show little if any correlation with recent photoelectric photometry. Watson (1940) obtained color indices for seven asteroids. His reliability is difficult to guage; although the mean color index for the seven is realistic, there is poor agreement with photoelectric colors for specific asteroids.

Perhaps the most ambitious and reliable of the early photographic colorimetry is that of Fischer (1941). Though Fischer's data show less scatter than Recht's, the random error is still uncomfortably large. Of the 33 asteroids for which Fischer obtained color indices, 13 have good photoelectric colors of which 12 are in good relative agreement with Fischer's values. In Figure 2-1, I have plotted Fischer's color indices after being re-scaled so that their mean and range approximate the photoelectric values; no absolute calibration is intended. It is probable that most of Fischer's bluer asteroid are in fact bluer than his redder ones, but finer distinctions probably have no meaning. Fischer reported statistically significant correlations between color index and two related orbital parameters: semi-major axis and Jacobi constant. The correlation is in the same sense as evident in subsequent photoelectric work (see Chap. V), but there was potential in this early photographic work for

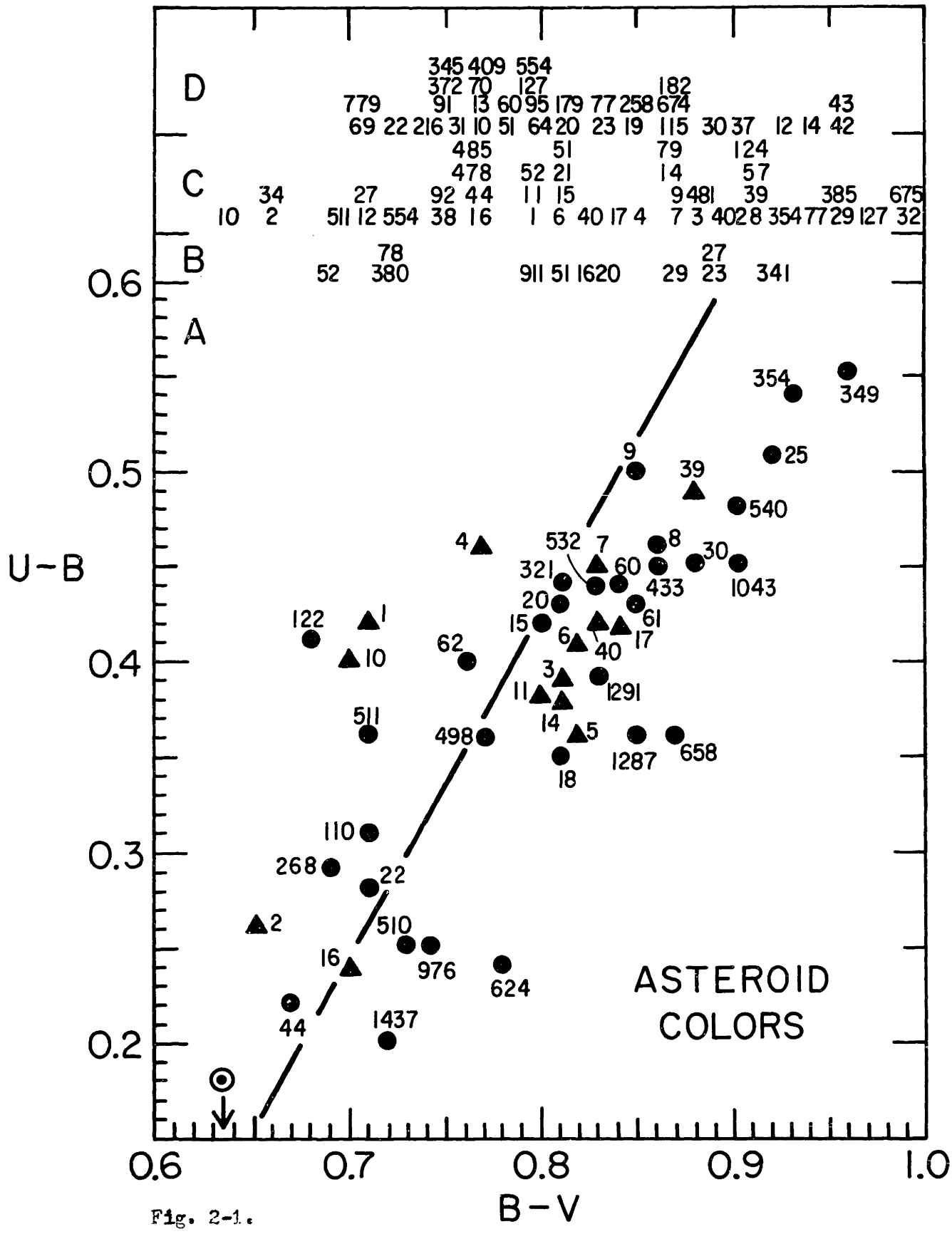
D
C
B
A
345 409 554
372 70 127
182
779 91 13 60 95 179 77 258 674 43
69 22 216 31 10 51 64 20 23 19 115 30 37 12 14 42
485 51 79 124
478 52 21 14 57
34 27 92 44 11 15 9 48 39 385 675
10 2 511 12 554 38 16 1 6 40 17 4 7 3 402 8 354 77 29 127 32
78 27
52 380 911 51 1620 29 23 341
0.6
0.5
0.4
0.3
0.2
U-B
354
349
25
9
39
540
4
532 7
8
30
321
60
433
1043
20
61
15
6
40
17
122
1
62
10
3
11
1291
14
5
511
498
1287
658
18
110
268
22
2
510
16
976
624
44
1437
ASTEROID
COLORS
0.6
0.7
0.8
0.9
1.0
B-V

Fig. 2-1.

systematic apparent magnitude dependent errors which themselves would be weakly correlated with semi-major axis.

The largest sample of asteroids for which color indices were determined is that compiled by Sandakova (1955; 1959; 1962). Photographic color indices are published for 56 asteroids. I have re-scaled them and grouped them into five color groups, from blue to red. The yearly averages for half a dozen of the frequently observed asteroids differ by two groups (e.g. from very red to medium), indicating large scatter; however one is 6 Hebe, which probably has real color variations. I have also considered a sub-set of 13 asteroids which Sandakova observed more frequently than the remaining 43 and which might be expected to have more reliable color indices. Table 2-1 shows the results of an approximate comparison between Sandakova's colors and those obtained by UBV photometry (Gehrels, 1970) and by myself (Chap. IV).

Table 2-1.

Comparison of Sandakova Asteroid Photometry with Photoelectric Results

	UBV Photometry		Spectral Reflectivities	
	Total 56 ast.	Selected 13 ast.	Total 56 ast.	Selected 13 ast.
Agreement	6	4	4	4
Some agreement	9	2	4	1
No agreement	9	1	10	0
No. in common	24	7	18	5

The comparisons demonstrate that little significance can be attached to most of Sandakova's results. However, it seems that the selected sample of 13 agrees well with recent results. Sandakova reports no correlation

of colors in his complete sample with a, but a large difference in color between asteroids with unusually small and unusually large orbital Jacobi constants.

C. PHOTOELECTRIC PHOTOMETRY

Forty-two asteroids were measured in two colors with a 1P21 photomultiplier by Kitamura (1959) in the mid-1950's. The effective wavelengths were somewhat longward of the standard B and V colors. From a graph presented by Kitamura of the color indices of 6 stars with known B-V colors, I have converted his color index into equivalent B-V colors. The resulting values have a slightly redder mean and greater range than B-V colors obtained by Gehrels, Kuiper, and their associates, so I have rescaled Kitamura's colors for plotting in Fig. 2-1. The several cases of multiple measurements of the same asteroid indicate small scatter in the data. Agreement for those asteroids with known B-V colors is good.

Kitamura reports negative attempts to correlate his color indices with proper orbital elements, absolute magnitude B(1,0), or rotation period. Though his figures show no correlation with B(1,0) or mean motion, there appears to be a real correlation with proper eccentricity. The sign of the correlation is such as to amplify the expected correlation of the Jacobi constant with respect to a correlation with semi-major axis a. Kitamura's table also shows a possible correlation of color index with extreme a, such that asteroids with $a > 3$ AU are bluer than those with $a < 2.3$ AU, but the statistics are poor.

Since the mid-1950's, Gehrels, Kuiper, and their associates have published a series of papers on photoelectric photometry of asteroids in the standard UBV system. A table summarizing these results (Gehrels,

1970) is the basis for parts A and B in Figure 2-1 (lunar-like phase corrections were applied; see Chaps. V and VI). The consistency of the UBV results is good and most of the plotted colors are probably known to 0.05 magnitudes. However, for most asteroids there is insufficient data to estimate the scatter introduced by the possible ranges of rotational and phase-angle variations in color.

All plotted asteroids are redder than the sun in both U-B and B-V, with the trend slightly redder than the stellar main sequence. There is a major clumping around (B-V, U-B) = (0.83, 0.4) and a lesser one near (0.7, 0.25). More data are needed to determine the significance of other possible clusters. The numbers of some asteroids for which only B-V colors have been measured are plotted in part B of the figure. They amplify the apparent dearth of objects with B-V colors near 0.75. Further implications of these UBV results are discussed in Chap. V.

UBV colors for several additional asteroids have been reported by observers not associated with Gehrels' group (e.g. Veverka, 1970; Tempesti and Burchi, 1969).

D. MULTICOLOR SPECTRAL REFLECTIVITY STUDIES

Fig. 2-2 summarizes the results of several multicolor studies of asteroids. In 1958 Haupt (see Gehrels, 1970) published the results of six-color photometry of 4 Vesta. It clearly shows the presence of an absorption near 1 micron, but its band-like shape and its full significance were not realized until it was rediscoverd (McCord *et al*, 1970). The other multicolor photometry shown in Fig. 2-2 is due to Gehrels *et al* (1970); the data are for asteroids 39, 51, and 1566 through UBVRI filters and some supplementary filters in the red and near-IR. 1566 Icarus shows

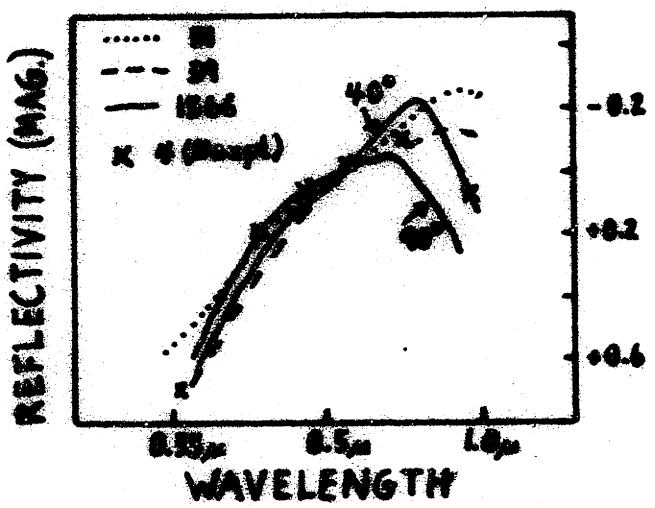

Fig. 2-2.

evidence for an absorption band possibly deeper than Vesta's band. Icarus also shows a strong tendency to become bluer with increasing phase angle over the range 40° to 90°; such behavior is found in laboratory measurements of rock powders and is theoretically understood as an increased surface component of the reflected radiation from a surface which preferentially absorbs in the red (Adams and Filice, 1967). Veverka (1970) published some six-color photometry of 15 Eunonia, but not in a form which permits a reflectivity curve to be sketched.

The first detailed spectral reflectivity study of an asteroid in many narrowband filters was carried out by McCord et al (1970). Measurements of Vesta made at Mt. Wilson in October 1968, and with a different set of 22 filters at Cerro Tololo in December 1969, show a deep absorption band centered in the 0.9 to 1.0 micron region. The band is the most prominent absorption feature yet found on a solid solar system body; it was interpreted as being due to a Mg-rich pigeonite, generally similar to the Nuevo Laredo basaltic achondrite. Supplementary observations of Pallas and Ceres were reported by McCord et al to show no similar strong absorption feature in the near-IR. Subsequent measurements of 4 Vesta by Johnson and Kunin (Chapman et al, 1971 b) showed little variation in the shape of the reflectivity curve or the absorption band as a function of rotational phase; some variation in the UV was noticed.

E. CONCLUSIONS

Work on asteroid spectrophotometry published prior to 1970 has yielded surprisingly little understanding of asteroid properties. Much of the data was of poor or worthless quality. All that could be said was that asteroids showed a variety of colors, averaging just slightly redder than the

sun. Suggestions of a correlation of asteroid color with a often had an unsound empirical basis; however, that result has been shown to be partly correct on the basis of high-quality data (see Chap. V).

Since Watson's (1938) thesis, there have been many detailed attempts to determine the mineralogical composition of asteroids from color indices. Most attention has been given, of course, to meteorites (e.g. Sytinskaya, 1965; Hapke, 1971). No firm conclusions have been reached, however, no doubt due to the large variety of color indices for rocks and minerals and the relatively ambiguous discrimination of spectral reflectivities by a single-dimensional color index (see Chap. VII).

Comparison of the results suggests that photographic photometry is definitely a marginal technique for obtaining even approximately accurate color indices. Bobrovnikoff's spectra, however, have withstood the test of time quite well. The chief advantage of UBV photometry is that it can be obtained rapidly, it is a well-standardized system, and some of the gross characteristics of the reflectivity curves can be determined rapidly. The full potential of spectrophotometry was not reached, however, until narrowband filters were employed, extending well into the near-IR where diagnostic mineral absorption bands are known to occur.

The results of this literature survey are applied in Chap. V.

CHAPTER III

SPECTRAL REFLECTIVITY OBSERVATIONAL PROGRAM

A. INTRODUCTION

An observational program was conducted to obtain spectral reflectivities for as many asteroids as possible using McCord's double-beam photometer (McCord, 1968) and the data system of the M.I.T. Planetary Astronomy Laboratory. This chapter briefly summarizes the program.

The aim of the program was to obtain photometry at about the 5% accuracy level for as many different asteroids as possible. Measuring changes correlated with phase angle and rotational phase for individual asteroids was of secondary concern. Asteroids were selected from among the sample brighter than apparent magnitude 13.0 for which ephemerides existed and which were readily available during the scheduled observing runs. I attempted to observe asteroids having typical and extreme values of many physical and orbital parameters. Special attempts were made to observe members of the same Hirayama families.

B. OBSERVING PROCEDURES AND INSTRUMENTATION

There were seven observing runs during the period June 1970 to May 1971 on the 200-inch telescope at Mt. Palomar, 24- and 60-inch reflectors at Mt. Wilson, and the no. 2 36-inch reflector at Kitt Peak National Observatory. Good data were obtained during 31 of the 42 nights of assigned telescope time.

Data were taken with McCord's photometer, operating in both the double- and single-beam modes, using a set of 24 narrowband interference

filters covering the spectral range 0.3 to 1.1 microns. Dry-ice cooled photomultipliers were used -- generally one with an S-1 surface, but sometimes one with an S-20 surface over its more limited spectral-response range. Complete runs through the 24 filters took from between several minutes, when spinning the filter wheel at 3 rpm and co-adding the signal, to about an hour when running in a filter-by-filter mode.

A high-speed pulse-counting data system was used for recording and monitoring the data in the two channels (object and sky, 40 msec samples). The data were dumped periodically onto magnetic tape. Dark current, scattered light, and differences in the double-beam mirror reflectivities were frequently monitored and also recorded on tape.

Asteroids were easily located in the finder with the use of computer-drawn finding charts at the scale of the Palomar Sky Survey. Several asteroids could not be located, either due to moonlight, their faintness, or possible ephemeris errors. Motion with respect to the stars was usually detected; it is unlikely that any observations were made of mis-identified objects.

Standard stars were selected from among the lists of Oke (1964) and Hayes (1970). Attempts were made to observe standards at or near the same airmass as for the asteroid observations -- also hopefully close in time and azimuth. Sufficient star observations were made to accurately determine the extinction coefficient for each filter, and usually to obtain some information on its spatial and temporal variations.

The data are believed to be generally free from errors at the several percent level. Runs seriously affected by atmospheric conditions and scattered light have been omitted. On the otherhand, there were differences

in observing conditions and equipment problems during the several observing runs which have potentially different effects on data accuracy at the level of a few percent or less. Observations with the Mt. Wilson 24-inch were more subject to systematic errors due to scattered light and other causes because of a lower signal-to-noise ratio. There were some problems with guiding during the January 1971 60-inch run because of bad seeing. Also, there remain some uncertainties in some data taken with the S-20 tube during February and May at Kitt Peak because of problems in calibrating neutral density (ND) filters used for the standard star observations. Accuracy is better in visible wavelengths than in the UV or IR because of higher count-rate and more constant atmospheric conditions. The internal consistency of the data demonstrates that it is little affected by the potential problems.

C. DATA REDUCTION

The raw data were examined, sorted, and corrected for any apparent problems. Forty-eight numbers were obtained from each run on an asteroid or standard star: the brightness of both the object and the sky in each of the 24 filters. The tests for beam mirror inequality, scattered light asymmetry, and other potential problems rarely showed effects large enough to require correcting the data. Therefore, in general, the sky count was directly subtracted from the object + sky count and associated with a sidereal time for final processing.

There were some uncertainties in calibrations of the ND filters used for some S-20 standard star observations. Although the adopted filter functions are believed to be accurate to several percent, the possibility remains of larger errors. "Coincidence" corrections were made to correct for non-linearity in the recorded signal at high count-rates; the

saturation was in a counter in the data system, not in the phototube. Corrections of 2% to 10% were required only for observations of stars without ND filters with the S-20 tube, which were used for calibrating the filters.

An elaborate computer extinction-correction program was written for making corrections for airmass differences between the asteroids and standard stars. However, in most cases the full sophistication of the program was unnecessary, although it was used, because of the relatively small differences in airmass involved.

The spectral reflectivity of an asteroid illuminated by the sun is obtained from the formula

$$\frac{\text{Ast.}}{\text{Sun}} = \left(\frac{\text{Ast.}_{ob}}{\text{Star}_{ob}}\right)\left(\frac{\text{Star}}{\text{Sun}}\right) \qquad (3\text{-}1)$$

where the quantities are fluxes integrated across the effective spectral response of each filter. For presentation in this thesis, and because I can obtain no information concerning absolute reflectivity (albedo), the reflectivities are scaled to unity at 0.57 microns (the 11th filter). Some curve-fitting is employed if the reflectivity in the 11th filter seems to have been displaced by scatter from the mean of reflectivities in neighboring filters.

The relative fluxes of the Oke and Hayes standard stars are interpolated from the calibrations against Alpha Lyrae at the effective wavelengths of each filter, taking due account of the spectral responses of the atmosphere, mirrors, and photocathodes. The star spectra are related to that of the sun using a model for Alpha Lyrae (Schild et al, 1971) which takes lines into account and agrees well with observational absolute

calibrations of the star (Oke and Schild, 1970). The new solar spectrum of Arvesen et al (1969) is adopted, which again takes account of lines in the solar spectrum. These new calibration sources are probably better, and detailed reduction procedures more complete, than these which have been used by the Planetary Astronomy Laboratory previously.

The errors in calibration are believed to be dominated by uncertainties in the relative calibrations between the standard stars used and Alpha Lyrae. These errors (mostly scatter but some systematic component) are of the order of 2% in the visible, but are somewhat larger in the UV and may approach 4% in the IR in some cases. These errors are important since they can significantly affect measurement of centers of mineralogical absorption bands. These calibration errors are probably larger than any systematic errors in the data and are much larger than the random scatter in the data for the brighter asteroids.

CHAPTER IV

SPECTRAL REFLECTIVITIES OF 32 ASTEROIDS (0.3 TO 1.1 MICRONS)

A. THE SAMPLE

Thirty-one asteroids were successfully observed. In this chapter I will present and describe their mean spectral reflectivity curves, along with that of 4 Vesta obtained by T. Johnson and J. Kunin (Chapman et al, 1971 a; Chapman et al, 1971 b). Good reflectivities throughout the range 0.3 to 1.1 microns were obtained for 21 asteroids, though with possible problems for 2; fair reflectivities for 7 more; and reflectivities only in the range 0.3 to 0.85 microns for 3 others. (Good data could not be salvaged for still 3 more and two asteroids could not be found.) Two asteroids were observed during 3 of the 5 observing trips and 12 during 2 trips, yielding some phase angle coverage. Twelve of the asteroids have also been observed by Matson (1971). Of the 32 asteroids, UBV colors have been measured previously for 17 and rotation periods measured or guessed for 22. Table 4-1 lists the ranges of some observational, physical, and orbital parameters which are known for asteroids in the sample.

Despite my attempts to observe asteroids with extreme values of various parameters, so many parameters were considered that the distribution of asteroids with regard to any particular parameter is quite representative; this is particularly true for the brighter asteroids, less so for the faint ones. The overwhelming selection factor was, of course, apparent magnitude. Hence the sample is biased, in order of decreasing strength toward large diameters, high albedos, and small a.

Table 4-1. Ranges of Parameters for Asteroid Sample.

	Minimum Value		Maximum Value	
Parameter	Value	Asteroid	Value	Asteroid
Semi-major axis, a	2.20	43	3.15	10
Proper eccentricity, e	0.020	40	0.288	324
Sine of proper inclin., $\sin i$	0.036	21	0.588	2
Rotation period (hours)	4.303	16	16.806 or 18?	5 10
Light-curve max. amplitude (magnitudes)	0.04	1,14,704	0.53	39
B-V color index (mag.)	0.65	2	0.88	39
Abs. magnitude, B(1,0)	4.11	1	10.31	82
Diameter (km)	35?	82	1160	1
Bond albedo	0.01	324	0.10	4
Apparent mag. when observed	7.7	1	12.6	43,68

B. MEAN REFLECTIVITIES

The final average reflectivities for the 32 asteroids are presented in Appendix I, in numerical order. The uniformity of presentation should not mislead the reader into believing that all final reflectivities are uniformly reliable. The data were obtained in many different modes and under different conditions. Of course, the reflectivities may be compared relative to each other with more reliability than can be given to their absolute characteristics; relative comparisons are even more reliable for asteroids reduced against the same standard star. The criteria important to guaging reliabilities are now briefly described.

There is scatter in the data for individual filters due to statistical fluctuations, minor guiding problems, as well as scatter in the calibrations. The reality of weak bands and other small wiggles is questionable.

The new calibrations used in this thesis have an oscillating character (peak-to-peak amplitude of 7%) when compared with those previously used by the Planetary Astronomy Laboratory. While the present calibrations are believed valid, it is hard to be sure at the few percent level. Also, in several cases the averaging of S-20 runs with S-1 runs made at different phases or rotational phases produces an unnatural effect near the 0.85 micron S-20 cut-off (the strongest effect is a spurious enhancement of the 0.9 micron band for 6 Hebe). Both the absolute calibration and individual runs made under inferior conditions are subject to systematic errors in slope over the 0.3 to 1.1 micron range, but such errors are probably relatively small.

The IR and, especially, the UV portions of reflectivities are subject to many times the random and systematic errors of the visible region, for many reasons. The calibrations of the standard stars relative to Vega have 3% - 4% scatter in both the UV and IR. The solar calibration is worst in the UV. Sky conditions are most variable in the UV and IR. Perhaps most important, the count-levels are much lower in the UV (especially for S-1 data) and the IR than in the visible due to photomultiplier response, yielding large scatter. Calibration of the first filter (0.3μ) is worthless and it is omitted from the graphs in Appendix I; the fifth filter (0.38 microns) is subject to 5% to 10% errors due to the Balmer jump.

Faint asteroids are more subject to a variety of problems including: low count statistics; systematic effects like unequal sky subtraction; greater probability of guiding errors in poor seeing; and higher probability of contamination by faint starlight (believed improbable). Asteroids that were relatively faint (considering telescope aperture and observing

conditions) are numbers 5, 17, 21, 43, 68, 82, 93, 324, 337, 356, 409, 554, 563, and 704. A single faint run on 40 Harmonia was given half weight and a faint run on 11 Parthenope was ignored entirely in calculating the final averages.

Reflectivities presented here may not be representative of all sides of an asteroid; there is evidence that rotational variations exist (see Chap. VI). Also, no color corrections for phase angle have been applied, for reasons discussed also in Chap. VI. Two separate runs on 43 Ariadne on January 7 are badly discordant in overall slope. I can find no probable cause of error, so it may be a real effect. The average reflectivity has been calculated using one of the two runs which agrees closely with a high-quality observation made on February 10.

There were special difficulties in reducing those asteroid runs made with the S-20 photomultiplier which were ratioed to standard stars observed through neutral density filters. The relative ND-filter calibrations are probably accurate to a few percent, but there is some possibility for larger errors. Particularly uncertain for some May data was the determination of the absolute filter calibration used for joining the IR segment observed with the S-1 tube to the UV-visible portion observed with the S-20. Other peculiar characteristics of some May runs may be real or may be due to unidentified problems.

This lengthy listing of sources for error is not intended to detract from the essential reliability and high quality of the results. The results are the epitome of the state-of-the-art, though the requirements for brevity in journal publications by other workers in this field may leave misleading impressions of greater accuracy. I feel the error bars assigned in Appendix I are reasonable, though a cautious person might multiply them

by two for some applications. It should be realized that exact calibration of Oke/Hayes standard stars to the sun, as observed through our system, may someday become available, in which case all data presented herein may be corrected to remove all errors due to calibration.

C. CLASSIFICATION OF SPECTRAL REFLECTIVITY CURVE TYPES

The 32 asteroids observed so far have a wide variety of spectral reflectivity curves. That asteroids differ in color has been known since Bobrovnikoff's (1929) early result. But the extent of variety is even greater than revealed in plots of B-V versus U-B (see Chap. V); some asteroids with nearly identical UBV colors have noticeably different spectral reflectivity curves. The asteroid reflectivity curves cannot be fit into a single-dimensional spectrum of classifications. On the otherhand, there is little obvious clustering into well-defined groups. Several investigators have attempted to find clusters or groups on a B-V versus U-B plot (Wood and Kuiper, 1963; Chapman et al, 1971 b; Hapke, 1971; Gehrels, comments at Tucson conference 1971). The present results show, however, that the UBV clusters are composed of a variety of reflectivities, hence presumably a variety of compositions.

Despite the lack of well-defined types, it is useful to attempt an approximate classification. The most obvious distinguishing characteristic of the reflectivities is their slope, or overall "color". They range from quite reddish to nearly flat or slightly bluish. I am defining three broad classes of curves -- red, medium, and blue (or flat) -- with somewhat arbitrary boundaries. The asteroids placed in the red (R) class constitute half the sample. Nearly all of them show absorption bands in the near IR (or could if counting statistics were higher); very few of the

Table 4-2-a. Red Asteroids.

Group	Sub-group	Characteristics	Asteroids
R1		Very red. Steep slope 0.3 to 0.85 microns; some leveling beyond 0.85 microns. No prominent band (43 Ariadne may have a deeper band on a different side).	43, 12, 5 (?)
R2		Red asteroids with band near 1.1 microns. Peak near 0.8 microns.	
	R2A	Very red.	39, 7, 5 (?)
	R2B	Moderately red.	68
R3		Red asteroids with 0.95 micron band (band not always statistically certain). Peak near 0.75 microns.	
	R3A	Very red.	192, 79, 40, 82, 5 (?)
	R3B	Moderately red. Weaker band (?)	3,6, 14
	R3C	Modestly red, weak band.	29
R4		Mostly reddish; curving reflectivities. May have 0.95 micron bands, but statistics low. Probably like Group R3B.	563, 17

Table 4-2-b. Medium Asteroids.

Group	Characteristics	Asteroids
M1	Modestly red. Flat (no curvature). No band.	16, 11 (??)
M2	Bent curves with dip at 0.65 microns. Steep slope 0.3 to 0.5 microns; flat 0.5 to 0.7 microns; rises again beyond 0.7 microns.	51, 324
M3	Vesta type. Similar to M2 but falls off beyond 0.8 microns. May (4) or may not (409) have deep 0.95 micron band.	4, 409
M4	Fairly flat beyond 0.5 microns. Drops off toward UV below 0.5 microns.	337, 356, 11 (?)

Table 4-2-c. Blue or Flat Asteroids.

Group	Characteristics	Asteroids
B1	Like Group M4, except UV downturn is at 0.45 microns.	554, 93 (?)
B2	Bluish. Sharp UV downturn shortwards of 0.4 microns.	13, 1
B3	Flatish or bluish into UV to 0.3 microns.	10, 2, 704
B4	Very bright in UV. Concave upwards.	21

M or B asteroids have such bands, often indicative of Fe^{2+} in various mineral crystals. Groups are defined within the classes based upon more refined characteristics of the reflectivity curves, such as band position or the location of the edge of a UV drop-off.*

Sub-groups are defined within the red groups based on the steepness of the red slope (see Table 4-2-a). Strength of the IR absorption bands in red asteroids may be positively correlated with steepness of slope. This is the reverse of the case with lunar regions for which the curves with steepest slopes have the weakest 0.95 micron bands, probably due to the admixture of dark reddish glasses which not only dominate the spectrum but reduce multiple scattering among the crystalline pyroxene grains that give rise to the band (Adams and McCord, 1971). Thus for asteroids, either there is not a red darkening material, or the strengths of the bands reflect other kinds of compositional variation among the asteroids

* Asteroids observed only with the S-20 phototube obviously cannot be grouped according to position of IR absorption bands. There is also difficulty assigning some poorly-observed asteroids to a particular group.

(see Chap. VII). It is significant that none of the reddish asteroids shows an absorption band with more than half the strength of Vesta's band (Vesta has an M-type curve and is the only M or B-type asteroid with a prominent IR band). There are differences in the center positions of the IR bands, with promising implications for mineralogical identifications.

The medium asteroids (Table 4-2-b) are a small but rather variegated sample of asteroids. By happenstance, the quality of the data is generally poorer than for the R and B type asteroids. Some have sharp drop-offs in the UV, while others do not. At least one has a strong IR absorption band; most do not. Some show evidence for a weak band near 0.65 microns.

Asteroids with blue or flat reflectivities comprise a quarter of the sample (Table 4-2-c). They all have quite flat curves throughout the visible and near-IR. Some show sharp drop-offs in the near UV, while others clearly do not. None have definite IR absorption bands.

Before considering the fundamental question of the compositional implications of these diverse reflectivities, I will analyse asteroid colors in the next two chapters.

CHAPTER V

ASTEROID COLORS

There are two main approaches to evaluating the spectral reflectivities presented in Chap. IV. One can examine and analyse the properties of the absolute spectral reflectivities, which I do in Chap. VII. Or one can compare the relative differences between reflectivities, in which we need not worry about the absolute calibration. In this chapter and the next I compare the general relative properties of the curves -- first differences between different asteroids, then differences between separate runs on individual asteroids. As a reconnaissance study, it is appropriate to relate the reflectivities to previous asteroid colorimetry, and to search for as many correlates with asteroid color as possible. In this chapter I mention many tantalizing possible correlations, to guide future research; however, some are not yet firmly established.

A. COMPARISON OF SPECTRAL REFLECTIVITIES WITH UBV PHOTOMETRY

UBV Colors Converted to Reflectivities

Gehrels (1970) has summarized most available UBV photometry of asteroids. I have converted his values to spectral reflectivities and plotted them as x's on the figures in Appendix I. An assumed solar color of B-V = 0.63, U-B = 0.14 was subtracted from the asteroid colors and the magnitudes were converted into intensities, setting V = 1.0. Since the effective wavelengths of U, B, and V are 0.374, 0.446, and 0.550 microns, respectively, (calculated for asteroid-like colors, with about 0.003 variation), a re-normalization to 0.57 microns is required for comparison with

spectral reflectivities. This is done by extrapolating the B to V slope from 0.55 to 0.57 microns, amounting to a 3% scaling change at most.

The reflectivities and UBV colors cannot be compared exactly because of the different bandpasses used. However the general agreement shown in Appendix I is excellent. There is a slight tendency for the UBV colors to show a more bent reflectivity curve and to be a little "redder" than the reflectivities, despite Gehrels' corrections for reddening with phase. This effect may be due to the solar calibration. The only major discrepancy is for 29 Amphitrite, and possibly 11 Parthenope, for which Gehrels gives appreciably redder colors.

UBV Colors Determined from Reflectivities

It is of interest to derive UBV colors for asteroids from the observed reflectivities since colors of astronomical objects are most frequently characterized in that photometric system. It must be emphasized that the derived UBV colors are a most incomplete characterization of the complete reflectivity curves. In addition, the derivations suffer from a variety of errors, some of which are peculiar only to the U and B regions of the spectrum and are not representative of the precision of the reflectivities as a whole. (1) The counting statistics in the U part of the spectrum are very low for data taken with the S-1 tube alone. (2) There is a potential calibration problem for some S-20 data. (3) The Balmer discontinuity in my standard stars near the U filter wavelength is a large source of error. (4) In any case, the derived colors, read off from the reflectivity curves at the respective UBV effective wavelengths, are not true UBV colors since the observations were not made through the standardized filters.

The colors listed in Table 5-1 and plotted in Figure 5-1 were derived

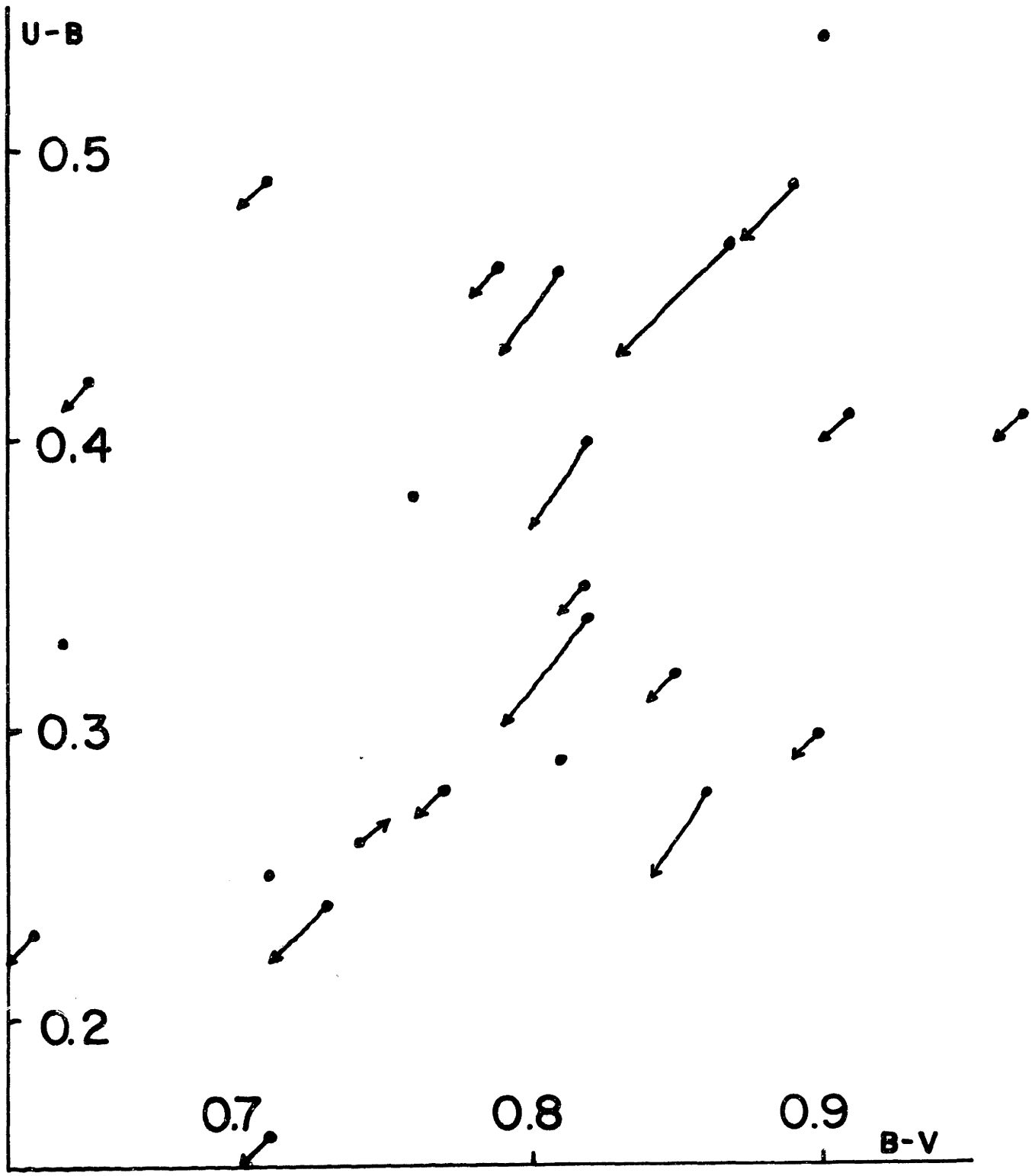

Fig. 5-1

by reversing the procedures already described for converting UBV colors to reflectivities. They suffer from any errors in the adopted solar colors. The colors are plotted both in raw form and corrected for reddening with phase according to the phase laws adopted by Gehrels (1970).* When available, UBV colors given by Gehrels are also tabulated, along with UBV colors not corrected for phase (Kuiper et al, 1958; Gehrels and Owings, 1962). For reasons discussed in Chap. VI, I believe there is little advantage in using corrected colors rather than raw colors.

The derived UBV colors are known absolutely to about 0.1 magnitude; relative colors are probably better than 0.05 magnitudes for most asteroids. Comparison of the derived colors (Figure 5-1) with actual UBV colors (triangles in Figure 2-1) shows good relative agreement. Positive corrections of about 0.015 and 0.07 magnitudes to the derived B-V and U-B colors respectively, would bring them into better absolute agreement with the UBV colors.

Earlier attempts to discern clustering on the U-B vs B-V plot were mentioned in Chap. IV. The general characteristics of the plot are not substantially modified by the addition here of more than a dozen approximate colors. I apparently did not sample as many extreme red asteroids as shown in Fig. 2-1. The new reddish asteroids I did observe may extend the main cluster upwards, filling in a region near or even above 9 Metis. Several new asteroid colors may increase the sparse population just left of the main cluster, near 62 and 498; there is no good reason to believe, as Anders (1971, personal communication) has suggested, that the

---

* The colors are corrected for reddening with phase to 5° phase using 0.0017 and 0.0020 magnitudes per degree for B-V and U-B, respectively.

Table 5-1. Approximate UBV Colors Derived from Spectral Reflectivities.

Ast. Number	Derived B-V		Derived U-B		Gehrels' B-V		Gehrels' U-B	
	raw	corrected	raw	corrected	raw	corrected	raw	corrected
1	0.64	0.64	0.33	0.33	0.72	0.71	0.44	0.42
2	0.63	0.62	0.23	0.22	0.65	0.65	0.27	0.26
3	0.82	0.79	0.34	0.30	0.83	0.81	0.43	0.39
4	0.74	0.74	--	--	0.78	0.77	0.48	0.46
5	0.83	0.80	--	--	0.83	0.82	0.38	0.36
6	0.86	0.84	0.28	0.25	0.82	0.82	0.40	0.41
7	0.81	0.79	0.46	0.43	0.85	0.83	0.46	0.45
10	0.71	0.71	0.25	0.25	0.71	0.70	0.40	0.40
11	0.78	0.78	--	--	0.81	0.80	0.40	0.38
12	0.87	0.83	0.47	0.43	--	--	--	--
13	0.65	0.64	0.42	0.41	--	--	--	--
14	0.82	0.81	0.35	0.34	0.82	0.81	0.40	0.38
16	0.73	0.71	0.24	0.22	0.71	0.70	0.25	0.24
17	0.82	0.81	--	--	0.85	0.84	0.42	0.42
21	0.61	0.59	0.10	0.08	--	--	--	--
29	0.76	0.76	0.38	0.38	0.88	0.87	--	--
39	0.91	0.90	0.41	0.40	0.89	0.88	0.51	0.49
40	0.82	0.80	0.40	0.37	0.85	0.83	0.44	0.42
43	0.97	0.96	0.41	0.40	--	--	--	--
51	0.79	0.78	0.46	0.45	0.83	0.81	--	--
68	0.85	0.84	0.32	0.31	--	--	--	--
79	0.90	0.90	0.54	0.54	--	--	--	--
82	0.90	0.89	0.30	0.29	--	--	--	--
93	0.71	0.69	--	--	--	--	--	--
192	0.89	0.87	0.49	0.47	--	--	--	--
324	0.81	0.81	0.29	0.29	--	--	--	--
337	0.82	0.82	--	--	--	--	--	--
356	0.77	0.76	0.28	0.27	--	--	--	--
409	0.73	0.72	--	--	--	--	--	--
554	0.74	0.75	0.26	0.27	--	--	--	--
563	~0.71	~0.70	0.49	0.48	--	--	--	--
704	0.71	0.70	0.16	0.15	--	--	--	--

colors for 62 and 498 are in error. Asteroid 21 Lutetia may be the bluest asteroid yet measured.

B. COMPREHENSIVE LIST OF ASTEROID COLORS

Asteroid colors are indicative of several properties of their surfaces, probably the most important being mineralogical composition. Studies of the correlations of colors with orbital parameters and other physical properties of asteroids may shed light on asteroid origin, subsequent evolution, and relationship to meteorites. We desire the largest sample of reliable asteroid colors in order to test hypotheses and find correlations. As demonstrated in Chap. II, much early work on asteroid colors was of such poor quality that most recent investigators have wisely restricted their work to the available UBV data summarized by Gehrels (1970) for 55 asteroids.

The critical review presented in Chap. II makes it possible to select colors from the earlier work which are reliable. By accepting them along with Gehrels' summary colors and the spectral reflectivities obtained in this thesis, it is possible to approximately double the list of asteroids with known colors, although the precision of color description must be quite low.

In Table 5-3, I have grouped the asteroids from the several sources into four color groups: blue (B), medium (M), medium-red (MR), and very red (VR). The precision of some of the data is too poor to permit discrimination between B and M or between MR and VR, so they are grouped into groups BM (blue or medium) and R (medium red or very red). Table 5-2 shows the relationship of the various color indices or classes to the adopted four color groups.

Table 5-2. Color Group Selection Criteria.

Source	B	BM	M	MR	R	VR
Spectral reflectivities, this thesis. Types	B		M	R2B, R3B, R3C, R4		R1, R2A, R3A
Gehrels (1970), B-V	<0.72	0.72 - 0.80		0.8 - 0.84		>0.84
Kitamura (1959), C color index	<0.40	0.40 - 0.51			>0.51	
Fischer (1941), FI color index		<1.0			>1.0	
Sandakova, selected, color index		<0.72			>0.72	

For deriving the final list (Table 5-4), I have given the greatest weight to the UBV colors and the spectral reflectivities. Three asteroids were omitted for which the existing color estimates were conflicting (nos. 60, 127, 216); they may be of intermediate color. In the table, colors have been underlined if they are particularly reliably determined (i.e. from UBV or spectral reflectivity data, or agreement between more than one of the lesser-weight sources). I expect that only a very few of the 102 asteroid colors will be found to have been in error when better data become available. It is important to remember, that these color groups are imprecise characterizations of spectral reflectivities. Many asteroids with the same colors may be expected to have significantly different reflectivity curve types.

Table 5-3. Asteroid Color Groups.

Source	B	M	MR	VR
This thesis	1, 2, 10, 13, 21, 93, 554, 704	4, 11, 16, 51, 324, 337, 356, 409	3, 6, 14, 17, 29, 68, 563	5, 7, 12, 40, 39, 43, 79, 82, 192
UBV	1, 2, 10, 16, 22, 44, 52, 78, 110, 122, 268, 380, 1437	4, 11, 15, 62, 498, 510, 624, 911, 976	3, 5, 6, 7, 14, 18, 20, 40, 51, 321, 532, 1291, 1620	8, 9, 17, 23, 25, 37, 29, 30, 39, 60, 61, 341, 349, 354, 433, 540, 658, 1043, 1287
Kitamura	2, 10, 12, 27, 34, 511, 554	1, 4, 6, 11, 15, 16, 17, 21, 38, 40, 44, 51, 52, 92, 478, 485	3, 7, 8, 9, 14, 29, 32, 39, 57, 77, 79, 124, 127, 354, 385, 402, 481, 675	
Fischer	10, 13, 22, 31, 51, 60, 64, 69, 70, 91, 95, 127, 216, 345, 372, 409, 554, 779		12, 14, 19, 20, 23, 30, 37, 42, 43, 77, 115, 179, 182, 258, 674	
Selected Sandakova	2, 4, 27, 45		3, 6, 9, 19, 40, 44, 115, 216	

C. CORRELATION OF COLORS WITH ORBITAL PARAMETERS

It is generally believed that the distribution of asteroid orbits, away from planets and commensurabilities, is similar to that at the time asteroids were formed. Certainly any correlation of asteroid compositions with semi-major axis a or with the Jacobi constant (Tisserand invariant) could indicate differences in the condensation of the solar nebula as a function of heliocentric distance.

Correlation of color with large perihelia could reflect the temperature

Table 5-4. Comprehensive List of Reliable Asteroid Colors

1	B	18	MR	42	R	89	VR	341	VR	532	MR
2	B	19	R	43	VR	91	BM	345	BM	540	VR
3	MR	20	MR	44	BM	92	M	349	VR	554	B
4	M	21	B	45	BM	93	B	354	VR	563	MR
5	VR	22	B	51	M	95	BM	356	M	624	M
6	MR	23	VR	52	BM	110	B	372	BM	658	VR
7	R	25	VR	57	R	115	R	380	B	674	R
8	VR	27	BM	61	VR	122	B	385	R	675	R
9	VR	29	R	62	M	124	R	402	R	704	B
10	B	30	VR	64	BM	179	R	409	M	779	BM
11	M	31	BM	68	MR	182	R	433	VR	911	M
12	VR	32	R	69	BM	192	VR	478	M	976	M
13	B	34	B	70	BM	258	R	481	R	1043	VR
14	MR	37	VR	77	R	268	B	485	M	1287	VR
15	M	38	M	78	B	321	MR	498	M	1291	MR
16	BM	39	VR	79	VR	324	M	510	M	1437	B
17	B	40	R	82	VR	337	M	511	B	1620	MR

environment in the asteroid belt, integrated over solar system history, since the boundary of the region where ices are stable throughout the age of the solar system may be near the asteroid belt (Watson et al, 1963). Studies of color correlations with inclination or eccentricity could clarify the role of the micro-particle population in eroding asteroid surfaces. For instance asteroids in highly elliptical or inclined orbits have high relative impact velocities -- possibly high enough to produce appreciable glassy material, which is known to affect the color of the lunar surface in a striking fashion (Adams and McCord, 1971).

The most fundamental orbital parameters are semi-major axis a, the proper eccentricity e, and the proper inclination i. The "proper elements"

are those for which periodic oscillations due to perturbations have been removed. I am using two sets of proper elements. J. Williams (1971) has recently completed a re-determination of asteroid proper elements taking into account higher terms in the expansions for both e and i, and considering both free and forced oscillations. In advance of publication, he has kindly listed for me the elements of those asteroids for which I have spectral reflectivities. For studying the entire sample of 102 asteroids with known colors, I must use the earlier proper elements of Arnold (1969), who has kindly provided me with a card deck tabulation. The agreement of the two sets of elements is sufficiently good for most purposes considered here.

Correlation of Colors with a, e, and i

A number of earlier investigators reported significant correlations between asteroid colors and a or the invariant Jacobi constant with respect to perturbations by Jupiter (a function of a, i, and e). Especially noted were correlations with extreme values of a or Jacobi constant. Let us re-examine these correlations.

In Figure 5-2, I have replotted Fig. 2-1, substituting the asteroid numbers with symbols for five ranges of a. A correlation is evident, though it is due almost entirely to the extreme values of a. Ten of the 13 asteroids with $a > 3.0$ have B-V $\leq$ 0.8 while none of the 5 with $a < 2.3$ are so blue. Asteroids with $2.75 < a < 3.0$ show the greatest range of colors. With a sample of several times as many asteroids, we might start to see significant clusterings of a-values in the plane of Fig. 5-2.

Figure 5-3 shows the colors of the 102 asteroids plotted as a function

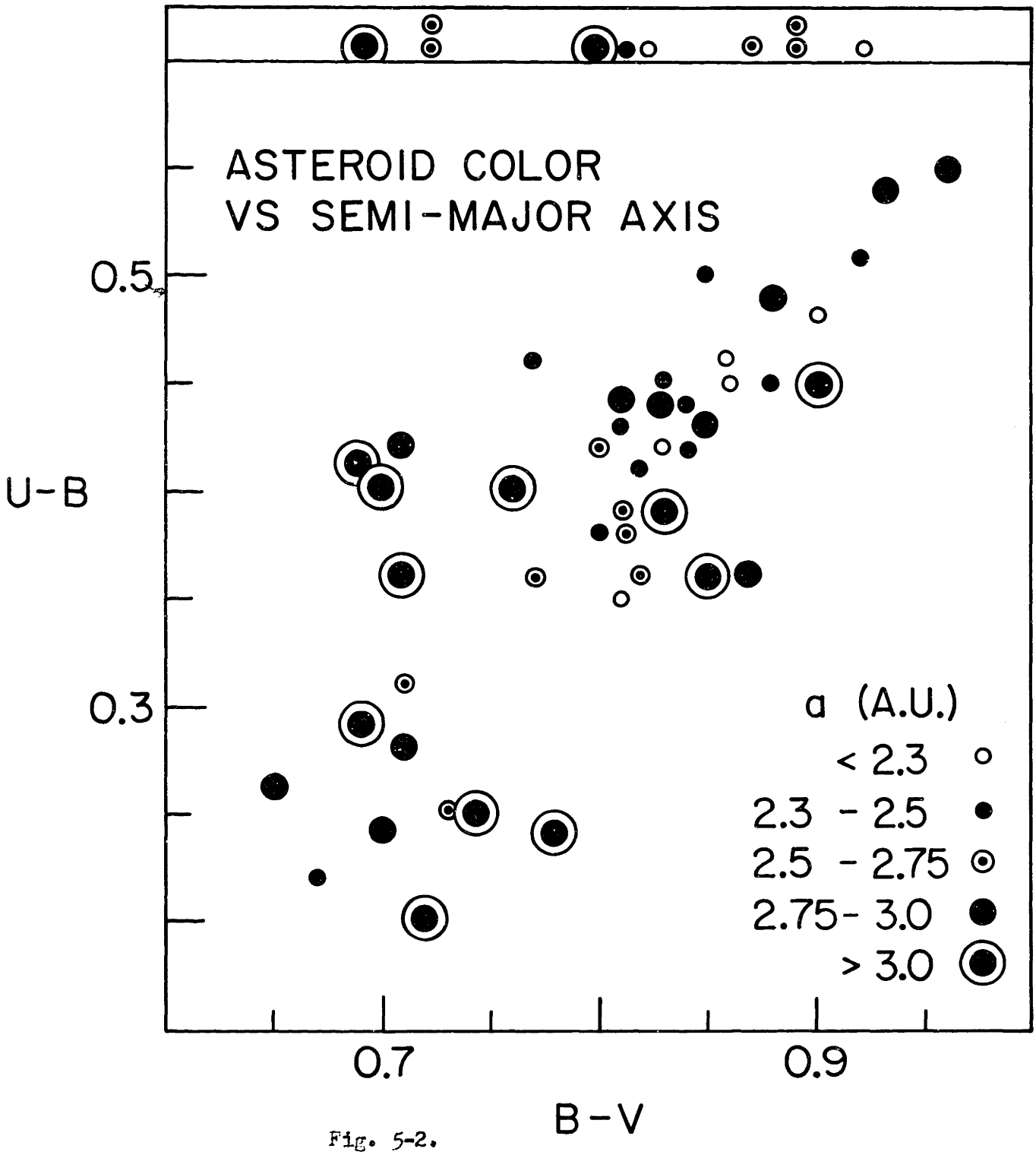
ASTEROID COLOR
VS SEMI-MAJOR AXIS
0.5
0.3
U-B
0.7
0.9
B-V
a (A.U.)
< 2.3
2.3 - 2.5
2.5 - 2.75
2.75- 3.0
> 3.0

Fig. 5-2.

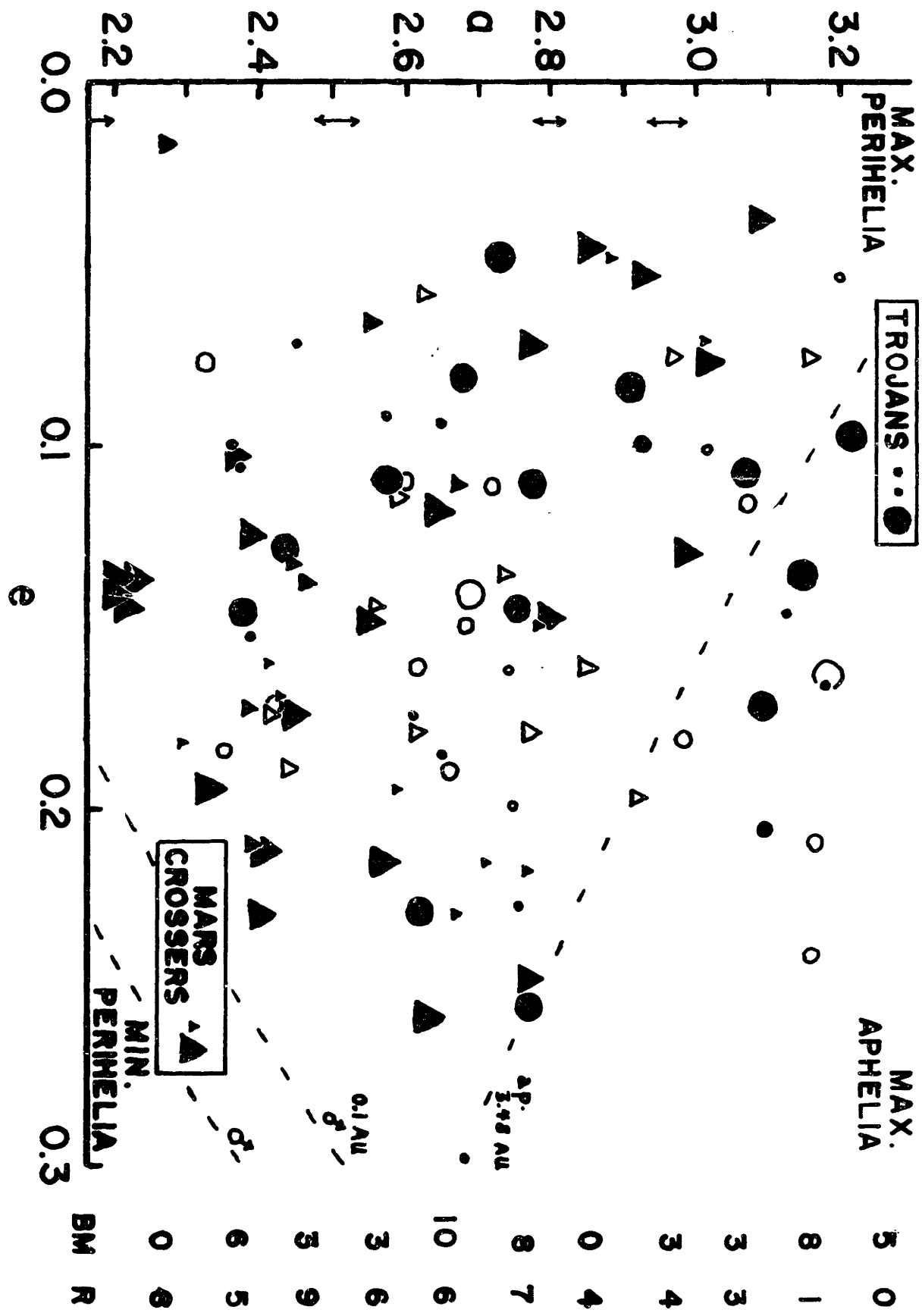
MAX. PERIHELIA
TROJANS
MAX. APHELIA
MARS CROSSERS
MIN. PERIHELIA
a
e
q
3.2
3.0
2.8
2.6
2.4
2.2
0.0
0.1
0.2
0.3
0.1 AU
3.4 AU
BM
R

Fig. 5-3

of a and e. Triangles are reds, circles are B's or M's. Larger symbols are for more extreme color; solid symbols are for the colors underlined in Table 5-4. The Trojans and Mars asteroids could not be plotted to scale. Plotted in the lower-right part of the figure are lines of closest approach to Mars' orbit (assuming 0° inclination and disregarding longitudes of perihelia). Lines of constant Jacobi constant would be approximately horizontal with a slight tilt upper-left to lower-right. The frequencies of R and of BM asteroid colors are shown to the right for each increment of 0.1 AU.

There is a clear but imperfect correlation of color with a. For $a < 2.6$ AU there are 12 BM asteroids and 28 R ones, while for $a > 2.6$ AU there are 37 BM's and 25 R's. The correlation exists even excluding the Trojans and Mars asteroids, but it is clearly strongest at the extreme values of a. Although the statistics are low, there is a suggestive tendency for asteroids near the borders of Kirkwood gaps to be red, and for asteroids far from the gaps to be blue, superimposed on the general correlation with a.

There is no correlation between asteroid color and either e or i, considered alone. This is true even so far as extreme values are concerned. Therefore, whatever correlation there is between asteroid colors and Jacobi constant is due solely to the correlation with a.

There are several additional striking features of Figure 5-3. First, nearly all asteroids in the upper-right part of the plot are B or M. In fact, it appears that there is a virtually sharp cut-off for red colors at an aphelion distance of about 3.5 AU. This might be consistent with a model for asteroidal accretion in which a bluish component which is restricted -- perhaps by temperature-pressure relations

in the solar nebula (e.g. carbonaceuous chondritic matter, see Larimer and Anders, 1967) -- to the outer regions of the asteroid belt, is the last component to accrete onto asteroid surfaces.

Another prominent characteristic of the distribution of colors in Fig. 5-3 is the tendency for asteroids with minimal perihelia to be red. Very few blue asteroids have perihelia within 2 AU. Processes like escape of volatiles are governed chiefly by maximum temperatures reached, rather than mean temperatures. Therefore, correlations with perihelion distance may reflect processes either of formation or of subsequent evolution governed by peak temperatures. (The absence of an obvious color difference correlated with larger perihelion distances, toward the upper left of Fig. 5-3 suggests that the ice-stability field is not readily recognizable in asteroid colors.)

It is generally accepted that meteorites must be fragments of Mars-crossing, or nearly-Mars-crossing, asteroids, if they are asteroidal fragments at all (Anders, 1971). To the extent that asteroids which approach within 0.2 AU of Mars are representative of those which give rise to meteorites, the correlation of red colors with minimal perihelia suggests that meteorite collections may be biased towards samples of red asteroids. Asteroid 324 Bamberga is the outstanding exception in this correlation; note, however, that it also reaches a rather large aphelion distance.

Correlation of Spectral Reflectivities with a, e, and i

Since spectral reflectivities are much more diagnostic of composition than are general colors, it is important to examine correlations of curve types with orbital parameters, even though the sample is quite small. Fig.

5-4 shows the correlation of reflectivity curve types with a and e. Asteroids with ~0.95 micron bands are indicated with an interior plus (+).

The general correlations of color with position on this plot are similar to those for the larger sample of asteroids. It seems possible that absorption bands are restricted to small and intermediate values of a. There is an intriguing clustering of 0.95 micron bands around a = 2.55 (±0.2), e = 0.2 (±0.5), spread along a track parallel to Mars-proximity. Some of the asteroids with longer wavelength bands (Groups R1 and R2) are still somewhat closer to Mars. Williams has listed the minimum distances of approach to Mars for all 32 asteroids, based on his analysis of asteroid orbit perturbations; see Appendix I. Of 12 asteroids with a minimum distance less than 0.2 AU, 8 are red, 2 M, and 2 B; of 6 asteroids that can approach Mars within 0.08 AU, 5 are red, 1 medium.

Another characteristic of asteroid reflectivity curves with important compositional implications is the presence or absence of a UV drop-off. It is important to verify or refute the slight tendency apparent in Fig. 5-4 for asteroids with bright UV reflectivities to be in the center and toward the upper-right of the plot, and for those with UV drop-offs to be in the center and toward the lower-left of the plot.

Although not borne out by the complete sample of 102 asteroids, the smaller sample seems to show a correlation between curve type and e. There seems to be no correlation, however, between curve types and i, or extreme i. Nor does consideration of i clarify any of the possible relationships shown in Fig. 5-4.

In conclusion, there are some enticing correlations, and possible

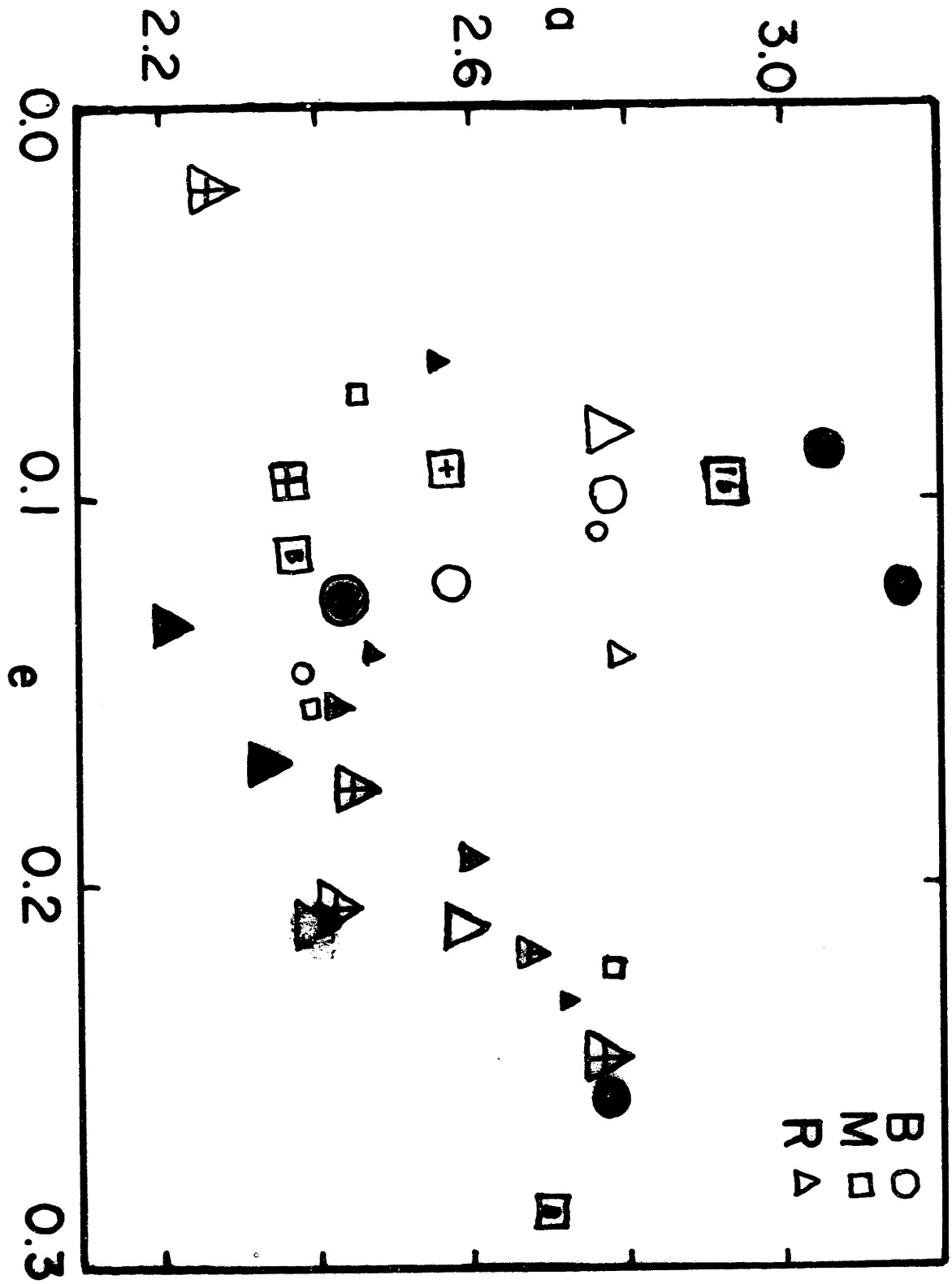

Fig. 5-4

correlations, between reflectivity curve types (and colors) and orbital parameters. For reasons discussed in later chapters, these curve types probably chiefly reflect mineralogical composition, so theories for the chemical origin of the asteroids may be elucidated by these correlations. More data is certainly needed.

D. CORRELATION OF COLORS WITH ASTEROID FAMILIES AND JET STREAMS

The Hirayama families of asteroids are usually thought to be composed of fragments from catastrophic collisions between asteroids. However, some workers suggest that they may be due, at least in part, to orbital dynamical processes not yet fully understood. Relationships of color and family membership can shed light on the nature of families.

If family members are all collisional fragments of a body of uniform composition, then colors would appear identical -- providing composition is the dominant color determinant. However, if fragmented asteroids were originally part of a large highly differentiated body, they might show a variety of colors. Some kinds of fragmentation are known to spall off spherical shells (Gault and Wedekind, 1969), which is a failure mode likely to yield family members of uniform but different colors; other modes which break off pieces might yield fragments with different colors on opposite sides of each fragment. Differing colors for family members could also result from the collisional break-up of two (or more) asteroids of different colors. But catastrophic collisions are much more likely between a large asteroid and one many times smaller than between similar-sized objects, so the fragments should dominantly reflect the colors of the large partner of a collision. If family members bear no genetic relationship to each other (for instance if they are

in the process of accreting, as proposed by Alfven and Arrhenius, 1970), then one might also expect a variety of colors.

It is difficult to determine whether or not a specific asteroid is a member of a family since there is no criterion for separating out "background" of "field" asteroids. The new determination of proper elements by Williams largely confirms the existence of the families reported by Arnold (1969). But the assignment of individual asteroids to the families is modified considerably by Williams' work. A first priority when Williams' complete list of proper elements is published is to re-evaluate earlier studies of family members (such as Anders' 1965 analysis of fragmentation). I now proceed to discuss the spectral reflectivities and colors of asteroids which may be members of the same families; I give preference to Williams' data for those asteroids for which it is available; otherwise I use Arnold's family lists.

Family B-25

Asteroids 17 and 79 are both listed by Arnold as members of family B-25. Although Williams did not originally assign 17 Thetis to his family which includes 79 Eurynome, he has examined the family and reports (personal communication, 1971) that Thetis is a borderline case and could as well be regarded as a member of the family. Thetis is type R4 (which resembles type R3B), while Eurynome is type R3A. Unfortunately, the error bars on the spectral reflectivity curve of Thetis are quite large, hence the two asteroids are identical to within errors, although there is a non-significant tendency for 79 to be redder. Based on the complete sample of 32 asteroids with known spectral reflectivities, I must revise my earlier conclusion (Chapman et al, 1971b) that the reflectivity curves for 17 and 79 are not only similar to each other but differ significantly from other

asteroids. They may be similar, but many others are also like them.

Ceres Family

According to Williams, 1 Ceres (B2), 39 Laetitia (R2A), and 93 Minerva (B1) belong to the same family. The errors on 93 are sufficiently large that it could conceivably be identical to Ceres, but Laetitia is obviously very different.

Family A-82

Both Arnold and Williams agree that 19 Fortuna (R) and 21 Lutetia (B4) are members of the same family. They are clearly different in color.

Flora Group

The Flora group is a large asteroid family at the inner edge of the asteroid belt with several recognizable sub-divisions. Williams regards 43 Ariadne (R1 = VR) to be a member of the Flora family. 8 Flora is also VR in color. Arnold regards 341 (VR) to be in the same sub-group, and 540 (also VR) in the next sub-group. These four asteroids form the cluster of triangles at the bottom of Fig. 5-3. The Flora family seems to contain only very-red asteroids, which is particularly important since many Flora group members are known to be Mars-crossers and are a likely source for meteorites.

Other Arnold Families

I list below other possible family members, obtained only from Arnold's lists. The families are identified by Arnold's designation.

H-1: 62 (M) and 268 (B) have UBV colors probably significantly different.

H-2: 1287 (VR) and 1291 (MR) have UBV colors that could be identical.

H-3: 321 ((MR) and 658 (VR) have UBV colors significantly different.

A-66: 38 (M), 68 (R2B = MR), and 93 (B1) do not seem very similar. 68 and 93 have spectral reflectivities that are obviously different.

A-72: 70 (BM) and 510 (M) may be the same, but the precision is poor.

A-83: 37 (VR) and 77 (R) may be the same, but the precision is poor.

Jet Stream J-2

The existence of jet streams is in some dispute, although Arnold (1969) lists seven possibilities. These are families of asteroids moving in nearly identical orbits, including the same longitudes of perihelion and ascending node. Asteroids 12 (R1 = VR), 115 (R), and 192 (R3A = VR) are all part of J-2. While their colors are similar, 12 Victoria and 192 Nausikaa differ significantly in the details of their reflectivities.

Conclusions about Family-Color Relationships

Although the similar red colors of Flora-group members may imply a genetic relationship between members of that family, most other asteroids with small semi-major axes are also red. So far as the other families are concerned, there is little evidence for family members to have the same color. There are too many differences to explain in terms of field asteroids being confused for family members.

The hypotheses which are consistent with these tentative implications are (1) that asteroid family members are not genetically related; or (2) that collisions are spalling off layers from highly differentiated larger asteroids; or (3) that asteroid colors are not highly indicative of compositional similarities. In the latter case, there might be a dominance of surface regolith-producing processes in determining asteroidal colors;

differences must depend on size or rotation of individual asteroids (i.e. effective surface gravity) since the impact environment is probably similar for family members.

E. CORRELATION OF COLOR WITH SPIN

It remains a subject of discussion what the relationship of asteroidal rotation periods might be to the accretion and fragmentation processes (Hartmann, 1969b; Alfven and Arrhenius, 1970). The spins of larger asteroids cannot be appreciably changed by impacts, but fragments might have very different spins. Certainly one might expect larger light-curve amplitudes for fragmented asteroids, especially if asteroids accrete spherically (Anders, 1964). The effective surface gravity, determined in part by rotation period and shape for rapidly spinning asteroids, is a dominant factor affecting regolith development (see Chap. VIII).

Asteroid obliquities are very badly known; but for those listed by Vesely (1971) there is no obvious correlation between obliquity and color. There is also no obvious correlation between color and rotation period for a sample of more than 40 asteroids.

There does appear to be a weak correlation between color and light-curve amplitude, as shown in Table 5-5. I have used the maximum amplitudes so far observed (Gehrels, 1970; Yang et al, 1965); of course some infrequently observed asteroids may have been observed nearly pole-on and may subsequently be revealed to have larger amplitudes. There seems to be a significant correlation of large amplitude with red color. There are several possible interpretations for this effect.

One might speculate that if red asteroids are stony and blue ones are metallic (see Chap. VII), then red asteroids would have larger

Table 5-5. Correlation of Color with Light-Curve Amplitude.

Max. Amplitude (magnitudes)	Blue or Medium	Red
> 0.2	7	17
0.1 - 0.2	10	7
< 0.1	3	2

amplitudes because rock is so much more easily fragmented than metal. A more plausible suggestion -- though not inconsistent with the first -- is that the color correlation is more directly one with size (see later part of this chapter), and that smaller asteroids are more likely to have non-spherical shapes than larger ones. Johnson and McGetchin (1971) have discussed the sphericity of asteroids as a function of size; larger ones may be gravitationally constrained to spherical shapes, while smaller ones are not. The fragmentation histories developed Anders (1965) and Hartmann and Hartmann (1968) suggest that larger asteroids are original condensations, and smaller ones are fragments likely to be less spherical. There is also observational support for the hypothesis that smaller asteroids have larger amplitudes (van Houten as mentioned by Gehrels (1970, p. 326)).

Although most asteroidal light-curve variation is believed due to non-sphericity because of the double-peaked character of the curves, a significant portion of the variation may be due to albedo differences across asteroid surfaces, recognized by odd-terms in the expansion of the light-curve (Lacis and Fix, 1971). Using available light-curves I have crudely estimated the components possibly due to spots (by comparing the two maxima and the the two minima). The statistics are too poor to reveal any significant correlation with color that may be present.

F. CORRELATION OF COLOR WITH ALBEDO AND DIAMETER

Correlation of Color with Absolute Magnitude

Authors of past studies of asteroid size-distributions (e.g. Anders, 1965; Dohnanyi, 1971) have assumed that asteroid absolute magnitudes can be directly converted into relative sizes; or even converted into absolute sizes by adopting albedo calibrations from direct diameter measurements of the four largest asteroids. The direct diameter measurements are very difficult to do accurately because asteroid diameters are generally smaller than seeing disks and are never many times bigger than the Airy disks. Moreover, we know from the work of Veverka (1970), Matson (1971), and Allen (1971) that there is a large scatter among asteroidal albedos -- at least a factor of 10. Hence absolute magnitudes B(1,0) are not a simple function of either diameter or albedo alone, but vary with both to a considerable degree. Let us nevertheless investigate the possible diameter implications of a color-B(1,0) correlation, remembering that the spread in albedos for asteroids of the same size yields a variation in B(1,0) of about 3 magnitudes. It is meaningless to group the absolute magnitudes in smaller intervals if we are interested in a size-dependence -- I use 2.5 magnitude intervals in Table 5-6. The table shows that the three largest asteroids (Ceres, Pallas, Vesta) are blue, which is no surprise, and also that the smallest asteroids are predominantly red. The slight reversal of the trend in the 6 to 11 magnitude range may or may not be physically significant.

Correlation of Color with Albdeo

I have read off approximate values for asteroid albdeos from Matson's (1971) Fig. 3. Also used are several additional albedo estimates or limits from thermal IR studies (Matson, 1971, personal communication). These were

Table 5-6. Correlation of Color with B(1,0).

B(1,0)	VR	R+MR	M+BM	B
< 6.0	0	0	1	2
6.0 - 8.5	10	12	9	5
8.5 - 11.0	7	14	21	10
> 11.0	6	3	1	0

placed in a relative sequence, bright to dark. Albedos deduced by Veverka (1970) from polarization studies were scaled against those in common with Matson, and added to the sequence. This procedure yields a total sample of 22 asteroids for which there exists some information about albedo, independent of B(1,0). Of these, I have color estimates for 20. Although no correlation is prominent -- there are examples of bright and dark asteroids of both M and R colors -- more data on low albedo asteroids may reveal most of them to be B. Colors should be determined for Asteroids 80, 145, and 313, which are apparently quite dark. If the suggested trend is found to exist, then 19 Fortuna would be an anomalously dark reddish asteroid. Vesta, of course, is an anomalously bright asteroid, and it is of type M3.

Correlation of Color with Diameter

By using the albedo sequence just described, and values for B(1,0) tabulated by Gehrels (1970), one can derive approximate relative diameters. The list which follows is necessarily crude and it should be checked and refined upon the final publication of Matson's results. (The diameter for 16 Psyche is at least "medium". In order to be "small" it must have an albedo higher than Vesta, but Matson (1971, personal communication) thinks

he detected it in the thermal IR, so it is not that bright.)

Large: 1, 2, 4, 324
Medium: 3, 6, 7, 15, (16), 19
Small: 5, 8, 9, 18, 20, 39, 27, 44, 68, 89, 192

Table 5-7. Correlation of Color with Diameter.

Relative Diam.	VR	R+MR	M+BM	B
large	0	0	2	2
medium	0	4	2	0
small	6	3	2	0

Table 5-7 shows a surprisingly strong correlation between color and diameter. No large asteroids are red, no small ones are clearly blue. Medium-size asteroids tend to have intermediate colors. This result is consistent with the crude results obtained from the correlation of the larger sample of colors with B(1,0). The result has important implications, of both a theoretical and a practical sort, so high priority should be given to attempts to verify it.

It appears that the diameter corresponding to the change from large blue asteroids to small red ones may be quite sharp, near 200 km. There may be no red asteroids as large as 300 km and no blue or medium ones as small as 150 km diameter. If this demarcation exists, what does it imply about asteroids? Several kinds of explanations suggest themselves.

(1) As previously suggested, possibly blue asteroids could be the relatively non-fragmented metallic (hence bluish) cores of parent bodies. The red asteroids would be fragments of the surfaces and mantles of those

parent bodies, as well as non-fragmented asteroids or fragments of asteroids too small to form cores. This simple picture does not explain the differences between the reflectivity curves for various bluish asteroids, but plausible modifications to the hypothesis are possible.

(2) On the other hand, perhaps most asteroidal surfaces initially were bluish, due to the nature of the last materials to accrete on their surfaces during the early history of the solar system. It is well-known that large asteroids have the lowest probabilities against collisions with other asteroids large enough to break them apart (catastrophic collisions). The smaller asteroids are more likely to have all been fragmented several times. Then the large blue asteroids are simply those objects which have not been disrupted during 4.5 billion years, leaving their surfaces reasonably intact. Agian, an elaboration is still required to explain differences between reflectivities of various B and M asteroids.

(3) Perhaps the colors have little to do with composition, and reflect chiefly various degrees of pulverization of surface material (see Chap. VII). Then large asteroids, which certainly can retain a regolith, may differ in color from smaller asteroids, which may not be able to retain regoliths (see Chap. VIII). The difficulty with this hypothesis is that most pulverized materials appear redder, so the correlation is in the wrong sense. Possible ways of forming blue regoliths are discussed in Chap. VII.

From the variety of logical alternatives -- big ones are formed and left blue, or become blue, or blue ones are left big, etc. -- one can devise other hypotheses. For instance, one might think that big ones are chemically differentiated, creating blue surface layers, while small ones are not (see Chap. IX). But the reported densities for Vesta and Ceres

(Schubart, 1971) suggest that there are more fundamental distinctions between large asteroids. Quite possibly the color correlation is fortuitous and only a much more sophisticated model for asteroidal origin and evolution will explain the great variety of spectral reflectivities.

If the suggestions made in this chapter that both albedo and diameter are correlated with color are borne out, then albedos and diameters are correlated. In that case, many earlier studies of the size-frequency distribution for asteroids must be re-evaluated.

CHAPTER VI

ASTEROID SPECTRAL REFLECTIVITIES: PHASE AND ROTATION VARIATIONS

So far, I have treated asteroid reflectivities as unique, invariant, reflective surface properties. But asteroids may have sufficiently large differences in composition and texture across their surfaces to be revealed as variations in spectral reflectivity as they rotate. Also it is important to investigate possible phase-angle variations in the reflectivity curves for two reasons: (1) comparison of the mean reflectivity curves in Appendix I could be confused since the average phase angles were different for different asteroids; (2) color-phase dependence is related to surface particle size, compaction, opaqueness, and composition in ways which are individually ambiguous but which are diagnostic in conjunction with other data.

A. PHASE ANGLE DEPENDENCE OF SPECTRAL REFLECTIVITIES

Since the search for phase-dependent variations in asteroid reflectivities was not the primary goal of the observational program, the data are not ideally suited to the task. For this reason the results must be regarded only as indicative, not conclusive. Because of the uncertainties in asteroid rotation-periods and pole positions, the absence of light-curve epochs in most cases (my data do not permit determination of a light-curve), and our lack of knowledge about rotational color variations even if the epoch were known, rotational color variations must be treated as noise in the search for phase-dependent effects.

For asteroids observed at several phase angles, I have measured the slopes of the reflectivity curves in the B and V regions of the spectrum,

and converted them to equivalent B-V magnitudes. (The counting statistics are too low to study slope changes in the UV.) The results are summarized, along with comments about phase-dependence of IR band strengths, in Table 6-1.

The quantitative results are not so precise as for standard UBV photometry; however, the precision is higher than for my determination of UBV colors from spectral reflectivities in Chap. V, for two reasons: (1) any systematic error in absolute B-V colors is not relevant to the slope comparisons, and (2) rather than just reading off values along the reflectivity curve at the effective wavelengths of B and V, I have considered the entire trend from about 0.4 to 0.7 microns. Still, there is significance only in the reality of the effect, and its order-of-magnitude, when "reality" is listed as probable.

There are three main results evident in Table 6-1: (1) Red asteroids seem to show a reddening with phase in the visible equivalent to a change in B-V of about $0.003^{+0.007}_{-0.002}$ magnitudes per degree. (2) However M-type asteroids may not show a prominent phase effect and two B-type asteroids seem to show a strong tendency to become bluer with phase (about 0.015 mag/deg). (3) In the 3 cases for which data were available for asteroids with prominent IR absorption bands, the depth of the bands seem to be greater at larger phase angles.

The apparent trends of color phase effects with color are physically reasonable. Silicate powders are known to redden with phase, over the range of phase studied here, because of the increased pathlength and transmission through grains, which enhances their coloration (Adams and Felice, (1967). The behavior of the bands is consistent with the observed reddening with phase; it implies an enhanced volume-component of the reflected

Table 6-1. Phase Variations in Asteroidal Spectral Reflectivities.

No.	Type	Color Change with Phase	B-V mag/deg	Reality	Range of $\underline{i}$, deg.	Band Stronger with Phase
7	R2A	redder	0.01	possible	$15\frac{1}{2}$ - 22	yes?
192	R3A	redder	0.002	probable	$9\frac{1}{2}$ - 25	yes?
40	R3A	redder	0.004	possible	$14\frac{1}{2}$ - 24	n.a.
3	R3B	redder	0.002	probable	20 - 29	n.a.
29	R3C	bluer	0.001	doubtful	2 - 24	yes?
16	M1	neither prominent			$12\frac{1}{2}$ - 20	n.a.
11	M4	blue	large	doubtful	4 - 25	n.a.
337	M4	ambiguous			4 - 7	n.a.
10	B3	neither prominent, data problems			3 - 9	n.a.
2	B3	bluer	0.01	probable	9 - 14	n.a.
704	B3	bluer	0.02	probable	5 - 10	n.a.

n.a. = not applicable, either because asteroid has no band or data taken with S-20 photomultiplier.

---

light from the increased multiple scattering and transmission at larger phase angles. It is reasonable that materials with less coloration would show a lesser tendency to redden. The tendency for asteroids with flatter reflectivities to become actually bluer with phase is more difficult to understand. It may imply that the flatter asteroids have surfaces composed of opaque grains (as seems plausible, see Chap. VII), with preferential red absorption, hence blue reflection. Then one might expect an enhancement of the surface component and a bluer coloration with increased phase angle (see Veverka, 1970).

The apparent color trends just described are not fully confirmed, however, by the several other available results. Taylor et al (1971) reports a reddening with phase for 4 Vesta (M) and 110 Lydia (B), but a bluing with phase for 20 Massalia (MR). Veverka (1970) found a reddening with

phase averaging about 0.002 mag/deg for all five asteroids studied, 8 (VR), 9 (VR), 15 (M), 89 (VR), and again 4 (M);* the effect was greatest for 89 and least for 9, both very red asteroids. The phase effect of the color of Massalia is especially difficult to understand in terms of a particulated surface in view of its reddish color and its apparently high albedo (Matson, 1971).

Although available evidence does not yet yield a clear understanding of asteroid color phase effects, it is clear that the magnitudes and even signs of the "reddening with phase" vary among asteroids. As a result, I conclude that the application of corrections to all asteroid colors, using a lunar-like phase law as applied by Gehrels (1970), is not justified. For asteroids for which phase changes have been accurately determined (e.g. by standard UBV photometry, taking account of rotational color variations), it would be desirable to apply the correct phase correction to any given observation. However, for spectral reflectivities presented in this thesis, few asteroids have well-determined phase laws (certainly those presented in Table 6-1 are not well known), so no corrections have been made. The available evidence suggests that typical color corrections are not sufficiently large, for instance, to change the reflectivity curve type classification presented in Chap. IV.

---

* The earliest published photoelectric photometry of asteroids (Giclas, 1950; 1951; 1952) yielded color indices which reddened with phase by 0.003 mag/deg for 9 Metis and 0.002 mag/deg for Vesta. Giclas observed in filters centered at 0.375μ and 0.5μ.

B. VARIATION OF COLOR WITH ROTATION

I have compared multiple observations of asteroids made during the same observing run in an attempt to identify rotational variations. No attempt has been made to compare data taken at time intervals longer than a few days, however, due to uncertainties in rotation period, orientation of axis, and the possibility of confusion with a phase angle effect. Since these results are merely a by-product of the main program, there are several limitations to the interpretation: (1) some observing modes required more than an hour between 1st and 24th filter, so any appreciable light-curve changes due to rotation during that interval could produce incorrect reflectivities. Few of the asteroids with measured light curves have sufficiently large amplitudes and rapid rotation for this to be a problem. (2) Without a simultaneous measurement of the light curve, it is difficult to know if I am observing the most significantly different sides (e.g. near maxima or minima). (3) I have poor coverage. For many asteroids both sides were not examined and for no asteroid are there two observations each of two differing sides. (4) Counting statistics on individual runs are frequently low, and systematic effects due to sky conditions cannot always be ruled out.

The following descriptions of possibly real rotational variations should be regarded as indicative only. They should spur further study of those asteroids which seem to show variations, and others as well.

43 Ariadne -- A large apparent discrepancy between two runs on the night of January 7 cannot be readily explained in terms of known sources of error. If real, the effect is very large and the change took place in a surprisingly, but not impossibly, short fraction of its reported $11\frac{1}{2}$ hour rotation period.

6 Hebe -- This is perhaps my most significant positive observation. There were three separate runs on three nights, with two runs showing one side and the third showing an approximately opposite side. The equivalent difference in B-V is 0.06 mag., with the trend changing throughout the 0.3 to 0.9 micron range. This observation is particularly significant in view of Matson's (1971, personal communication) report of rotation-correlated changes in thermal flux by a factor of three! Perhaps his observations can be explained by a large albedo -- and perhaps color -- difference across the asteroid. The color variation could sometimes be far greater than that I observed, since Hebe's pole was strongly tipped toward earth during my runs; Matson observed with the axis more perpendicular. There may be sufficient data on light curves now (Ahmad, 1954; Yang et al, 1965; perhaps Gehrels and Taylor as referenced by Gehrels, 1970) to permit accurate spin determination and correlation with the observations reported here and by Matson.

68 Leto -- There are probable or possible differences between mean reflectivities for the separate nights and between separate runs during each night. These would imply large color differences on the surface or a fairly rapid rotation period. It should be noted, however, that Leto was quite faint during these observations.

16 Psyche -- I explicitly searched for rotational differences on October 11. The counting statistics are low, but there may be real differences (see Fig. 6-1). Data were averaged over durations no longer than 15 minutes so there is no spurious effect due to the light-curve. Successive averages are approximately 120° apart on the asteroid. The filled-circle reflectivity is the flattest and occurs on a side probably appreciably brighter (near the normalizing wavelength, 0.57 microns) than for

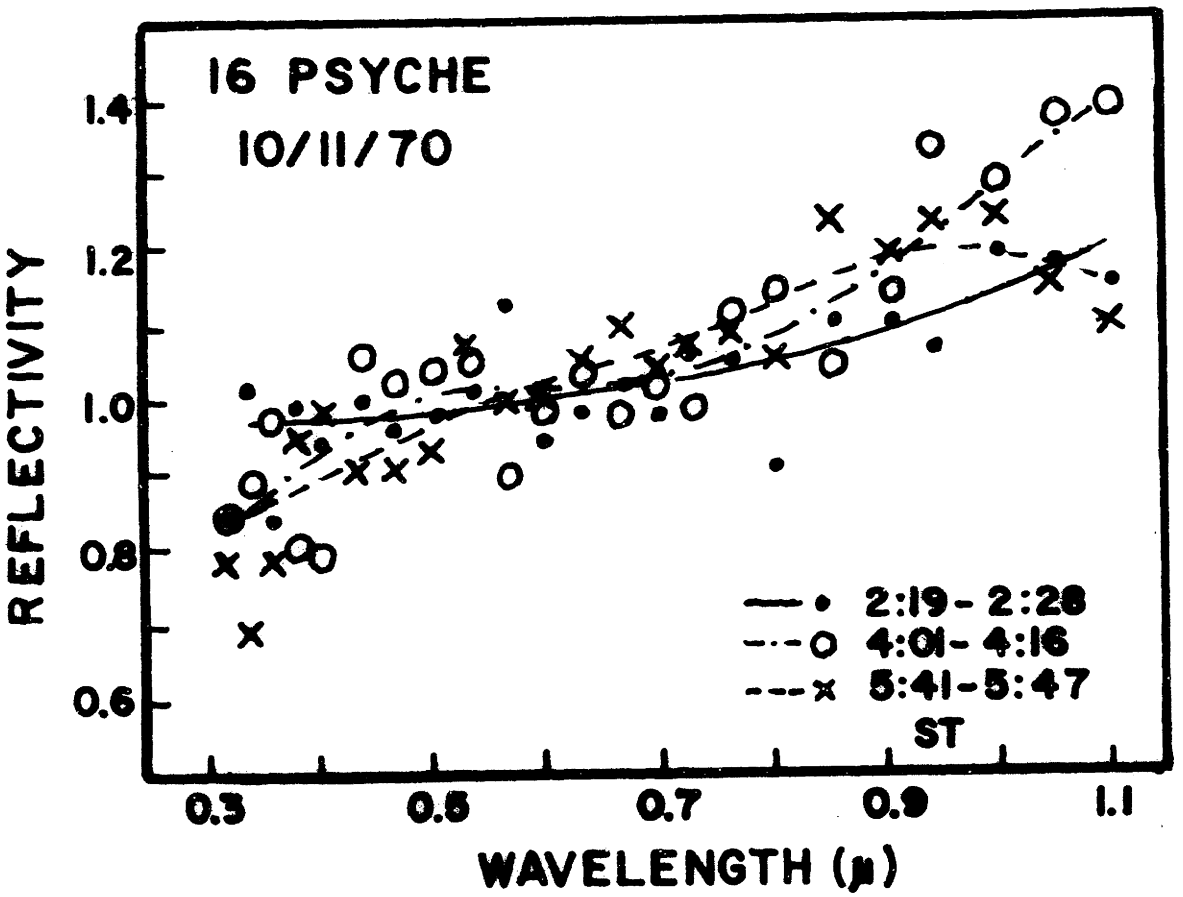
16 PSYCHE
10/11/70
REFLECTIVITY
1.4
1.2
1.0
0.8
0.6
0.3
0.5
0.7
0.9
1.1
WAVELENGTH (μ)
2:19 - 2:28
4:01 - 4:16
5:41 - 5:47
ST

Fig. 6-1

the other two averages. The open circles may show a significant IR rise; the crosses show a possible UV fall-off. Although these conclusions are statistically marginal, I include them here more to illustrate the technique than to prove a real effect on Psyche.

93 Minerva -- Data taken on two successive nights look substantially different. This may be a rotational effect or due to other problems.

10 Hygiea -- Opposite sides of this asteroid were observed. Rotational differences may partly account for large color differences (up to 0.08 mag. B-V), but there were other problems with these data so the reality of the effect is uncertain.

In conclusion, there are suggestions -- some quite strong, others weak -- that some asteroids show significant differences in reflectivity on different sides. One previous positive case has already been reported for Vesta (Bobrovnikoff, 1929; Gehrels, 1967; Chapman et al 1971b). Several asteroids I observed showed no prominent color variations. In view of the possible relevance of such color differences to interpreting regolith development on asteroids, fragmentation of differentiated asteroids, etc., more work is certainly warranted. Simultaneous light curves should be obtained in the future.

CHAPTER VII

SURFACE COMPOSITIONS INFERRED FROM SPECTRAL REFLECTIVITIES

A. INTRODUCTION

Of the knowledge of asteroid surfaces that can be derived from telescopic observations, perhaps that of mineralogy has most far-reaching implications. McCord *et al* (1970) have demonstrated how fruitful mineralogical interpretations of asteroid spectrophotometry can be. In the case of the 31 additional asteroids which I have measured, the task is somewhat more difficult, partly because of the less definitive measurements possible in this reconnaissance survey, and partly due to intrinsic properties of the spectral reflectivities of most asteroids.

Before discussing the compositional implications of the reflectivities, it is appropriate to ask whether or not we are truly observing *surface reflectivities*. Due to their low surface gravity, it is inconceivable that asteroids possess atmospheres sufficiently thick to produce absorptions. But it is not inconceivable that one or more of the observed asteroids -- particularly those with orbits of large semi-major axes *a* -- are in fact comets, with weak comas that have not been recognized. Marsden (1970) has shown that it is very unlikely that dead comets *become* asteroids; but that it is by no means unlikely for some comets to temporarily *look* like asteroids. It seems very unlikely that the relatively bright ring asteroids that I have observed could be such asteroidal comets; but, for the record, I note that none of the observed reflectivities show significant superimposed peaks which correlate with CN or C_3 emission (the most common features in cometary spectra at large *a*; cf. Wurm, 1963). The

possibility that asteroid reflectivities indicate surface compositions (e.g. dirty ices) which might be compatible with completely "dead" comets is briefly discussed later.

B. PRINCIPLES OF COMPOSITIONAL IDENTIFICATION

The process of identifying a mineral or rock from its spectral reflectivity curve can be broken into two parts. The most diagnostic features in the curves are absorption bands, the center positions of which are often precise indicators of mineralogy. But there are few bands in the visible spectral region and ambiguities sometimes arise, particularly in cases of mixtures of more than one mineral. General shape and slope of the reflectivity curve can then be used to sort out the ambiguities. Although curve shape alone is not very diagnostic, when it is used in conjunction with band measurements the combination can be very powerful.

Band Positions

Burns (1965) and other workers have measured precisely the absorption bands, along the several optical axes, for some common mineral crystals, and have explained the origin of the absorptions in terms of crystal-field theory. Many of the bands which occur in the 0.3 to 1.1 micron spectral region arise from transitions of the d-shell electrons of various transition element ions, notable iron, within the crystals. The band positions vary among minerals due to different distortions of these shells with the ions in different coordinations. Burns described a functional relation between band position and mineralogy in some of the most common mineral series, including orthopyroxenes and olivines. Adams (1971, in preparation) has extended this work to observing a shift in position of the Fe^{2+} 0.9 micron band in diffuse spectra of pyroxenes up to about

1.0 microns (and similar shifts in a 2 micron band) as one moves from enstatite to the more iron- or calcium-rich pyroxenes.

Much of the light reflected from a rocky or powdery surface is transmitted through crystals so the absorption features show up in reflection spectra. A large sample of laboratory spectral reflectivities for common terrestrial minerals has been published by Hunt and Salisbury (1970a; 1970b) and Hunt et al (1971; 1970). The positions of bands in these spectra, and in measurements by others (e.g. Adams, unpublished), generally agree well with the results of single-crystal measurements and with the expectations of crystal-field theory; when they do not, the mineralogical characterization of the laboratory sample has been found to be at fault.

Reflectivity spectra of mineral assemblages and rocks show bands due to the component minerals. Some progress has been made in understanding how the combination spectrum is derived from the components -- the variables are the relative opacities of the mineral grains and how well they are mixed (see below).

Curve Shapes

There is a less rigorous understanding of the compositional implications of general slopes, inflection points, and other non-band characteristics of transmission and reflection spectra. Many minerals are known to be reddish due to deep UV charge-transfer absorptions, the wings of which extend through the visible to different degrees for different minerals.

The slopes of reflectivity curves are appreciably affected by compaction, phase angle, and especially particle size and opacity (Adams and Filice, 1967). In cases where these characteristics of a surface are unknown, the compositional implications of slopes become obscured. The

spectral reflectivity catalogs of Hunt et al show curves for samples of different particle sizes.

Although their origins are not well understood, some bends and inflections in spectra of minerals and rocks are fairly repeatable and provide some diagnostic help. The reflectivities for a variety of terrestrial rocks published by Ross et al (1969) show some differences between rock groups.

C. PROBLEMS IN APPLICATIONS TO ASTEROIDS

Compared with the scientist trying to interpret reflectivities of terrestrial regions taken from airplanes or satellites, the astronomer is at some disadvantage for several reasons: (1) Asteroid albedos are poorly known, if at all; hence in principle we cannot distinguish a clean white snow from carbon black, if both have the same spectral characteristics. (2) The crystal minerals of the earth are only a small subset of those which may be present in the asteroid belt. The minerals observed in meteorites may be far from a complete sample, and even an adequate catalog of meteorite reflectivities has yet to be made. We must consider the possibility that asteroid surfaces contain not only silicates, but metals, ices, and perhaps very exotic compounds. (3) Several processes associated with hypervelocity impact may have important effects on asteroid reflectivities. These include shock, vitrification, and the textural development of regoliths and breccia lenses on low-gravity surfaces (see Chap. VIII).

If asteroids were composed of single minerals, there would be no difficulty in assigning unambiguous identifications. But if meteorite mineralogy is any guide, we may expect some asteroids to have mixtures of

minerals on their surfaces. A few general comments will suffice to illustrate the problems to expect.

It is common that trace components can dominate the spectral reflectivities of surfaces. First, there is the simple case of weighting by albedo. A small amount of sulphur on any dark background will produce a strong spectral signature of sulphur. Secondly, there is the case of opaque powders which, when mixed even in small quantities with another mineral, will reduce multiple scattering and transmission of light through the crystals of the mineral so as to diminish or remove entirely the spectral signature of the dominant mineral (cf. Salisbury, 1970). Finally, there is the intermediate case of a highly transmitting mineral being mixed with a more absorbing mineral. Whereas the more transparent mineral may show strong spectral features by itself due to long pathlength of transmitted light, the more absorbing mineral will act like opaque particles and greatly reduce the pathlength. But, the absorbing mineral may still produce a strong spectral signature of its own.

All three effects of mixtures may be important for asteroids. Many meteorites are rich in such opaques as metals, magnetite, and carbon which may swamp the spectral features of other minerals present. The existence of stony-iron meteorites, with silicate crystals well separated from each other in a metal matrix, could result in the domination of the silicate fraction in spectra due to its higher albedo. Finally, a common pair of minerals found in some meteorites is orthopyroxene (strongly absorbing) and olivine (much more transparent); measurements of such meteorites show that orthopyroxenes very largely determine the character of the spectrum, even when olivine is the dominant mineral present (Adams, 1968).

Despite these problems, there is much promise in the technique of remote-mineralogy, especially if we apply Occam's Razor and consider only the more likely mineral candidates. Before applying these techniques to the sample of 31 asteroids, I exemplify both the difficulties and the power of the technique by re-examining the work of McCord et al (1970) on Vesta.

D. THE SURFACE COMPOSITION OF 4 VESTA

McCord et al (1970) presented spectral reflectivity data for Vesta showing its prominent absorption band. They concluded that the band "arises from electronic absorptions in ferrous iron on the M2 site of a magnesian pyroxene" and that the surface of Vesta "has a composition very similar to that of certain basaltic achondrites". They argued that no gases or ices have absorption bands like that on Vesta, and that the only common mineral which does is orthopyroxene. They set limits of ± 0.015 micron on their measurement of the center of the band at 0.915 microns, and further suggested that the position might be accurate to ± 0.005 micron if one assumed band symmetry. McCord et al concluded that a magnesium-rich pigeonite was the most likely identification; some other orthopyroxenes have incorrect band positions and mixtures of orthopyroxenes and either calcic clinopyroxenes or olivines have the wrong curve shapes in the visible and UV.

The reflectivity curve for Vesta presented in this thesis (due to Johnson and Kunin, Chapman et al 1971a,b) has a relative shift for the 0.9 and 0.95 data points, yielding an apparent band position nearer to 0.95 microns. There are two reasons for the shift: (1) the raw data show some shift, though within the error bars of both runs, and (2) a

new standard-star/solar flux calibration was used which is different as a result of taking stellar lines into account. Though I feel the new calibration is superior, a realistic error bar on band position is at least ± 0.03 micron, taking into account statistical error, calibration error, and the 0.05 micron sampling interval. In view of these small changes, I have re-examined the compositional implications for Vesta.

Vesta Composition from Band Position Alone

From the band position alone, we can probably rule out pure enstatite or bronzite -- their bands are at too short a wavelength. Olivine and some calcic clinopyroxenes have bands too far in the opposite direction. Augite is close to the upper limit, but can be ruled out because its band is much too broad. A variety of less likely minerals have bands at or near the position of Vesta's band: cummingtonite, tremolite, montmorillonite, smithsonite. All bands are probably due to Fe^{2+}, though sometimes present in only trace amounts. Appropriate mixtures of enstatite or bronzite with most of the other minerals just mentioned might yield absorption bands in the correct place. But the simplest choice is an iron- or calcium-rich pigeonite, some samples of which have absorption bands near 0.94 or 0.95 microns (Burns, 1965). The magnesium-rich pigeonites, proposed for Vesta by McCord *et al* have bands which now fall near the lower error limit for Vesta.

Vesta Composition Considering the Full Reflectivity Curve Shape

McCord *et al* showed that the shape of the reflectivity curve in the visible and UV rules out mixtures of such minerals as orthopyroxenes and olivine. The reasonably flat curve in the visible, with shoulder near 0.4 microns, is characteristic of a variety of other minerals, including

some plagioclases, actinolites, diopsides, augites, and others. But some of these minerals lack IR absorption bands or would not be expected to contribute much to the spectrum of a mineral assemblage due to their high transparency. Others (such as diopside) have absorption bands which are much too wide, or secondary absorptions in the visible which are not apparent in Vesta's curve.

It is possible that some unusual mixtures of minerals could be devised that would resemble Vesta's curve. However, by applying Occam's Razor one can easily agree with McCord et al that the eucritic composition of Nuevo Laredo or Pasamonte -- or a somewhat more calcium-rich type -- is probably the composition of the surface of Vesta. Therefore it is reasonable that Vesta's curve is also similar to the reflectivity curves of some lunar rocks (Adams and Jones, 1970) and certain fresh lunar regions (e.g. Aristarchus).

It may also be pointed out that the strong depth of Vesta's absorption band rules out the presence of much opaque material, whether lunar-type glasses, iron, or carbon compounds. This is confirmed by Vesta's relatively high albedo (Matson, 1971). Finally, Vesta's surface is certainly covered with a regolith (see Chap. VIII; also Veverka, 1970), so the comparisons with spectral reflectivities of meteorite powders and lunar regions is probably not distorted by extreme differences in particle size. Thus I conclude that Vesta's surface is probably a regolith of calcium-rich eucritic composition with predominant pigeonite.

E. MAJOR BAND POSITIONS IN ASTEROID REFLECTIVITIES

Absorption band positions (with possible errors), for all asteroids which seem to show them, are presented in Table 7-1 and in Fig. 7-1. The

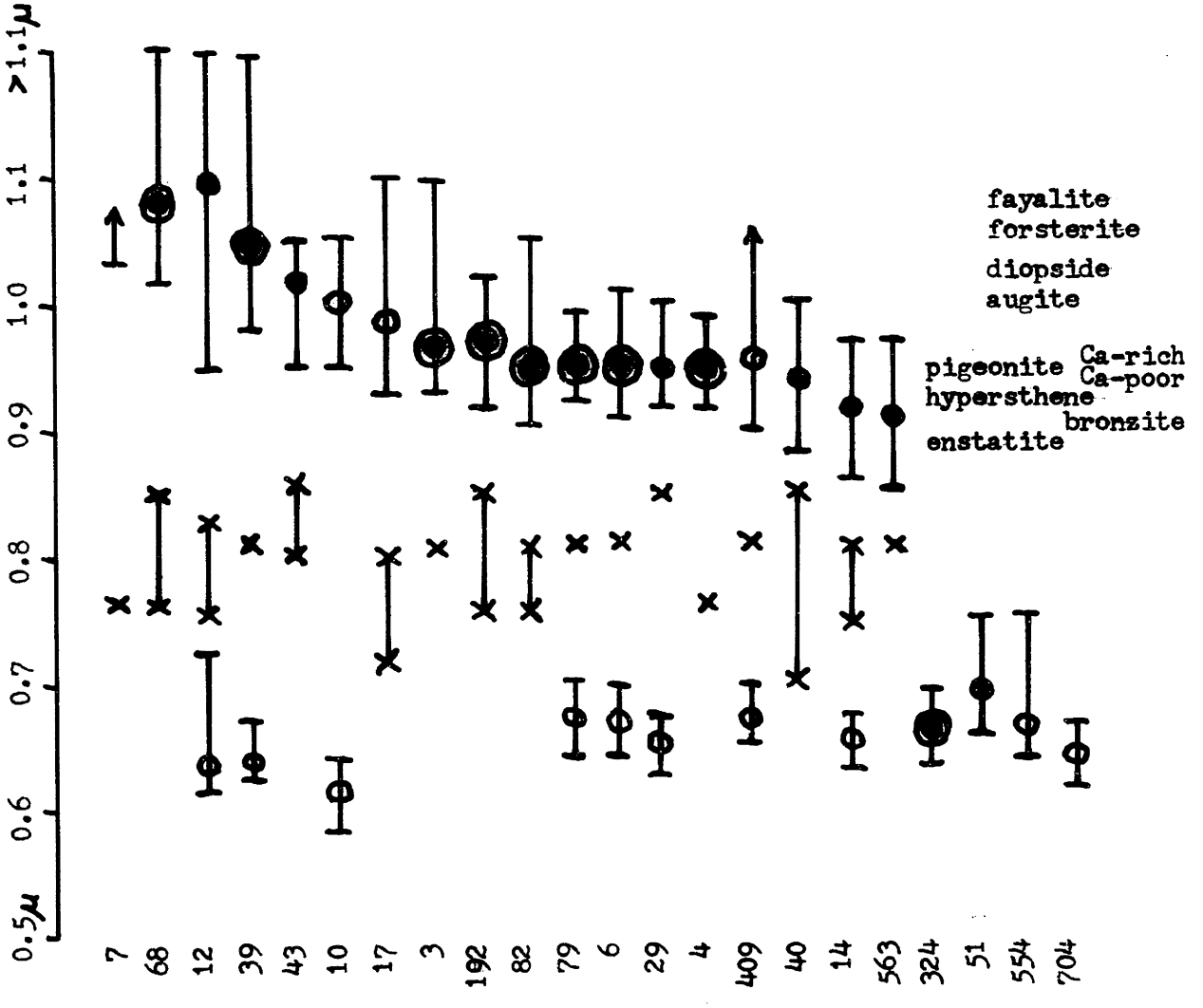
>1.1μ
1.1
1.0
0.9
0.8
0.7
0.6
0.5μ
fayalite
forsterite
diopside
augite
pigeonite
hypersthene
enstatite
Ca-rich
Ca-poor
bronzite
7
68
12
39
43
10
17
3
192
82
79
6
29
4
409
40
14
563
324
51
554
704

Fig. 7-1

confidence of the band identification is indicated both in the table and the figure. The figure also shows the band positions for some common pyroxenes and olivines known to occur in meteorites. Tentative mineralogical identifications can be made on the basis of band position alone, using two hypotheses: (1) that we are observing a single mineral reflectivity, of (2) that we are observing mineral assemblages in which more than one component contributes significantly to the band position. Subsequently I will consider other characteristics of bands and curve slopes.

Single Mineral Compositions

Asteroids 7, 12, 39, and 68 have long-wavelength bands which seem most consistent with olivine (especially fayalite), although forsterite, which is most common in meteorites, is acceptable. Diopside and even augite cannot be excluded.

Asteroids 14, 40, and 563 (whose bands are not certain), and asteroids with bands near 0.95 microns but having large error bars, could possibly be enstatite or bronzite. Hypersthene is a possibility for all asteroids with bands centered at or less than 0.97 microns, although in most cases its band is toward the short end of the error bars.

Calcium or iron-rich pigeonites have band positions closest to the centers of most asteroid bands. Only asteroids previously considered consistent with olivine are clearly inconsistent with pigeonite. Unfortunately we cannot discriminate with confidence between calcium-rich and calcium-poor pyroxenes since most bands fall near the border between the two fields and have large errors.

Table 7-1. Band Positions in Asteroid Spectral Reflectivities.

Ast. No.	Certainty	Center microns		Possible range	Comments
12	probable		1.10	0.95 - >1.10	
	possible	0.64		0.62 - 0.73	
39	certain		1.05	0.98 - >1.10	deep
	possible	0.64		0.63 - 0.67	
7	v. probable		>1.05	1.03 - >1.05	deep
43	probable		1.02	0.95 - >1.05	
192	certain		0.97	0.92 - 1.02	
40	probable		0.94	0.88 - 1.00	
79	certain		0.95	0.92 - 0.99	fairly sharp
	possible	0.67		0.64 - 0.70	
3	certain		0.97	0.93 - 1.10	broad, deep
	possible	0.61		0.59 - 0.63	
82	v. probable		0.95	0.90 - 1.05	seems deep, poor stat.
6	v. probable		0.95	0.91 - 1.01	not so deep
	possible	0.67		0.64 - 0.69	as appears
68	certain		1.08	1.02 - >1.10	deep
17	possible		0.98	0.93 - 1.10	poor stat.
14	probable		0.92	0.86 - 0.97	poor stat.
	possible	0.65		0.63 - 0.67	
29	probable		0.95	0.92 - 1.00	not very deep
	possible	0.65		0.63 - 0.67	
563	probable		0.91	0.85 - 0.97	
4	certain		0.95	0.92 - 0.98	very deep
324	v. probable	0.66		0.63 - 0.69	quite deep, narrow
51	probable	0.69		0.66 - 0.75	broad
554	possible	0.66		0.64 - 0.75	shallow
409	possible	0.67		0.65 - 0.70	
10	possible		1.00	0.95 - 1.05	shallow
	probable	0.61		0.58 - 0.64	
704	possible	0.64		0.62 - 0.66	

Mixed Mineral Compositions

Since the bands for R1 and R2 asteroids are at long wavelengths, no mixtures of short-band minerals are possible. However appropriate mixtures of orthopyroxenes with clinopyroxenes or with olivine can yield all other band positions in the range 0.91 to 1.0 microns. A large proportion of olivine is required to shift the orthopyroxene band, due to their relative opacities.

F. OTHER CHARACTERISTICS OF ASTEROID ABSORPTION BANDS

The determination of mineralogy is made less ambiguous by considering band strengths, band widths, over-all slopes, inflection points, absorption edges, additional minor bands, and so on. I examine first the more detailed characteristics of asteroid bands.

Band Strengths

Bands become weaker as a rock is pulverized, due to the increased component of surface reflections from the grains in the total reflected light. However, the effect is not strong, except at very small particle sizes. Even the 0 to 5 micron fraction of samples measured by Hunt and Salisbury (1970a) show absorption bands as deep as 20% to 30%. The weakness of most asteroid bands requires either (1) that a fair fraction of opaque material is mixed in to quench the bands or (2) band-producing minerals comprise a small fraction of the surface rocks.

Band Widths

Weak bands are relatively narrow. But if bands are scaled to the same depth, there remain intrinsic differences in width due to composition. Orthopyroxenes have the narrowest bands of most common minerals. Olivine

has much wider bands, in part due to the substantial differences in band positions for light transmitted through different crystallographic axes (see Burns, 1965). Diopsides and augites often show an extremely wide near-IR band. Available curves for pigeonites suggest they have moderately narrow bands, but not quite so narrow as for orthopyroxenes.

When absorption bands are superimposed on a general reddish-sloping reflectivity, the onset of the band at the short-wavelength side produces a relative maximum in the curve. For well-developed bands, these occur at about 0.75 to 0.8 microns for orthopyroxenes and pigeonites, around 0.7 microns for olivines, and around 0.55 microns for augites and diopsides. For the weaker asteroid bands, we expect curve maxima to be at longer wavelengths.

The wavelengths of relative maxima in the asteroid curves are plotted in Fig. 7-1. In nearly all cases these maxima are in the 0.75 to 0.85 micron range, confirming the general trend for short-wavelength bands to be narrower than the longer ones. There is a hint that the asteroids with absorptions centered at the longest wavelengths have maxima at the shortest wavelenghhs, and vice versa. The positions of the maxima confirm the earlier guess that the shorter-wavelength bands are due to orthopyroxenes or pigeonites. Furthermore, they suggest that the longer bands are probably due to olivine, rather than clinopyroxenes.

Minor Absorption Bands

Somewhat less than half of the asteroids sampled show hints of an absorption band in the 0.6 to 0.7 micron region. This feature, or others similar to it, have shown up in many of our solar system spectral reflectivities, so the question arises as to whether there is a calibration

problem. A detailed examination of the problem, including division of all asteroid reflectivities by the mean of several others, convinces me that the band is real, in at least some cases.

Though few common minerals have strong absorptions in this region, numerous transition element ions (Cr, Ni, Fe, Co, Ti) are responsible for weak bands in this region for several minerals. Some samples measured by Hunt and Salisbury (1970a) show similar weak bands which they ascribe to ferric ions. They occur in actinolites, hornblendes, and chlorites, which are not common in meteorites. Measurements of diopsides show moderately strong absorptions at these wavelengths (J. Adams and M. Charette, 1971, personal communication).

There seem to be other significant wiggles and dips in some asteroid reflectivities which, however, are too weak to interpret confidently. More data are required to verify and identify these features.

G. SLOPES OF ASTEROID SPECTRAL REFLECTIVITIES

Compositional Implications

The charge-transfer absorptions in different minerals yield different overall slopes in reflectivity throughout the visible. Some minerals, such as hydrated iron oxides are redder in color than any observed asteroids. Other minerals are similar to asteroids in this respect. Some minerals can be distinguished by the location and sharpness of the slope of the charge-transfer band. Orthopyroxenes have reflectivities with constant slopes throughout the visible, while pigeonites, clinopyroxenes, and calcium-rich plagioclase feldspars have reflectivities which are flat in the visible, but decrease sharply in the UV. The absorption edge is even sharper in many minerals containing sulphur.

The red asteroids have curve shapes like those of many chondritic meteorites, in which orthopyroxenes control the spectral features. Asteroids with curve types M3, M4, B1, and B2 (fairly flat visible reflectivity, but prominent UV drop-off) resemble the "bluest" basic and ultrabasic terrestrial rocks. Of the rocks studied by Ross et al (1969), the coarse-grained peridotites and basalts and gabbros rich in calcic feldspar (e.g. bytownite or anorthite) have reflectivities most nearly resembling these asteroids, but few terrestrial rocks are so blue when pulverized (see below).

Flat Reflectivities

Some asteroids show flat reflectivities into the UV (type B3), unlike any common terrestrial rock. Two kinds of materials tend to have flat reflectivities: highly transparent materials like ices and clear glasses, and highly opaque materials. In powdered metals, most of the incident light is absorbed (not transmitted) in a wavelength-independent fashion; what little reflected light there is resembles the incident light in spectral character. Powdered opaque materials have reflectivities which are especially dark and flat. The most likely opaque minerals one might expect on the surfaces of type B3 asteroids are nickel-iron, carbon, and magnetite. Transparent compounds are less likely to have flat reflectivities because they are prone to have impurities which give rise to strong colors, even though the materials are colorless and without absorptions themselves. Hence a "dirty-ice" is unlikely to have such a flat reflectivity, but it cannot be ruled out.

Pulverization

Pulverization of many materials changes their colors. Adams and Filice (1967) defined an R/B ratio (the ratio of reflectivity at 0.7 micron to that at 0.4 micron) and demonstrated that increasing pulverization of rocks reddened them to the point where the grains became quite transparent; further pulverization enhances surface reflections and the reddening decreases. For purposes of comparison I have tabulated approximate R/B ratios for 30 asteroids, obtained by reading off reflectivities at 0.7 and 0.4 microns (Table 7-2).

Basalts and gabbros measured by Adams and Filice have R/B values near 1.00 for coarse rocks which increase to the range of 1.3 to 1.5 for moderately small size fractions, then decrease to 1.2 to 1.3 for sizes less than 40 microns. Bulk samples of all sizes tend to look like the smallest sizes, since the dust coats the larger particles. Acidic rocks have R/B ratios of 1.6 to 1.9 which rise to 2.0 to 2.3 with slight pulverization, then rapidly diminish towards lower values as the rocks become further pulverized. The redder asteroids are redder than most pulverized terrestrial basalts and gabbros. The bluer asteroids are too blue (and evidently too dark -- Matson, 1971) to be composed of pulverized terrestrial basalt.

Albedo rises with pulverization for most common rocks. Basalts and gabbros which have albedos near 0.03 when unbroken are in the 0.2 to 0.25 range when pulverized. But while the larger asteroids seem to be dusty (Veverka, 1970) and must have regoliths (Chap. VIII), evidence accumulates that some are not only very blue but are also very dark, with albedos of less than 0.05. The only kinds of powdered materials that are so blue and

Table 7-2. R/B Colors for Asteroids.

No.	R/B	No.	R/B	No.	R/B	No.	R/B
43	1.95	5	1.61	356	1.39	93	1.15
39	1.84	68	1.58	4	1.34	10	1.11
82	1.72	3	1.57	324	1.30	704	1.09
7	1.70	17	1.54	51	1.29	13	1.05
192	1.66	14	1.50	554	1.27	21	0.99
40	1.64	6	1.48	409	1.26	2	0.95
12	1.63	29	1.47	16	1.22	1	0.94
79	1.63	337	1.42				

so black are opaques. The darkest asteroids, such as Bamberga, must have surfaces comprised largely of such opaque materials. Other asteroids can be darkened and have their spectra flattened sufficiently by relatively minor fractions of opaques.

Adams and Filice also demonstrate that rock powders redden with phase angle up to about 30° or 40° phase angle, due to increased optical path length in the powders enhancing the volume component or reflected radiation; at still larger phases they become bluer as the surface component starts to dominate. These color changes are small compared to the effects of particle size, but they have been measured for asteroids (Chap. VI). Some asteroids seem to become bluer with phase even at small phase angles, which may also be understood in terms of a high proportion of opaques (Chap. VI).

The question was asked in Chap. V whether or not regoliths can be bluer than unbroken rock of the same composition. It may be possible by addition of opaques in a special manner. Some meteorites, such as

pallasites, contain silicate crystals imbedded in an iron matrix. An unbroken sample would show a spectrum largely determined by the high-albedo colored silicates, with the metal matrix simply lowering the overall albedo of the rock. But if such a material were pulverized, the metal grains would effectively coat the silicate grains, flattening and (if the silicate is red) bluing the spectral reflectivity.

Shock, Vitrification, and Other Factors

Asteroid surfaces are in an environment of repeated hypervelocity impacts. They might be heavily shocked, so it is of interest to consider the effects of shock on reflectivity curves. Experience with lunar rocks (subject to higher impact velocities than asteroid surfaces) and with meteorites (more likely to have been shocked than typical asteroids because of accelerations required to get them to earth) suggests that the effects are not important, at least in so far as band positions are concerned. But Adams and Jones (1970) warn of the possibility that band positions might be changed by shock, and there is even more reason to guess that heavy shock might affect colors in view of the extreme darkening of heavily shocked meteoritic olivine crystals. But laboratory work has yet to be carried out on the reflectivities of shocked minerals.

The lunar surface is extensively vitrified, with small glassy materials making up a large fraction of surface fines. These glasses are highly colored, probably due to metallic ions, and give rise to a very reddish color to the lunar maria. Glasses appear to be caused only by impacts exceeding 10 km/sec (Hörz et al, 1971), so one expects a relatively smaller proportion of micro-meteoriod-produced glasses on asteroids than on the moon. Glass formed by unusually high-velocity impacts will be eroded off most asteroid surfaces by less energetic impacts before it can

collect (see Chap. VIII). The absence of lunar-like red colors for asteroids suggests that the vitrification process is not important on asteroids, but it cannot rule out comparatively colorless glasses produced by impact on a surface with a different mineralogy than that of the lunar surface.

The large rate of net mass-loss from asteroids (Chap. VIII) precludes appreciable contamination of asteroid surfaces by other kinds of meteoritic or asteroidal material. Thus the surfaces we are observing should be representative of the surface layers of each individual asteroid. This supposition is confirmed by the variety of different spectral reflectivities observed.

H. SUMMARY OF PROBABLE ASTEROID SURFACE COMPOSITIONS

Before listing some probable compositional identifications for the various spectral reflectivity curve types, a number of qualifications should be discussed. First, I accept the probable results of Chap. VIII that most asteroids studied here have regoliths and powdery surfaces; hence, no effect of particle size differences will be considered. Secondly, I showed in Chap. V that there is no correlation between color and the orbital elements which would imply differences in impact environment. Therefore, I assume no color differences due to shock or vitrification of surface materials. The only factors I consider are mineral composition and percentage of opaques. The latter can be considered only qualitatively until laboratory measurements are made.

In suggesting probable identifications, I assume that the simple straightforward explanations are correct. My suggestions are guided by, though not based upon, the known mineralogy of meteorites. Exotic

materials will not be considered. Speculations concerning surface compositions based largely on asteroidal models rather than on diagnostic reflectivity curve characteristics are saved for Chap. IX. Other investigators with hypotheses concerning the chemical evolution of the asteroid belt are free to reject my suggestions and to compare the reflectivity curves of Appendix I with published catalogs of minerals they might expect to find in the asteroid belt.

As further warning, let me exemplify the ambiguities which arise. A variety of hydrated or altered minerals have been suggested as likely forming in the outer parts of the asteroid belt during the late stages of cooling of the solar nebula (Larimer and Anders, 1967). Reflectivities for three of them -- magnetite, serpentine, and montmorillonite (the last two of which have been shown by Bass (1971) to be the dominant mineral constituents of the Orgueil meteorite) -- agree reasonably well with B, M, and R type asteroids, respectively. Reflectivities of minerals like montmorillonites are variegated, depending considerably on the nature of the minerals from which they are derived, so the prominent reddish slope and deep 0.95 micron absorption feature for one published by Hunt and Salisbury (1970a) may not resemble any hypothetical asteroidal montmorillonites. Also, these minerals are usually found all together in meteorites -- in carbonaceous chondrites -- for which one expects relatively feature less reflectivities due to carbonaceous and other opaque materials. But if someone finds reason to hypothesize the existence of asteroids of pure montmorillonite, magnetite, and serpentine, he will find a good first-order separation among the reflectivities presented in this thesis. With that extreme example in mind, I proceed to more plausible interpretations of the asteroid reflectivity curve types.

Group R1 and R2. The long-wavelength bands seem to be chiefly due to olivine, although the bands are not very deep. Asteroid 68 Leto is less red and its band is broadened toward shorter wavelengths; it could have an appreciable admixture of pigeonites or clinopyroxenes.

Group R3A. The bands and steep reddish slope in the visible are most consistent with mixtures of orthopyroxenes (hypersthene) and olivines. The band positions for pigeonites and some clinopyroxenes are a slightly better match but they are ruled out by the steep slope in the visible.

Groups R3B, R3C, and R4. These groups cannot be dominantly pigeonite or clinopyroxene for the same reason as R3A; but an admixture of them along with olivine and/or orthopyroxenes might explain the less steep reddish slope. A more likely explanation is that they are of orthopyroxene/olivine composition but with a larger percentage of opaques, which would reduce the slopes and reduce the band intensities, as observed. This is especially likely for 29 Amphitrite which has a greatly weakened band and a greatly reduced slope, but without the bend characteristic of pigeonites or clinopyroxenes. A predominance of calcic plagioclase might cause a less red, but somewhat bent reflectivity, but it would have to be present in very large proportions.

16 Psyche. The overall shallow, reddish, flat slope of the reflectivity curve for Psyche is similar to that for pulverized terrestrial basalts. However, the absence of a UV fall-off suggests Psyche more resembles Group B3, although the explanation for the difference in slope is unclear. A ground but solid nickel-iron octahedrite measured by Watts (1966) has a reflectivity similar to Psyche. No definitive identification is possible.

Group M2. The cause of the 0.6 - 0.7 micron band is not known. But no reasonable origin of the band seems consistent with the extremely low

albedo reported by Matson (1971, personal communication) for 324 Bamberga.

Vesta. This large asteroid was re-analysed earlier in this chapter. It is likely of eucritic composition, with predominant calcium-rich pigeonite and a relative absence of opaques.

409 Aspasia. This asteroid could perhaps be similar to Vesta, but it apparently lacks the strong absorption band. There is some resemblance to diopside.

Groups M4, B1, B2. These look like unpulverized basic basalts, diabases, etc. Similar rocks, with even higher percentages of opaques, are likely identifications. There are no diagnostic absorption bands. The UV drop-off rules out metals and other opaques as sole constituents.

Group B3. These asteroids most likely have surfaces composed of metals or other opaques. Less likely, but possible, are pure ices, which would have to be mixed with a large percentage of black material to yield sufficiently low albedos.

Group B4. Asteroid 21 Lutetia has an unusual spectrum. Its coloration suggests it is not composed of opaques, but of something which is truly bright in the UV and in the IR relative to the visible.

I. COMPARISONS WITH METEORITES

Because of the wide interest in possible connections between asteroids and meteorites, I now compare asteroid reflectivities with what is known about meteorite reflectivities. Unfortunately very few reflectivity curves for meteorites have been published. The majority of those that have cover just the visible portion of the spectrum.

The most extensive study of meteorite colors is that of Sytinskaya (1955) who later related them to asteroid colors (Sytinskaya, 1965). He published albedos and color indices for both the interiors and crusts of 83 meteorites, apparently of whole rock samples at a moderately large phase angle.* It is uncertain to what extent the samples were free of rust and other impurities -- there are certainly a wide range of colors for meteorites of the same class and albedo. In general, the H chondrites are the reddest, followed by L chondrites, achondrites, olivine-pigeonite chondrites, amphoterites, and carbonaceous chondrites (types II and III), in that order. There are only a few samples of all but the H and L chondrites. The achondrites consisted of 3 howardites, 3 eucrites, 1 aubrite, and 3 diogenites. A single octahedrite was quite red and a single pallasite even redder.

Watson (1938) measured the spectral reflectivities of 8 meteorites in the visible only. A Canyon Diablo iron and the bronzite and hypersthene stones appeared reddish, especially those with rust specks visible. A type II carbonaceous chondrite was slightly bluish, and a brecciated chondrite grey. Watts (1966) measured two meteorites from 0.25 to 0.7 microns; the Colby (Wisc.) hypersthene chondrite shows a curving reddish reflectivity while a Canyon Diablo octahedrite has a flat but somewhat reddish reflectivity.

The only published reflectivities of meteorites which extend into the infrared are those of John Adams (Adams, 1968; McCord et al, 1970). They

---

* I have not had the complete 1955 article translated. However, M. Gaffey has kindly transliterated the names of the 83 meteorites and found their classifications in meteorite catalogs.

are of powders of two hypersthene chondrites, a bronzite chondrite, and a eucrite. The 0.9 micron band in the bronzite is only about an 8% feature compared with the 15% to 20% bands in the hypersthenes and the 35% band in Nuevo Laredo. This is consistent with a possible quenching due to progressively more free iron in the hypersthene and bronzite chondrites.

The following brief discussions of meteorite classes are based on the little available laboratory work just described combined with an understanding of how spectral reflectivities arise from the mineralogy of rocks. But there is no substitute for more laboratory work. For instance, the expectation of Hapke and Wells (1970) that chondrites should be blue due to free iron is plausible but not confirmed by the several published reflectivities for meteorites.

Chondrites

Enstatite chondrites are nearly pure enstatite. It is unlikely that any of the asteroids (except possibly 14, 40, or 563) have bands at sufficiently short wavelength to be consistent with enstatite-rich orthopyroxene. Pure enstatite has no band at all, but a reddish slope, possibly consistent with 16 Psyche.

The 0.90 micron absorption band of bronzite should dominate the reflectivity of olivine-bronzite chondrites, which are composed of approximately equal proportions of both minerals. Adams' (1968) measurement of Richardton shows the band at 0.90 microns. Hence only 14, 40, or 563 are possible matches; their only moderately reddish slopes might be consistent with the higher iron content of these H-type chondrites, but the laboratory measurements discussed above suggest bronzites are quite red.

The measured olivine-hypersthene chondrites (L-type) show bands near 0.93 microns, very near the 0.92 micron center for hypersthene alone, despite the preponderance of olivine in these meteorites. However, the band is noticeably broadened toward longer wavelengths. Holbrook (R/B = 1.55) is a reasonably good match for most R3 and R4 asteroids of moderate slope; Ladder Creek is much redder. Both hypersthene chondrites measured have bands deeper than shown by most asteroids, however.

Olivine-pigeonites (carbonaceous chondrites type III) are a very plausible class to associate with reddish asteroids, but no laboratory reflectivities are available. Such meteorites are predominantly olivine, with small amounts of pigeonite, and some carbonaceous material. They might show a reddish reflectivity, perhaps somewhat bent, with relatively shallow bands near 0.95 microns.

Carbonaceous chondrites (Types I and II) are composed of such altered minerals as montmorillonite and serpentine, with tarry hydrocarbons. Type II have chondrules of olivine or enstatite composition. It is likely such meteorites have fairly flat reflectivities, but laboratory measurements are needed.

Achondrites

Nickel-iron is largely absent from achondrites, so we expect brighter colors and stronger bands. Vesta is the only obvious identification -- it has a band near that measured for Pasamonte and looks similar to Nuevo Laredo, both eucrites. Diogenites are nearly pure hypersthene, which has a band at too short a wavelength to be the best fit for most asteroids; also the asteroid bands are quite weak. Howardites contain more opaques than either eucrites or diogenites, and are chiefly hypersthene and calcic

plagioclase. If the hypersthene controls the reflectivity, similar comments hold as for diogenites. But if the bands are quenched by the opaques, howardites may resemble asteroid types M4, B1, and B2. The same comments hold for aubrites as for enstatite chondrites.

Chassignites are nearly pure olivine which has a band stronger than observed for type R1 and R2 asteroids. Perhaps the added opaques from the metal matrix of a pallasite would improve the match. Asteroid 409 might look like a nakhlite, which is mostly diopside with some fayalite-rich olivine. There is no clear asteroid comparison for angrites which are nearly pure augite. The dark, heavily shocked ureilites have intriguing asteroidal possibilities, being composed of olivine, clinobronzite, and nickel-iron; laboratory measurements are needed.

Stony-Irons and Irons

Pallasites have already been discussed. Laboratory measurements are also needed for simulated regoliths of siderophyres, lodranites, and mesosiderities, although the silicate portions for most representatives are composed of minerals with bands centered toward the short-end of the asteroid band-center error bars. The nickel-iron meteorites must, of necessity, look flat if finely ground and should resemble type B3 asteroids.

J. CONCLUSIONS

I cannot delve as deeply into asteroid mineralogy as I hoped at the outset of this project. Vesta's prominent band is unique among asteroids so far surveyed. Higher counting statistics and better calibrations are necessary before the weak bands present in most asteroid curves can be measured to the precision required for unambiguous identification. The confidence of identifications will also be increased once complete rock

and meteorite reflectivity catalogs are produced. I believe the results presented in this chapter justify optimism concerning the future usefulness of this remote-sensing technique.

It is clear that some asteroids are composed of silicates, rich in pyroxenes and perhaps olivines, while others have high percentages of opaque powders. The variety of spectral reflectivities found among asteroids is very similar to the variety among the different meteorite classes. Several asteroids have unusual features in their reflectivities, however, which require further study.

CHAPTER VIII

ASTEROID REGOLITHS

A. INTRODUCTION

The question of whether or not asteroids have regoliths -- fragmental surface layers produced by repeated, superimposed impacts -- is a sub-topic of the general field of the fragmentation and evolution of the small-body population in the solar system. I do not intend a complete examination of even the sub-topic, though it has not been studied in detail before. I will chiefly address the question of whether or not asteroids have regoliths which would appear dusty as detected by polarization observations (Veverka, 1970) and of the sort that would influence the slope of spectral reflectivities.

What is Known About Asteroidal Fragmentation

The approximate power-law form of the size-frequency relationship for asteroids has been determined most recently by the Palomar-Leiden Survey (van Houten et al, 1970). But large uncertainties remain. First, there are normalization problems with the Survey, with at least one major revision since publication. Secondly, only magnitudes are known for asteroids and if there are correlations of albedo with size, the derived power-law will be wrong.

The physics, evolution, and stability of the asteroid population have been investigated by many authors from Piotrowski (1953) to Dohnanyi (1971). Asteroids are probably only modestly fragmented at large sizes

(Anders, 1965) but completely so at small sizes.* Rocky materials are more "fully fragmented" than is iron. The mass-loss mechanism for asteroids of any size is chiefly by catastrophic collision with smaller bodies (but no smaller than about 1/100th of the mass) rather than by collision with bodies of similar size or by progressive erosion of the surfaces by very small particles. The root-mean-square impact velocity for particles with orbits distributed like those of the visible asteroids is about 5 km/sec.

Mass-Wasting from Airless Bodies: Discussion of a Paper by Marcus

In a most interesting though speculative paper, Marcus (1969) discusses accretion and erosion on airless bodies in an environment of hypervelocity impacts. He applies to the problem the meager amount of available laboratory data (Gault et al, 1963) concerning the percentage of mass ejected at various velocities from a specified hypervelocity impact. On an airless body, the degree to which the impact velocity is much greater than escape velocity from that body determines the rate of net mass loss. For impact velocities due mostly to the self-gravity of the body, there is no net mass loss; for impact velocities much greater than escape velocity, most of the ejected mass is lost. Since the ratio of ejecta mass to projectile mass at 5 km/sec is of the order of 20,000 for unbonded sand and 500 for dense, strong basalt, the rate of mass loss from most asteroids can be very large. Even the largest asteroids, with V_{esc} of the order of $\frac{1}{2}$ km/sec, probably show net mass loss, although they could be close to equilibrium if they had rocky -- rather than fragmental --

* A particle distribution evolving in a fragmentation process is said to be "fully fragmented" when its population index has reached a steady-state value. This is discussed later.

surfaces. (Regolith development processes on Ceres are probably similar to those on the moon, which is known to be losing mass. Ceres' lower escape velocity is largely off-set by the lower average impact velocity for incoming debris.)

Gault (personal communication, 1970) has criticized Marcus for over-interpreting his laboratory data. But he does not complain they were misinterpreted. Certainly extrapolations to asteroidal and planetary scale are insecure since most mass loss is due to large-scale impacts, not the more frequent laboratory-scale sand-blasting type of impacts (see below). But we can certainly accept Marcus' results to order-of-magnitude accuracy.

The heart of the problem for Marcus -- and for other reasons our problem in this thesis -- is whether or not asteroids have rocky or fragmental surfaces. Marcus writes:

> At best, only a few of the largest asteroids might be growing by accretion -- if they have rocky surfaces. All of the smaller asteroids... must surely be suffering erosion. The erosion is extremely rapid if the asteroids have sandy surfaces. In fact, it is difficult to see how initially rocky small asteroids could ever acquire a sandy surface, since all of the ejecta from an impact is thrown off the asteroid. Initially rocky asteroids must therefore still have rocky surfaces... Only initially sandy asteroids can be expected to have sandy surfaces at present.

I have two criticisms of the sentences quoted. (1) Even if large asteroids had rocky surfaces, how could they remain rocky while accreting? Without some lithification process, any material accreted would presumably create a fragmental regolith. The asteroid would then be subject to the greatly increased erosion from impacts on the regolith. I conclude that all asteroids are losing mass. (2) Also, I find it hard to see why the

initial state of an asteroidal surface must be sandy in order for the surface to be sandy now. If an asteroid can retain a sandy surface, then surely an initially rocky surface will be converted to "sand" and will remain fragmented.

B. THE ANALYSIS

Definition of Population Index

I will discuss the incremental size-frequency distribution for particles

$$N = a D^{b} \qquad (1)$$

where N is the number of particles of diameter D (meters) per m^2 per m diameter increment. The exponent b is a negative number; its absolute value is usually called the population index and is the slope of a log N vs log D plot. The cumulative population index is (b+1). Mass-frequency relations are often discussed, both cumulative and incremental; the cumulative mass exponent is derived from the cumulative size distribution by dividing by 3. Table 8-1 lists some important population indices (see Alfven and Arrhenius, 1970, parts 3.8 and 3.9, for a concise summary).

Table 8-1. Population Indices.

Diameter		Mass	
Incremental	Cumulative	Incremental	Cumulative
3	2	1.67	0.67
3.5	2.5	1.83	0.83
4	3	2	1
5	4	2.33	1.33

I will examine the regolith problem from the standpoint of crater diameters rather than impacting particle diameters. I use A and B to replace a and b when discussing crater populations (craters per m^2 per

m diameter increment). In order to compare the results with data on particle populations, I assume that an impacting particle produces a crater 20 times its own diameter, which is typical; hence B = b. Actually a given crater distribution is produced by particles with a slightly larger population index, but the difference is not important in view of observational uncertainties in particle population indices.

Particle Mass Distributions

Observations bearing on the mass distribution of space debris over the mass range 10^{-14} to 10^{22} g come from diverse sources; estimates vary by several orders of magnitude in the mass ranges of interest. Simplified representation of the frequency relation for particles impacting on the moon is shown in Fig. 8-1 (adapted from Whipple, 1967, and Hörz et al, 1971).

At large masses, the population index (cumulative mass) is about 2/3 which is known to be a stable asymptotic solution at large sizes for catastrophic fragmentation (Hellyer, 1970). Known terrestrial fragmentation processes yield such a population index (Hartmann, 1969a).

At lesser masses, the population index increases to values approaching 1.3. A steepening to 0.83 for smaller asteroids is predicted by Dohnanyi (1971) and Hellyer (1970), but still larger values are not expected in these derivations. Part of the increase in small particles of centimeter sizes in the earth's environment may be due to particles spiralling in from the asteroid belt due to the Poynting-Robertson effect. This probably cannot explain the entire effect. A current model for the particle distribution in the asteroid belt (Kessler, 1970) has a population index of 0.84 with the frequency tied to visible asteroids at the

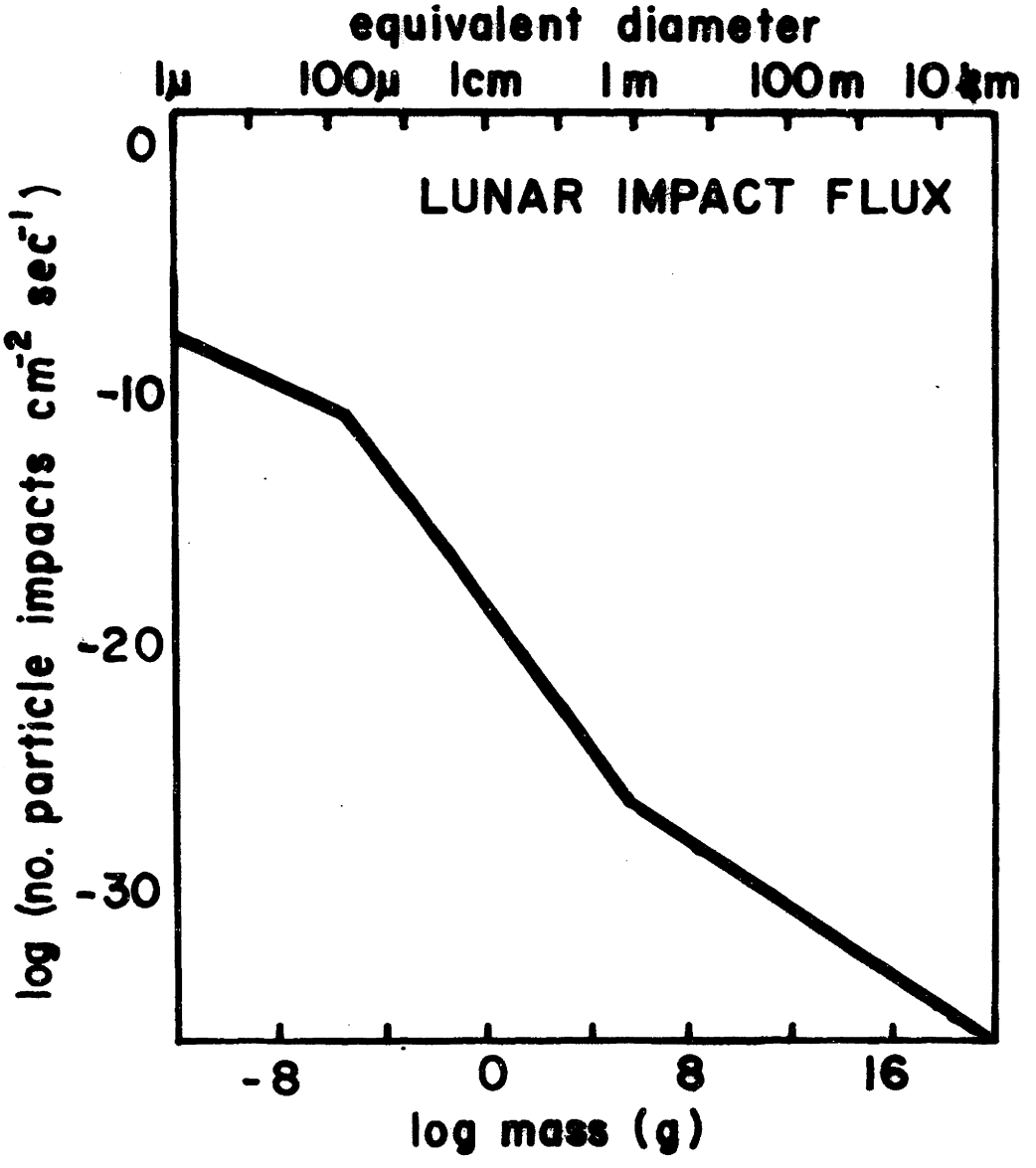
equivalent diameter
1μ
100μ
1cm
1m
100m
10km
LUNAR IMPACT FLUX
0
-10
-20
-30
log (no. particle impacts cm⁻² sec⁻¹)
-8
0
8
16
log mass (g)

Fig. 8-1

large end and continued as a straight line to a 10^{-9} gram cut-off required by the brightness of the gegenschein. There is no observational justification for the constant population index in the mass-range where the terrestrial debris steepens; it derives solely from Dohnanyi's theory. The gegenschein observation can also be accounted for by a steeper population index and larger cut-off.

It is beyond the scope of this chapter to derive a new fragmentation model; but in view of the importance to regolith formation of both the population index and a small-mass cut-off for particles, a brief discussion is warranted. An important part of the fragmentation process is creation of small particles by surface erosion (cratering) of larger ones. This has been explicitly ignored by Hellyer and has probably been effectively ignored by Dohnanyi. Dohnanyi includes an erosional term but concludes that its effect can be ignored compared with catastrophic collisions; however, he adopts a population index for his erosional comminution law which is identical to that for his catastrophic-collision comminution law (0.8). But it is well-known that the comminution law for particles created by hypervelocity cratering events on semi-infinite targets is usually in the range of 1.0 to 1.2 (Shoemaker, 1965; Walker, 1966; Chapman, 1968; Hartmann and Hartmann, 1968; Hartmann, 1969a). Such a particle distribution for impact debris often extends orders of magnitude in size, though geometrically limited to a small-size cut-off. For particle sizes many orders of magnitude smaller than the largest asteroids, there may well begin to be a significant contribution to the particle size distribution by such cratering debris with a much larger population index than the value adopted by Dohnanyi.

What are reasonable estimates for the population index and the small-size cut-off? Wetherill (1967 a) concluded that the incremental size population index is <3.4. But his conclusion must be re-evaluated in the light of several new facts: (1) Roosen (1971) has demonstrated that indeed all of the gegenschein originates in the asteroid belt. (2) The albedo of asteroidal material may be much lower than previously believed. Matson (1971) derived very low albedos for most asteroids. Also there are indirect reasons for believing that most asteroidal debris is composed of carbonaceous chondritic material, which is very dark (Mazor and Anders, 1967). (3) The scaling for the Palomar-Leiden Survey (PLS) asteroid frequencies may be as much as an order of magnitude below those extrapolated from the McDonald Survey (MDS) to smaller sizes.

Table 8-2 summarizes plausible approximate values for the small-mass cut-off (and equivalent particle diameter) as a function of cumulative mass population index (and equivalent incremental size index) for a variety of cases. I assume that there is a slope of -0.83 from the observed asteroid distribution down to either 10^9 or to 10^6 grams, below which there is a steep slope to the specified cut-off. I have used Roosen's (1971) gegenschein brightness for calculating these limits. Unlikely values are shown in parentheses or omitted.

I conclude that at medium mass ranges, the particle mass population index is at least 0.83 and could be as high as 1.2. (The comparable size population indices are 3.5 to 4.6.) At some smaller size, given in Table 8-2, the particle distribution curves over to an effective cut-off (see Fig. 8-1). This is an expected result of a variety of processes (Poynting-Robertson effect, light pressure, and electromagnetic forces; see Alfven and Arrhenius, 1970), not all of which are sufficiently understood

Table 8-2. Asteroid Belt Particle Population Small-Size Cut-off.

Source for Ast.	Break in Slope	Albedo	Population Indices (cum. mass, incr. size) 0.83, 3.5	1.0, 4.0	1.12, 4.36
MDS	10^9 g	0.07	10^{-9}g, 10μ	(10^0g, 1 cm)	-
		0.02	10^{-11}g, 2μ	(10^{-1}g, 4 mm)	-
	10^6 g	0.07	10^{-9}g, 10μ	$10^{-2\frac{1}{2}}$g, 1mm	(10^0g, 1 cm)
		0.02	10^{-11}g, 2μ	$10^{-3\frac{1}{2}}$g, 600μ	($10^{-\frac{1}{2}}$g, 6 mm)
PLS (MDS /10)	10^9 g	0.07	(10^{-14}g, 0.2μ)	$10^{-3\frac{1}{2}}$g, 600μ	-
		0.02	-	$10^{-4\frac{1}{2}}$g, 300μ	-
	10^6 g	0.07	(10^{-14}g, 0.2μ)	10^{-6}g, 100μ	$10^{-3\frac{1}{2}}$g, 600μ
		0.02	-	10^{-7}g, 40μ	10^{-4}g, 400μ

to predict accurately the cut-off size.

Asteroid Cratering

Consider a time interval T such that the frequency of 1 m diameter craters* per m^2 is $\lesssim 0.1$. As just shown, $|b| > 3.5$; therefore I certainly may assume that $|B| > 3$. Thus craters of diameters >1 m are quite sparsely scattered over the asteroid surface -- not near saturation (cf. Chapman, et al 1970). I will approximate a crater diameter/depth ratio as 3 and the volume of ejecta produced as $(D^3)/6$, of which a proportion p is

* I could choose any diameter, but the 1 m example helps visualizing the model.

scattered widely around the neighborhood of the crater (hence 1-p of it is ejected from the asteroid at greater than escape velocity). Table 8-3 gives values of p for representative asteroids; see Fig. 8-2, adapted from Gault et al (1963).

Table 8-3. Approximate Values of p for Some Asteroids.

Diameter (km)	Example	V_{esc} (km/sec)	p
3400	Moon	2.4	0.998
1200	1 Ceres	0.35	0.97
400	324 Bamberga	0.12	0.75
120	192 Nausikaa	0.04	0.25
30	82 Alkmene	0.01	0.02

The average depth d of ejecta from craters of diameters D_1 to D_2 is given by

$$d = \int_{D_1}^{D_2} p\left(\frac{D^3}{C}\right) A D^B dD = \frac{Ap}{6(B+4)}\left[D_2^{(4+B)} - D_1^{(4+B)}\right], \qquad (2)$$

$$= \frac{Ap}{6(B+4)}\left[D_2^{4+B}\right] \quad \text{for } B \gg -4 .$$

That is, for $|B| < 4$ most of the ejecta is produced by the largest craters in the diameter interval considered; in our example these are 1 meter craters. It can be shown readily that for $|B| < 4$, most ejecta is removed from a surface by large craters, not by the much more frequent small ones; but the large ones only sparsely cover the surface during time interval T, so we must rely on small craters, which do saturate the surface area, to scour away the widely-spread blanket remaining from ejecta thrown out of craters of size D_2. Saturation by smaller craters occurs for $|B| > 3$.

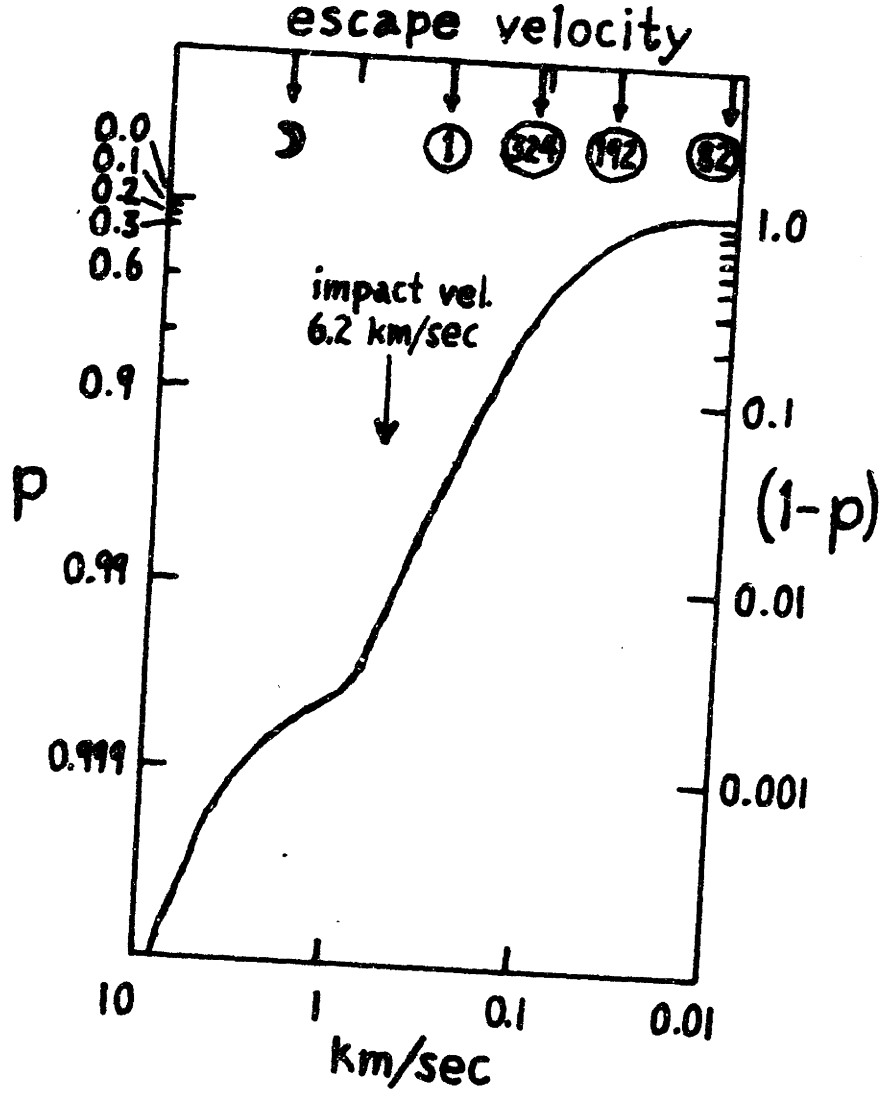
escape velocity
1
324
192
82
0.0
0.1
0.2
0.3
0.6
0.9
0.99
0.999
p
impact vel.
6.2 km/sec
1.0
0.1
0.01
0.001
(1-p)
10
1
0.1
0.01
km/sec

Fig. 8-2

Let us calculate the effectiveness of small craters in removing the ejecta of larger ones for the interesting case of $3<|B|<4$. Let us approximate the removal of a fraction (1-p) of the ejecta from the asteroid by the condition that craters of diameter 3d and larger saturate the surface during time T (these are primarily craters very near 3d in diameter because of the large population index). Such craters saturate the surface x times during T and eject from the asteroid a depth x(3d)(1-p) when

$$x = \frac{A\pi}{4(B+3)} \left\{ -\left[\frac{3Ap}{6(B+4)} \left(D_2^{4+B} \right) \right]^{B+3} \right\}, \quad B \ll -3 \qquad (3)$$

(see Chapman et al, 1970).

If x(1-p) is greater than 1, the smaller craters eject all of the larger crater's ejecta in interval T or less. If x(1-p) is very large then the removal is very efficient; it is tabulated in Table 8-4 for several values of p and B. Let us consider the implications for developing asteroid regoliths.

Table 8-4. Values of x(1-p).

B	-3.2	-3.5	-3.8
p			
0.3	0.4	0.85	1.4
0.1	0.7	1.8	4.5
0.01	1.3	5	40

(1) Assume uniform deposition around the entire asteroid of crater ejecta that is not permanently lost from the asteroid. For values of $|B| \gtrsim 3.2$ we expect a rocky surface, provided p is less than a few percent. The same is true for p as large as 10% if $|B|>3.5$. For $p>0.5$ we certainly see

a regolith unless $|B| > 4.5$. No reasonable value of B yields rocky surfaces for $p > 0.9$.

(2) Suppose instead there is a more localized distribution of ejecta around a crater, out to half of a typical intercrater distance (i.e. ejecta covers 10 m^2 in our example for 1 m craters). Then the most recent $(x(1-p))^{-1}$ of the craters of size D_2 which are formed during T will not have had their ejecta blankets removed by the end of the interval. Thus a proportion of the surface equal to $1 - (x(1-p))^{-1}$ will be rocky, but the rest fragmental. For small p and large B , large fractions of an asteroid surface will be rocky.

Size Range Validity of the Model

Whatever ejecta our 1 m diameter craters leave on an asteroid surface is rapidly removed by a smaller generation of craters for suitable values of p and B. The small craters in turn leave a portion p of their ejecta to be scoured away by a still smaller generation of craters at a rate still exceeding the ejecta production rate. Thus down to any lower size-limit for which $|B|$ is suitably large, the present model is valid. But as previously discussed, there is a cut-off in small particles at some size. With $|B| < 3$ small craters no longer saturate the surface faster than large craters, hence ejecta is not only contributed by, but also chiefly removed by relatively large craters (i.e. about the size of the cut-off). The formation of each such relatively large crater removes pre-existing regolith within its rim but spreads its own ejecta around a wide area. The steady-state depth of regolith then is of the order p/3 times the cut-off crater diameter δ. Such steady-state regolith depths are given in Table 8-5. For regolith depths similar to or less than the wavelength of

Table 8-5. Small-scale Steady-state Regolith Depths.

Cut-off crater diam. δ :	1 cm	1 mm	100μ	10μ
Equiv. particle diam. :	500μ	50μ	5μ	0.5μ
p				
0.3	1 mm	100μ	10μ	1μ
0.1	300μ	30μ	3μ	0.3μ
0.01	30μ	3μ	0.3μ	0.03μ

light, spectral reflectivities and polarization measurements will be of an effectively rocky surface; otherwise the surface appears dusty. It is not certain, however, that cratering and regolith development occurs at such tiny scales in a fashion analogous to larger scales. Hörz et al (1971) counted abundant microcraters on lunar rocks down to the 100μ size range, but we can learn nothing about regolith development at such scales since lunar rocks have no appreciable self-gravity.

A better determination of cut-off limit δ is required; but at least it seems possible that asteroid surfaces which are macroscopically rocky might have very thin dust layers of photometric importance if δ is sufficiently large. I now turn my attention to the validity of the model at very large sizes.

The model is valid only for $3<|B|<4$. Fig. 8-1 suggests that $|B|$ could be less than 3 at very large diameters, although it is perhaps unlikely in view of the studies by Hellyer (1970) and Dohnanyi (1971). Consider the double-segment frequency relation shown in Fig. 8-3. One can calculate that

$$A' = A D_2^{(B-B')} \qquad (4)$$

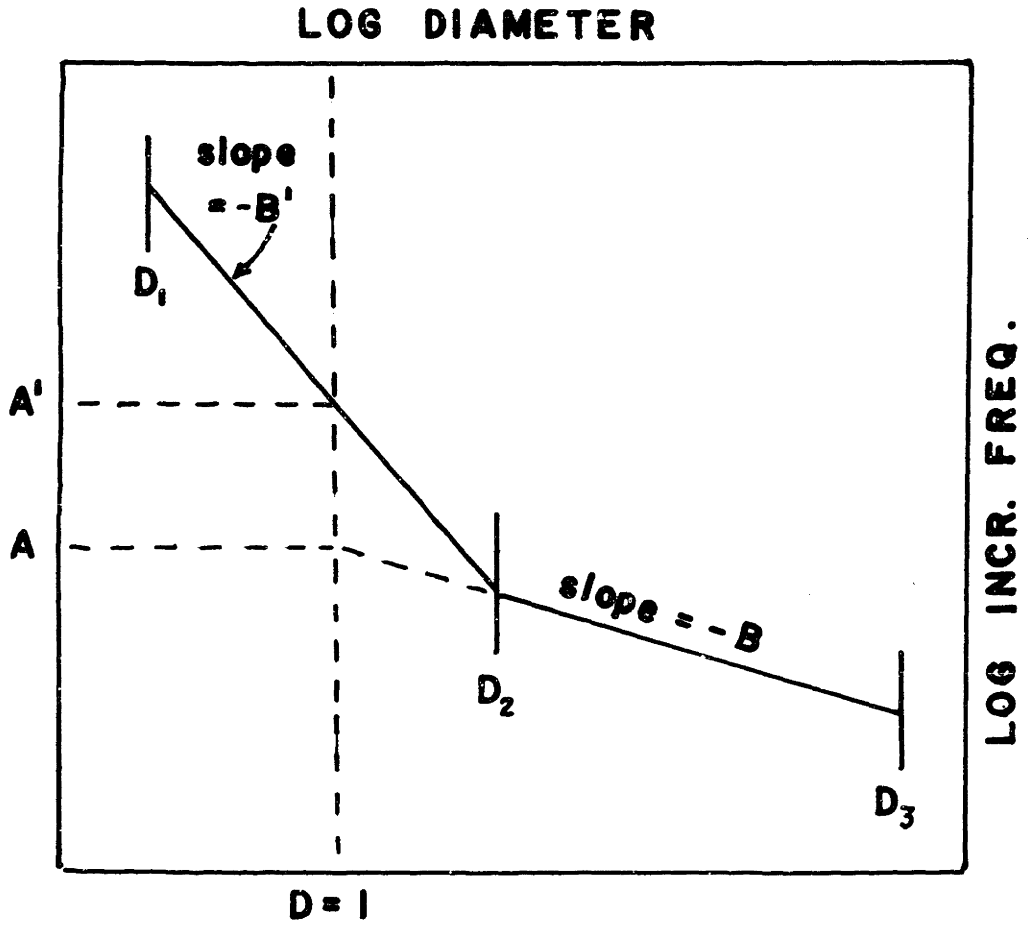

Fig. 8-3

Let us determine the condition for which the small craters in the steep part of the frequency relation can eject from the asteroid all of the ejecta blanket deposited by the large craters with the shallow distribution. The relevant quantity is the ration R of the cumulative depth of material ejected at escape velocity by the little craters to the depth of ejecta deposited by the big ones:

$$R = \left[\frac{A D_2^{(B-B')}(1-p)}{(B'+4)\,6}\right]\left[D_2^{(4+B')} - D_1^{(4+B')}\right] \div \left[\frac{Ap}{6(B+4)}\right]\left[D_3^{(4+B)} - D_2^{(4+B)}\right]$$

$$= D_2^{(B-B')}\left(\frac{1-p}{p}\right)\left(\frac{B+4}{B'+4}\right)\left[\frac{D_2^{(4+B')} - D_1^{(4+B')}}{D_3^{(4+B)} - D_2^{(4+B)}}\right] . \qquad (5)$$

For R>1 the surface is rocky; otherwise there remains a regolith. Possible values for some of the parameters are: D_1 = 0.001 m, D_2 = 20 m, D_3 = 20 km (i.e. an asteroid larger than 100 km diameter), and B' = -4.5. For |B| as low as 2.5, p must be $\leq$ 0.01 for there to be a rocky surface; this is too low for such a large asteroid, hence large asteroids must have a regolith under such circumstances. But for |B| = 3.0, p$\leq$0.3 yields a rocky surface. The ratio is sensitively dependent on both the degree to which |B'| is appreciably larger than 4 and on the lower diameter limit to which it is valid. The more smaller particles there are to erode away the surface, the less likely an asteroid can maintain a regolith. Note that small impacts erode a greater depth than larger ones for |B| > 4.

Crater Breccia Lenses as Regolith

So far, by lunar analogy, I have considered only actual crater ejecta as the source for potential asteroid regoliths. But in the case of a small asteroid which is being sand-blasted and scoured clean as discussed, do we really see hard rock beneath? In addition to throwing out ejecta, a

cratering event crushes rocks beneath the crater forming a lens of breccia. Perhaps such a brecciated zone would be sufficiently rubbly or powdery to photometrically resemble a powder.* We must probably talk about breccia lenses under rather small craters; the breccias generated by giant impacts may not meet the photometric requirements of a powdery surface.

Breccia lenses have thicknesses approximating the crater depth. Such a layer is eaten away faster than it is generated if $|B|>4$. For $|B|<4$, such a brecciated layer remains in steady-state even for $p = 0.0$. It is quite possible that $|B|$ is in fact greater than 4 for small particles, in which case an asteroid might appear rocky down to a scale corresponding to the depth of a crater with cut-off diameter δ' produced by the smallest particle in the range for which $|b|>4$. (δ' must be $\geq\delta$.) I tabulate below the depth of such a brecciated zone:

Crater diameter δ':	1 cm	1 mm	100μ	10μ
Brecciated layer depth:	0.3 cm	300μ	30μ	3μ

Comparison with Table 8-5 shows that micro-brecciation (if it occurs and produces powders at these scales) produces more regolith than does blanketing by ejecta from tiny craters. Experimental verification is required.

C. CONCLUSIONS ABOUT ASTEROID REGOLITHS

In order to be confident of predicting the existence or non-existence of asteroidal regoliths we require better determinations of two important

---

* Such a brecciated regolith does <u>not</u> meet Marcus' requirements for a sandy surface for craters of the sizes which create the breccias. It is just the energy lost in generating breccias which reduces the production of ejecta in rock compared with sand.

parameters -- the population index for particles in the asteroid belt of less than 10^4 g and the low diameter cut-off for micro-particles. We also require experimental verification for two hypothesized regolith-producing processes: small scale ejecta-blanketing and small-scale brecciation. (Possibly even large-scale brecciation will produce dusty, fragmental surfaces which would be very difficult to scour away.)

Nevertheless it can be stated confidently that the largest asteroids must retain regoliths, both because p approaches 1 and because more regolith is created by large impacts on such asteroids. Just as certainly, such small asteroids and asteroidal fragments as Icarus will be free of any kind of regolith. For moderate-to-large asteroids, such as the majority of those with measured spectral reflectivities, the presence of a regolith due to normal ejecta blanketing is possible, but it becomes unlikely if |B| approaches or exceeds 4. Such a regolith is unlikely for asteroids with diameters under 50 km. Moderately small asteroids may retain a skin-deep surface dust layer provided the lower particle size cut-off is not too small and provided that small-scale regolith formation is a viable process. A summary is presented in Table 8-6.

It is especially important to determine b for centimeter-sized particles in the asteroid belt and elsewhere in the solar system. If it is appreciably larger in absolute magnitude than the 3.5 predicted by Dohnanyi, there are several important implications: (1) even moderately large asteroids will lack macroscopic regoliths; (2) if Mazor and Anders (1967) are correct about the origin of gas-rich meteorites, then their origin can be further restricted to the surfaces of the largest asteroids; (3) the possibility of finding "soft-landed" meteorites remaining on asteroid surfaces, as proposed by Alfven and Arrhenius (1971), may be

Table 8-6. Likely Existence of Asteroidal Regoliths.

Asteroid	Large-scale Regoliths	Possible Skin-Deep Regoliths	
		Micro Ejecta Blankets	Micro-brecciation
Ceres	yes	yes	yes
324 Bamberga	yes	yes	yes
192 Nausikaa	no?	yes	yes
82 Alkmene	no	no?	yes
1566 Icarus	no	no	no

virtually eliminated; (4) the short cosmic-ray exposure ages for stony meteorites may find a ready explanation which many investigaters have previously been unwilling to accept (e.g. Wetherill, 1967 a,b) and (5) spacecraft attempting to pass through the asteroid belt may be more vulnerable to destruction or impairment by impact of particles too large for shielding protection. Since observational data are difficult to obtain at this size range, more theoretical treatment is required, taking due account of plausible erosive comminution laws.

In this chapter, I have assumed that typical impact velocities for particles of all sizes is about 5 km/sec. In order for the net accretional process proposed by Alfven and Arrhenius (1970) to work, relative impact velocities for the accreting particles must be an order of magnitude smaller.

CHAPTER IX

IMPLICATIONS AND DISCUSSION

A. IMPLICATIONS FOR THE PRESENT ENVIRONMENT OF THE ASTEROID BELT

Asteroid spectral reflectivities show a considerable diversity. One might have supposed that asteroid surfaces would all be the same due to similarities in the final stages of their formation. Or perhaps the similarity of their current impact, temperature, or radiation environments would be expected to modify all asteroids to likenesses of each other. But it is becoming increasingly clear that asteroids are very different from each other, not only in color, but in the presence of absorption bands and in albedo.

There seems to be little significant contamination of asteroid surfaces by any ubiquitious kind of small particulate debris in the asteroid belt. Moreover, there is little evidence that asteroid surface colors are dominantly controlled by the effects of hypervelocity impacts. At least the effects of vitrification as seen on the moon are not evident in asteroid reflectivities. On the other hand, cratering theory shows that all larger asteroids must have regoliths, in agreement with observed negative polarization brances, opposition effects, and some meteorite characteristics. But regoliths are not possible for the smaller asteroids; the exact cut-off size cannot be determined. One might expect an asteroid regolith to be well-mixed around the entire surface of the asteroid due to low gravity, but the suggestions of color differences with rotational phase for several asteroids imply that the regoliths are steady-state blankets composed of rock exposed relatively recently as the surface

erosion digs deeper and deeper into the asteroids.

Thus in planning possible asteroid spacecraft missions, we can be confident that true asteroidal material will be accessible on all asteroid surfaces, although there will be a fragmental layer on the larger ones and only hard rock on the smaller ones.

The current temperature environment does not play a dominant role in the color characteristics of asteroid surfaces. It is quite possible that kilometers of material have been eroded from asteroid surfaces during the age of the solar system, so any early icy layers might no longer exist. If there are asteroids of largely icy composition, the ice does not dominate their surface reflectivity characteristics.

For a complete understanding of the effects of asteroidal environments on their surface properties, it is most important to determine the population index of small debris in the asteroid belt (perhpas as a function of a). Also we need laboratory experiments on the velocity distribution of ejecta from simulated asteroid surfaces and a study of breccia lenses formed by small hypervelocity impacts.

B. THE ORIGIN AND EVOLUTION OF THE ASTEROIDS AND METEORITES

Over the years there have been many hypotheses for the origin of the smaller objects in the solar system. A once-popular concept was that of an "exploded planet" between Mars and Jupiter. During the past decade, estimated sizes of meteorite parent bodies have steadily dwindled, to the point where some investigators doubt that some meteorites had anything to do with asteroids. Perhaps the most typical picture of a parent body is the one constructed by Mason (1968), which contains a pallastic core, a diogenitic mantle, topped by a basaltic crust; he would derive

chondrites from smaller asteroids insufficiently large to have differentiated. With Larimer and Anders (1967), he would agree that enstatite chondrites came from a hotter part of the solar nebula, and carbonaceous chondrites from a colder part, which is presumably a function of a. A different parent body model was drawn by Wood (1965). He would derive all meteorites from common parent bodies with an iron core surrounded by an achondritic layer which in turn is surrounded by a chondritic mantle, topped off with carbonaceous chondritic material.

If we are not constrained by the existence of meteorites (let them come from comets or elsewhere in the solar system), then a model asteroid can be considerably simpler -- in particular, differentiation would not be required. If meteorites do not originate in the asteroid belt, then this asteroid study has little to say about meteorites. If they do come from the belt, then we can begin to elucidate the locations of meteorite parent bodies, and in turn meteorite studies can then tell us about the asteroids. On the latter assumption, a few speculations are possible about asteroid-meteorite relations.

First, there is the obvious correlation of blue colors with large a, or large aphelia. The three B3 asteroids with flat reflectivities are located in the outer part of the asteroid belt which suggests that these have carbonaceous chondritic surfaces. One of these -- 2 Pallas -- may be an occasional Mars-crosser (Anders, 1971) and would be a likely source for these primitive meteorites if they can be accelerated the several hundred m/sec necessary to eject them into escape velocity from the surface of Pallas.

Also intriguing is the qualitative agreement between Mason's model and the apparent correlation between color and size of asteroids (Chap. V). This requires that achondrites look bluer than chondrites, which seems to agree with the limited laboratory measurements available (Chap. VII). Vesta, with an M-type reflectivity, is strikingly similar to basaltic achondrites. Other large, blue asteroids such as Ceres have reflectivities that differ from Vesta's, but they still seem similar to terrestrial basalts. Having already explained the still different BM reflectivities of the B3 type as being due to carbonaceous material, we have made partial progress towards answering some of the questions posed at the end of Chap. V.

The red asteroids, which are a more uniform group than are the BM asteroids, would be the ordinary chondrites in this model. Though the band position for the majority of them may be consistent with Type III carbonaceous chondrites, hypersthene chondrites also suffice. Let us consider evidence for something resembling Larimer and Anders' (1967) predicted variation in chondrite class with a. A possible correlation of carbonaceous chondrites in the outer part of the belt has been already discussed. It was mentioned in Chap. V that the R1 asteroids seem to be at slightly smaller a than other red asteroids. I have already ascribed the flattening of their spectral curve slopes in the IR to a weakened form of the olivine band, which seems strongest for 68 Leto and 39 Laetitia (R2). But possible pure enstatite would work for the R1's, judging from curves published by Adams (1968), though it would have to be iron-free since a trace of iron in the pyroxene yields a very deep absorption feature near 0.89 microns, which is not observed. There seem to be no clear representatives of the bronzite chondrite class in any asteroid spectra. The outermost reddish asteroids (68 and 39) are both of type R2,

which might be consistent with the olivine-pigeonites.

Thus the model is consistent with the observed reflectivities. However, the data by no means prove that it is correct. The identification for several of the chondrite classes is only circumstantial. But this model is amenable to further tests, and the prospects for conclusive results are good. Supporting laboratory studies of meteorite reflectivities are essential for this project and initial steps have already been taken to make such measurements.

C. FRAGMENTATION OF ASTEROIDS

Most evidence suggests that fragmentation is a dominant process in the asteroid belt. It presumably is responsible for creating the smaller asteroids and for generating the fragments which fall on earth as meteorites. It also seems to leave evidence of its role in the numerous families which are composed of a large fraction of all asteroids. I showed in Chap. V that there is little correlation between color and family. Unfortunately there is only one family, as determined unequivocably by Williams, for which I have complete spectral reflectivities for more than one representative. The fact that 1 Ceres and 39 Laetitia belong to the same family is somewhat distrubing. Although Laetitia has a large light-curve amplitude, suggesting fragmentation, Ceres itself does not appear particularly irregular; possibly it is too large to maintain a non-spherical shape.

Clearly more spectral reflectivity observations of family pairs would be very enlightening. A good candidate might be the Flora family -- it is a possible source of meteorites, and the red colors of some of its members suggest the likely presence of diagnostic absorption bands. If Mason's model were correct, one might find two kinds of families: (1) families

with a relatively small combined mass composed of similar reddish chondritic fragments, and (2) families with larger combined masses composed of fragments with a variety of different colors, with some possibly showing large rotational variations in color.

Two Mars-approaching asteroids may show color differences across their surfaces: 6 Hebe and 43 Ariadne (Chap. VI). While 43 Ariadne is part of the Flora group, Hebe appears not to be part of any family, leading one to wonder about the origins of its obvious asymmetries.

From what fraction of the asteroid belt can meteorites come? Jaeger and Lipschutz (1967) and Jain and Lipschutz (1970) have discussed evidence for shock in some iron meteorites, which suggests they might have been ejected with large accelerations from the main asteroid belt. Further theoretical work is needed to ascertain for sure the impossibility of obtaining other meteorites from the belt. Fortunately, it appears from the distribution of asteroid spectral reflectivities on the a-e plot (Fig. 5-4) that there is a sufficient variety of asteroids with moderately small perihelia to be sources for most meteorites. In fact the relative proportions of red to EM asteroids is similar to the proportions of different colored meteorites, if one identifies ordinary chondrites with the red asteroids.

It will be very important to re-analyse the correlation of various asteroidal parameters with family membership, using Williams' new family designations. Anders' (1965) application of his criteria of fragmentation is probably obsolete since many of the previous family designations seem incorrect. In calculating the total pre-fragmentation mass of a family parent, consideration now should be given to possible correlations of albedo with diameter (Chap. V). It will be very interesting to see how light-

curve amplitudes correlate with family membership.

The correlation of blue-dark-big asteroids (Chap V) has several important implications for the size-frequency relation. It tends to decrease the slope of the frequency relation near the size corresponding already to an apparent shelf in the distribution near the boundary between the McDonald and Palomar-Leiden surveys. This enhances the feature which Anders (1965) has ascribed to an original Gaussian population of bodies prior to the creation of the small-size tail by fragmentation (see Hartmann and Hartmann, 1968, for an elaboration). An enhancement of the shelf in the distribution implies that catastrophic collisional fragmentation has been less important than previously believed in disrupting the biggest asteroids.

D. 324 BAMBERGA -- AN INTERESTING ASTEROID

Anders (1964) considered the possibility that 324 Bamberga might be a source of meteorites. But he rejected the possibility, on the grounds that an ejection velocity of 370 m/sec is required to get crater ejecta into Mars crossing orbits from Bamberga's perihelion distance of about 0.1 AU from Mars (cf. Öpik, 1968). Öpik's theory may be too pessimistic about the possibilities for accelerating fragments to large velocities (Chapman, 1971). Moreover, Williams (1971, personal communication) now believes that Bamberga comes to within 0.05 AU of Mars, which means that some fragments from impacts against Bamberga can achieve Mars-crossing orbits.

This fact is especially interesting now that we have evidence that Bamberga has interesting surface properties. Matson's (1971) measurements of its thermal flux, as calculated using his most recent Vesta calibration

(1971, personal communication), indicate a Bond albedo of about 0.013. Even using his maximum permissible Bond albedo of 0.018, it is hard to raise the geometric albedo above 3% and it is more likely near 2% making Bamberga the blackest object known in the solar system and the fourth largest known asteroid (bigger even than Juno).

It is difficult to make any substance as dark as Bamberga. Even carbon black or finely particulated magnetite or ilmenite are somewhat brighter (Hunt et al, 1971). But it is more difficult to understand how the spectral reflectivity of Bamberga can show so much structure. The reflectivity has a modest red slope with a prominent absorption band in the vicinity of 0.65 microns -- an unusual location for a prominent band. How a surface which is darker even than particulated opaques can show a prominent absorption feature is very difficult to understand, especially if there is a surface regolith.

Bamberga has a very large eccentricity and a moderately large orbital inclination, which enhances its uniqueness. Perhaps not too surprisingly for such a large black asteroid, Bamberga shows little light variation -- not enough to determine a rotation period with any confidence (Gehrels and Owings, 1962). Not only does Bamberga come closest to Mars of any asteroid yet studied in detail, but it reaches a larger aphelion distance than most. This interesting asteroid clearly deserves further study.

CHAPTER X

SUGGESTIONS FOR FUTURE ASTEROID SPECTROPHOTOMETRY PROGRAMS

A. INTRODUCTION

The results obtained so far are sufficiently important to justify further work on spectral reflectivities. However, as expected, experience suggests some modifications to the previous routine. A primary need is for data similar to those included here to develop better statistics. With spectral reflectivities for several times the present sample of asteroids, the suggestive correlations with physical and orbital parameters discussed in Chap. V can be conclusively verified, modified, or rejected. We have by no means exhausted the asteroids bright enough to be observed by this technique. There are about 200 asteroids as bright or brighter than the faintest asteroids successfully observed so far. This is nearly twice the number of asteroids for which colors of any sort are currently available. By using more efficient observing techniques, there is no reason that reconnaissance reflectivity measurements of most of the 200 could not be obtained using about twice the amount of observing time used for the present program (i.e. 60 clear nights on telescopes 36-inches aperture or larger).

B. MORE EFFICIENT OBSERVING SCHEDULE

By utilizing more efficient equipment-control electronics, with the photometer operating in the dual-photomultiplier incremental-filter-advance mode, it should be possible to improve efficiency by about a factor of 3. The following observing schedule would be a good one:

S-20	C	0	11-24	0	18-24	0	18-24	0	18-24	0	18-24	C		8 min.
S-20	C	0	11-24	0	18-24	0	18-24	0	18-24	0	18-24			8 min.
find star		0	1-24	C	S-20	find asteroid								8 min.
repeat entire sequence														24 min.

"S-20" refers to observations with the S-20 tube through filters 1-18. All other observations are with the S-1. Tubes are changed at time C. Observations are taken of all light (through an open filter) at time 0. This observing sequence will yield, per hour, about 3 standard star observations, 25 data points for a light curve, 5 S-20 runs, 5 S-1 runs on filters 11-24 (providing overlap and normalization information), and 15 runs in filters 18-24 (where most absorption bands occur). Each "run" consists of 50 seconds integration, divided among the specified filters. The tubes must be switched six times an hour.

The advantages of this observing schedule are: (1) emphasizes acquisition of data near the important IR absorption bands; (2) it utilizes the high quantum efficiency of the S-20 tube to good advantage; (3) it provides sufficient overlap and standardization between the two tubes to reduce the kinds of problems encountered in the February and May runs; (4) it permits data to be taken in all filters in times short compared with changes in sky conditions or asteroid rotation; (5) it permits sufficiently frequent standard star observations; (6) it provides for the taking of a simultaneous light-curve for the asteroid (see below), and (7) it standardizes the format of the recorded data for easy computer reduction.

C. PRECISION OF DATA

Some of the difficulties in interpreting the reflectivities reported in this thesis stem from the fairly large error bars on many reflectivities.

Vesta-type bands would have been resolved easily, but the shallower bands which are much more common, are marginal features in the noiser spectra. For future programs we must clearly distinguish between two goals: further reconnaissance and detailed study of specific asteroids, especially of absorption bands.

For purposes of further reconnaissance the resolution of 24 filters in the 0.3 to 1.1 micron region is probably not necessary. The major features of all spectral reflectivity types thus far recognized could probably be determined from 8-color photometry, given well-chosen effective wavelengths. I propose that filters similar to the U, B, and V standard filters be used for the shorter wavelengths, and that medium-band filters centered at 0.65, 0.75, 0.85, 0.95, and 1.05 microns constitute the rest of the set. Measurements in the 0.65 and 0.95 micron filters would reveal the presence of the only two bands thus far recognized (or the 1.05 filter would reveal the olivine band). Data could be taken more rapidly, or of fainter objects, with such a filter set and interesting asteroids could be noted for more detailed spectrophotometry. There is always a chance however of missing some important spectral feature by reducing the resolution.

In order to measure band positions, higher spectral resolution in the 0.9 - 1.05 micron region is desirable (perhaps twice as many filters). The current resolutinn can only marginally distinguish between some very important orthopyroxenes. For such measurements, one should hope to achieve 1 to 2% statistics, since that is about the level to which we may reasonably expect the absolute and relative calibrations to be improved during the next couple years. The current resolution is probably adequate for detailed studies of the reflectivities away from the near-IR; better counting

statistics, also to 1 or 2%, would be useful, however.

D. SPECIAL PROJECTS

Going to fainter magnitudes. It is worthwhile to try for fainter asteroids, especially Mars-crossers, the Trojans, small family fragments, and perhaps some very dark, small asteroids. Problems with finding, guiding, and star-light contamination get severe for magnitudes fainter than 15th. But it should be possible to take reconnaissance data with the S-20 tube, and to spend long periods of time integrating in the near-IR for a few particularly promising faint asteroids. A large telescope is necessary.

Spectral data out to 2.5 microns. It would probably be feasible on a large telescope to obtain some spectral information in the 1.1 to 2.5 micron region using a PbS detector. There are diagnostic bands in this region of great interest. The technique could only be used on the few brightest asteroids, and even then it would take a lot of telescope time. I do not feel that such a project is warranted at this time, in comparison with the priority for extending the visible reflectivity data.

Simultaneous light-curve. A serious handicap in interpreting possible rotational color effects in Chap. VI is the absence of knowledge about the phase of the light-curve or the pole direction. It would probably be well worth the slight additional investment in time to make observations in an open filter (to obtain better statistics) with sufficient frequency to derive a fair light-curve. These added data would help in deriving pole positions and in keeping track of the rotational phase. It would also permit direct comparison of color variations with light-curve.

Phase Variations. Evidence was presented in Chap. VI that band strengths may increase with increasing phase angle. Therefore asteroids possessing bands should be observed at relatively large phase-angles, if they are sufficiently bright. There is little advantage, however, in trying to measure color variations with phase angle using all 24 filters. Color phase relationships are probably uniform over a wide wavelength interval and are best determined by UBV photometry or its equivalent.

E. INTERESTING ASTEROIDS FOR SPECIAL STUDY

Along with a continuing reconnaissance study (perhaps with fewer filters), detailed spectral reflectivity measurements should continue for the more interesting asteroids. I present here a partial list of interesting candidates for special study.

Asteroids already observed, but which should be re-observed, are 324 Bamberga (extend observations beyond 0.85 microns); 79, 192, 68, and 39 (for detailed band position measurements); 43 and 6 (for possible rotational color variations).

Mars-crossers or near Mars-crossers. High priority should be given to studying these asteroids which most likely give rise to meteorites. Some of the larger asteroids are 8 Flora, 6 Hebe, 18 Melpomene, 25 Phocaea, 2 Pallas and 324 Bamberga. Some of the small true Mars-crossers and Apollo objects should be observed whenever possible.

Observations of family pairs are of the greatest interest; the choices should be obtained from Williams' lists when they are available.

Some effort should be made to find other asteroids like Vesta. Possible candidates are the brighter bluish asteroids 15 and 44. Also, Williams (1971, personal communication) describes Vesta and 409 Aspasia

as having family members sufficiently bright to be observed using these techniques.

Of the spread of colors on the B-V vs U-B plot, the extremely reddish asteroids have not been adequately covered in my present sample. Possibly some of these asteroids will be bronzite chondritic in appearance.

Rotational variations in color should be examined for those asteroids with large "spottedness" components to their light-curves, such as 9 Metis and 18 Melpomene.

Examination of asteroids with extreme orbital elements should be continued, especially extending outward in the asteroid belt and hopefully including a Trojan.

F. SUPPORTING STUDIES

Coordination with Other Observing Programs

The greatest promise for learning about asteroid surfaces is for coordinated studies of spectral reflectivity, thermal IR flux, polarization, and light-curve photometry. Nearly simultaneous observations of the same asteroids by all techniques might be particularly interesting since phase angle, pole position, and rotational phase would be the same.

Spectral Reflectivity Studies of Cometary Nuclei

A particularly fruitful project is to observe reflectivities of cometary nuclei. They may have surface compositions radically different from asteroids, but perhaps not. It will be particularly interesting to try to identify ices and perhaps carbonaceous chondritic matter. The relationship between dead comets and asteroids could be further elucidated.

Stellar and Solar Calibrations

A primary impediment to the detailed study of band positions is the uncertainty in the relative standard star calibrations and their absolute calibration against the sun. The Oke-Hayes standard stars should be calibrated against each other in the filters used for asteroid observations; perhaps the calibration sequence can be extended to some G-type stars.

Laboratory Studies of Rocks, Mineral, Ices, and Meteorites

Veverka (1970) noted the extreme importance of measuring the spectral reflectivities of meteorites. This project has still not been carried out. When it is, the opportunities for making much firmer compositional identifications will be excellent. Further studies of other rocks and materials should be continued, varying such parameters as particle size, phase angle, and percentage of opaques.

REFERENCES

Adams, J.B. (1968). Lunar and Martian surfaces: petrologic significance of absorption bands in the near-infrared. Science 159, 1453-1455.

Adams, J.B. and Filice, A.L. (1967). Spectral reflectance 0.4 to 2.0 microns of silicate rock powders. J. Geophys. Res. 72, 5705-5715.

Adams, J.B. and Jones, R.L. (1970). Spectral reflectivity of lunar samples. Science 167, 737-739.

Adams, J.B. and McCord, T.B. (1971). Alteration of lunar optical properties: age and composition effects. Science 171, 567-571.

Ahmad, I.I. (1954). Photometric studies of asteroids. IV. The light-curves of Ceres, Hebe, Flora, and Kalliope. Astrophys. J. 120, 551-559.

Allen, C.W. (1963). "Astrophysical quantities," 2d ed. Univ. of London Press, London.

Allen, D.A. (1970). Infrared diameter of Vesta. Nature 227, 158-159.

Allen, D.A. (1971). The method of determining infrared diameters. In "Physical studies of minor planets," (T. Gehrels, ed.), Proc. 12th Colloq. Intl. Astron. Union, Tucson, March 8-10, NASA SP-267.

Alfven, H. and Arrhenius, G. (1970). Structure and evolutionary history of the solar system, I; Origin and evolution of the solar system, II. Astrophys. Space Sci. 8, 338-431; Astrophys. Space Sci. 9, 3-33.

Alfven, H. and Arrhenius, G. (1971). Arguments for a mission to an asteroid. In "Physical studies of minor planets," (T. Gehrels, ed.), Proc. 12th Colloq. Intl. Astron. Union, Tucson, March 8-10, NASA SP-267.

Anders, E. (1964). Origin, age and composition of meteorites. Space Sci. Rev. 3, 583-718.

Anders, E. (1965). Fragmentation history of asteroids. Icarus 4, 399-408.

Anders, E. (1971). Interrelations of meteorites, asteroids, and comets. In "Physical studies of minor planets," (T. Gehrels, ed.), Proc. 12th Colloq. Intl. Astron. Union, Tucson, March 8-10, NASA SP-267.

Anders, E. and Mellick, P.J. (1969). Orbital clues to the nature of meteorite parent bodies. In "Meteorite research," (P.M. Millman, ed.), Springer-Verlag, New York. 559-572.

Arnold, J.R. (1969). Asteroid families and "jet streams". Astron. J. 74, 1235-1242.

Arvesen, J.C., Griffin, R.N., and Pearson, B.D.jr. (1969). Determination of extraterrestrial solar spectral irradiance from a research aircraft. Appl. Optics 8, 2215-2232.

Bass, M.N. (1971). Montmorillonite and serpentine in Orgueil meteorite. Geochim. Cosmochim. Acta 35, 139-147.

Bobrovnikoff, N.T. (1929). The spectra of minor planets. Lick Observatory Bulletin 18, 18-27.

Breger, M. (1971). A spectrophotometric scanner catalog. S.U.N.Y. Stony Brook, Communications in Astronomy, no.1.

Burns, R.G. (1965). Electronic spectra of silicate minerals: application of crystal-field theory to aspects of geochemistry. Ph.D. dissertation, Univ. of Calif. (Berkeley), Berkeley, Calif., 1965.

Chapman, C.R. (1968). Interpretation of the diameter-frequency relation for lunar craters photographed by Rangers 7, 8, and 9. Icarus 8, 1-22.

Chapman, C.R., Johnson, T.V., Kunin, J.S. and McCord, T.B. (1971a). Spectral reflectivity studies of 12 asteroids (0.3 to 1.1μ). Bull. Am. Astron. Soc. 3, 279.

Chapman, C.R., Johnson, T.V., and McCord, T.B. (1971b). A review of spectrophotometric studies of asteroids. In "Physical studies of minor planets," (T. Gehrels, ed.), Proc. 12th Colloq. Intl. Astron. Union, Tucson, March 8-10, NASA SP-267.

Chapman, C.R., Mosher, J.A., and Simmons, G. (1970). Lunar cratering and erosion from Orbiter 5 photographs. J. Geophys. Res. 75, 1445-1466.

Chapman, D.R. (1971). Australasian tektite geographic pattern, crater & ray of origin, and theory of tektite events. J. Geophys. Res. 76, 6309-6338.

Chebotarev, G. (1969). "Ephemerides of minor planets for 1970." Institute of Theoretical Astronomy, Academy of Sciences, U.S.S.R., Moscow.

Chebotarev, G. (1970). "Ephemerides of minor planets for 1971." Institute of Theoretical Astronomy, Academy of Sciences, U.S.S.R., Moscow

Dohnanyi, J.S. (1971). Fragmentation and distribution of asteroids. In "Physical studies of minor planets," (T. Gehrels, ed.), Proc. 12th Colloq. Intl. Astron. Union, Tucson, March 8-10, NASA SP-267.

Dollfus, A. (1971). Diameters of asteroids and possibilities for future work. In "Physical studies of minor planets," (T. Gehrels, ed.), Proc. 12th Colloq. Intl. Astron. Union, Tucson, March 8-10, NASA SP-267.

Fischer, V.H. (1941). Farbmessungen an kleinen Planeten. Astron. Nachr. 272, 127-147.

Gault, D.E., Shoemaker, E.M. and Moore, H.J. (1963). Spray ejected from the lunar surface. NASA TN-D-1767.

Gault, D.E. and Wedekind, J.A. (1969). The destruction of tektites by micrometeoroid impact. J. Geophys. Res. 74, 6780-6794.

Gehrels, T. (1967). Minor planets. I. The rotation of Vesta. Astron. J. 72, 929-938.

Gehrels, T. (1970). Photometry of asteroids. In "Surfaces and interiors of planets and satellites," (A. Dollfus, ed.), Academic Press, London, 317-375.

Gehrels, T. and Owings, D. (1962). Photometric studies of asteroids. IX. Additional light-curves. Astrophys. J. 135, 906-924.

Gehrels, T., Roemer, E., Taylor, R.C., and Zellner, B.H. (1970). Minor planets and related objects. IV. Asteroid (1566) Icarus. Astron. J. 75, 186-195.

Giclas, H.L. (1950). Direct photoelectric photometry. In "The project for the study of planetary atmospheres," Annual Report, 1950 to AFCRL, Lowell Observatory, Flagstaff, Arizona, 47-63.

Giclas, H.L. (1951). Direct photoelectric photometry. In "The project for the study of planetary atmospheres," Annual Report, 1951, no.9 to AFCRL, Lowell Observatory, Flagstaff, Arizona. 33-71.

Giclas, H.L. (1952). Measurement of solar variation. In "Final report on the study of planetary atmospheres," Lowell Observatory, Flagstaff, Arizona. 250-269.

Goldstein, R.M. (1969). Radar observations of Icarus. Icarus 10, 430-431.

Goldstein, R.M. (1971). Radar methods and surface roughness of asteroids. In "Physical studies of minor planets," (T. Gehrels, ed.), Proc. 12th Colloq. Intl. Astron. Union, Tucson, March 8-10, NASA SP-267.

Groeneveld, I. and Kuiper, G.P. (1954). Photometric studies of asteroids. II. Astrophys. J. 120, 529-546.

Hapke, B. (1971). Possible surface texture of asteroids. In "Physical studies of minor planets," (T. Gehrels, ed.), Proc. 12th Colloq. Intl. Astron. Union, Tucson, March 8-10, NASA SP-267.

Hardie, R.H. (1962). Photoelectric reductions. In "Astronomical techniques," (W.A. Hiltner, ed.), Univ. of Chicago Press, Chicago. 178-208.

Hartmann, W.K. (1969a). Terrestrial, lunar, and interplanetary rock fragmentation. Icarus 10, 201-213.

Hartmann, W.K. (1969b). Angular momentum of Icarus. Icarus 10, 445-446.

Hartmann, W.K. and Hartmann, A.C. (1968). Asteroid collisions and evolution of asteroidal mass distribution and meteoritic flux. Icarus 8, 361-381.

Hayes, D.S. (1970). An absolute spectrophotometric calibration of the energy distribution of twelve standard stars. Astrophys. J. 159, 165-176.

Hellyer, B. (1970). The fragmentation of the asteroids. Mon. Not. R. Soc. 148, 383-390.

Hertz, H.G. (1968). Mass of Vesta. Science 160, 299-300.

Hodge, P.W. (1971). Large decrease in the clear air transmission of the atmosphere 1.7 km above Los Angeles. Nature 229, 549.

Hörz, F., Hartung, J.B. and Gault, D. (1971). Micrometeorite craters on lunar rock surfaces. J. Geophys. Res. 76, 5770-5798.

Hunt, G.R. and Salisbury, J.W. (1970a). Visible and near-infrared spectra of minerals and rocks: I. Silicates. Modern Geology 1, 283-300.

Hunt, G.R. and Salisbury, J.W. (1970b). Visible and near-infrared spectra of minerals and rocks: II. Carbonates. Modern Geology 2, 23-30.

Hunt, G.R., Salisbury, J.W., and Lenhoff, C.J. (1970). Visible and near-infrared spectra of minerals and rocks: IV. Sulphides and sulphates. Preprint.

Hunt, G.R., Salisbury, J.W., and Lenhoff, C.J. (1971). Visible and near-infrared spectra of minerals and rocks: III. Oxides and Hydroxides. Modern Geology 2, 195-205.

Jaeger, R.R. and Lipschutz, M.E. (1967). Implications of shock effects in iron meteorites. Geochim. Cosmochim. Acta 31, 1811-1832.

Jain, A.V. and Lipschutz, M.E. (1970). On preferred disorder and the shock history of chemical group IVA meteorites. Geochim. Cosmochim. Acta 34, 883-892.

Johnson, T.V. and McGetchin, T.R. (1971). Topography on planetary surfaces and the shape of asteroids. Preprint.

Johnson, W.A. (1939). Spectrophotometric study of three asteroids. Harvard College Obs. Bull. 911, 13-15.

Kessler, D.J. (1970). Meteoroid environment model-1970 (interplanetary and planetary). NASA SP-8038.

Kitamura, M. (1959). A photoelectric study of colors of asteroids and meteorites. Pub. Astron. Soc. Japan 11, 79-89.

Kuiper, G.P, Fujita, Y., Gehrels, T., Groeneveld, I., Kent, J., Van Biesbroeck, G., and Van Houten, C.J. (1958). Survey of asteroids. Astrophys. J. Suppl. 3, 289-427.

Labs, D. and Neckal, H. (1968). The radiation of the solar photosphere from 2000Å to 100μ. Zeitschrift Astrophys. 69, 1-73.

Lacis, A.&Fix, J. (1971). Light-curve inversion and surface reflectivity. In "Physical studies of minor planets," (T. Gehrels, ed.), Proc. 12th Colloq. Intl. Astron. Union, Tucson, March 8-10, NASA SP-267.

Larimer, J.W. and Anders, E. (1967). Chemical fractionations in meteorites: II. Abundance patterns and their interpretation. Geochim. Cosmochim. Acta 31, 1239-1270.

Lunar Sample Preliminary Examination Team. (1971). Preliminary examination of lunar samples from Apollo 14. Science 173, 681-693.

Marcus, A.H. (1969). Speculations on mass loss by meteoroid impact and formation of the planets. Icarus 11, 76-87.

Marsden, B.G. (1970). On the relationship between comets and minor planets. Astron. J. 75, 206-217.

Mason, B. (1968). Composition of stony meteorites. In "Extra-terrestrial matter," (C.A. Randall, jr, ed.), Proc. Central states universities and Argonne Nat. Lab. conf., Argonne, Ill., Mar. 7-8, 1968, De Kalb, Illinois, Northern Illinois Univ. Press, 3-22.

Matson, D.L. (1971). Infrared observations of asteroids. In "Physical studies of minor planets," (T. Gehrels, ed.), Proc. 12th Colloq. Intl. Astron. Union, Tucson, March 8-10, NASA SP-267.

Mazor, E. and Anders, E. (1967). Primordial gases in the Jodzie howardite and the origin of gas-rich meteorites. Geochim. Cosmochim. Acta 31, 1441-1456.

McCord, T.B. (1968). A double beam astronomical photometer. Appl. Optics 7, 475-478.

McCord, T.B., Adams, J.B., and Johnson, T.V. (1970). Asteroid Vesta: Spectral reflectivity and compositional implications. Science 168, 1445-1447.

McCord, T.B. and Johnson, T.V. (1970). Lunar spectral reflectivity (0.30 to 2.50 microns) and implications for remote mineralogical analysis. Science 169, 855-858.

Oke, J.B. (1964). Photoelectric spectrophotometry of stars suitable for standards. Astrophys. J. 140, 689-693.

Oke, J.B. and Schild, R.E. (1970). The absolute spectral energy distribution of Alpha Lyrae. Astrophys. J. 161, 1015-1023.

Opik, E.J. (1968). The cometary origin of meteorites. Irish Astron. J. 8, 185-208.

Pettengill, G.H., Shapiro, I.I., Ash, M.E., Ingalls, R.P., Rainville, L.P., Smith, W.B. and Stone, M.L. (1969). Radar observations of Icarus. Icarus 10, 432-435.

Piotrowski, S. (1953). The collisions of asteroids. Acta Astronomica ser a. 5, 115-138.

Recht, A.W. (1934). Magnitudes and color indices of asteroids. Astron. J. 44, 25-32.

Roosen, R.G. (1971). The gegenschein. Rev. Geophys. and Space Phys. 9, 275-304.

Ross, H.P., Adler, J.E.M. and Hunt, G.R. (1969). A statistical analysis of the reflectance of igneous rocks from 0.2 to 2.65 microns. Icarus 11, 46-54.

Salisbury, J.W. (1970). Albedos of lunar soil. Icarus 13, 509-512.

Sandakova, E.V. (1955). Concerning color indices of minor planets. Astron. Circ., Acad. Sci. U.S.S.R., no.163.

Sandakova, E.V. (1959). Interpretation of color indices of minor planets. Publ. Kiev Univ. Astron. Obs. 8.

Sandakova, E.V. (1962). Concerning the color indices of minor planets. Publ. Kiev Univ. Astron. Obs. 10.

Schild, R.E., Peterson, E.M., and Oke, J.B. (1971). Effective temperatures of B and A type stars. Astrophys. J. 166, 95.

Schubart, J. (1971). Asteroid masses and densities. In "Physical studies of minor planets," (T. Gehrels, ed.), Proc. 12th Colloq. Intl. Astron. Union, Tucson, March 8-10, NASA SP-267.

Shoemaker, E.M. (1965). Preliminary analysis of the fine structure of the lunar surface in Mare Cognitum. In "Ranger VII: part II. Experimenters' analyses and interpretations," Cal. Inst. Tech. J.P.L. TR-32-700, 75-144.

Sytinskaya, M.N. (1955). Photometric and colorimetric studies of meteorites and meteorite crusts. Meteoritika 13, 65-75.

Sytinskaya, M.N. (1965). Experiment in colorimetric comparison of asteroids and terrestrial rocks. Sov. Astron. A.J. 9, 100-104.

Taylor, G.E. (1962). Diameters of minor planets. Observatory 82, 17-20.

Taylor, R.C. (1971). Photometric observations and reductions of light-curves of asteroids. In "Physical studies of minor planets," (T. Gehrels, ed.), Proc. 12th Colloq. Intl. Astron. Union, Tucson, March 8-10, NASA SP-267.

Taylor, R.C., Gehrels, T., and Silvester, A.B. (1971). Minor planets and related objects. VI. Asteroid (110) Lydia. Astron.J. 76, 141-146.

Tempesti, P. and Burchi, R. (1969). A photometric research on the minor planet 12 Victoria. Mem. Soc. Astr. Italiana 40, 415-432.

van Houten, C.J., van Houten-Groeneveld, I., Herget, P., and Gehrels, T. (1970). The Palomar-Leiden survey of faint minor planets. Astron. Astrophys. Suppl. Ser. 2, 339-448.

Vesely,C. (1971). Summary on orientations of rotation axes. In "Physical studies of minor planets," (T. Gehrels, ed.), Proc. 12th Colloq. Intl. Astron. Union, Tucson, March 8-10, NASA SP-267.

Veverka, J.F. (1970). Photometric studies of minor planets and satellites. Ph.D. dissertation, Harvard Univ. Cambridge, Mass.

Walker, E.H. (1967). Statistics of impact crater accumulation on the lunar surface exposed to distribution of impacting bodies. Icarus 7, 233-243.

Watson, F.G. (1938). Small bodies and the origin of the solar system. Ph.D. dissertation, Harvard Univ. Cambridge, Mass.

Watson, F.G. (1940). Colors and magnitudes of asteroids. Harvard College Obs. Bull. 913, 3-4.

Watson, K., Murray, B.C., Brown, H. (1963). The stability of volatiles in the solar system. Icarus 1, 317-327.

Watts, H.V. (1966). Reflectance of rocks and minerals to visible and ultraviolet radiation. IIT Research Inst. Tech. Mem. W6137-1.

Wetherill, G.W. (1967a). Collisions in the asteroid belt. J. Geophys. Res. 72, 2429-2445.

Wetherill, G.W. (1967b). Dynamical studies of asteroidal and cometary orbits and their relation to the origin of meteorites. In "Origin and distribution of the elements," (L.H. Ahrens, ed.), Proc. of the Intl. Symp. Paris, May 8-11, 1967, New York, Pergamon, 423-443.

Wetherill, G.W. (1969). Relationships between orbits and sources of chondritic meteorites. In "Meteorite research," (P.M. Millman, ed.), Springer-Verlag, New York. 573-589.

Whipple, F.L. (1967). The meteoritic environment of the Moon. Proc. Roc. Soc., A 296, 304-315.

Williams, J. (1971). Proper elements, families, and belt boundaries. In "Physical studies of minor planets," (T. Gehrels, ed.). Proc. 12th Colloq. Intl. Astron. Union, Tucson, March 8-10, NASA SP-267.

Wood, H.J. and Kuiper, G.P. (1963). Photometric studies of asteroids X. Astrophys. J. 137, 1279-1285.

Wood, J.A. (1965). Meteorites and asteroids. Adv. Astronaut. Sci. 19, 99-118.

Wood, J.A. (1968). "Meteorites and the origin of planets" New York, McGraw-Hill.

Wurm, K. (1963). The physics of comets. In "The moon, meteorites and comets," (B.M. Middlehurst and G.P. Kuiper, eds.), Chicago, Univ. of Chicago Press, 573-617.

Wyszecki, G. and Stiles, W.S. (1967). "Color science." New York, Wiley, 344-351.

Yang, Xiu-yi, Zhang, You-yi, and Li, Xiao-qing. (1965). Photometric observations of variable asteroids, III. Acta Astronomica Sinica 13, 66-74.

APPENDIX I

AVERAGE ASTEROID SPECTRAL REFLECTIVITIES

This appendix includes information about each asteroid observed, including the best mean spectral reflectivity curves presented in both tabular and graphical format. Also listed is information about each individual run, including sources of error and a description of how the nightly means were weighted in deriving the final averages. There is a paragraph about the reliability of the data and its relationship to other physical parameters known for the asteroid. Certain orbital and physical parameters are listed for each asteroid, although this appendix is not intended as a complete summary of known information.

I wish to emphasize a point about the reliability of the data. Many entries in the appendix concern various problems including weather, guiding, standard star reductions, neutral density filter calibrations, and so on. This information is listed for the record and to assist potential users of the data. It does not imply that the data are poor, nor that interpretations in the text of this thesis have weak bases. For example, the lists of filters for which there may have been guiding errors refer to effects of a few percent at most on a single run (as judged by comparing separate runs); the effects on the final averages are almost always negligible compared with the adopted errors.

The following information is supplied in identical format for each observed asteroid (plus Vesta). The asteroids are arranged in numerical order.

Orbital parameters

The first line lists semi-major axis (a), proper eccentricity (e), sine of the proper inclination (sin i), and the minimum distance to Mars reached by each asteroid (Mars dist.). This information was supplied by J. G. Williams, of J.P.L., who has recently completed an as-yet-unpublished re-evaluation of the proper elements of asteroids using a more complete perturbation theory than that adopted by Arnold (1969). Williams has made tentative new family assignments (named for the brightest asteroid in the family), given as the last entry of the first line. Arnold's (1969) family assignments are listed in parentheses.

Photometric parameters

The second line lists photometric parameters given by Gehrels (1970). These are absolute magnitude B(1,0), UBV colors in magnitudes (as corrected for phase by Gehrels), the rotation period as inferred from the light curve, and the range of observed light curve amplitudes (in magnitudes).

Information on Nightly Spectral Reflectivity Runs

Each nightly summary is given a number, in chronological order. Nightly averages are given, in graphical format only, in Appendix VII. The dates are calendar dates for the day beginning at midnight on the night in question. The number of runs is the number of times data were taken through the series of 24 filters (generally, but not always, starting with filter 1 and ending with filter 24); in the case of the spinning-filter-wheel mode, a "run" refers to co-added data from 4, 8, or 16 revolutions of the filter wheel. The Local Sidereal Time (ST) is given for each run, generally for the 11th filter, followed by the maximum duration (in hours) for an individual run.

Given next (right-adjusted) is the phase angle, to the nearest degree, and the apparent magnitude (from the ephemeris). On the next line are the name/s of the standard star/s used, the range of asteroid airmass (sec z, for the 11th filter only), the quality of the standard star reduction, estimated by: the number of standard star observations and their consistency, the quality of the skies, the degree of extrapolation (in either time or airmass) between the star and the object, and the apparent accuracy of the computer reductions.

The series of comments which follow include: (1) The first item mentions the use of the S-20 photomultiplier tube and any ND filter used for the standard star observations, if the S-20 was used. No entry means the data were taken exclusively with the S-1. (2) "Counts =" gives the number of signal pulses counted for the asteroid in the 11th filter (usually) during the entire night. Experience suggests that twice the square-root of this number approximates the statistical uncertainty in the data, except for the first five and last couple filters for which the signal is lower. This entry is omitted for S-20 data for which the error is dominated by filter calibrations, guiding errors, etc. (3) Entries in the observing log regarding the certainty of identification of the asteroid (ID) are quoted. No entry implies neither certain nor uncertain identification. (4) Guiding errors were occasionally listed in the log; more frequently they were suspected from uneveness on graphical output of the raw data. Sometimes errors could not be corrected or were of a minor nature. Listed after "Guiding:" are filter numbers for which minor guiding errors may exist for <u>one</u> run during the night in question. Such errors are for the asteroid unless specifically indicated to be for the star. Cases of serious guiding errors or minor ones for more than one one run in the same filter are underlined. A guiding error for the object

will depress the reflectivity, but a guiding problem for a standard star will spuriously raise the asteroid's reflectivity. Most of these guiding problems are small effects and can be ignored.

The final entry for each night is the weight given the nightly average (presented in Appendix VII) in deriving the final average reflectivity for the asteroid. If certain filters were omitted in deriving the final average, they are so indicated. In some cases, for purposes of more accurate curve fitting, all reflectivities in a nightly average were multiplied by some factor prior to final averaging; any such factor is indicated. (In some more extreme cases, a multiplier was applied prior to deriving the nightly averages shown in Appendix VII. These are not indicated here.)

Commentary

A paragraph of comments is given for each asteroid. It is largely self-explanatory. The spectral reflectivity group assigned in Chap. IV is given at the end.

Average Spectral Reflectivity

The final averages are tabulated on the second page and are shown graphically in the final page of each section devoted to an asteroid. The standard deviation of the mean (mu) has been derived from the internal consistency of the data, where possible. Otherwise errors have been assigned on the basis of the counting statistics and expected systematic errors. All derived errors less than 0.03 have been arbitrarily set to 0.03 to indicate the approximate uncertainty in standard star calibrations and other possible sources of systematic error.

1 CERES

a = 2.766 AU e = 0.101 sin i = 0.169 Mars dist. = 0.62 AU Ceres (A-67)
B(1,0) = 4.11 B-V = 0.71 U-B = 0.42 L. Curve: $9^h.078$, 0.04 m.

(1) 10/12/70. 6 runs: 22:56, 23:00, 23:06, 23:57, 0:01, 0:03 ST ($0^h.05$).
i = 7° m = 7.7
Standard: χi^2 Ceti, sec z = 1.45 - 1.90, good. Counts = 5540.

Comments: There are no obvious differences among the six runs. Ceres, the ~~largest~~ asteroid, has a low albedo according to diverse kinds of measurements. Its mass has been estimated (Schubart, 1971), indicating a low density. Ceres has a flattish or even slightly bluish spectral reflectivity longwards of a sharp UV drop-off near 0.4 microns. There may be additional real structure in the reflectivity curve, but no obvious bands. Group B2.

1 CERES

Wavelength	Reflectivity	Mu
0.301	0.898	0.19
0.322	0.570	0.08
0.341	0.703	0.03
0.360	0.758	0.03
0.383	0.910	0.03
0.402	0.949	0.03
0.434	0.963	0.03
0.468	0.984	0.03
0.500	0.936	0.03
0.533	0.975	0.03
0.566	1.000	0.03
0.599	0.953	0.03
0.632	0.903	0.03
0.665	0.929	0.03
0.699	0.873	0.03
0.729	0.904	0.03
0.763	0.920	0.03
0.807	0.887	0.03
0.855	0.936	0.03
0.906	0.903	0.03
0.947	0.920	0.03
1.003	0.866	0.03
1.053	0.890	0.03
1.101	0.928	0.03

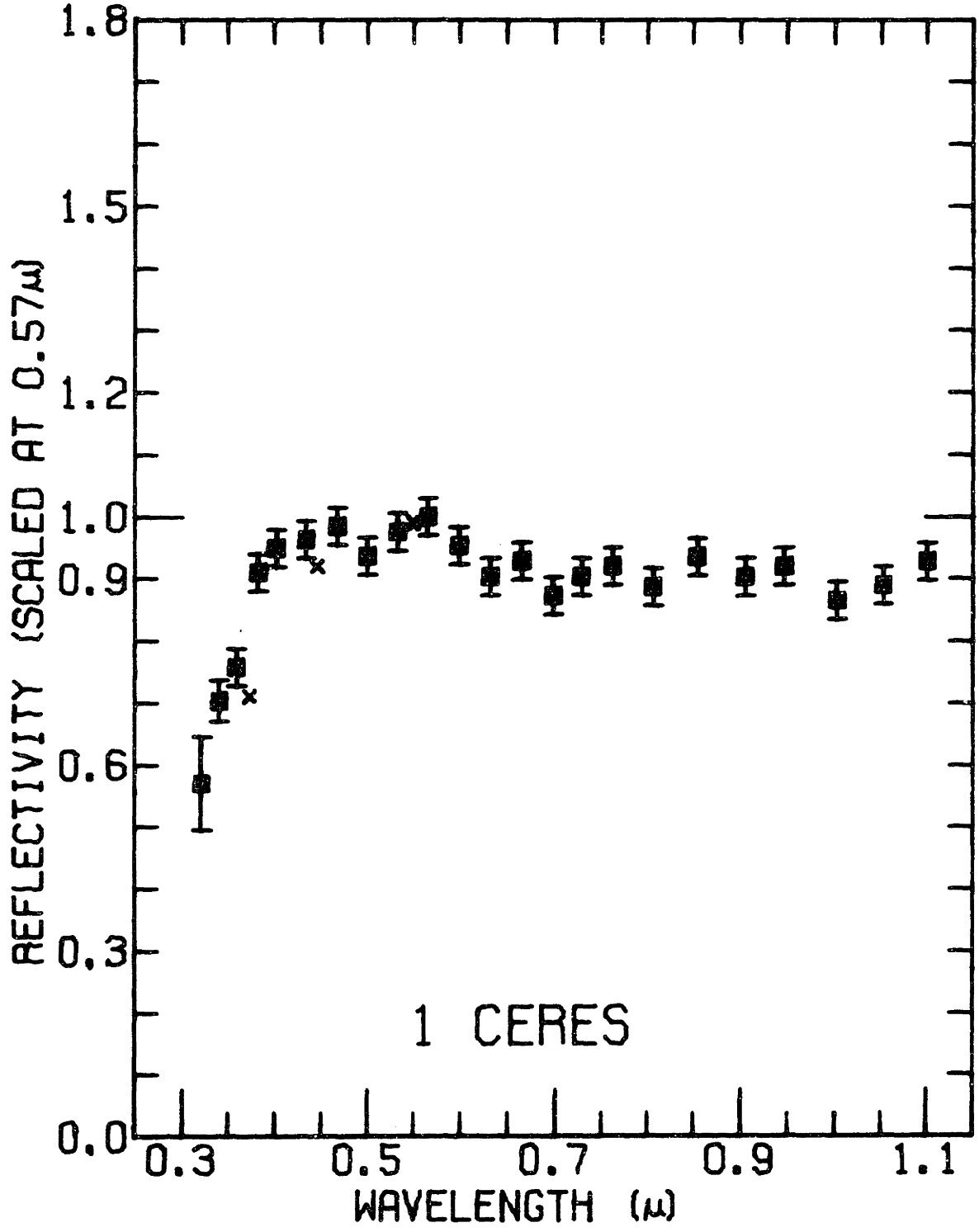
1.8
1.5
1.2
1.0
0.9
0.6
0.3
0.0
REFLECTIVITY (SCALED AT 0.57μ)
1 CERES
0.3
0.5
0.7
0.9
1.1
WAVELENGTH (μ)

2 PALLAS

a = 2.769 AU e = 0.256 sin i = 0.588 Mars dist. = 0.14 AU Pallas (B-28)
B(1,0) = 5.18 B-V = 0.65 U-B = 0.26 L. Curve: 9 - 12^h, 0.12 - 0.15 m.

(1) 8/8/70. 2½ runs: 20:53, 23:19, 1:30 ST (0^h.83). i = 9° m = 9.6
Standard: 29 Pisc., sec z = 1.13 - 1.56, very good. Counts = 1160.
Last run stopped due to dawn, Fil. 1 - 11 only. Single weight.

(2) 10/10/70. 9 runs: 20:37, 20:40, 20:43, 20:50, 20:52, 21:11, 21:15, 21:17, 21:21 ST (0^h.05). i = 14° m = 9.7
Standard: Epsilon Aqr., sec z = 1.25 - 1.30, very good. Counts = 1100. Double weight.

(3) 10/12/70. 5 runs: 20:54, 20:56, 20:58, 21:09, 21:21 ST (0^h.05)
i = 14° m = 9.7
Standard: Xi^2 Ceti, 29 Pisc., Epsilon Aqr., sec z = 1.25 - 1.28, fair. Counts = 530. ID: "certain". Single weight.

Comments: Comparison of runs (1) and (3) suggests a bluer color with increasing phase angle. The suggestion of bands near 0.7 and 0.95 microns is probably not significant. Both Veverka's (1970) polarization review and Matson's (1971) studies indicate a low albedo for this large and unusually bluish asteroid. The blue color of Pallas has been commented upon frequently by many workers since Bobrovnikoff's (1929) early reference. Group B3.

2 PALLAS

Wavelength	Reflectivity	Mu
0.301	1.173	0.48
0.322	0.867	0.15
0.341	0.906	0.17
0.360	0.783	0.10
0.383	1.050	0.08
0.402	0.967	0.05
0.434	1.021	0.08
0.468	0.996	0.05
0.500	0.998	0.07
0.533	0.999	0.03
0.566	1.000	0.03
0.599	1.001	0.05
0.632	0.953	0.04
0.665	0.961	0.05
0.699	0.922	0.05
0.729	0.972	0.04
0.763	0.974	0.05
0.807	1.035	0.04
0.855	0.968	0.05
0.906	0.985	0.04
0.947	0.939	0.05
1.003	0.975	0.03
1.053	0.960	0.04
1.101	1.052	0.11

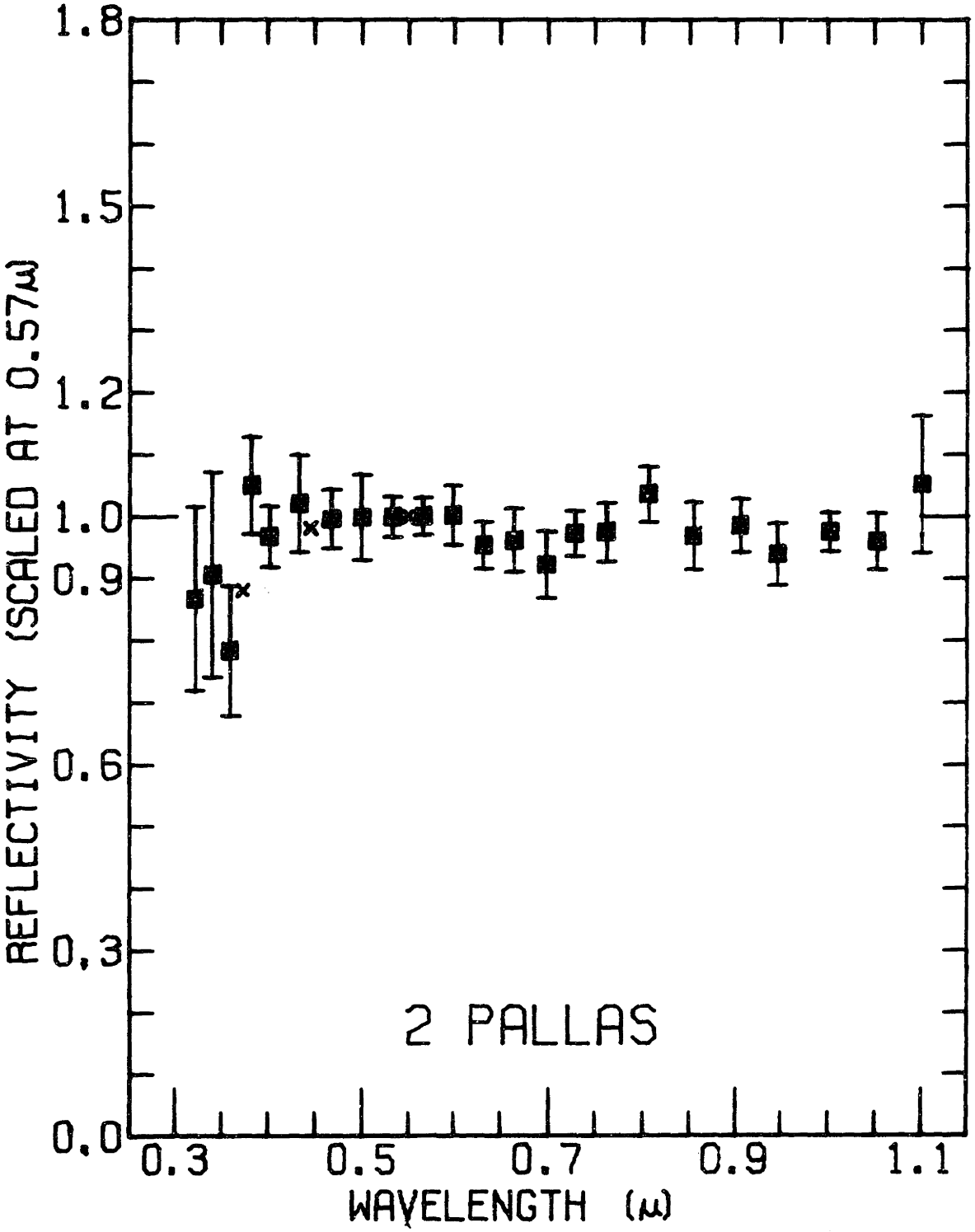
1.8
1.5
1.2
1.0
0.9
0.6
0.3
0.0
REFLECTIVITY (SCALED AT 0.57μ)
2 PALLAS
0.3
0.5
0.7
0.9
1.1
WAVELENGTH (μ)

3 JUNO

a = 2.668 AU e = 0.22 sin i = 0.246 Mars dist. = 0.23 AU Juno B(1,0) = 6.43 B-V = 0.81 U-B = 0.39 L. Curve: $7^h.213$, 0.15 m.

(1) 10/9/70. 7 runs: 3:13, 3:18, 3:20, 3:24, 4:06, 4:09, 4:13 ST ($0^h.03$). i = 20° m = 8.2
Standard: Xi^2 Ceti, sec z = 1.17 - 1.18, very good. Counts = 1380.
Double weight.

(2) 2/10/71. 2 runs: 4:40, 4:54 ST ($0^h.15$) i = 29° m = 9.0
Standard: Xi^2 Ceti, sec z = 1.15 - 1.17, good. S-20 (no ND).
Guiding: 14. Single weight.

Comments: There is a probable slight reddening with phase between the two sets of observations. The strength of the 0.97 micron band is not affected by the averaging of the S-20 run with the complete run (1). The band was possibly a bit stronger during the last three runs of Oct. 9 than it was earlier that night. A weak 0.6 micron band evident in the October observations is nearly absent in the February data. Several kinds of measurements indicate that Juno has a fairly high albedo (Dollfus, 1971; Allen, 1971; Veverka, 1970). It is difficult to be sure of the center position of the absorption band, but it is likely that Juno belongs to Group R3B.

3 JUNO

Wavelength	Reflectivity	Mu
0.322	0.577	0.09
0.341	0.629	0.08
0.360	0.708	0.05
0.383	0.700	0.05
0.402	0.723	0.03
0.434	0.776	0.04
0.468	0.868	0.03
0.500	0.912	0.03
0.533	0.989	0.03
0.566	1.000	0.03
0.599	0.999	0.03
0.632	1.052	0.03
0.665	1.104	0.03
0.699	1.151	0.03
0.729	1.122	0.04
0.763	1.178	0.04
0.807	1.189	0.03
0.855	1.166	0.03
0.906	1.106	0.03
0.947	1.071	0.03
1.003	1.107	0.03
1.053	1.127	0.05
1.101	1.085	0.08

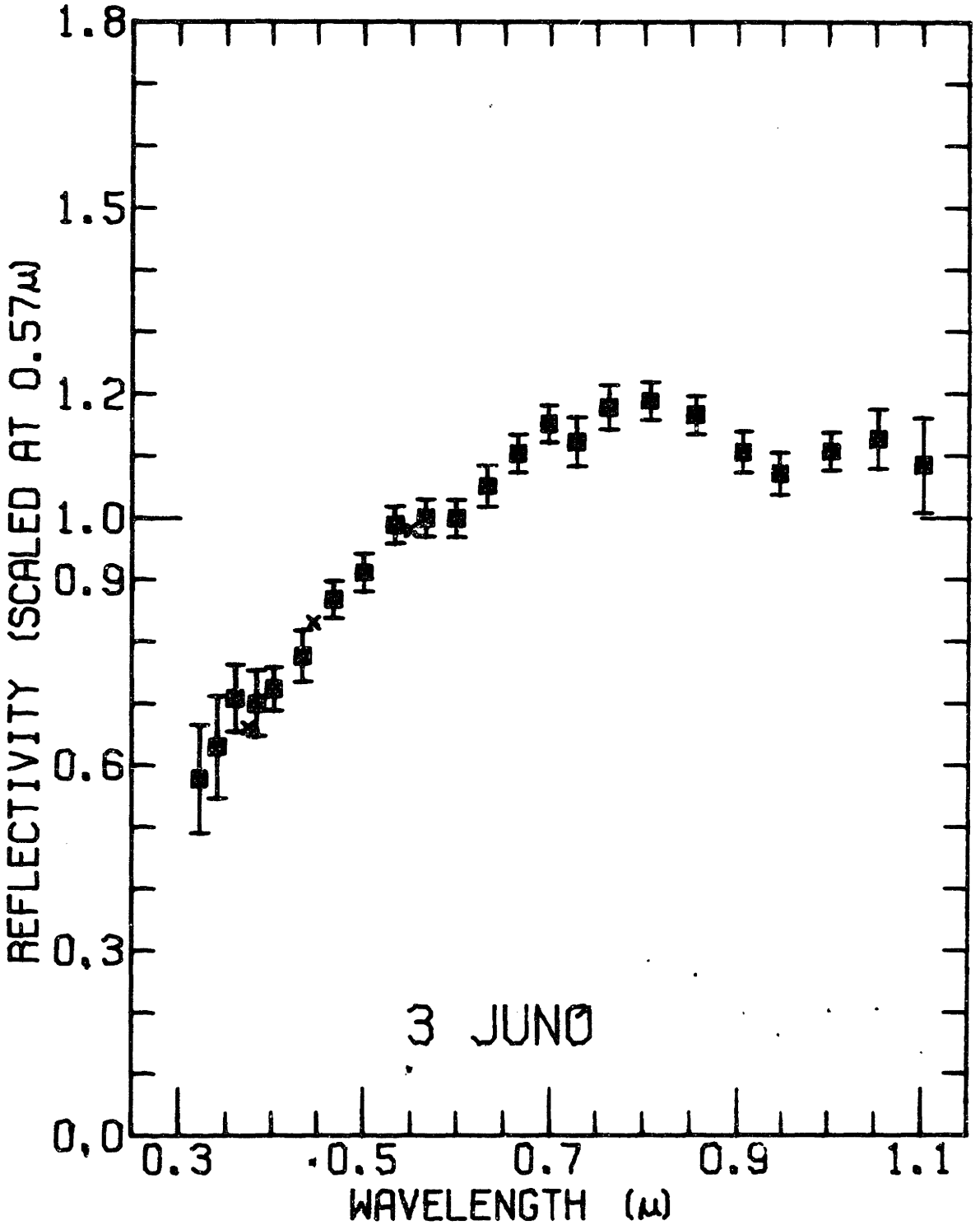
1.8
1.5
1.2
1.0
0.9
0.6
0.3
0.0
REFLECTIVITY (SCALED AT 0.57μ)
3 JUNO
0.3
0.5
0.7
0.9
1.1
WAVELENGTH (μ)

4 VESTA

a = 2.362 AU e = 0.263* sin i = 0.111* Vesta

B(1,0) = 4.31 B-V = 0.77 U-B = 0.46 L. Curve: $5^{h}.342129$, 0.1 - 0.13 m.

Comments: The data presented here were obtained on 2/16/70 by Torrence Johnson and Jay Kunin, using equipment and methods similar to those I have used for other asteroids. The data were taken over several hours ($i = 5^{\circ}$, m = 6.9) but not in the far UV. The albedo of Vesta is quite high as determined by direct diameter measurements, polarization, and thermal IR (Dollfus, 1971; Veverka, 1970; Allen, 1970). Matson (1971, private communication) informs me that he has adopted 10% as a final absolute (Bond) albedo for Vesta from his thermal IR measurements, which implies a geometric albedo appreciable less than those derived by other methods, but still among the highest yet found for an asteroid. The mass of Vesta determined by Hertz (1968) yields a density considerably higher than that of Ceres, but the new albedoes and diameters suggest densities similar to (or less than) that of the moon, not the 8 gm cm^{-3} originally indicated. Vesta shows a band near 0.95 microns which is much stronger than any yet observed on another asteroid. The standard star reduction adopted in this thesis results in a different band position than that reported by McCord et al (1970), but the indicated composition is changed in only a minor way (see Chap. VII for a complete discussion). The proper elements listed above are from a list by Arnold, not from Williams. Group M3.

4 VESTA

Wavelength	Reflectivity	Mu
0.402	0.787	0.03
0.434	0.866	0.03
0.468	0.917	0.03
0.500	0.928	0.03
0.533	0.987	0.03
0.566	1.000	0.03
0.599	1.008	0.03
0.632	1.012	0.03
0.665	1.004	0.03
0.699	1.047	0.03
0.729	1.076	0.03
0.763	1.072	0.03
0.807	1.023	0.03
0.855	0.936	0.03
0.906	0.830	0.03
0.947	0.794	0.03
1.003	0.878	0.03
1.053	0.939	0.03
1.101	1.161	0.15

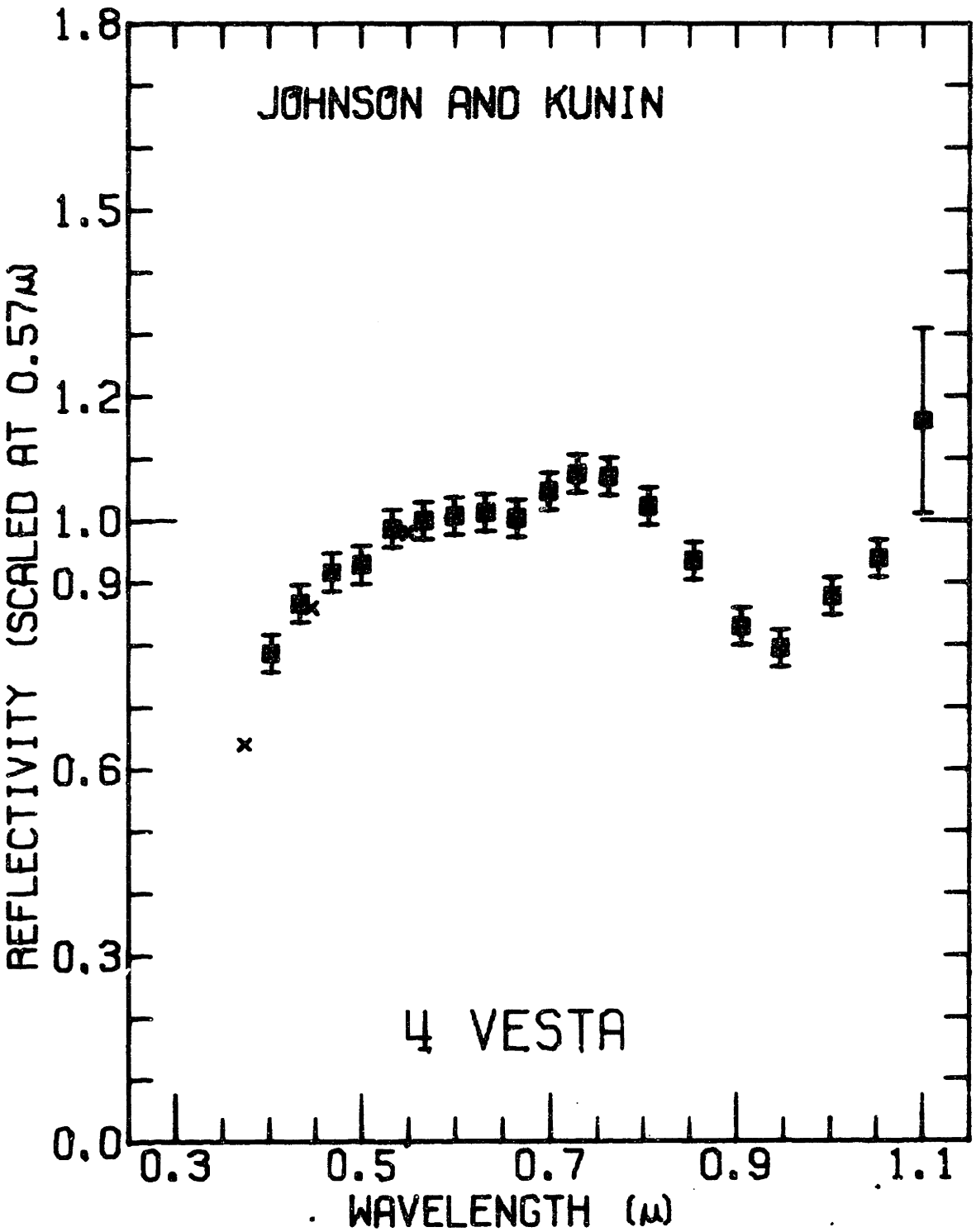
JOHNSON AND KUNIN
4 VESTA
REFLECTIVITY (SCALED AT 0.57μ)
WAVELENGTH (μ)
1.8
1.5
1.2
1.0
0.9
0.6
0.3
0.0
0.3
0.5
0.7
0.9
1.1

5 ASTRAEA

a = 2.579 AU e = 0.214 sin i = 0.082 Mars dist. = 0.20 AU Astraea

B(1,0) = 8.00 B-V = 0.82 U-B = 0.36 L. Curve: $16^{h}.806$, 0.21 - 0.27 m.

(1) 2/10/71. 1 run: 14:01 ST ($0^{h}.15$). i = 25° m = 11.9

Standard: 109 Vir. and Zeta Oph., sec z = 1.45, good. S-20 + ND2.

ID: "probably correct asteroid; in right place but Palomar Sky Survey reproduction poor".

Comments: No data were taken in the IR. This red asteroid could be in Group R1, R2A, or R3A.

5 ASTRAEA

Wavelength	Reflectivity	Mu
0.322	1.165	0.03
0.341	0.510	0.03
0.360	0.791	0.03
0.383	0.523	0.03
0.402	0.723	0.03
0.434	0.754	0.03
0.468	0.814	0.03
0.500	0.806	0.03
0.533	0.892	0.03
0.566	1.000	0.03
0.599	1.033	0.03
0.632	1.026	0.03
0.665	1.104	0.03
0.699	1.065	0.03
0.729	1.192	0.03
0.763	1.164	0.03
0.807	1.320	0.03
0.855	0.954	0.03

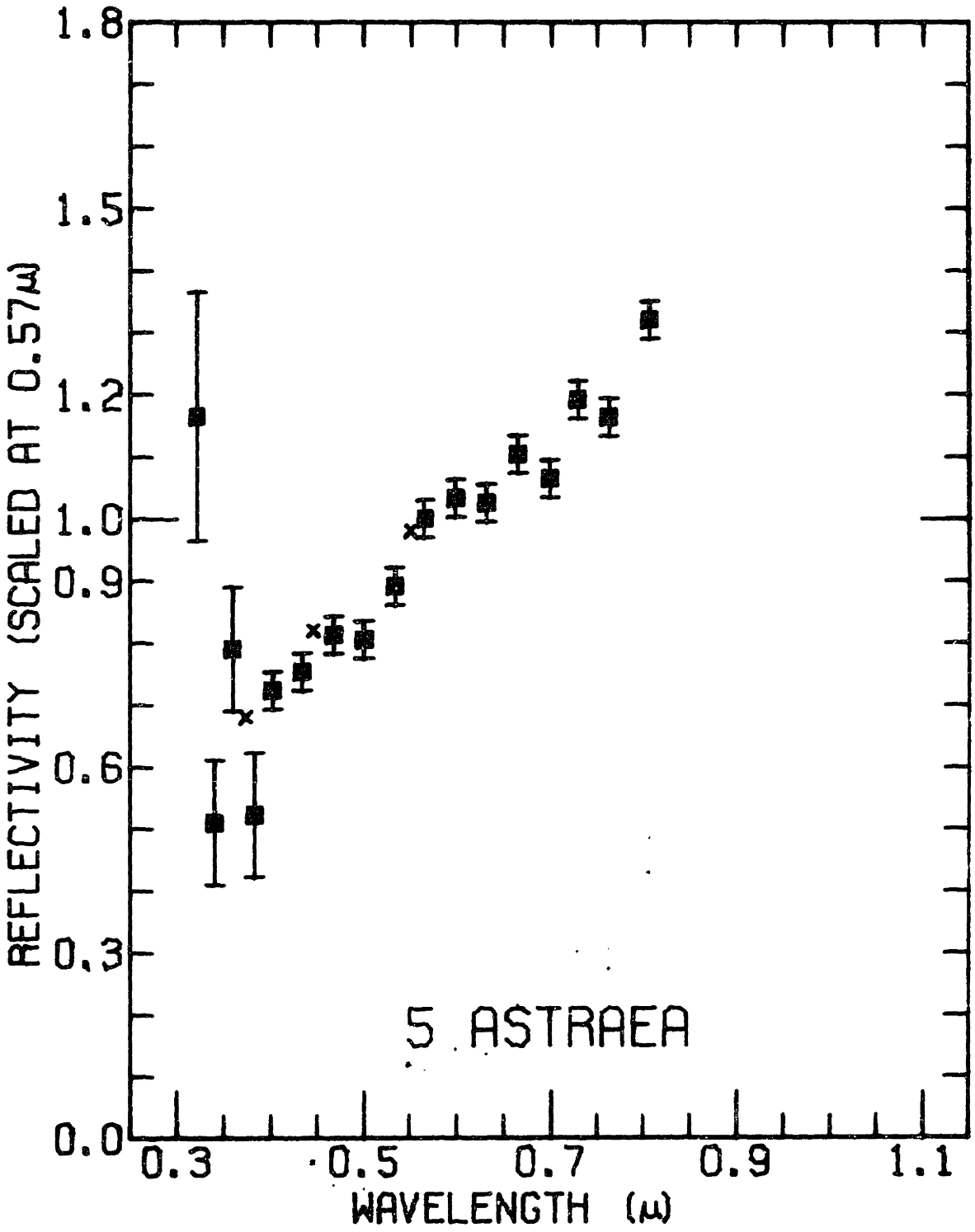
1.8
1.5
1.2
1.0
0.9
0.6
0.3
0.0
REFLECTIVITY (SCALED AT 0.57μ)
5 ASTRAEA
0.3
0.5
0.7
0.9
1.1
WAVELENGTH (μ)

6 HEBE

a = 2.426 AU e = 0.155 sin i = 0.249 Mars dist. = 0.08 AU None

B(1,0) = 6.70 B-V = 0.82 U-B = 0.41 L. Curve: $7^h.275$, 0.06 - 0.16 m.

(1) 2/9/71. 1 run: 13:41 ST ($0^h.3$). i = $18\frac{1}{2}^\circ$ m = 11.4
Standard: 109 Vir., sec z = 1.17, very good. S-20 + ND2. ID: "easily identified". Single weight (fil. 19 omitted).

(2) 2/10/71. 1 run: 13:22 ST ($0^h.2$). i = $18\frac{1}{2}^\circ$ m = 11.4
Standard: 109 Vir., sec z = 1.18, good. S-20 + ND2. Single weight. (fil. 19 omitted).

(3) 2/12/71. $1\frac{1}{2}$ runs: 12:30, 13:44 ($0^h.8$) i = $18\frac{1}{2}^\circ$ m = 11.3
Standard: Theta Vir., 109 Vir., and Zeta Oph., sec z = 1.16 - 1.27, good. Counts = 2360. ID: "positive due to relative motion". Guiding: 14, 18. No obvious differences between two runs; first for fil. 11-23 only. Double weight.

Comments: The strength of the 0.95 micron absorption band is considerably enhanced in the final average due to the spurious effect of averaging in the redder S-20 runs. However, the existence of the band seems real from run (3) alone. The differences in redness seem to be a real effect of rotational phase. Run (2) is the reddest, run (3) the least red, and run (1) most nearly like run (3). The color difference corresponds approximately to 0.06 magnitudes for B-V although it extends at least through the range 0.3 to 0.9 microns. Assuming the rotation period given above, run (2) shows a side of Hebe more than a quarter of a revolution away from the side seen in run (1). This is consistent with the color

6 HEBE

Wavelength	Reflectivity	Mu
0.322	0.556	0.03
0.341	0.598	0.06
0.360	0.704	0.06
0.383	0.716	0.03
0.402	0.722	0.03
0.434	0.733	0.03
0.468	0.823	0.03
0.500	0.828	0.03
0.533	0.946	0.03
0.566	1.003	0.03
0.599	0.997	0.03
0.632	1.024	0.03
0.665	0.990	0.06
0.699	1.031	0.03
0.729	1.129	0.05
0.763	1.141	0.06
0.807	1.158	0.05
0.855	1.147	0.07
0.906	1.067	0.03
0.947	1.036	0.03
1.003	1.096	0.04
1.053	1.148	0.03
1.101	1.274	0.03

differences observed. The shape of Hebe's light curve is consistent with appreciable albedo variations across the surface of the asteroid. A discussion of the possible correlation of these observations with thermal IR flux variations observed by Matson is given in Chap. VI. Hebe is a moderately reflective asteroid. Group R3B.

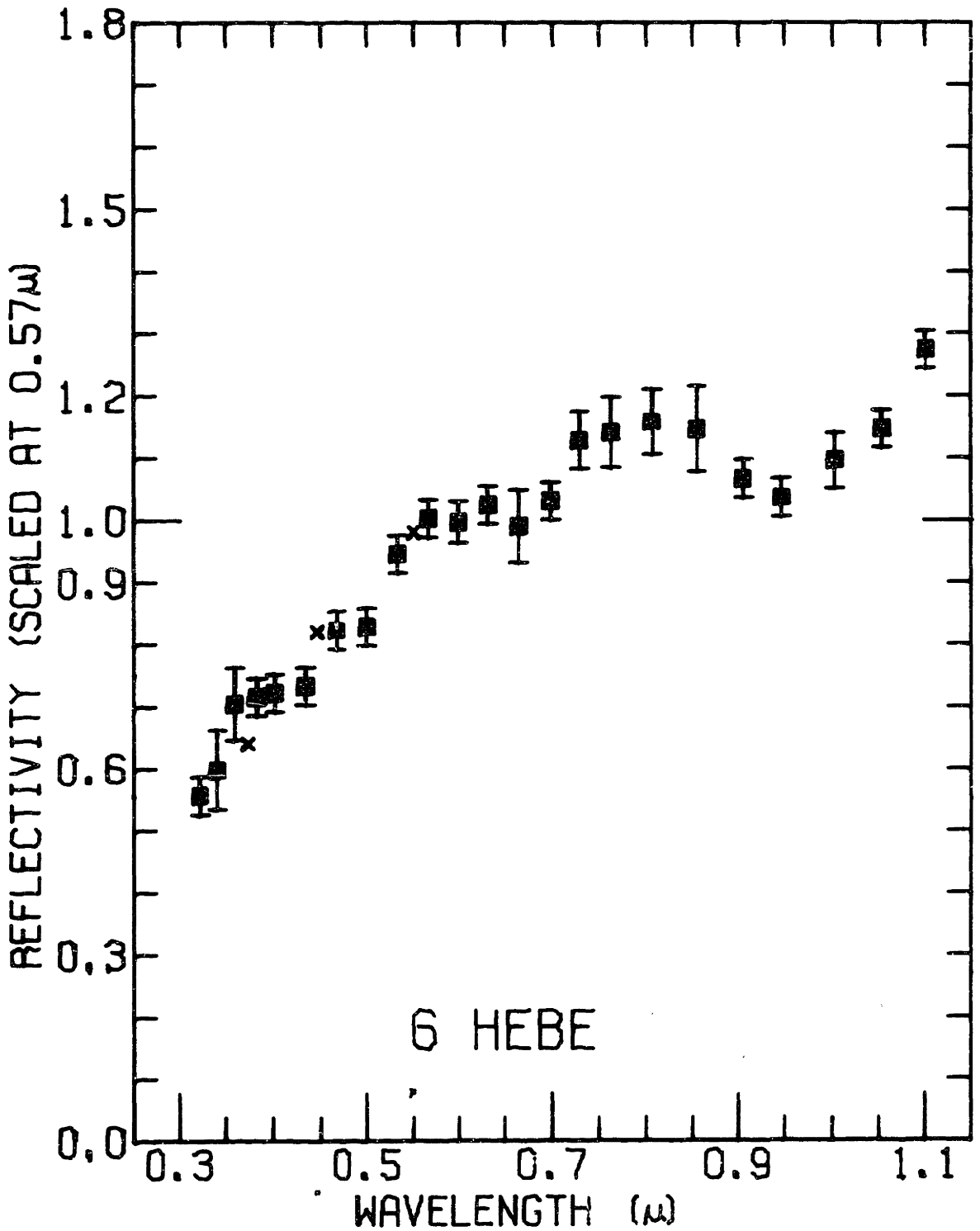
1.8
1.5
1.2
1.0
0.9
0.6
0.3
0.0
REFLECTIVITY (SCALED AT 0.57μ)
6 HEBE
0.3
0.5
0.7
0.9
1.1
WAVELENGTH (μ)

7 IRIS

a = 2.386 AU e = 0.210 sin i = 0.115 Mars dist. = 0.05 AU None

B(1,0) = 6.84 B-V = 0.83 U-B = 0.45 L. Curve: $7^h.135$, 0.04 - 0.29 m.

(1) 1/7/71. 1 run: 12:19 ST ($1^h.0$). i = 22° m = 11.4

Standard: Theta Vir., sec z = 1.42, very good. Counts = 810. ID: "easily located as a bright star, but not observed long enough to detect motion." Guiding: 6,18,20. Located low in southerly sky, possibly some thin clouds. Single weight.

(2) 2/7/71. 2 runs: 12:54, 13:49 ST ($0^h.4$). i = 18° m = 11.0

Standard: Theta Vir., sec z = 1.41 - 1.47, fair. S-20 (no ND). Guiding: 8, 13, 14, 15. Single weight (except fil. 16 - 18 omitted).

(3) 5/9/71. 5 runs: 11:23, 11:32, 11:37, 11:41, 11:46 ST ($0^h.44$).

i = 15° m = 11.0

Standard: Theta Crt., sec z = 1.27 - 1.28, very good. S-20 (no ND) for UV and visible, S-1 for IR. Counts (IR) = 2200. Single weight.

Comments: There were some minor problems with all runs, but the average should be good. The separate runs on individual nights are in good agreement. There may be a reddening with phase angle, but it should be noted that Iris shows a light curve with large amplitude (though probably due mainly to shape). According to Gehrels (1970) the pole appears to be so oriented that I was looking approximately pole-on in February, toward the equator in May, and at an intermediate latitude in January. Thus we cannot remove possible effects due to either rotational phase angle or aspect in measuring possible phase angle effects. There is a suggestion

7 IRIS

Wavelength	Reflectivity	Mu
0.322	0.500	0.05
0.341	0.628	0.07
0.360	0.617	0.03
0.383	0.597	0.03
0.402	0.696	0.03
0.434	0.736	0.03
0.468	0.862	0.03
0.500	0.892	0.03
0.533	0.956	0.03
0.566	1.000	0.03
0.599	1.062	0.03
0.632	1.062	0.03
0.665	1.108	0.05
0.699	1.098	0.03
0.729	1.194	0.09
0.763	1.266	0.09
0.807	1.252	0.03
0.855	1.155	0.03
0.906	1.181	0.03
0.947	1.146	0.03
1.003	1.146	0.03
1.053	1.093	0.04

of an 0.65 micron absorption feature in the May data (least i) and a weakened IR absorption band, but possible difficulties in the May reduction procedures cannot be ruled out. It is interesting to note the very prominent fall-off longwards of 0.7 microns in the February S-20 data (omitted for computing a final average). This may have been the beginning of a very strong absorption feature, but more likely is a problem with the standard star data. Group R2A.

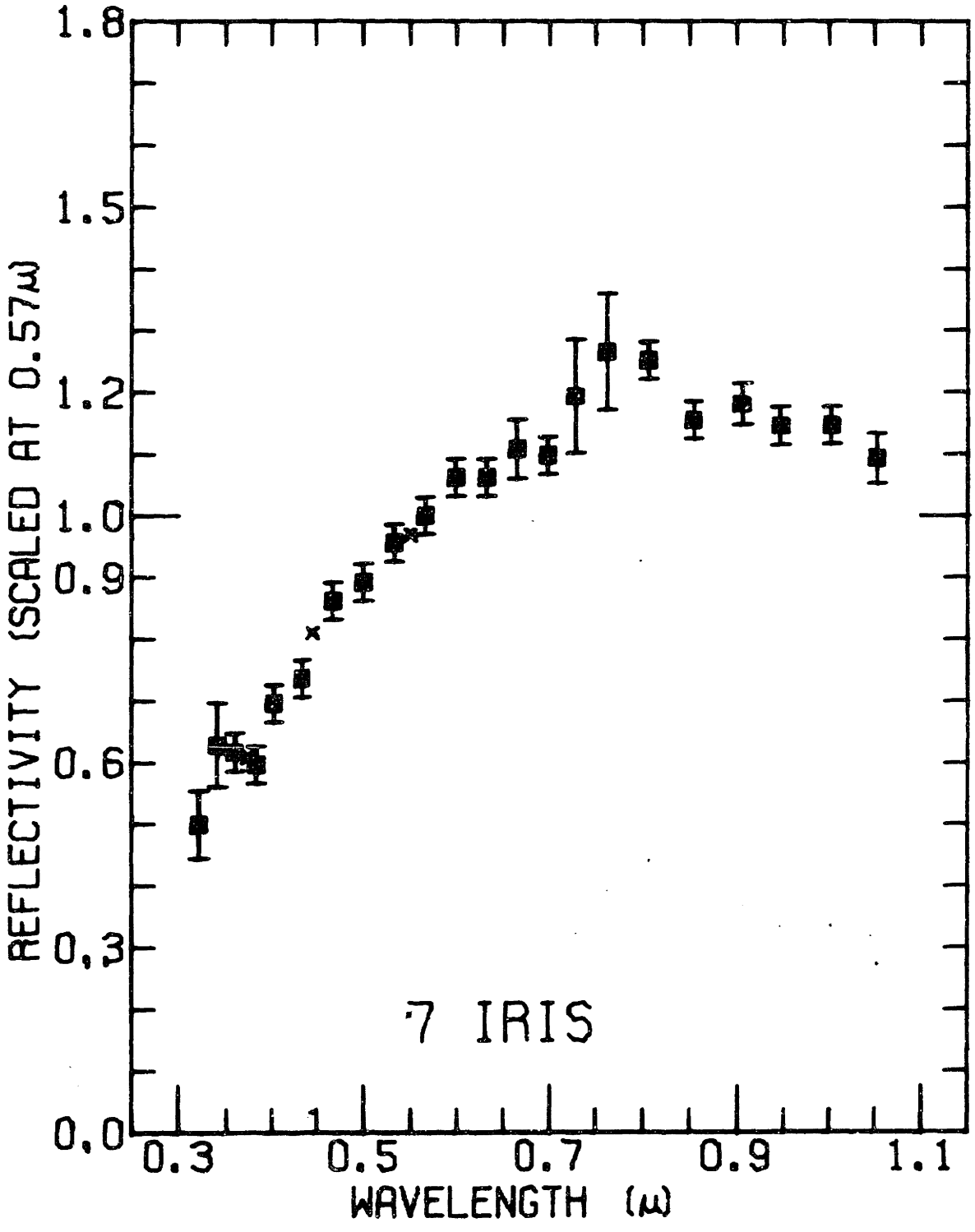
1.8
1.5
1.2
1.0
0.9
0.6
0.3
0.0
REFLECTIVITY (SCALED AT 0.57μ)
7 IRIS
0.3
0.5
0.7
0.9
1.1
WAVELENGTH (μ)

10 HYGIEA

a = 3.151 AU e = 0.127 sin i = 0.09 Mars dist. = 0.90 AU Hygiea B(1,0) = 6.57 B-V = 0.70 U-B = 0.40 L. Curve: $18^{h}.?$, 0.10 m.

(1) 1/5/71. 1 run: 10:56 ST ($0^{h}.97$). i = 9° m = 10.8
Standard: Gamma Gem., sec z = 1.17, good. Counts = 1110. ID: "was quite bright and must have been Hygiea though no motion was observed". Guiding: 6, 22. Guiding only fair; no data for fil. 20 and 24. Single weight.

(2) 2/9/71. 1 partial run: 5:27 ST ($0^{h}.6$). i = 3° m = 10.7
Standard: Alpha Leo, sec z = 1.47, fair to good. Counts = 2920. Problems with city power supply; data for fil. 1 - 8 destroyed. Double weight.

(3) 2/9/71. 1 run: 12:46 ST ($0^{h}.12$). i = 3° m = 10.7
Standard: Alpha Leo and 109 Vir., sec z = 1.85, fair. S-20 + ND2. Telescope dome flooded with moonlight. Zero weight.

(4) 2/10/71. 1 run: 10:31 ST ($0^{h}.1$). i = $3\frac{1}{2}$° m = 10.7
Standard: Alpha Leo, sec z = 1.15, good. S-20 + ND2. Guiding: 14. Single weight.

Comments: The quality of the data for Hygiea is only fair due to a variety of problems. Apparent discrepancies in color (a range of about 0.08 mag. in B-V) may be due to rotational differences or to problems; in any case the data show too much variation to determine a phase variation of color. There is a tendency for S-1 data to be flat, S-20 data

10 HYGIEA

Wavelength	Reflectivity	Mu
0.322	0.783	0.06
0.341	0.832	0.04
0.360	0.992	0.21
0.383	0.845	0.04
0.402	0.836	0.04
0.434	0.923	0.07
0.468	0.916	0.03
0.500	0.961	0.03
0.533	1.005	0.03
0.566	1.000	0.03
0.599	0.922	0.03
0.632	0.908	0.03
0.665	0.967	0.05
0.699	0.939	0.05
0.729	0.992	0.05
0.763	0.984	0.03
0.807	0.966	0.05
0.855	0.980	0.04
0.906	0.946	0.03
0.947	0.884	0.03
1.003	0.872	0.03
1.053	0.879	0.03
1.101	0.934	0.03

to show a reddish trend. There can be no doubt, however, of the primary qualitative characteristic of Hygiea's spectral reflectivity: it is relatively flat over the entire range 0.3 to 1.1 microns. A dip near 0.6 microns is apparent in all four runs and is probably real. The evidence for a long-wavelength band is weak. Group B3.

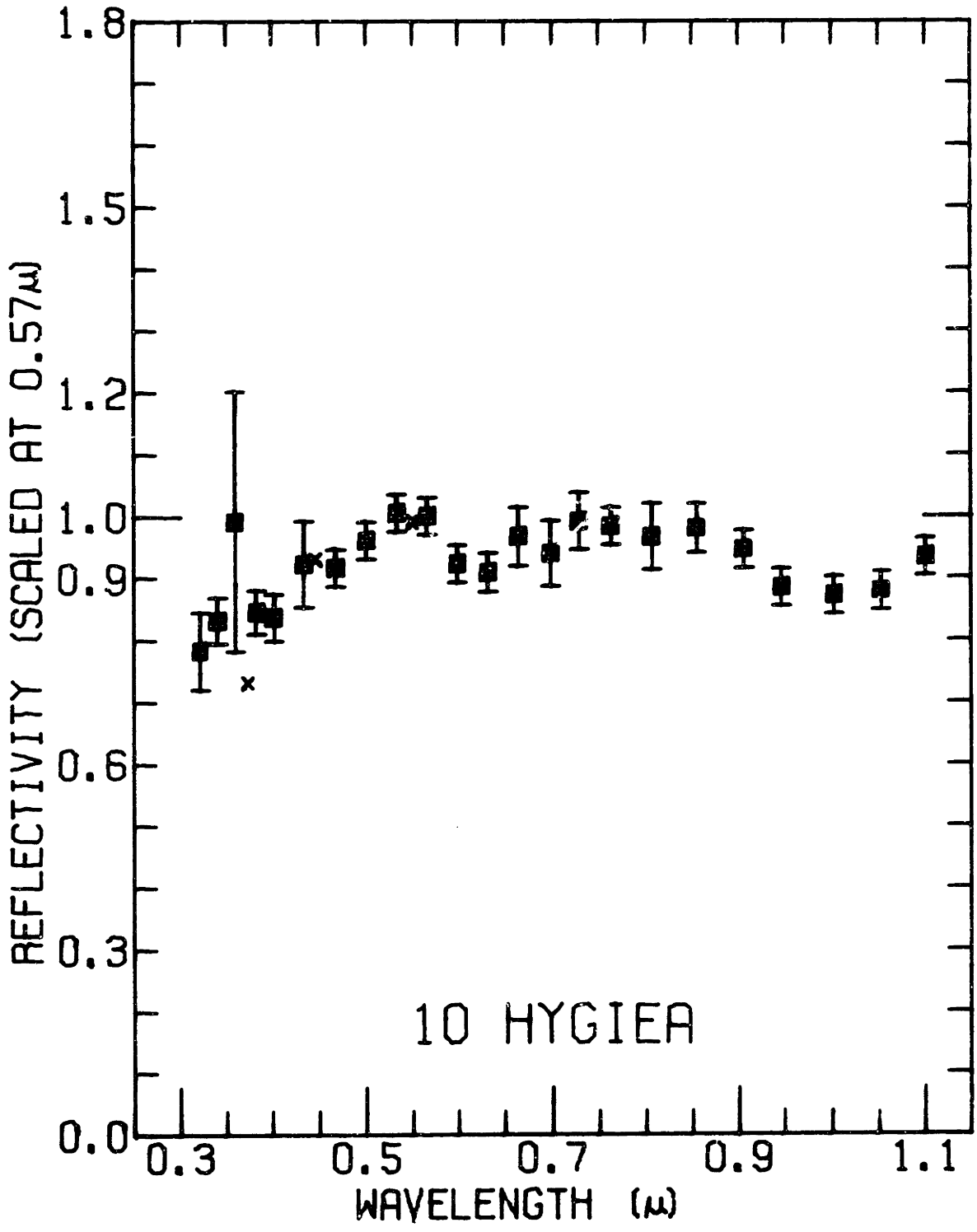
1.8
1.5
1.2
1.0
0.9
0.6
0.3
0.0
REFLECTIVITY (SCALED AT 0.57μ)
10 HYGIEA
0.3
0.5
0.7
0.9
1.1
WAVELENGTH (μ)

11 PARTHENOPE

a = 2.452 AU e = 0.074 sin i = 0.069 Mars dist. = 0.46 Parth. (A-76)
B(1,0) = 7.78 B-V = 0.80 U-B = 0.38 L. Curve: $10^{h}.67$, 0.07 - 0.12 m.

(1) 8/6/70. 2 runs: 22:07, 0:52 ST ($0^{h}.87$). i = 25^{o} m = 10.7
Standard: Eta Pisc., sec z = 1.17 - 1.84, fair. Counts = 260.
Dawn was beginning during second run. Eta Pisc. not well calibrated.
Zero weight.

(2) 10/12/70. 3 runs: 22:11, 22:16, 22:22 ST ($0^{h}.05$). i = 4^{o} m = 10.2
Standard: 29 Pisc. and Xi^{2} Ceti, sec z = 1.74 - 1.87, very good.
Counts = 540. Single weight.

Comments: Run (1) looks very peculiar; in view of the low counting statistics and possibilities for systematic errors in the 24-inch procedures, it has been ignored in determing the final average. Run (2) also has low counting statistics -- too low to reveal any possible 0.9 absorption band that may be present. The overall shape of the reflectivity curve of Parthenope places it in Group M4 or maybe M1.

11 PARTHENOPE

Wavelength	Reflectivity	Mu
0.301	1.055	2.56
0.322	1.043	0.21
0.341	0.407	0.34
0.360	0.954	0.13
0.383	0.705	0.04
0.402	0.876	0.10
0.434	0.755	0.05
0.468	0.982	0.05
0.500	0.914	0.03
0.533	0.966	0.14
0.566	1.000	0.03
0.599	1.034	0.06
0.632	1.016	0.03
0.665	1.135	0.08
0.699	1.123	0.06
0.729	1.063	0.05
0.763	1.205	0.07
0.807	1.105	0.04
0.855	1.141	0.05
0.906	1.088	0.05
0.947	1.090	0.05
1.003	1.138	0.04
1.053	1.183	0.07
1.101	1.107	0.08

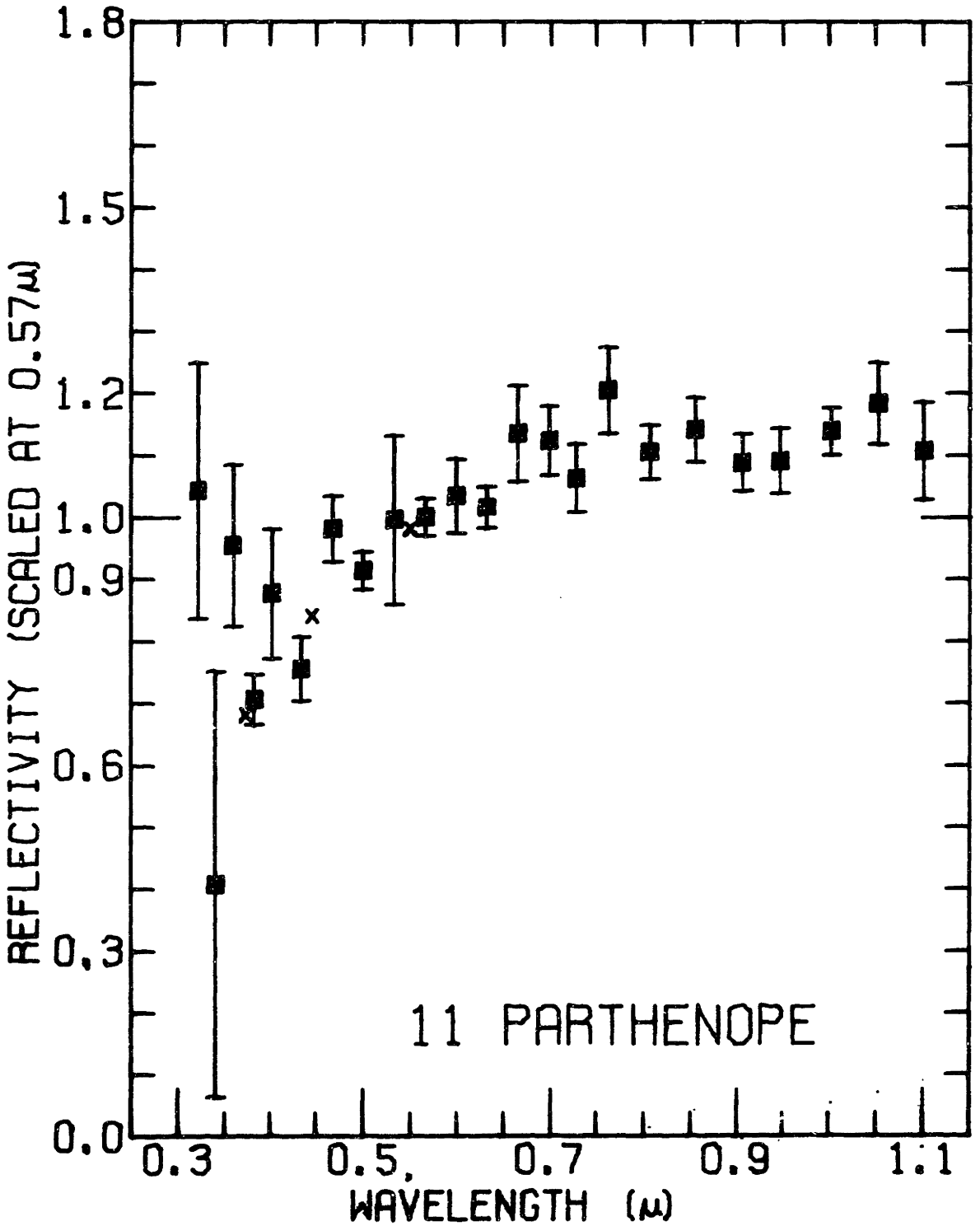
1.8
1.5
1.2
1.0
0.9
0.6
0.3
0.0
REFLECTIVITY (SCALED AT 0.57μ)
11 PARTHENOPE
0.3
0.5
0.7
0.9
1.1
WAVELENGTH (μ)

12 VICTORIA

a = 2.333 AU e = 0.170 sin i = 0.164 Mars dist. = 0.07 AU Victoria (A77)

B(1,0) = 8.81 B-V = 0.87* L. Curve: $8^h.654$*

(1) 5/9/71. $2\frac{1}{2}$ runs: 19:11, 19:13, 19:03 ST ($0^h.26$). l = 27° m = 11.3 Standard: Epsilon Aqr., sec z = 1.51, good. S-20 + ND1 for UV and visible, S-1 for IR. Counts (IR) = 1000. Guiding: star, 6,7.

Comments: There is good agreement between the separate runs. Unfortunately there appears to be a problem in matching the IR part of the reflectivity curve to that obtained with the S-20 tube; the off-shift of about 10% should not be regarded as significant in view of problems calibrating the ND1 filter. The data listed for B-V and rotation period are from Tempesti and Burchi (1969). This appears to be a very red asteroid. There is little suggestion of a long wavelength absorption feature, making 12 Victoria definitely different from 192 Nausikaa; both are part of possible jet stream J2. Group R1.

12 VICTORIA

Wavelength	Reflectivity	Mu
0.322	0.323	0.08
0.341	0.508	0.08
0.360	0.596	0.03
0.383	0.580	0.03
0.402	0.665	0.03
0.434	0.758	0.03
0.468	0.825	0.03
0.500	0.889	0.03
0.533	0.963	0.03
0.566	1.000	0.03
0.599	1.047	0.03
0.632	1.023	0.03
0.665	1.016	0.04
0.699	1.076	0.03
0.729	1.099	0.06
0.763	1.133	0.04
0.807	1.307	0.05
0.855	1.324	0.08
0.906	1.286	0.03
0.947	1.318	0.08
1.003	1.376	0.04
1.053	1.187	0.14
1.101	0.843	0.06

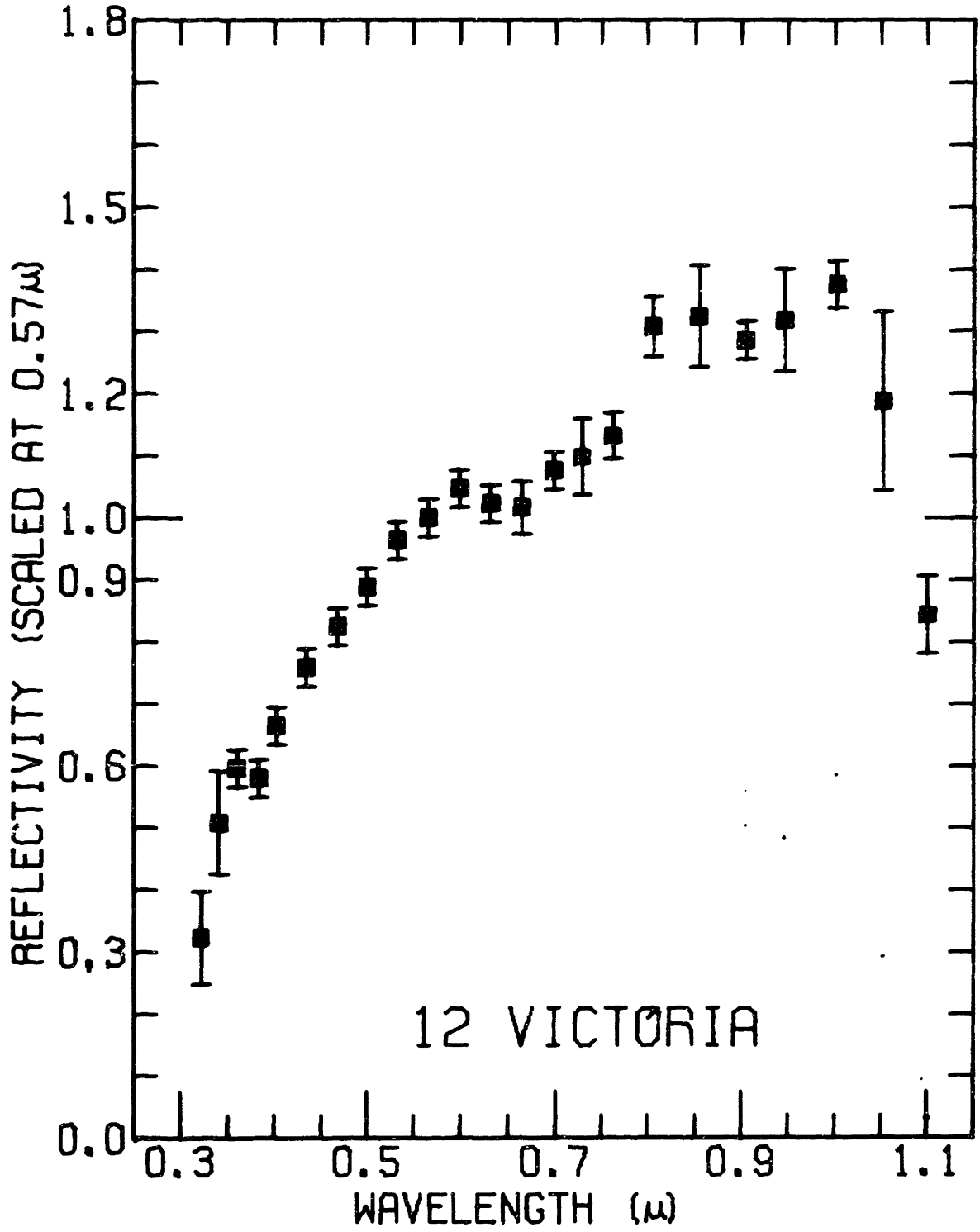
1.8
1.5
1.2
1.0
0.9
0.6
0.3
0.0
REFLECTIVITY (SCALED AT 0.57μ)
12 VICTORIA
0.3
0.5
0.7
0.9
1.1
WAVELENGTH (μ)

13 EGERIA

a = 2.576 AU e = 0.124 sin i = 0.282 Mars dist. = 0.34 Triplet

B(1,0) = 7.97 L. Curve: $7^{h}.045$, 0.12 m.

(1) 10/12/70. 6 runs: 0:18, 0:23, 0:28, 0:34, 0:57, 1:04 ST ($0^{h}.1$).

$i = 11^{\circ}$ m = 11.0

Standard: Xi^{2} Ceti, sec z = 1.20 - 1.34, very good. Counts = 840.

Comments: The separate runs are in good agreement. Egeria looks very much like Ceres. Group B2.

13 EGERIA

Wavelength	Reflectivity	Mu
0.301	1.103	1.15
0.322	0.405	0.17
0.341	0.581	0.13
0.360	0.502	0.08
0.383	0.898	0.14
0.402	0.784	0.05
0.434	0.935	0.09
0.468	1.069	0.04
0.500	0.931	0.05
0.533	1.008	0.03
0.566	1.000	0.03
0.599	0.944	0.05
0.632	0.914	0.03
0.665	0.944	0.03
0.699	0.866	0.05
0.729	0.936	0.05
0.763	0.959	0.03
0.807	0.916	0.05
0.855	1.068	0.03
0.906	0.906	0.06
0.947	0.933	0.04
1.003	0.888	0.03
1.053	0.978	0.05
1.101	0.796	0.09

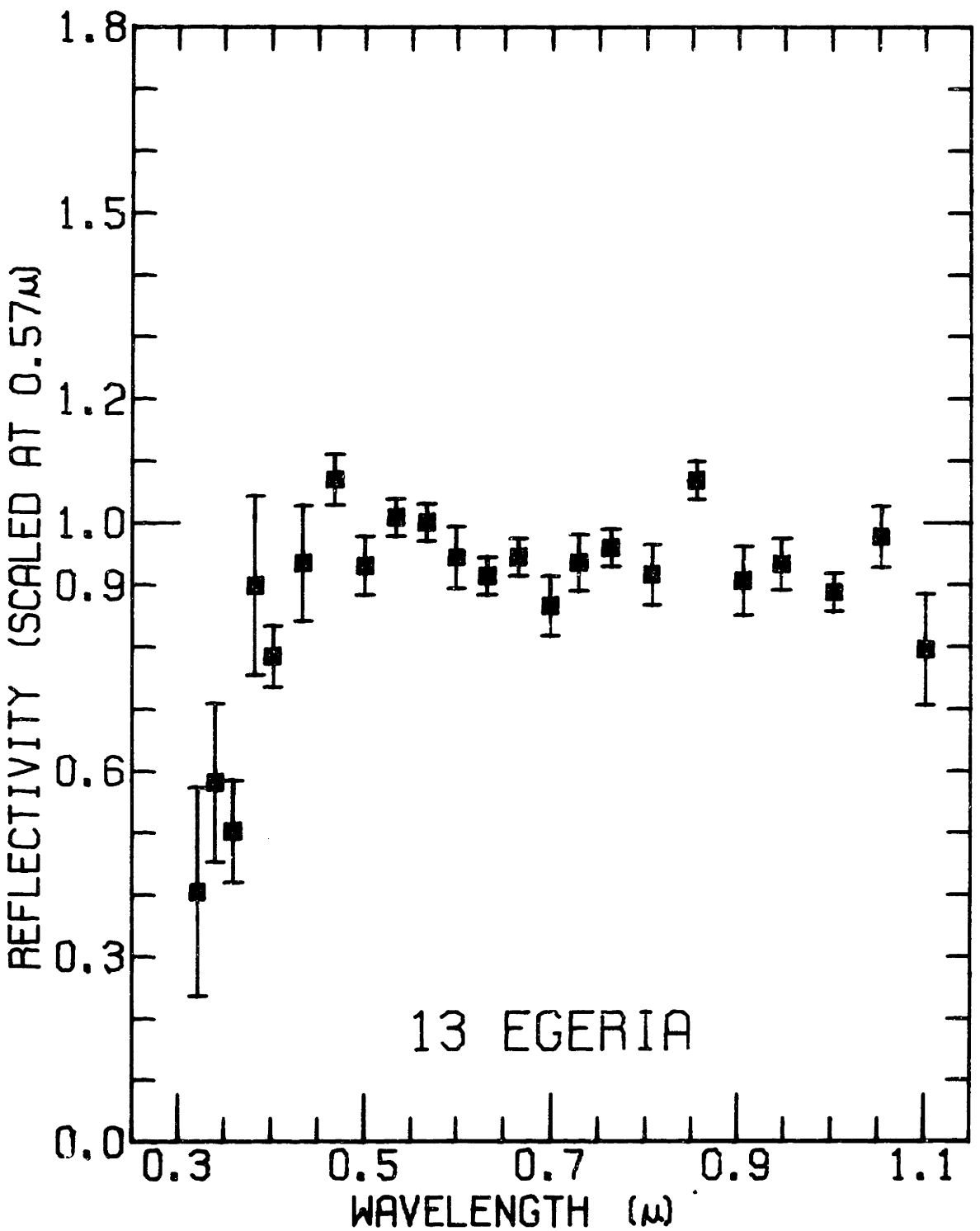
1.8
1.5
1.2
1.0
0.9
0.6
0.3
0.0
REFLECTIVITY (SCALED AT 0.57μ)
13 EGERIA
0.3
0.5
0.7
0.9
1.1
WAVELENGTH (μ)

14 IRENE

a = 2.588 AU e = 0.194 sin i = 0.151 Mars dist. = 0.25 AU Triplet
B(1,0) = 7.41 B-V = 0.81 U-B = 0.38 L. Curve: $11^{h}?$, 0.04 m.

(1) 12/29/70. 2 runs: 8:09, 10:45 ST ($1^{h}.35$) i = 10° m = 10.3
Standard: Gamma Gem., sec z = 1.01 - 1.19, fair. Counts = 1060. ID: "certain". Slight possibility of uncertainty in filter count for second run, but there are no obvious differences between the two runs and both show evidence of an absorption band. Single weight.

(2) 2/6/71. 1 run: 10:40 ST ($1^{h}.1$) i = 11° m = 10.2
Standard: Alpha Leo, sec z = 1.27, very good. Counts = 1810. ID: "definite". Sky conditions poor with gradually diminishing haze. Systematic color trends may not be real. Single weight.

(3) 2/7/71. 2 runs: 5:10, 6:05 ST ($0^{h}.67$) i = 11° m = 10.2
Standard: Gamma Gem., sec z = 1.07 - 1.18, very good. S-20 + ND2. Two runs identical. Single weight.

Comments: The February runs agree perfectly, but are different from the December run which is less red and shows an 0.9 micron band of which there is only a vague hint in run (2). The differences are unlikely to be a phase effect because the implied reddening of 0.4 mag. per degree is unrealistic. The reliability of the data is not too good. Clouds and haze could have reddened run (2) and run (1) was made with the 24-inch telescope in less-than-perfect conditions. Group R3B.

14 IRENE

Wavelength	Reflectivity	Mu
0.322	0.603	0.05
0.341	0.633	0.03
0.360	0.827	0.06
0.383	0.695	0.06
0.402	0.648	0.03
0.434	0.786	0.03
0.468	0.844	0.03
0.500	0.924	0.03
0.533	0.940	0.03
0.566	1.000	0.03
0.599	1.027	0.03
0.632	1.026	0.03
0.665	1.012	0.03
0.699	1.083	0.03
0.729	1.097	0.03
0.763	1.192	0.09
0.807	1.138	0.04
0.855	1.054	0.07
0.906	1.123	0.07
0.947	1.023	0.11
1.003	1.189	0.08
1.053	1.254	0.03
1.101	1.227	0.03

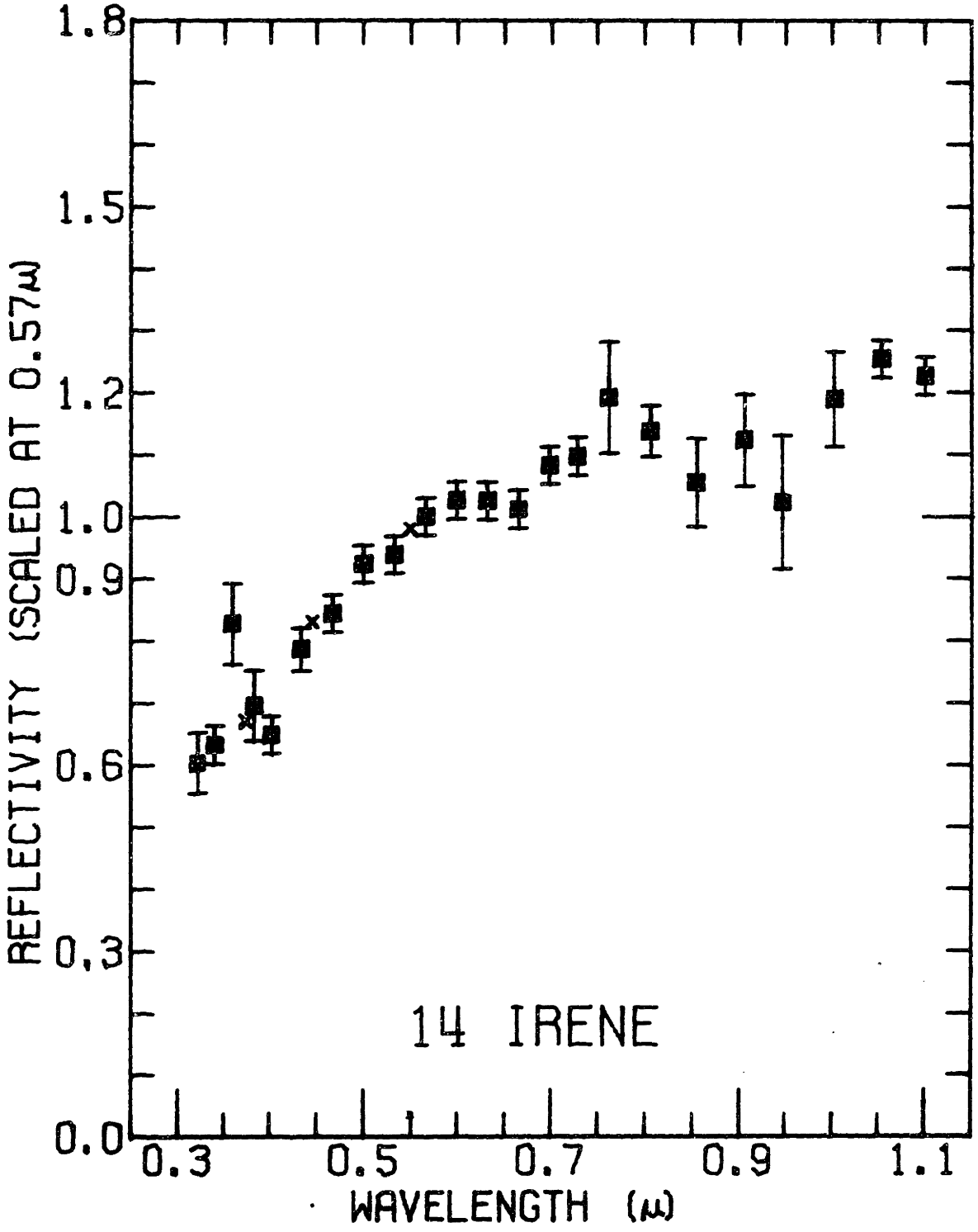
1.8
1.5
1.2
1.0
0.9
0.6
0.3
0.0
REFLECTIVITY (SCALED AT 0.57μ)
14 IRENE
0.3
0.5
0.7
0.9
1.1
WAVELENGTH (μ)

16 PSYCHE

a = 2.923 AU e = 0.099 sin i = 0.045 Mars dist. = 0.81 AU (B-13)

B(1,0) = 6.89 B-V = 0.70 U-B = 0.24 L. Curve: $4^h.303$, 0.11 m.

(1) 10/11/70. 10 runs: 2:19, 2:22, 2:28, 4:01, 4:06, 4:10, 4:16, 5:41, 5:44, 5:47 ST ($0^h.05$). i = 20° m = 10.3
Standard: Xi^2 Ceti, sec z = 1.04 - 1.32, very good. Counts = 790. Single weight.

(2) 1/4/71. 2 runs: 2:18, 4:59 ST ($0^h.97$). i = 12½° m = 10.3
Standard: Gamma Gem., sec z = 1.06 - 1.18, good. Counts = 1540. ID: "certain". Guiding: 9, 10, 15; star, 5, 7, 9, 15, 17, 20, 23, 24. Seeing horrible, reflectivities good to only 5% for first run. First run slightly brighter in IR (?). Run duration was an appreciable fraction of the rotation period. Single weight.

(3) 1/6/71. 1 run: 3:23 ST ($1^h.1$). i = 13° m = 10.3
Standard: Xi^2 Ceti and Gamma Gem., sec z = 1.07, fair. Counts = 1120. Guiding: 10, 16, 17; star, 11, 14, 17, 18, 21, 22. Possible scattered light (?). Run duration was an appreciable fraction of the rotation period. Single weight.

(4) 2/10/70. 1 run: 5:31 ST ($0^h.18$). i = 20° m = 10.8
Standard: Gamma Gem., sec z = 1.06, good. S-20 + ND2. Single weight.

Comments: There is no clearcut reddening with phase. The run at largest phase angle (run 4) is quite red (B-V about 0.73), but run (1) at a similar phase angle is not nearly so red (0.67). The January runs (least

16 PSYCHE

Wavelength	Reflectivity	Mu
0.301	1.747	0.43
0.322	0.871	0.07
0.341	0.831	0.06
0.360	0.830	0.06
0.383	0.814	0.08
0.402	0.823	0.04
0.434	0.904	0.04
0.468	0.907	0.03
0.500	0.949	0.04
0.533	0.991	0.05
0.566	0.981	0.03
0.599	0.995	0.05
0.632	1.000	0.04
0.665	1.034	0.04
0.699	1.037	0.04
0.729	1.069	0.03
0.763	1.093	0.05
0.807	1.118	0.05
0.855	1.187	0.04
0.906	1.143	0.04
0.947	1.144	0.06
1.003	1.242	0.04
1.053	1.83	0.07
1.101	1.198	0.10

phase angles) have B-V about 0.68. The differences are more likely due to slight rotational differences. Psyche has the shortest known rotation period for a major asteroid and much of its brightness fluctuations appear due to spots rather than shape. An attempt to search for color differences with rotation on Oct. 11 suffers from poor statistics but may have a positive result (see Chap. VI). The reflectivity curve for Psyche

is unique among asteroids studied; it has a flat slope throughout the range 0.3 to 1.1 microns, but with a reddish trend. Group M1.

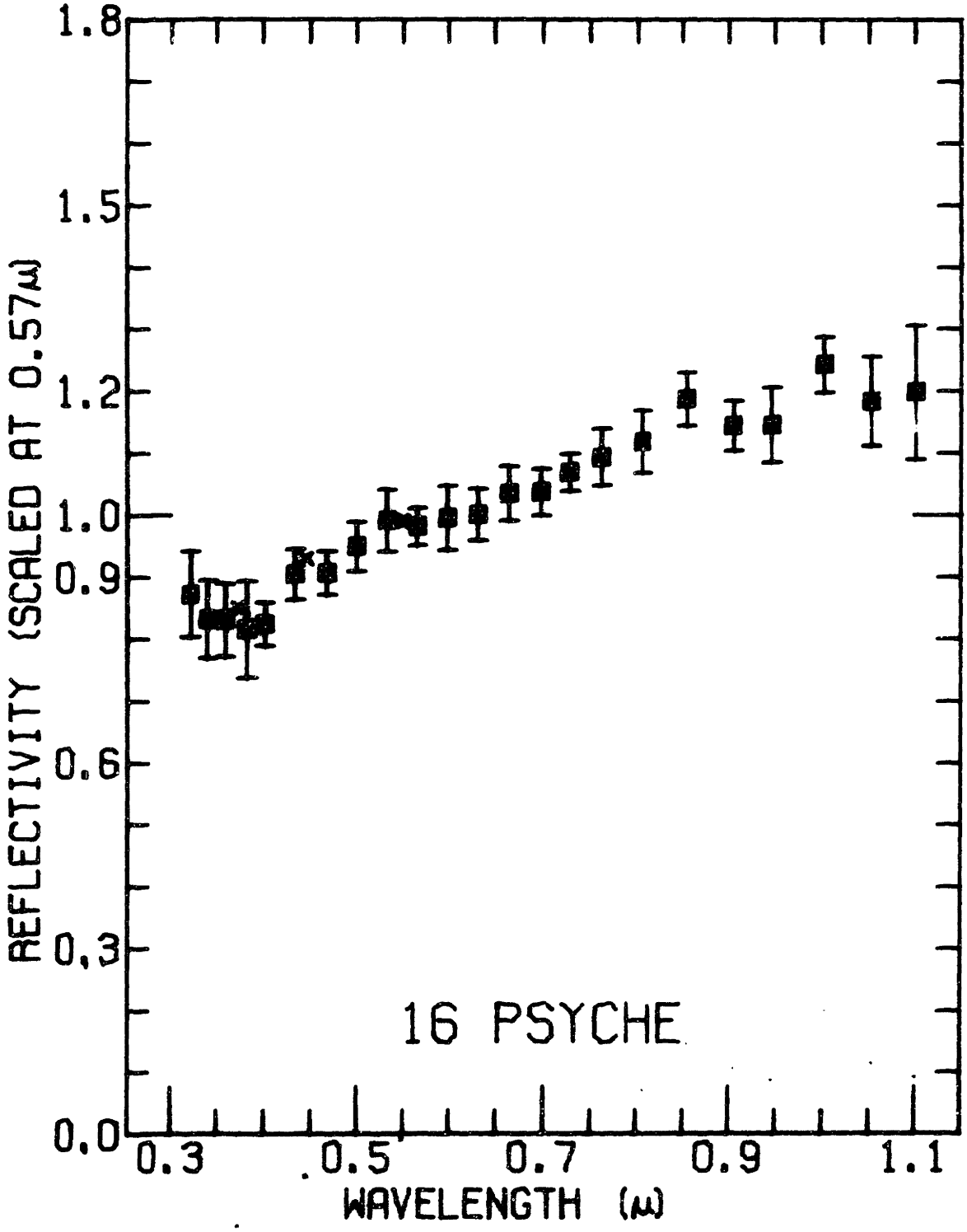
1.8
1.5
1.2
1.0
0.9
0.6
0.3
0.0
REFLECTIVITY (SCALED AT 0.57μ)
16 PSYCHE
0.3
0.5
0.7
0.9
1.1
WAVELENGTH (μ)

17 THETIS

a = 2.469 AU e = 0.142 sin i = 0.085 Mars dist. = 0.30 AU (B-25)
B(1,0) = 8.69 B-V = 0.84 U-B = 0.42 L. Curve: $12^{h}.275$, 0.12 - 0.36 m.

(1) 10/10/70. 8 runs: 0:24, 0:29, 0:33, 0:41, 1:50, 2:00, 2:05, 2:11 ST ($0^{h}.05$). i = $10\frac{1}{2}^{\circ}$ m = 12.0
Standard Xi^{2} Ceti, sec z = 1.14 - 1.39, very good. Counts = 320.
Single weight, multiplied by 1.1.

(2) 10/11/70. 8 runs: 23:24, 23:28, 23:38, 23:43, 0:10, 0:13, 0:16 ST ($0^{h}.05$). i = $10\frac{1}{2}^{\circ}$ m = 12.0
Standard: Xi^{2} Ceti, sec z = 1.43 - 1.77, very good. Counts = 200.
ID: "confirmed by motion from previous night". Single weight.

(3) 10/12/70. 7 runs: 5:57, 6:00, 6:19, 6:27, 6:31, 6:34, 6:37 ST ($0^{h}.05$). i = 10° m = 12.0
Standard: Xi^{2} Ceti, sec z = 1.52 - 1.83, good. Counts = 200. Single weight.

Comments: The counting statistics are too low to determine significant differences between reflectivities on the three different nights (on Oct. 12 the side opposite to that observed on the other two nights was observed). The asteroid was quite faint, so its apparent brightness in some UV filters is not significant. The spectral reflectivity of 17 Thetis may resemble that of 79 Eurynome which is also in family B-25. Williams (1971, private communication) did not include Thetis in the small family whose brightest member is Eurynome, but he feels it is a borderline case and might as-well have been included. That would be consistent

17 THETIS

Wavelength	Reflectivity	Mu
0.301	0.399	0.03
0.322	0.868	0.12
0.341	0.790	0.25
0.360	0.432	0.09
0.383	0.868	0.10
0.402	0.729	0.04
0.434	0.756	0.07
0.468	0.921	0.08
0.500	0.911	0.06
0.533	0.944	0.05
0.566	0.908	0.14
0.599	1.077	0.05
0.632	1.068	0.04
0.665	1.118	0.03
0.699	1.057	0.03
0.729	1.176	0.03
0.763	1.161	0.09
0.807	1.156	0.03
0.855	1.113	0.04
0.906	1.211	0.05
0.947	1.019	0.03
1.003	1.190	0.03
1.053	1.043	0.06
1.101	1.257	0.19

with the trend he thinks may exist for the brightest member of a family to be located near the boundary of the family. Thetis has a fairly large amplitude light curve, probably due largely to non-spherical shape. Group R4.

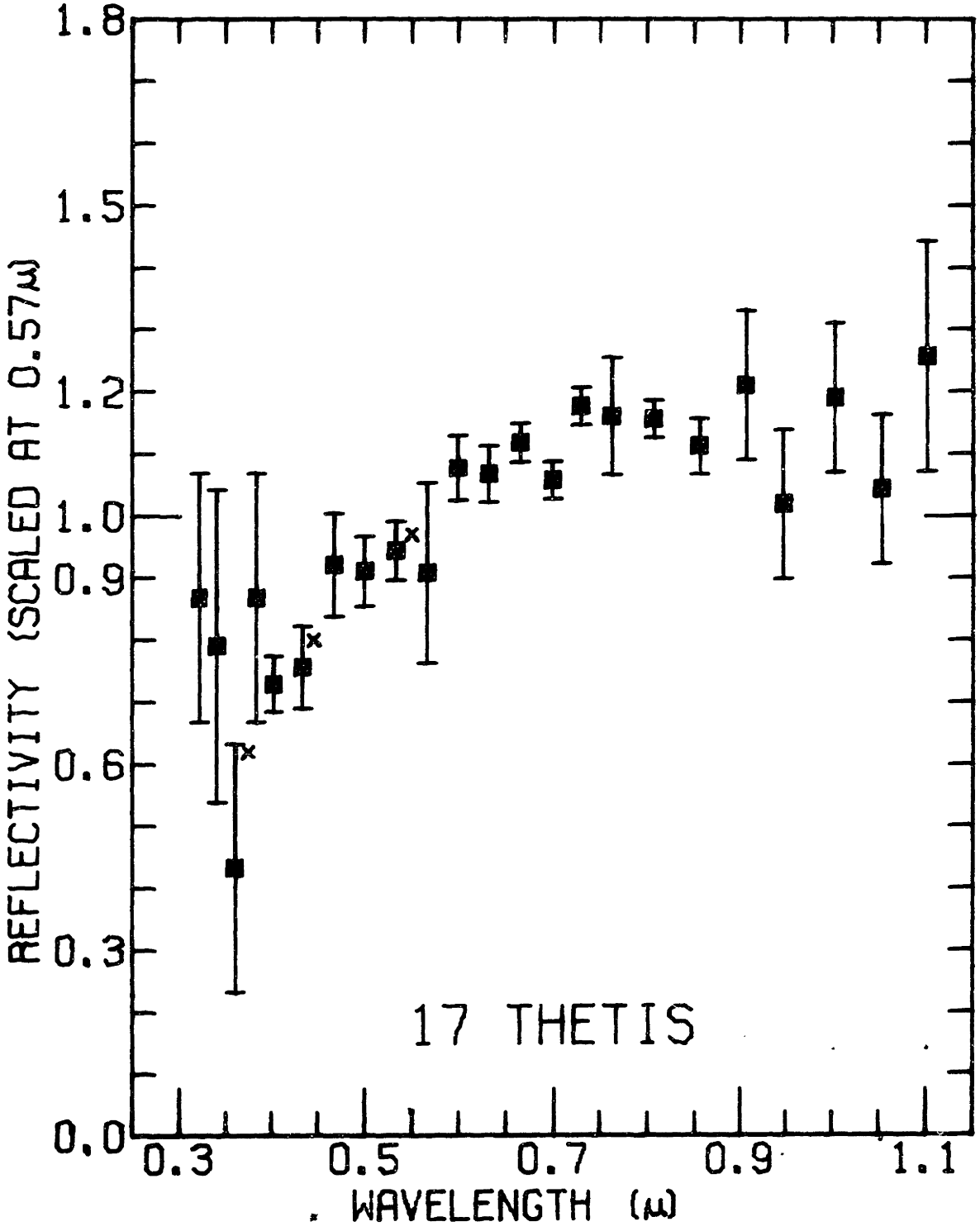
1.8
1.5
1.2
1.0
0.9
0.6
0.3
0.0
REFLECTIVITY (SCALED AT 0.57μ)
17 THETIS
0.3
0.5
0.7
0.9
1.1
WAVELENGTH (μ)

21 LUTETIA

a = 2.435 AU e = 0.128 sin i = 0.036 Mars dist. = 0.31 AU Fortuna (A-82)

B(1,0) = 8.68 L. Curve: $6^h.133$, 0.15 m.

(1) 12/30/70. 2 runs: 5:02, 7:26 ST ($1^h.17$). i = 13° m = 11.6

Standard: Xi^2 Ceti and Epsilon Ori., sec z = 1.05 - 1.43, fair. Counts = 230. ID: "certain". Filters 21 - 24 omitted for second run due to haze and telescope drive problems. Single weight.

(2) 1/5/71. 1 run: 4:04 ST ($0^h.97$) i = 15° m = 11.7

Standard: Xi^2 Ceti and Gamma Gem., sec z = 1.03, very good. Counts = 610. Small aperture used, guiding difficulties probable. Guiding: 8, 13, 20. Double weight.

Comments: The data for 21 Lutetia suffer from low counting statistics. Within that limitation, the agreement between the two runs is good. Run (2) seems somewhat bluer, but not significantly so. The dip at 0.63 microns is also not significant. The tendency for the reflectivity curve to be concave upwards (bright in the UV and IR relative to the visible) may be real. The evidence suggests that Lutetia is the bluest asteroid yet observed. Group B4.

21 LUTETIA

Wavelength	Reflectivity	Mu
0.322	1.165	0.16
0.341	1.034	0.03
0.360	1.225	0.27
0.383	1.010	0.04
0.402	0.987	0.04
0.434	0.964	0.03
0.468	1.014	0.03
0.500	0.962	0.03
0.533	0.957	0.03
0.566	0.964	0.04
0.599	0.965	0.11
0.632	0.839	0.09
0.665	0.912	0.05
0.699	1.007	0.03
0.729	0.934	0.05
0.763	0.924	0.05
0.807	1.080	0.15
0.855	1.034	0.07
0.906	1.107	0.12
0.947	1.117	0.13
1.003	1.007	0.06
1.053	1.368	0.20
1.101	0.974	0.03

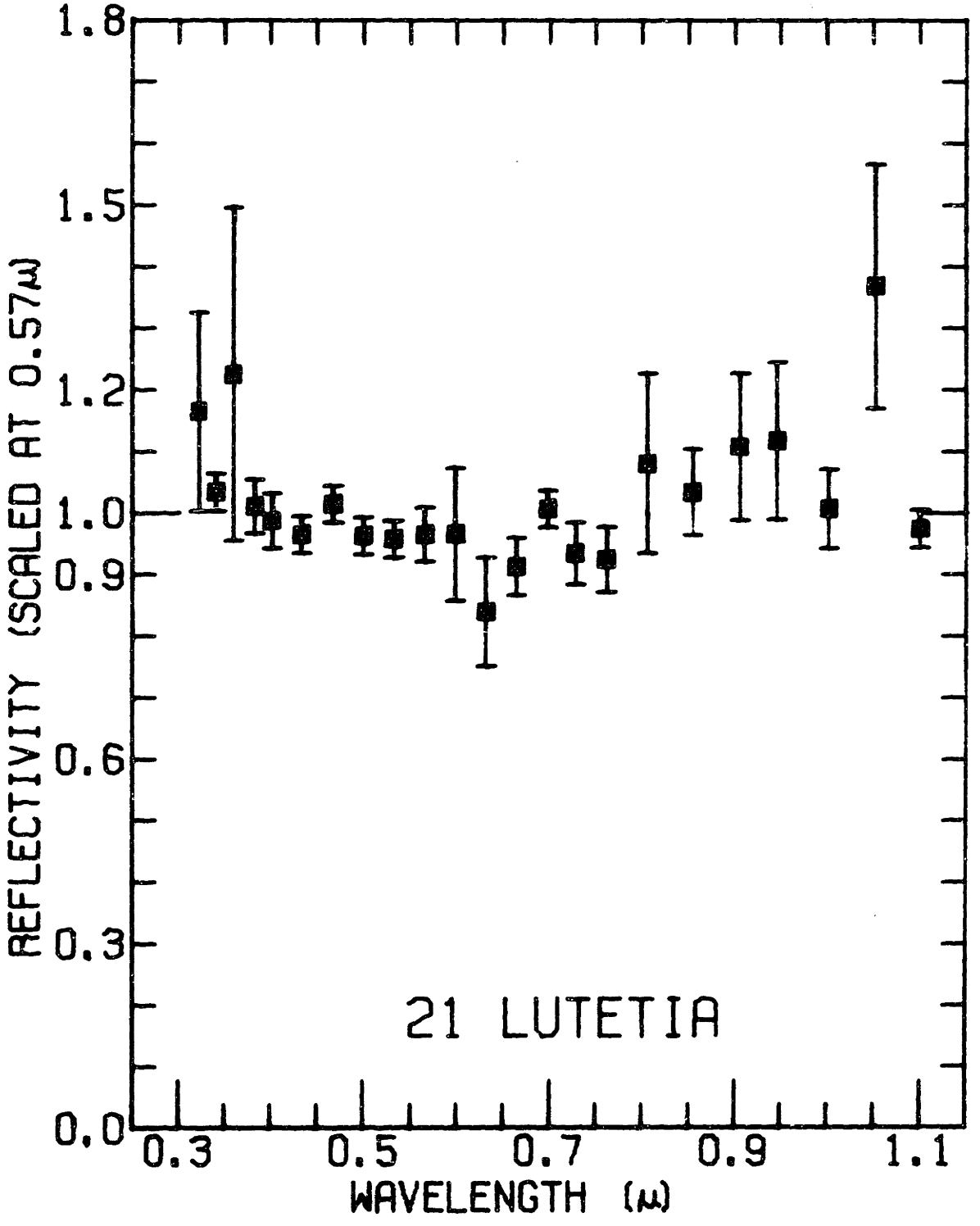
1.8
1.5
1.2
1.0
0.9
0.6
0.3
0.0
REFLECTIVITY (SCALED AT 0.57μ)
21 LUTETIA
0.3
0.5
0.7
0.9
1.1
WAVELENGTH (μ)

29 AMPHITRITE

a = 2.554 AU e = 0.065 sin i = 0.110 Mars dist. = 0.57 AU Amphitrite B(1,0) = 7.26 B-V = 0.87 L. Curve: $5^h.389$, 0.13 m.

(1) 10/11/70. 11 runs: 21:24, 21:27, 21:29, 21:55, 21:59, 22:01, 22:04, 22:20, 22:22, 22:25 ST ($0^h.05$). i = 2° m = 9.8
Standard: 29 Psc., sec z 1.35 - 1.74, very good. Counts = 2050.
ID: "definite". No differences between the runs. Triple weight.

(2) 1/7/71. 1 run: 3:36 ST ($1^h.0$). i = 24° m = 10.7
Standard: Gamma Gem., sec z = 1.35, fair. Counts = 780. ID: "98% certain: in correct location, but no star chart available". Some problems with moonlight, guiding and standard star data. Guiding: 7, 10, 12, 13, 14, 17, 18, 19, 21, 22, 23. Single weight.

Comments: No reddening with phase is evident. A slight tendency in the opposite sense is not statistically significant. The agreement between the runs is good. If run (2) can be trusted, then the 0.95 micron band may be more prominent at large phase angle, but a faint 0.65 micron dip more prominent at small phase angle. The evident color of this asteroid is at variance with the B-V color published by Gehrels (1970). Group R3C.

29 AMPHITRITE

Wavelength	Reflectivity	Mu
0.301	0.764	0.37
0.322	0.649	0.09
0.341	0.697	0.08
0.360	0.773	0.03
0.383	0.670	0.05
0.402	0.735	0.03
0.434	0.849	0.04
0.468	0.901	0.04
0.500	0.925	0.03
0.533	0.988	0.03
0.566	1.000	0.03
0.599	1.059	0.03
0.632	1.036	0.04
0.665	1.039	0.04
0.699	1.109	0.04
0.729	1.161	0.04
0.763	1.157	0.03
0.807	1.190	0.05
0.855	1.234	0.03
0.906	1.192	0.05
0.947	1.133	0.04
1.003	1.206	0.05
1.053	1.232	0.05
1.101	1.194	0.06

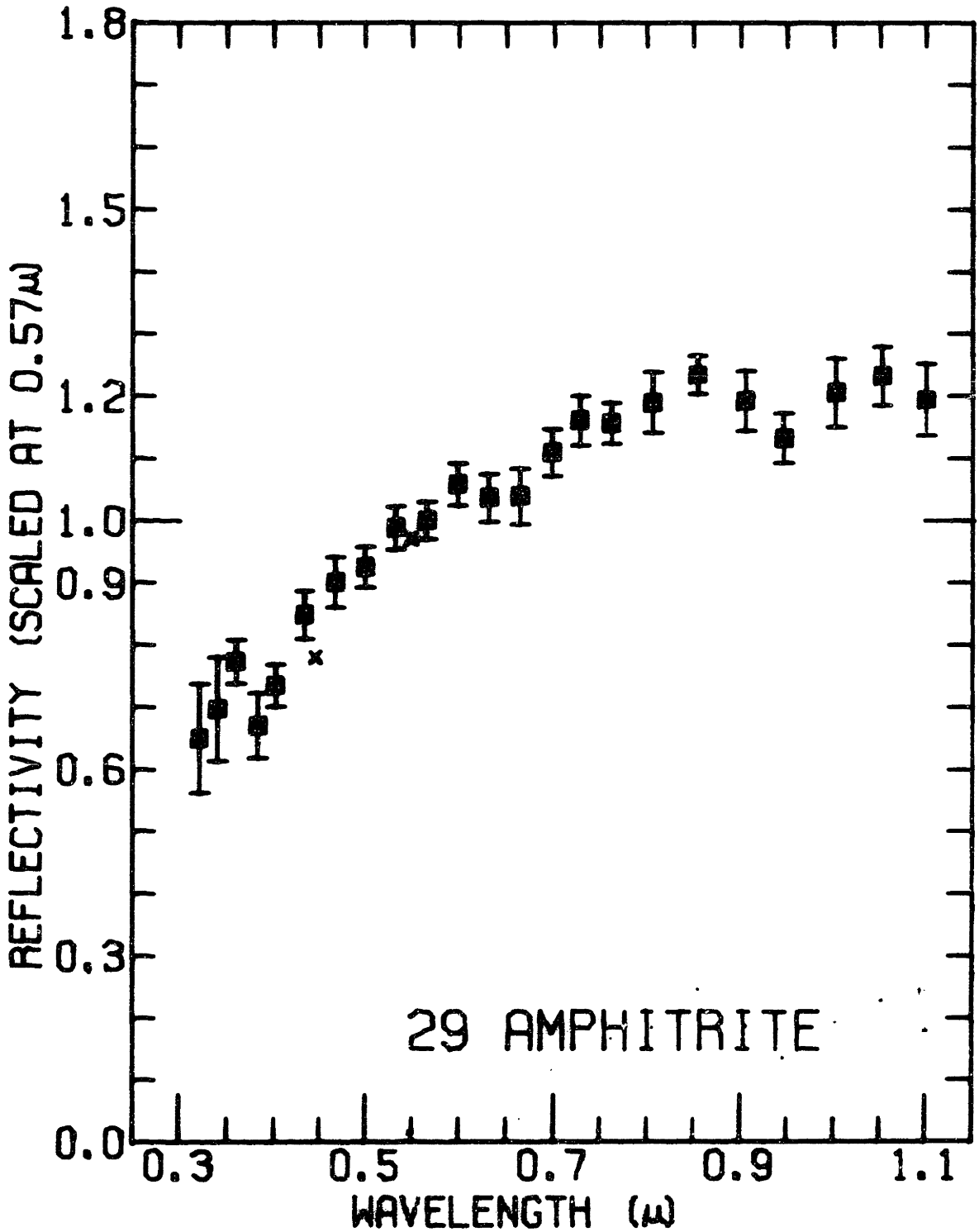
1.8
1.5
1.2
1.0
0.9
0.6
0.3
0.0
REFLECTIVITY (SCALED AT 0.57μ)
29 AMPHITRITE
0.3
0.5
0.7
0.9
1.1
WAVELENGTH (μ)

39 LAETITIA

a = 2.769 AU e = 0.084 sin i = 0.172 Mars dist. = 0.68 AU Ceres

B(1,0) = 7.41 B-V = 0.88 U-B = 0.49 L. Curve: $5^h.138$, 0.18 - 0.53 m.

(1) 2/7/71. 2 runs: 7:32, 8:25 ST ($0^h.5$). i = 8° m = 11.4

Standard: Alpha Leo, sec z = 1.23 - 1.44, good. S-20 + ND2.

Guiding: 6, 7, 9, 10, 12, 16; star 6,8. Single weight; all reflectivities multiplied by 1.04 (fil. 19 omitted).

(2) 2/9/71. 1½ runs: 9:50, 11:23 ST ($1^h.3$). i = 8° m = 11.4

Standard: Alpha Leo, sec z = 1.10 - 1.13, very good. Counts = 3270.

Guiding: 6, 7, 8, 9. Possibility of city voltage fluctuations during first run, though no evidence of it in the data. Second run for fil. 11 -- 24 only. Single weight.

Comments: 39 Laetitia has a very large light amplitude associated with its rotation. Inequalities in successive maxima or minima suggest that, while most of the variation may be due to shape, at least 0.1 magnitude is due to surface features. Lacis (1971) has noted this characteristic of the light curve. Although there is a suggestion that the second of the two runs on Feb. 9 is slightly darker than the first in the IR, there is in general no significant differences between individual runs on the same night, or between averages for the separate nights. For the given rotation period, however, I was observing approximately the same side of the asteroid. Also Gehrels (1970) suggests that the asteroid is approximately pole-on when observed near opposition in February. Ast. 39 has one of the highest albedos among asteroids observed by Matson (1971). This red

39 LAETITIA

Wavelength	Reflectivity	Mu
0.322	0.501	0.03
0.341	0.533	0.03
0.360	0.645	0.03
0.383	0.577	0.03
0.402	0.620	0.05
0.434	0.731	0.05
0.468	0.819	0.05
0.500	0.880	0.03
0.533	0.998	0.05
0.566	1.018	0.03
0.599	1.073	0.03
0.632	1.067	0.03
0.665	1.107	0.03
0.699	1.171	0.03
0.729	1.235	0.03
0.763	1.238	0.04
0.807	1.297	0.03
0.855	1.271	0.05
0.906	1.252	0.04
0.947	1.214	0.03
1.003	1.195	0.09
1.053	1.208	0.09
1.101	1.180	0.16

---

asteroid falls off in the IR. Group R2A.

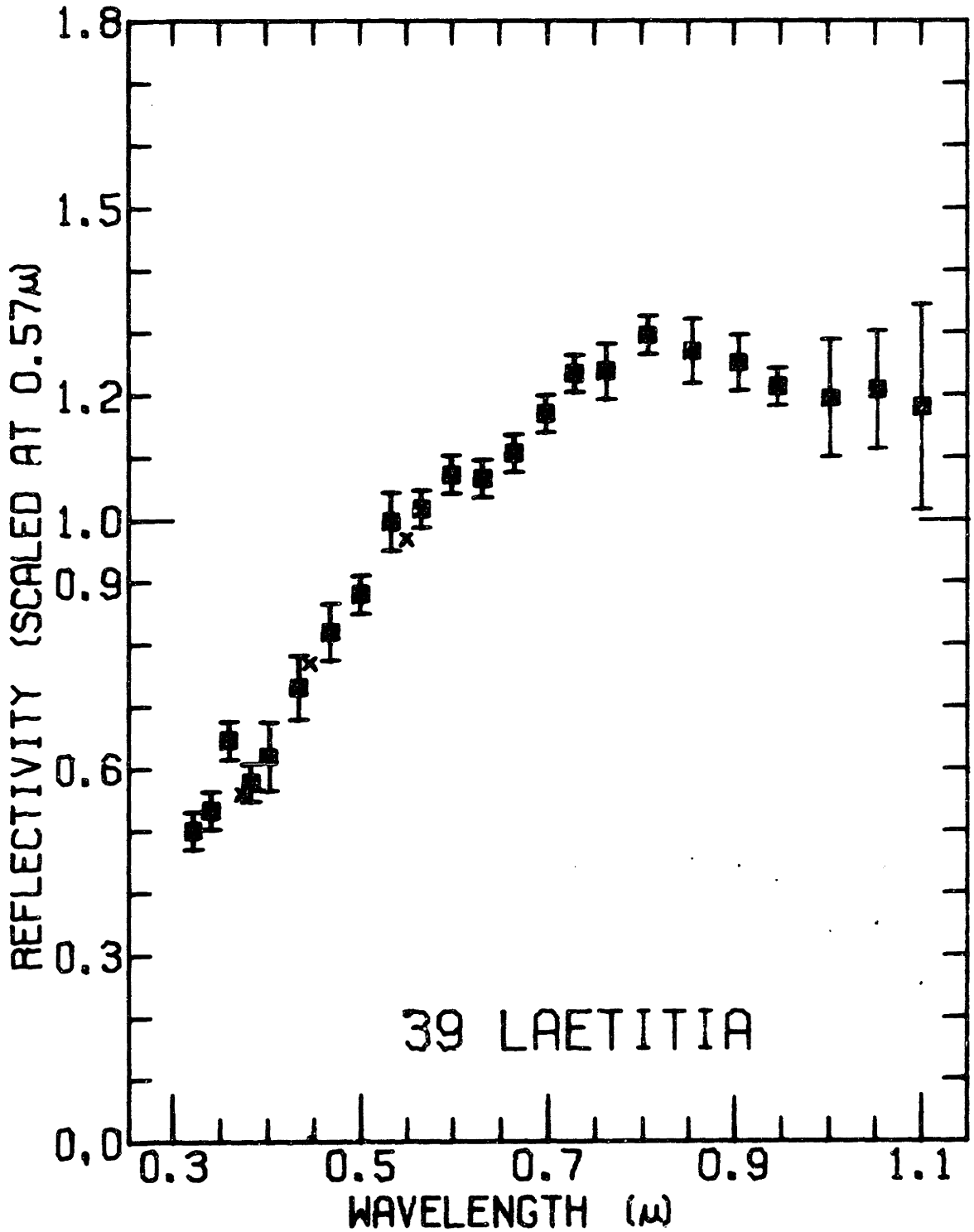
1.8
1.5
1.2
1.0
0.9
0.6
0.3
0,0
REFLECTIVITY (SCALED AT 0.57μ)
39 LAETITIA
0.3
0.5
0.7
0.9
1.1
WAVELENGTH (μ)

40 HARMONIA

a = 2.267 AU e = 0.02 sin i = 0.066 Mars dist. = 0.39 AU None
B(1,0) = 8.45 B-V = 0.83 U-B = 0.42 L. Curve: $9^h.1358$, 0:22 m.

(1) 10/11/70. 6 runs: 0:52, 0:56, 1:01, 1:16, 1:20, 1:22 ST ($0^h.05$).
i = $14\frac{1}{2}^\circ$ m = 10.6
Standard: Xi^2 Ceti, sec z = 1.21 - 1.30, very good. Counts = 610.
Double weight.

(2) 1/2/71. 2 runs: 2:09, 4:28 ST ($1^h.27$). i = 24° m = 11.1
Standard: Xi^2 Ceti, sec z = 1.09 - 1.24, very good. Counts = 290.
Immediately following the last run clouds suddenly formed on the mountain and it was snowing within a couple hours. A rapidly increasing humidity, just prior to cloud formation, may have caused the very low counts in filters 22 - 24 of the last run. Single weight (fil. 22 - 24 omitted).

Comments: The counting statistics are quite low for 40 Harmonia. In view of a slight reddening with phase, which may be real, the omission of filters 22 - 24 of run (2) may cause a slight strengthening of any 0.95 micron band in the average reflectivity spectrum. In any case, the data are too poor to definitively describe any such absorption feature. Group R3A.

40 HARMONIA

Wavelength	Reflectivity	Mu
0.301	2.690	1.00
0.322	0.545	0.14
0.341	0.644	0.06
0.360	0.548	0.08
0.383	0.843	0.10
0.402	0.668	0.09
0.434	0.821	0.07
0.468	0.817	0.06
0.500	0.888	0.05
0.533	0.940	0.05
0.566	1.000	0.03
0.599	1.108	0.06
0.632	1.137	0.07
0.665	1.198	0.09
0.699	1.228	0.07
0.729	1.160	0.07
0.763	1.233	0.07
0.807	1.136	0.03
0.855	1.265	0.08
0.906	1.161	0.07
0.947	1.143	0.07
1.003	1.222	0.08
1.053	1.334	0.08
1.101	1.292	0.10

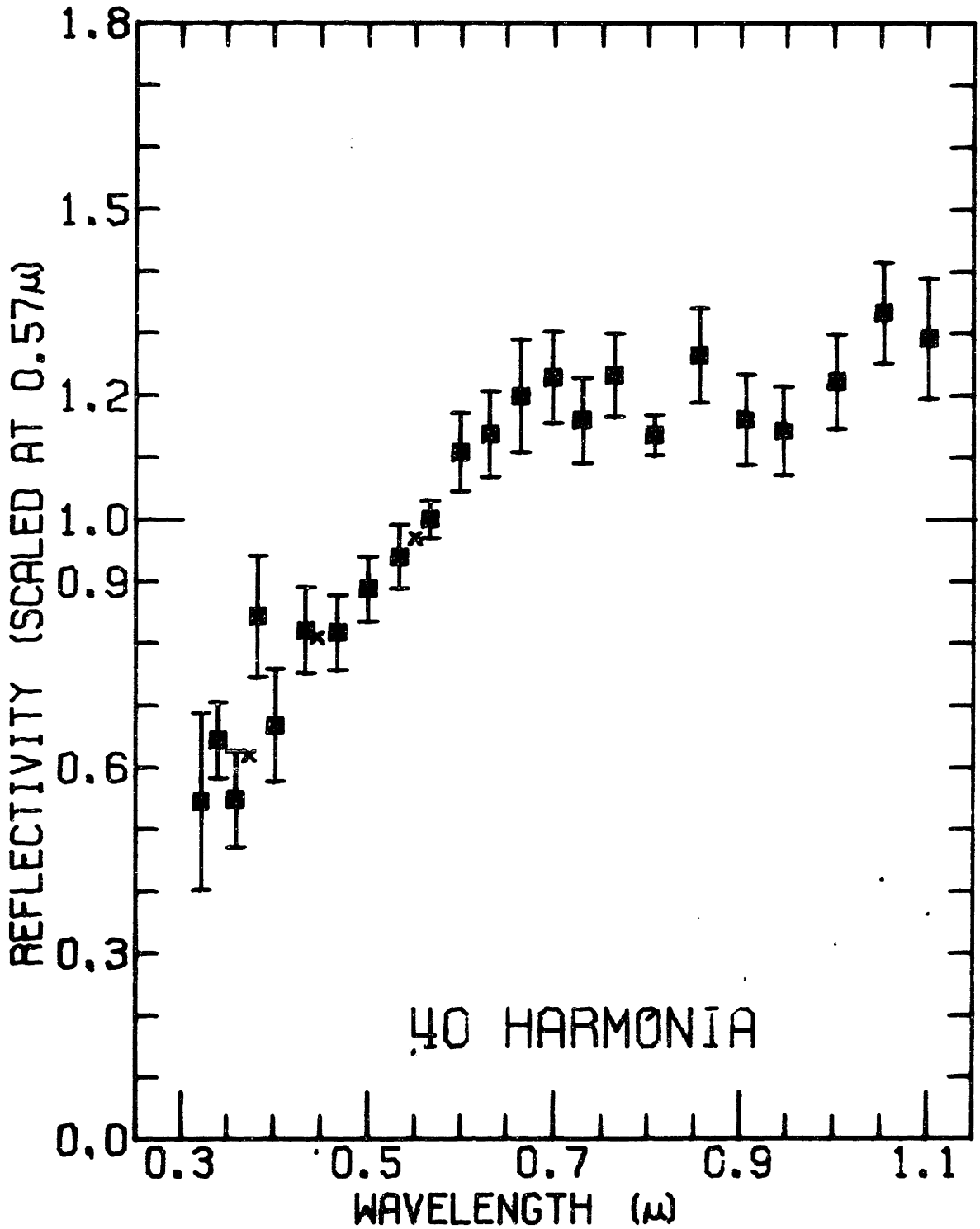
1.8
1.5
1.2
1.0
0.9
0.6
0.3
0.0
REFLECTIVITY (SCALED AT 0.57μ)
40 HARMONIA
0.3
0.5
0.7
0.9
1.1
WAVELENGTH (μ)

43 ARIADNE

a = 2.203 AU e = 0.135 sin i = 0.07 Mars dist. = 0.04 AU Flora II (7)
B(1,0) = 9.18 L. Curve: 11 - 47^h, 0.15 m.

(1) 1/7/71. 2 runs: 9:08, 10:35 ST ($0^h.45$). i = 15° m = 12.6
Standard: Alpha Leo, sec z = 1.11 - 1.12, good. Counts = 420. ID: "asteroid in exact location; appeared to move slightly during runs". Guiding: 12, 14, 16, 22. Large difference between runs (see below). 10:35 run given single weight, multiplied by 1.07; 9:08 run omitted.

(2) 2/10/71. 2 runs: 9:09, 9:30 ST ($0^h.26$). i = $2\frac{1}{2}^\circ$ m = 12.0
Standard: Alpha Leo, sec z = 1.07, very good. S-20 + ND2. ID: probably secure; during second run the log records: " 2 objects side-by-side and closing; this one is presumably the asteroid" due to direction of motion. Guiding: 7. Single weight.

Comments: The two runs on January 7 show the worst discrepancy of any two runs for a single asteroid. The 9:08 run has a nearly flat spectral reflectivity, while the other shows the reddest slope, throughout the entire range 0.03 to 1.1 microns, yet seen on an asteroid. Both February runs are nearly identical to the red January run over the range covered with the S-20 tube. The log and the original data have been checked for signs of a mistake in the January data, but no obvious problem is apparent, either with the sky, the moon and other sources of scattered light, the dark current, or in identification of the asteroid. It is true that the asteroid was very faint, and seeing conditions were poor (as was usually the case in January), but it is not clear how such a large error

43 ARIADNE

Wavelength	Reflectivity	Mu
0.322	0.364	0.13
0.341	0.610	0.09
0.360	0.615	0.08
0.383	0.561	0.06
0.402	0.556	0.06
0.434	0.724	0.03
0.468	0.806	0.03
0.500	0.884	0.03
0.533	1.036	0.07
0.566	1.035	0.04
0.599	1.037	0.05
0.632	1.113	0.03
0.665	1.177	0.03
0.699	1.218	0.03
0.729	1.134	0.16
0.763	1.320	0.03
0.807	1.444	0.09
0.855	1.611	0.16
0.906	1.382	0.08
0.947	1.454	0.08
1.003	1.387	0.08
1.053	1.464	0.08
1.101	1.693	0.08

could occur.

The tentative hypothesis I choose to accept is that there are large color differences on different parts of the asteroid, despite the fact the asteroid had supposedly rotated less than 50° during the interval separating the two dissimilar runs. This hypothesis requires verification. The average reflectivity adopted for 43 Ariadne is the mean of the February data and the red January run. The counting statistics are therefore

very poor for the IR part of the reflectivity curve, and the possible existence of a band centered near 1.02 microns cannot be given much weight. The apparent red color of this member of the Flora goup of families may be consistent with that of Flora itself. Group R1.

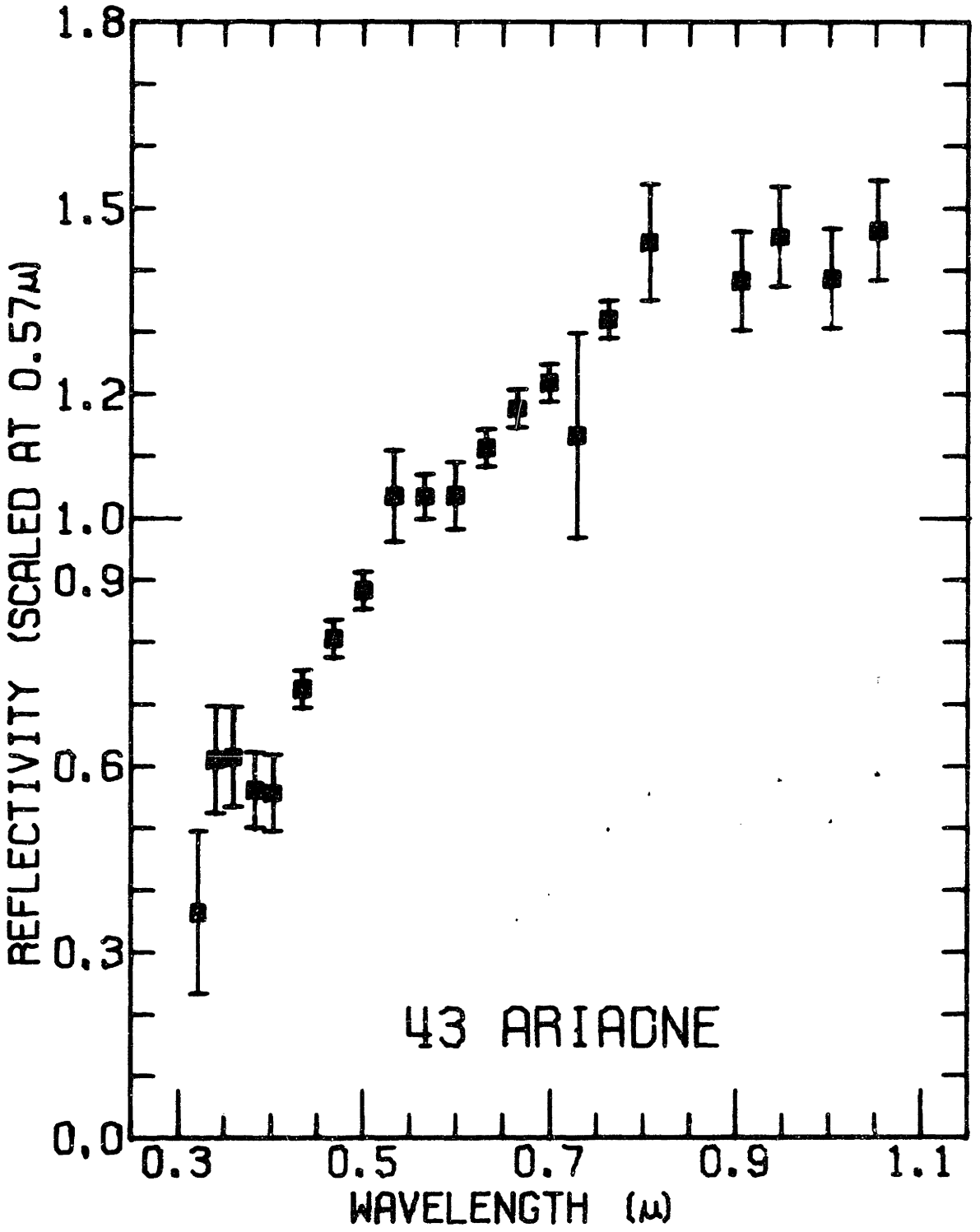
1.8
1.5
1.2
1.0
0.9
0.6
0.3
0.0
REFLECTIVITY (SCALED AT 0.57μ)
43 ARIADNE
0.3
0.5
0.7
0.9
1.1
WAVELENGTH (μ)

51 NEMAUSA

a = 2.366 AU e = 0.116 sin i = 0.177 Mars dist. = 0.23 AU None

B(1,0) = 8.66 B-V = 0.81 L. Curve: $7^{h}.785$, 0.14 m.

(1) 5/10/71. 2 full and 2 partial runs: 12:25, 12:27, 12:36, 12;38 ST ($0^{h}.18$). i = 12^{o} m = 11.1

Standard: Theta Vir., sec z = 1.21, good. S-20 + ND1 for UV and visible, S-1 for IR. Counts (IR) = 1100. Last two runs fil. 18 - 23 only.

Comments: There is uncertainty in the calibration of the ND filter, through which the IR data are tied to the scaling at 0.57 microns. If there were a 20% error (unlikely), the IR data could be reduced to a level such that the reflectivity of Nemausa would resemble that of asteroids 409 or 13 in general form, but retaining a narrow absorption band near 0.66 microns. On the otherhand, multicolor photometry by Gehrels et al (1970) shows a reflectivity curve for 51 Nemausa nearly as red over the range 0.33 to 1.0 microns as that for 12 Victoria. An upward shift of my IR data would bring the endpoints of the reflectivity curve into greater agreement with Gehrels et al, but would magnify a wide absorption band between 0.65 and 0.75 microns. Verification of the reflectivity curve I present here would be desirable. Group M2.

51 NEMAUSA

Wavelength	Reflectivity	Mu
0.322	0.554	0.33
0.341	0.543	0.13
0.360	0.623	0.06
0.383	0.595	0.03
0.402	0.745	0.03
0.434	0.802	0.05
0.468	0.914	0.03
0.500	0.967	0.04
0.533	1.004	0.03
0.566	1.000	0.03
0.599	0.983	0.03
0.632	0.982	0.03
0.665	0.890	0.04
0.699	0.932	0.03
0.729	0.975	0.03
0.763	0.942	0.06
0.807	1.030	0.03
0.855	1.119	0.07
0.906	1.125	0.04
0.947	1.099	0.05
1.003	1.134	0.03
1.053	1.176	0.15

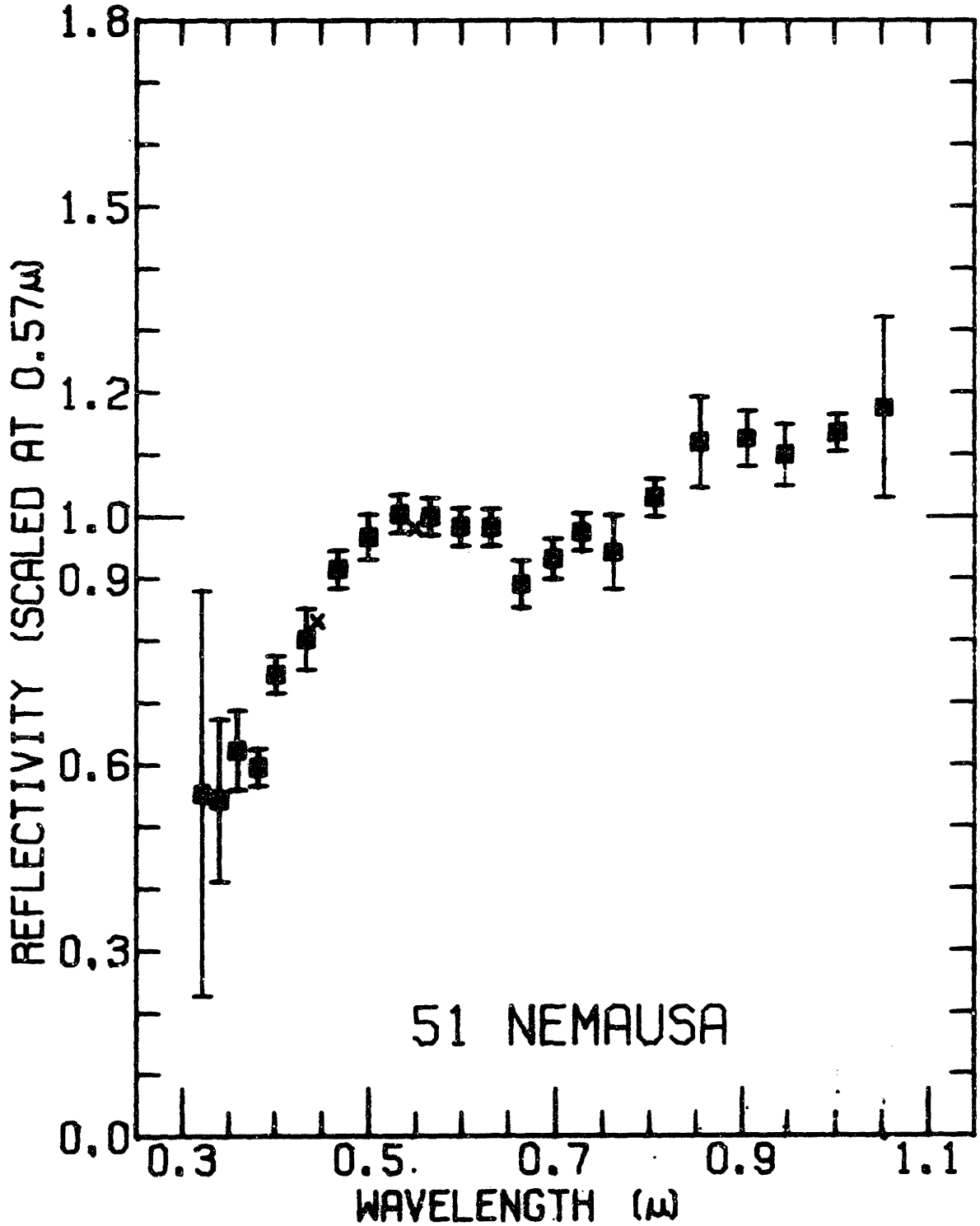
1.8
1.5
1.2
1.0
0.9
0.6
0.3
0.0
REFLECTIVITY (SCALED AT 0.57μ)
51 NEMAUSA
0.3
0.5
0.7
0.9
1.1
WAVELENGTH (μ)

68 LETO

a = 2.784 AU e = 0.142 sin i = 0.132 Mars dist. = 0.54 AU Leto (A-66)
B(1,0) = 8.29

(1) 1/4/71. 2 runs: 8:42, 11:22 ST ($1^h.27$). i = 9° m = 12.6
Standard: Alpha Leo, sec z = 1.00 - 1.18, fair to good. Counts = 860. ID: "obvious". Guiding: 20; star, 18. The first run is probably good to only 5 - 10% due to bad seeing and image faintness, which made guiding difficult. The band is more prominent in the first run. Single weight.

(2) 2/8/71. 2 runs: 5:05, 6:23 ST ($1^h.8$, second run interrupted by clouds near fil. 16). i = 7° m = 12.5
Standard: Gamma Gem., sec z = 1.10 - 1.32, very good. Counts = 580. ID: "asteroid moved between 2 runs; no doubt of ID". Single weight, multiplied by 1.02.

(3) 2/10/71. 2 runs: 6:13, 6:28 ST ($0^h.28$). i = 7° m = 12.5
Standard: Eta Hya., sec z = 1.09 - 1.12, very good. S-20 (no ND). Single weight.

Comments: There are probable differences in the spectral reflectivity of Leto between the separate nights and between the separate runs in (1) and, especially, (2). These could be due to rotational phase angle differences, but the spin of Leto is not known. The asteroid was very faint, however, so great weight should not be attached to either these differences or to the apparently long-wavelength position of its absorption band. The strength of the absorption band in the final average is not affected by

68 LETO

Wavelength	Reflectivity	Mu
0.322	0.205	0.04
0.341	0.584	0.16
0.360	0.796	0.15
0.383	0.691	0.04
0.402	0.750	0.03
0.434	0.772	0.06
0.468	0.860	0.03
0.500	0.893	0.03
0.533	0.971	0.03
0.566	1.007	0.03
0.599	1.095	0.03
0.632	1.042	0.03
0.665	1.085	0.03
0.699	1.149	0.04
0.729	1.161	0.05
0.763	1.252	0.03
0.807	1.165	0.03
0.855	1.525	0.25
0.906	1.166	0.03
0.947	1.141	0.05
1.003	1.114	0.03
1.053	1.109	0.04
1.101	1.121	0.03

averaging the S-20 runs. Leto shows a fairly sharp drop-off into the UV shortwards of 0.38 microns. Group R2B.

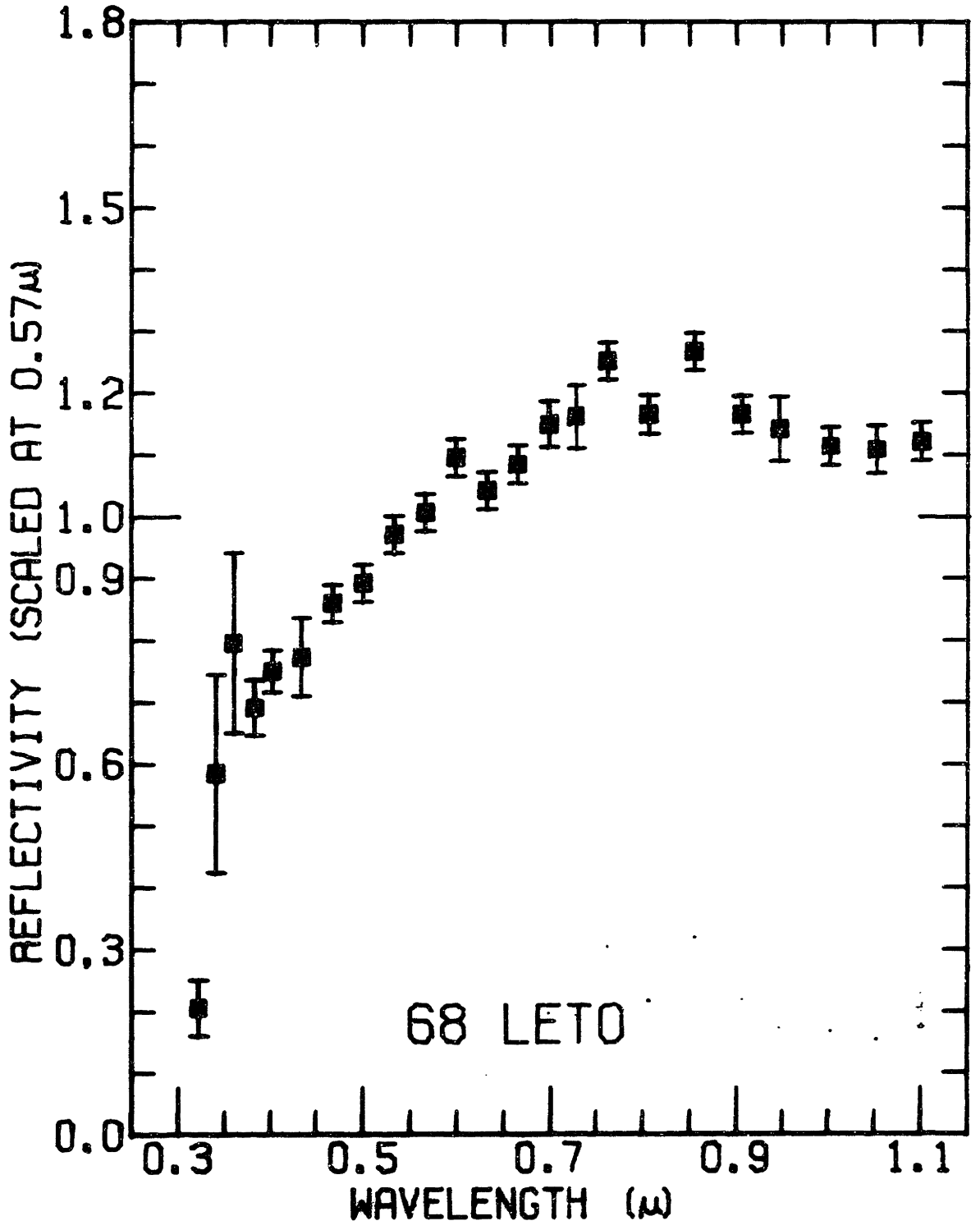
1.8
1.5
1.2
1.0
0.9
0.6
0.3
0.0
REFLECTIVITY (SCALED AT 0.57μ)
68 LETO
0.3
0.5
0.7
0.9
1.1
WAVELENGTH (μ)

79 EURYNOME

a = 2.444 AU e = 0.175 sin i = 0.090 Mars dist. = 0.19 AU Eurynome (B-25)
B(1,0) = 9.28

(1) 10/10/70. 8 runs: 22:48, 22:52, 22:57, 23:23, 23:30, 23:34, 23:36, 23:41 ST ($0^h.05$). i = $3\frac{1}{2}^\circ$ m = 10.8
Standard: 29 Pisc., sec z = 1.16 - 1.25, very good. Counts = 1215.

Comments: This is an excellent set of runs on 79 Eurynome. There are no obvious differences between the separate runs. This asteroid shows a prominent absorption feature at 0.95 microns. Group R3A.

79 EURYNOME

Wavelength	Reflectivity	Mu
0.301	1.853	1.01
0.322	0.621	0.16
0.341	0.465	0.04
0.360	0.429	0.05
0.383	0.575	0.06
0.402	0.648	0.06
0.434	0.734	0.04
0.468	0.814	0.06
0.500	0.838	0.04
0.533	0.891	0.03
0.566	1.000	0.03
0.599	0.994	0.08
0.632	1.028	0.05
0.665	1.003	0.08
0.699	1.026	0.03
0.729	1.117	0.05
0.763	1.128	0.04
0.807	1.146	0.05
0.855	1.139	0.06
0.906	1.089	0.05
0.947	1.064	0.03
1.003	1.145	0.05
1.053	1.230	0.07
1.101	1.275	0.09

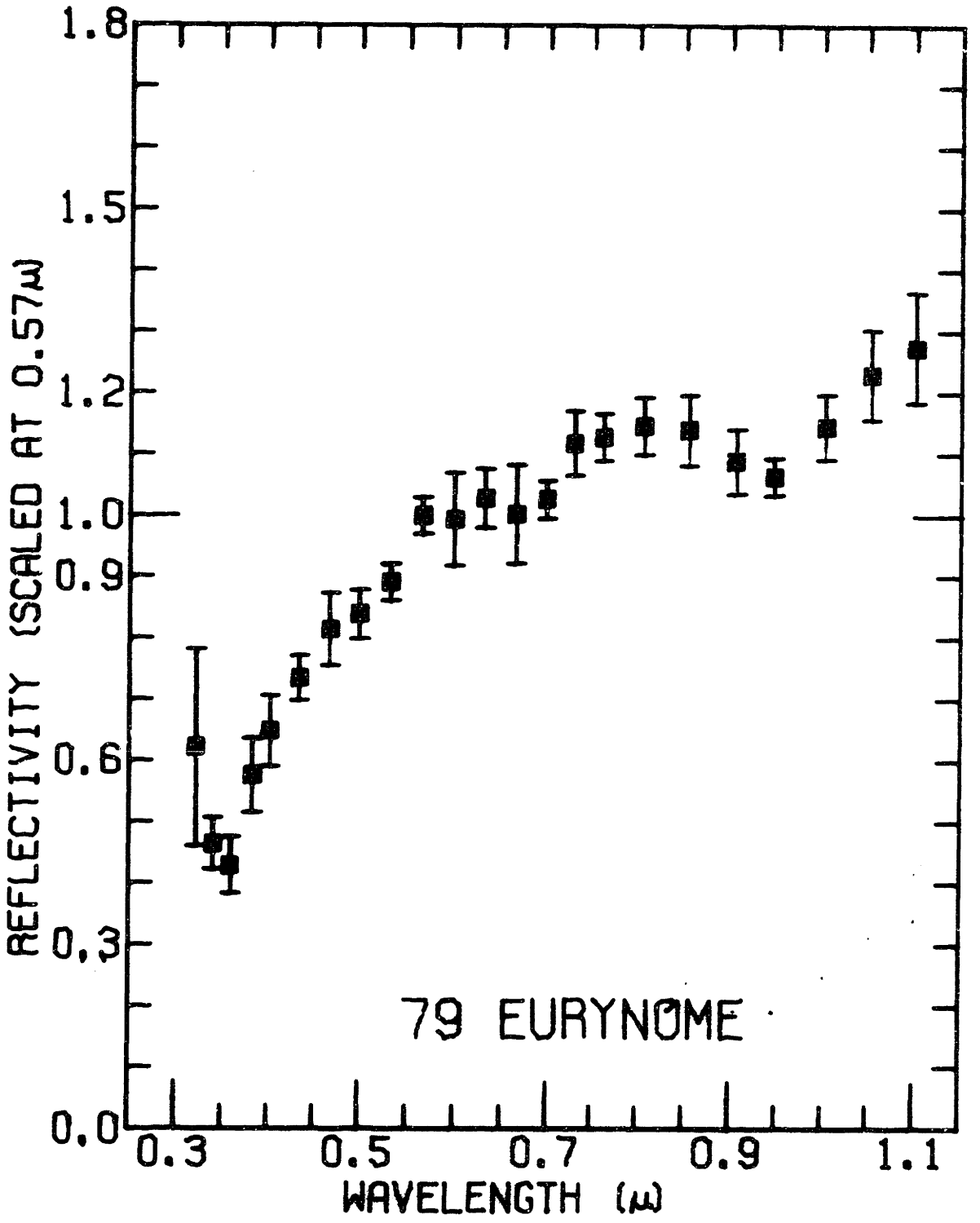
1.8
1.5
1.2
1.0
0.9
0.6
0.3
0.0
REFLECTIVITY (SCALED AT 0.57μ)
79 EURYNOME
0.3
0.5
0.7
0.9
1.1
WAVELENGTH (μ)

82 ALKMENE

a = 2.763 AU e = 0.248 sin i = 0.048 Mars dist. = 0.25 AU Triplet B(1,0) = 10.31

(1) 2/10/71. 2 runs: 7:46, 8:14 ST ($0^h.2$) i = 10° m = 11.6

Standard: Eta Hya., sec z = 1.01 - 1.02, good. S-20 (no ND).

Guiding: 10, 11, 12. Single weight.

(2) 2/11/71. 1 and 2 partial runs: 4:53, 5:51, 8:39 ST ($0^h.8$)

i = 10° m = 11.6

Standard: Gamma Gem. and Eta Hya., sec z = 1.01 - 1.40, fair to good. Counts = 2950. ID: "asteroid is very well identified". Guiding: 10, 17, 22. Last two runs for fil. 11 - 24 only. Double weight.

Comments: Excellent agreement among all runs. The depth of the 0.95 micron absorption feature is either unaffected or slightly reduced by averaging the S-20 data. Group R3A.

82 ALKMENE

Wavelength	Reflectivity	Mu
0.322	0.528	0.05
0.341	0.676	0.10
0.360	0.782	0.05
0.383	0.580	0.05
0.402	0.680	0.05
0.434	0.691	0.05
0.468	0.786	0.05
0.500	0.877	0.05
0.533	0.938	0.05
0.566	0.989	0.05
0.599	1.019	0.03
0.632	1.052	0.03
0.665	1.076	0.03
0.699	1.112	0.04
0.729	1.139	0.05
0.763	1.243	0.08
0.807	1.163	0.07
0.855	1.166	0.06
0.906	1.098	0.06
0.947	1.069	0.07
1.003	1.214	0.12
1.053	1.174	0.07

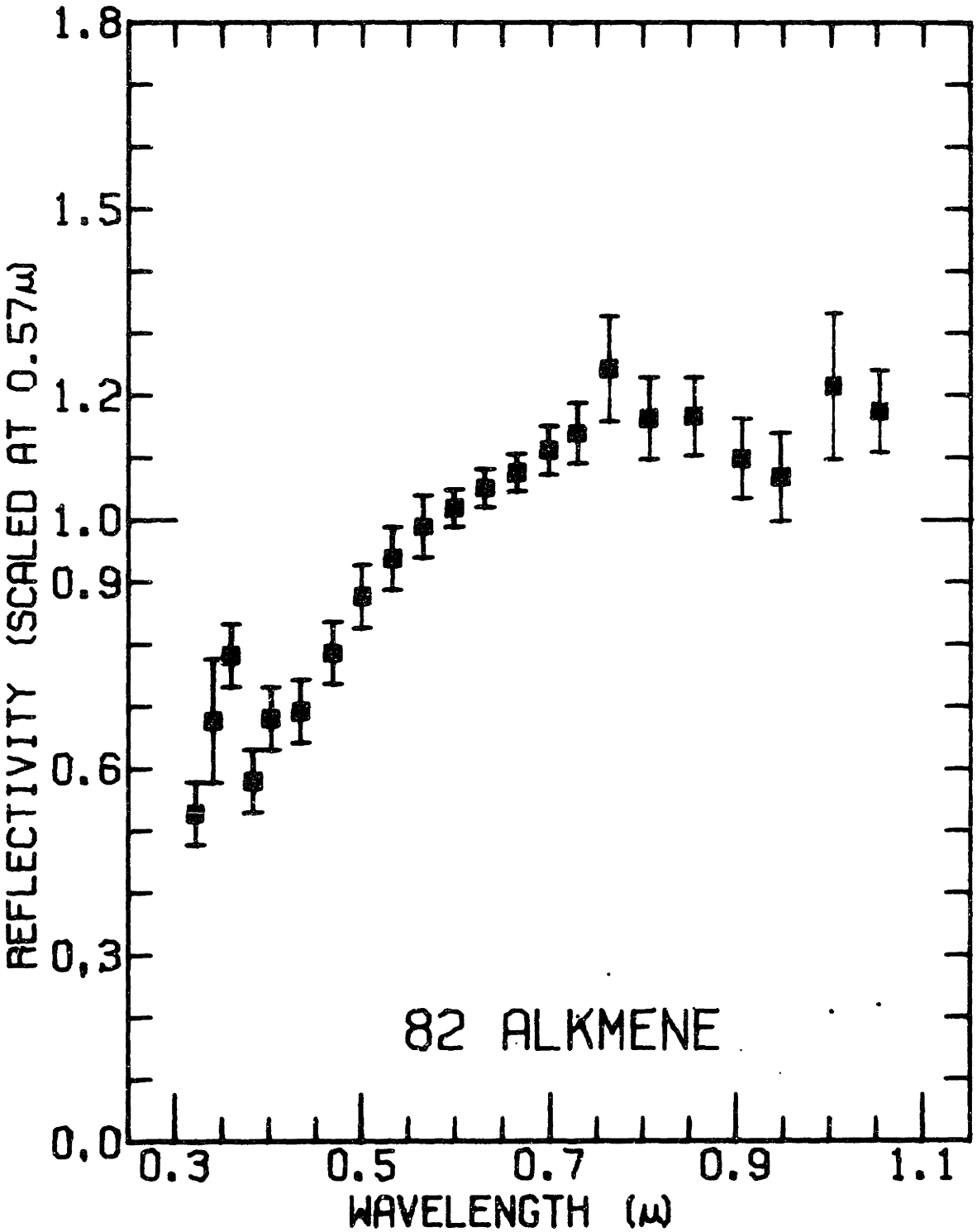
1.8
1.5
1.2
1.0
0.9
0.6
0,3
0.0
REFLECTIVITY (SCALED AT 0.57μ)
82 ALKMENE
0.3
0.5
0.7
0.9
1.1
WAVELENGTH (μ)

93 MINERVA

a = 2.754 AU e = 0.109 sin i = 0.156 Mars dist. = 0.53 AU Ceres (A-66) B(1,0) = 8.75

(1) 5/8/71. 5 full and 3 partial runs: 12:10, 12:23, 12:24, 12:27, 12:33, 12:52, 12:55, 12:56 ST ($0^h.38$). i = 15° m = 12.3 Standard: Theta Crt., sec z = 1.30 - 1.31, good. S-20 (no ND) in UV and visible, S-1 in IR. Last 3 runs fil. 18 - 24 only. Counts = 460. Single weight.

(2) 5/9/71. $2\frac{1}{2}$ runs: 12:34, (12:37), 12:44 ST ($0^h.23$) i = 15° m = 12.3 Standard: Theta Crt., sec z = 1.30, good. S-20 (no ND) in UV and visible, S-1 in IR. Second run IR only. Counts (IR) = 350. Single weight.

Comments: The results look a little peculiar for uncertain reasons. A small dip near 0.63 microns is evident in run (1) along with a larger but noiser dip near 0.9 microns. In run (2) there is a large dip of 0.7 microns and the IR reflectivity seems very high relative to the rest of the spectrum. One can suspect problems with the data, perhaps complicated by the extreme faintness of the asteroid. Otherwise large variations with rotation are indicated, of an unusual form. That the asteroid has a fairly flat reflectivity in the visible and a UV drop-off seesm fairly secure; the IR behavior is more problematical. Group B1 (?).

93 MINERVA

Wavelength	Reflectivity	Mu
0.322	1.722	0.48
0.341	0.998	0.16
0.360	0.721	0.11
0.383	0.553	0.15
0.402	0.868	0.06
0.434	0.841	0.05
0.468	0.956	0.07
0.500	0.970	0.06
0.533	0.975	0.06
0.566	1.000	0.03
0.599	0.973	0.06
0.632	0.946	0.07
0.665	0.971	0.11
0.699	0.979	0.13
0.729	1.025	0.05
0.763	0.973	0.14
0.807	1.057	0.16
0.855	1.053	0.23
0.906	0.980	0.12
0.947	1.105	0.20
1.003	1.365	0.29
1.053	1.496	0.65

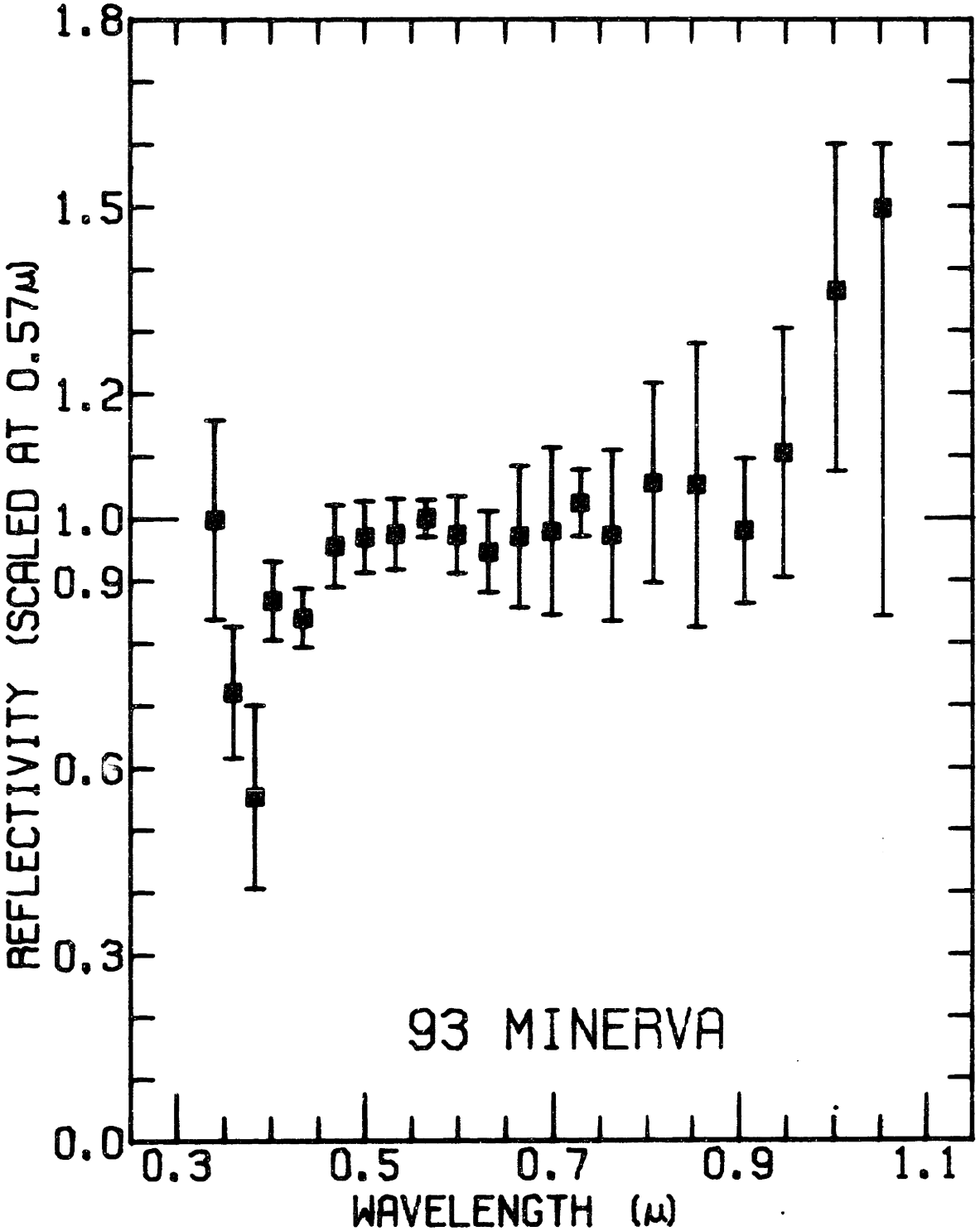
1.8
1.5
1.2
1.0
0.9
0.6
0.3
0.0
REFLECTIVITY (SCALED AT 0.57μ)
93 MINERVA
0.3
0.5
0.7
0.9
1.1
WAVELENGTH (μ)

192 NAUSIKAA

a = 2.402 AU e = 0.206 sin i = 0.130 Mars dist. = 0.07 AU (J-2)

B(1,0) = 8.40 L. Curve*: $13^{h}.625$, 0.2 m.

(1) 8/7/70. 3 runs: 20:58, 23:09, 0:32 ST ($1^{h}.15$). i = 11° m = 9.9
Standard: Epsilon Aqr., sec z = 1.67 - 1.78, good. Counts = 1380. Guiding: 6, 7, 10, 14, 16, 22; star, 2. Single weight, multiplied by 0.94.

(2) 8/9/70. 3½ runs: 19:59, 21:25, 0:10, 1:19 ST ($0^{h}.84$).
i = 9½° m = 9.9
Standard: 29 Pisc. and Epsilon Aqr., sec z = 1.58 - 2.14, very good. Counts = 2280. Guiding: 9, 10, 13; star, 5, 17, 21, 20. Last run for fil. 1 - 14 only (interrupted by dawn). Single weight, multiplied by 1.09

(3) 10/10/70. 9 runs: 21:36, 21:40, 21:44, 21:47, 21:50, 22:18, 22:21, 22:25, 22:30 ST ($0^{h}.05$). i = 25° m = 10.4
Standard: Epsilon Aqr., sec z = 1.43 - 1.45, very good. Counts = 1300. Guiding: possible slight problems towards ends of 2 of the 9 runs. Double weight.

Comments: Run (3) is of excellent quality and may be a better representation of Nausikaa's spectral reflectivity than the average which includes the August 24-inch data. When run (3) is compared with the average of runs (1) and (2), there is a strong indication that the 0.97 micron absorption band is stronger for run (3) (larger phase angle). There is also a probable reddening with phase in the B-V color; an even stronger

192 NAUSIKAA

Wavelength	Reflectivity	Mu
0.301	1.284	1.53
0.322	0.481	0.15
0.341	0.482	0.12
0.360	0.509	0.07
0.383	0.574	0.08
0.402	0.722	0.04
0.434	0.745	0.06
0.468	0.867	0.03
0.500	0.838	0.03
0.533	0.951	0.04
0.566	1.005	0.03
0.599	1.015	0.05
0.632	1.068	0.03
0.665	1.058	0.05
0.699	1.162	0.03
0.729	1.124	0.04
0.763	1.188	0.03
0.807	1.165	0.03
0.855	1.156	0.04
0.906	1.136	0.05
0.947	1.085	0.03
1.003	1.123	0.03
1.053	1.200	0.04
1.101	1.227	0.07

phase effect in U-B is apparent. There were no obvious differences between the separate runs on individual nights. Nauskiaa is a reddish asteroid with one of the best defined absorption bands yet seen. The light-curve data is from Yang et al (1965). Group R3A.

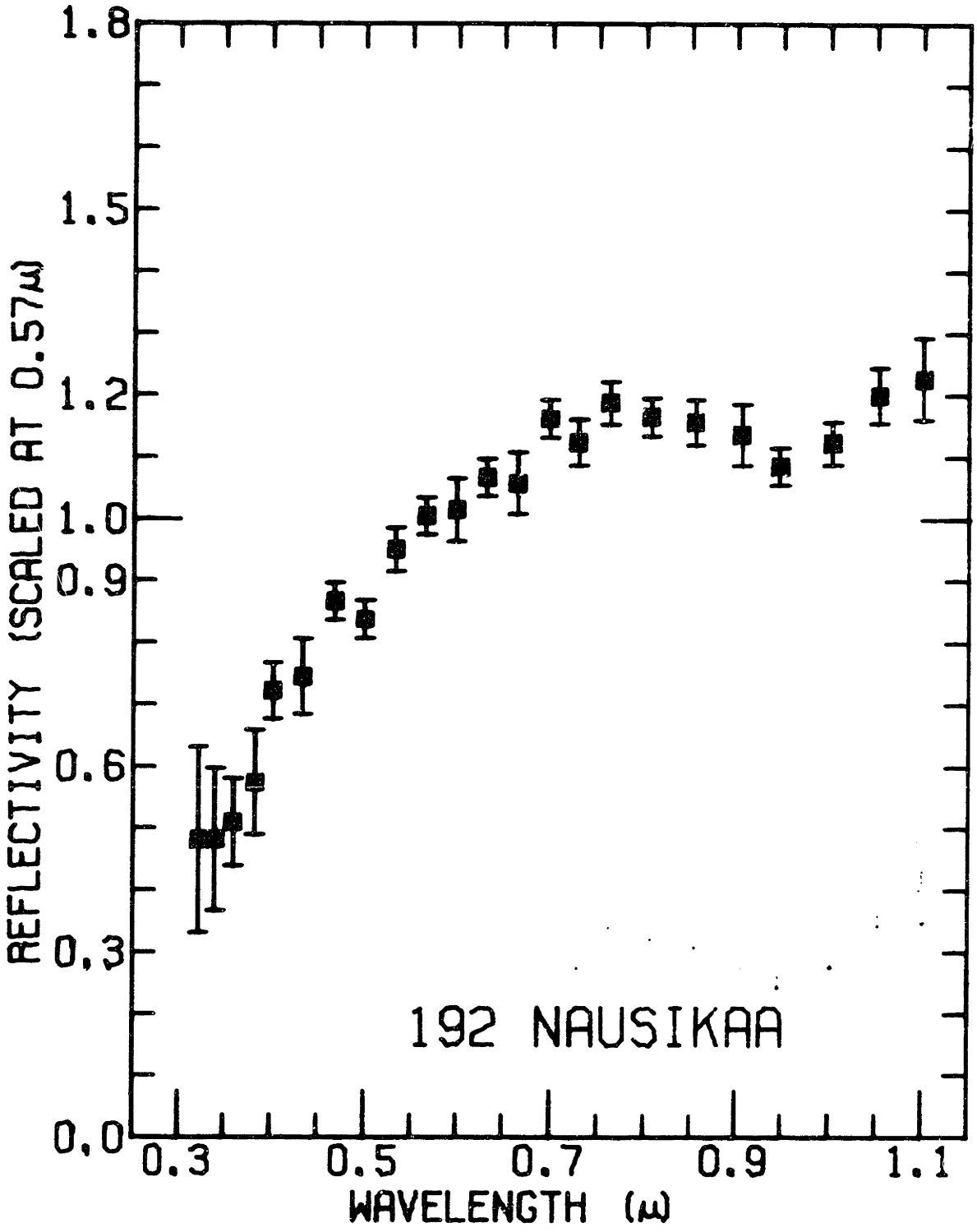
1.8
1.5
1.2
1.0
0.9
0.6
0.3
0.0
REFLECTIVITY (SCALED AT 0.57μ)
192 NAUSIKAA
0.3
0.5
0.7
0.9
1.1
WAVELENGTH (μ)

324 BAMBERGA

a = 2.682 AU e = 0.288 sin i = 0.229 Mars dist. = 0.05 AU None

B(1,0) = 8.14 L. Curve: $8^h.?$, 0.07 m.

(1) 2/10/71. 2 runs: 11:04, 11:21 ST ($0^h.13$). $i = 3^\circ$ m = 12.3

Standard: Alpha Leo, sec z = 1.09 - 1.12, very good. ID: "positive by relative motion". Second run may be subject to scattered moonlight, although both runs appear similar.

Comments: There is evidence of the 0.66 micron dip in both runs. Bamberga was located very near standard star Alpha Leo and only a few degrees from the moon, emerging from total eclipse. During the first run the umbra covered about half the moon; about a quarter of the moon during the second run. There is no evidence the data were affected by scattered light, however. The intriguing problems raised by the unusually low albedo determined by Matson (1971, and private communication) for this nearly-Mars-crossing asteroid are discussed in more detail elsewhere in the thesis.

Group M2.

324 BAMBERGA

Wavelength	Reflectivity	Mu
0.322	0.753	0.48
0.341	0.719	0.13
0.360	0.739	0.03
0.383	0.876	0.03
0.402	0.759	0.03
0.434	0.854	0.03
0.468	0.855	0.06
0.500	0.931	0.03
0.533	1.006	0.03
0.566	1.000	0.03
0.599	0.968	0.04
0.632	0.982	0.03
0.665	0.914	0.03
0.699	0.979	0.05
0.729	1.104	0.05
0.763	1.097	0.04
0.807	1.144	0.09

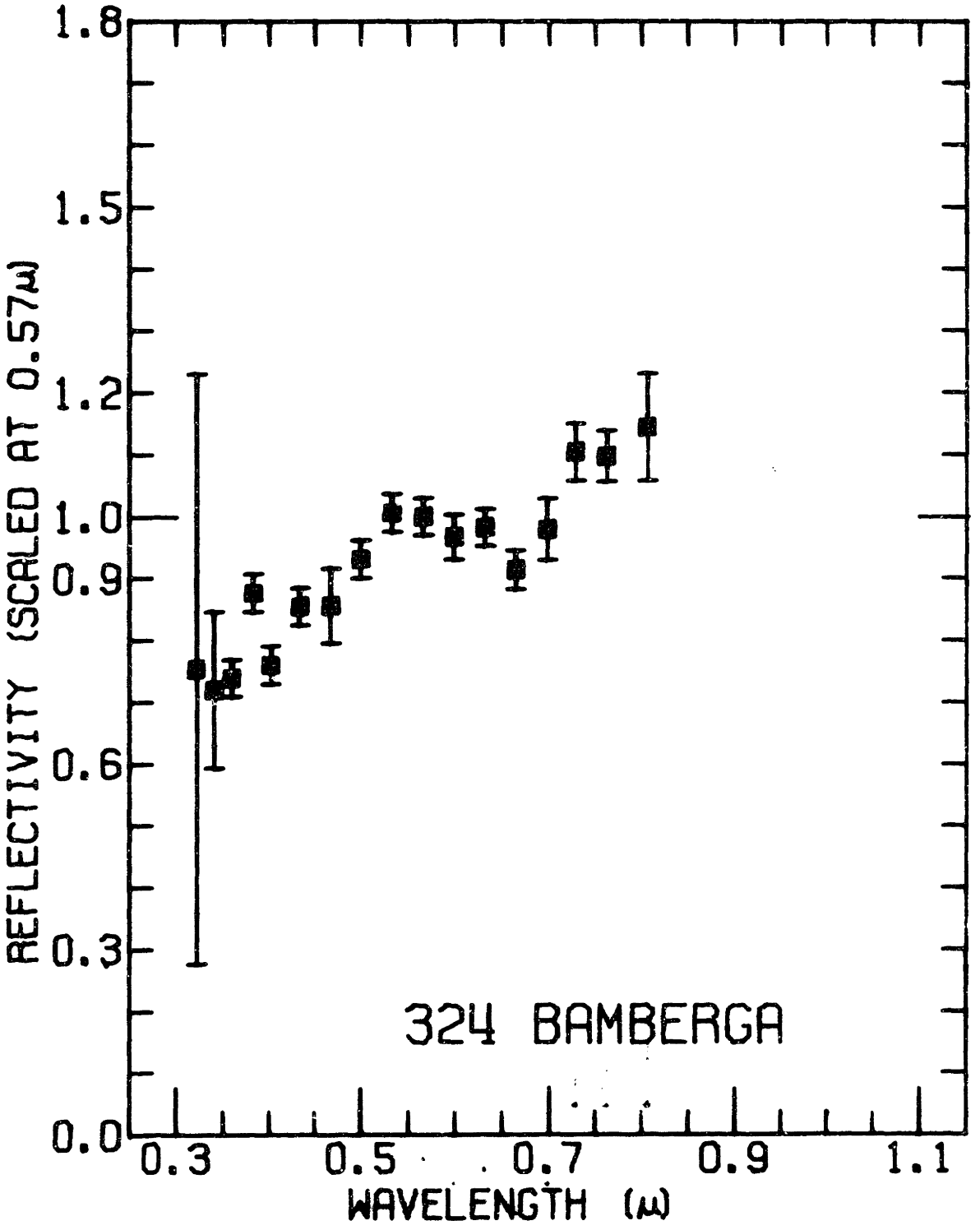
1.8
1.5
1.2
1.0
0.9
0.6
0.3
0.0
REFLECTIVITY (SCALED AT 0.57μ)
324 BAMBERGA
0.3
0.5
0.7
0.9
1.1
WAVELENGTH (μ)

337 DEVOSA

a = 2.383 AU e = 0.154 sin i = 0.142 Mars dist. = 0.18 AU Triplet B(1,0) = 10.05

(1) 2/7/71. 1 run: 11:10 ST ($0^h.6$). i = 7° m = 12.2

Standard: Alpha Leo, sec z = 1.05, good. S-20 + ND2. Guiding: 5, 11. Single weight (fil. 19 omitted).

(2) 2/12/71. 3 partial runs: 7:23, 7:54, 11:51 ST ($0^h.4$)

i = 4° m = 12.1

Standard: Alph Leo, sec z = 1.11 - 1.34, fair. Counts = 500. Guiding: 12, 19. Runs interrupted by cloudy periods; average probably good to 3 - 5%. Single weight.

Comments: The data on the two nights are in reasonably good agreement. Group M4.

337 DEVOSA

Wavelength	Reflectivity	Mu
0.322	0.869	0.03
0.341	0.584	0.33
0.360	1.116	0.13
0.383	0.599	0.16
0.402	0.855	0.13
0.434	0.780	0.03
0.468	0.853	0.03
0.500	0.786	0.12
0.533	0.957	0.04
0.566	1.000	0.03
0.599	1.112	0.11
0.632	0.987	0.07
0.665	1.051	0.09
0.699	1.017	0.03
0.729	1.109	0.03
0.763	1.02	0.03
0.807	1.068	0.07
0.855	1.038	0.03
0.906	1.106	0.03
0.947	1.102	0.07
1.003	1.087	0.09
1.053	1.001	0.03
1.01	1.016	0.03

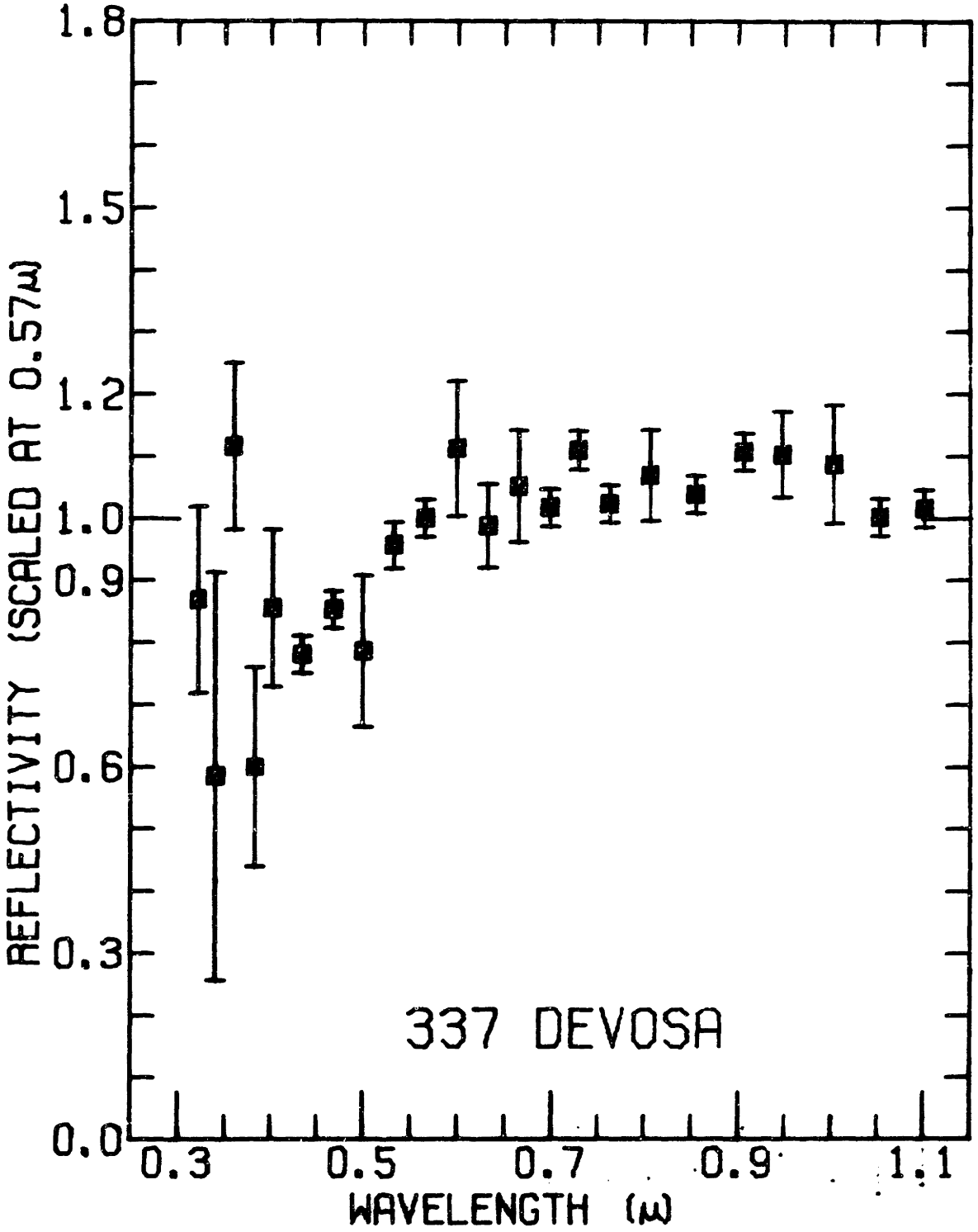
1.8
1.5
1.2
1.0
0.9
0.6
0.3
0.0
REFLECTIVITY (SCALED AT 0.57μ)
337 DEVOSA
0.3
0.5
0.7
0.9
1.1
WAVELENGTH (μ)

356 LIGURIA

a = 2.758 AU e = 0.224 sin i = 0.168 Mars dist. = 0.24 AU None

B(1,0) = 9.11

(1) 2/10/71. 2 runs: 12:01, 12:29 ST ($0^h.25$). i = 9° m = 12.2
Standard: Alpha Leo, sec z = 1.10 - 1.14, good. S-20 + ND2. ID:
"probable that this is correct". Guiding: 6.

Comments: Both runs are identical. Group M4.

356 LIGURIA

Wavelength	Reflectivity	Mu
0.322	0.397	0.10
0.341	0.743	0.10
0.360	0.788	0.10
0.383	0.448	0.10
0.402	0.745	0.03
0.434	0.791	0.03
0.468	0.920	0.05
0.500	0.958	0.03
0.533	0.981	0.03
0.566	1.000	0.10
0.599	1.061	0.03
0.632	1.026	0.03
0.665	1.023	0.03
0.699	1.024	0.04
0.729	1.071	0.03
0.763	1.018	0.05
0.807	1.280	0.04

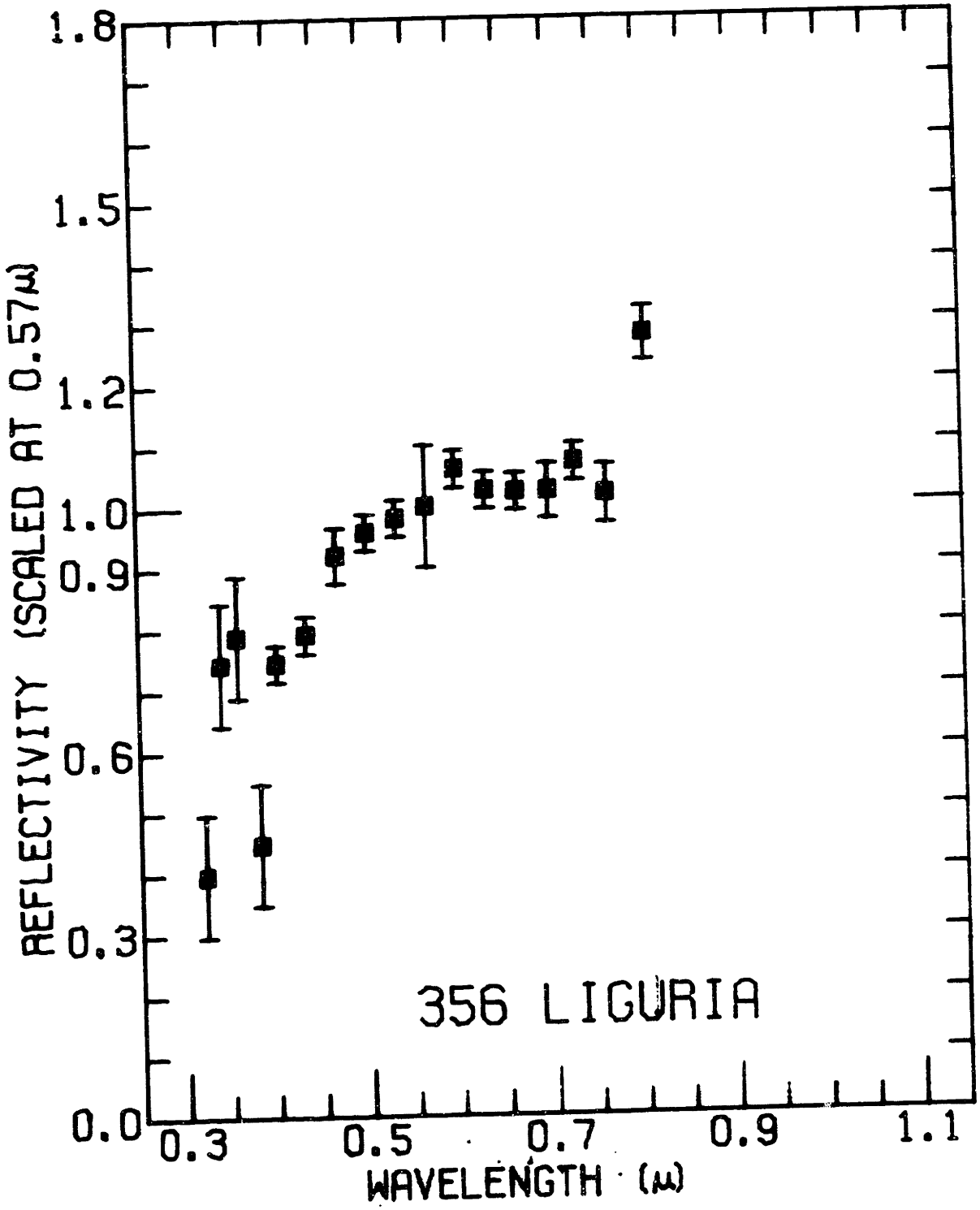
1.8
1.5
1.2
1.0
0.9
0.6
0.3
0.0
REFLECTIVITY (SCALED AT 0.57μ)
356 LIGURIA
0.3
0.5
0.7
0.9
1.1
WAVELENGTH (μ)

409 ASPASIA

a = 2.575 AU e = 0.094 sin i = 0.212 Mars dist. = 0.50 AU Sophrosyne B(1,0) = 8.63

(1) 2/10/71. 2 runs: 7:01, 7:17 ST ($0^h.27$). i = $8\frac{1}{2}^\circ$ m = 12.0 Standard: Eta Hya., sec z = 1.17 - 1.19, very good. S-20 (no ND). ID: "motion observed with respect to stars". Guiding: 4 - 8, 10, 18. Single weight (fil. 19 omitted).

(2) 2/11/71. $1\frac{1}{2}$ runs: 10:49, 11:22 ST ($0^h.83$). i = 9° m = 12.0 Standard: Theta Vir., Zeta Oph., Gamma Gem., and Eta Hya., sec z = 1.47 - 1.68, good. Counts = 860. ID: "absolutely certain, by relative motion". Guiding: 3, 10, 15, 22. Second run, fil. 15 - 23 only. Single weight, multiplied by 1.03.

Comments: Agreement between the separate runs is good except near 0.75 microns where the S-20 runs are somewhat brighter. This effect causes a probably spurious suggestion of an absorption band near 0.95 microns. Group M3.

409 ASPASIA

Wavelength	Reflectivity	Mu
0.322	1.199	0.03
0.341	1.003	0.32
0.360	0.613	0.20
0.383	0.717	0.03
0.402	0.811	0.03
0.434	0.867	0.04
0.468	0.965	0.03
0.500	0.962	0.03
0.533	0.947	0.07
0.566	1.106	0.11
0.599	1.031	0.03
0.632	1.009	0.03
0.665	0.964	0.04
0.699	1.002	0.03
0.729	1.077	0.04
0.763	1.093	0.04
0.807	1.113	0.09
0.855	1.052	0.03
0.906	1.018	0.05
0.947	0.961	0.03
1.003	1.124	0.03
1.053	0.897	0.10

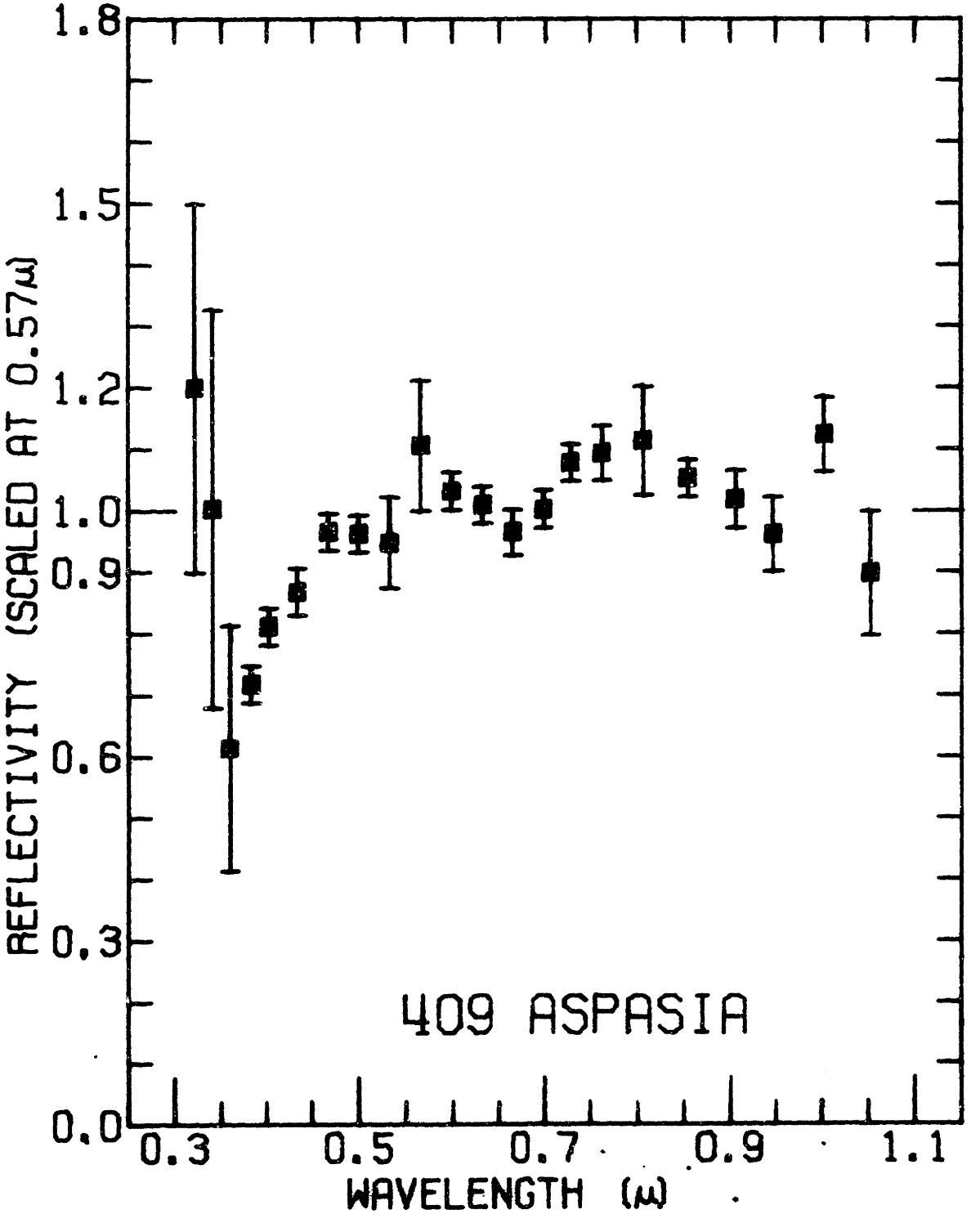
1.8
1.5
1.2
1.0
0.9
0.6
0.3
0.0
REFLECTIVITY (SCALED AT 0.57μ)
409 ASPASIA
0.3
0.5
0.7
0.9
1.1
WAVELENGTH (μ)

554 PERAGA

a = 2.375 AU e = 0.148 sin i = 0.066 Mars dist. = 0.20 AU Peraga B(1,0) = 9.49

(1) 2/10/71. 1 run: 10:00 ST ($0^h.32$). i = 1° m = 11.7
Standard: Alpha Leo, sec z = 1.07, good. S-20 + ND2. Single weight.

(2) 2/12/71. 1 run: 6:34 ST ($0^h.73$). i = 1° m = 11.7
Standard: Alpha Leo, sec z = 1.46, fair. Counts = 640. Guiding: 11. Single weight.

Comments: The S-20 run shows a more prominent break in slope near 0.5 micron, but the runs are similar and agree quite well. The observations were made unusually near 0° phase angle. Peraga appears to be reasonably bright into the UV, although it has a slightly reddish slope. Group B1.

554 PERAGA

Wavelength	Reflectivity	Mu
0.322	0.735	0.09
0.341	0.919	0.11
0.360	0.913	0.04
0.383	0.754	0.08
0.402	0.790	0.03
0.434	0.827	0.03
0.468	0.969	0.07
0.500	0.934	0.03
0.533	0.994	0.03
0.566	1.000	0.10
0.599	0.967	0.03
0.632	0.977	0.03
0.665	0.941	0.03
0.699	0.990	0.03
0.729	1.009	0.03
0.763	0.987	0.06
0.807	1.072	0.03
0.855	0.957	0.29
0.906	1.051	0.10
0.947	1.019	0.10
1.003	0.975	0.10
1.053	0.980	0.10
1.101	0.976	0.10

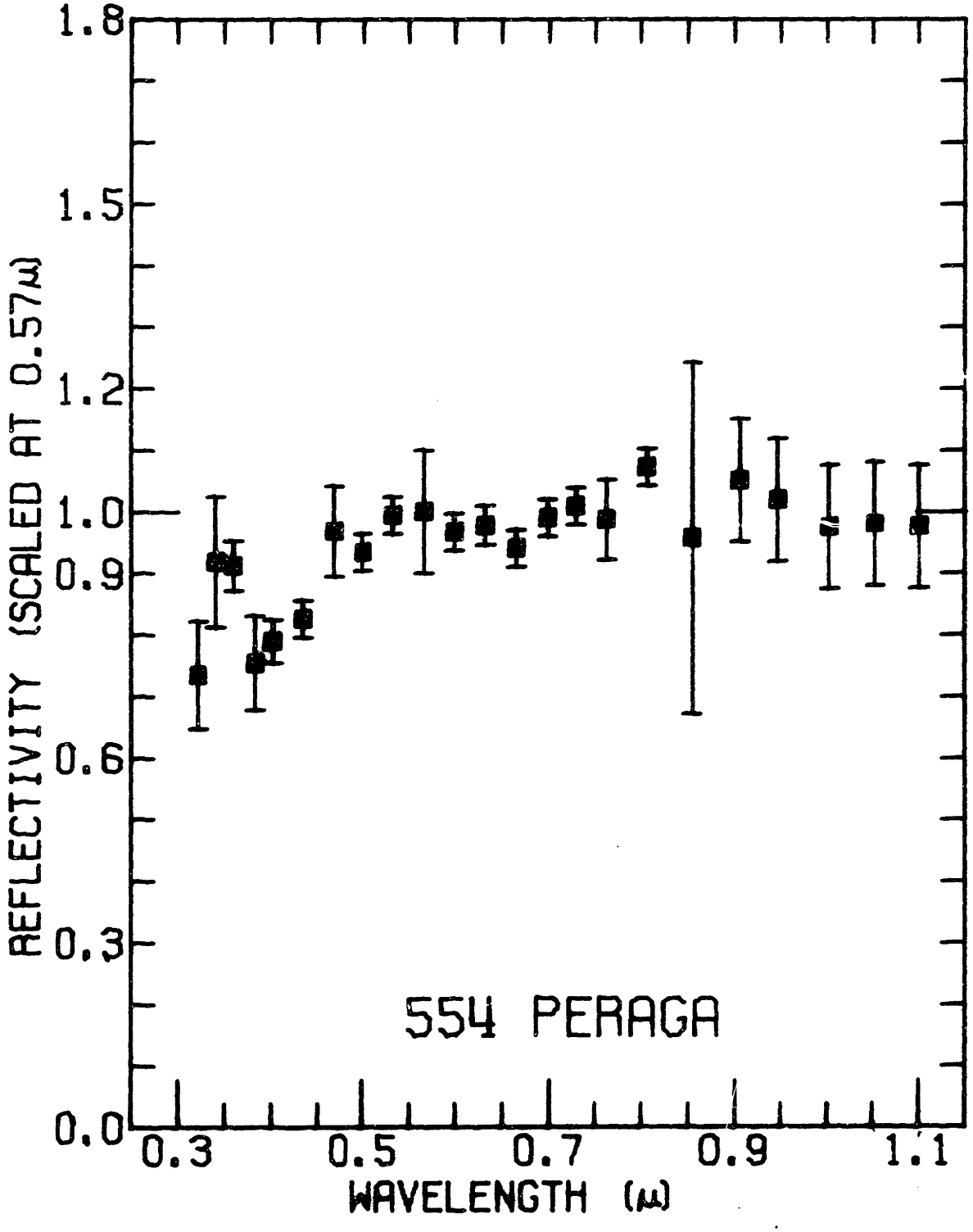
1.8
1.5
1.2
1.0
0.9
0.6
0.3
0.0
REFLECTIVITY (SCALED AT 0.57μ)
554 PERAGA
0.3
0.5
0.7
0.9
1.1
WAVELENGTH (μ)

563 SULEIKA

a = 2.713 AU e = 0.232 sin i = 0.160 Mars dist. = 0.20 AU Triplet (A-84)

B(1,0) = 9.57

(1) 1/7/71. 1 run: 7:17 ST ($1^h.26$). i = 9° m = 12.0

Standard: Gamma Gem., sec z = 1.05, very good. Counts = 350. ID: "seems very likely to be correct; agrees with expected motion from last night's position; some motion probably detected tonight". Guiding: 10, 15, 18, 21.

Comments: This run seems good but the counting statistics are too poor to confidently measure the band position. The asteroid could not be found in February. Group R4.

563 SULEIKA

Wavelength	Reflectivity	Mu
0.322	0.708	0.08
0.341	0.581	0.08
0.360	0.689	0.08
0.383	0.674	0.08
0.402	0.604	0.08
0.434	1.026	0.08
0.468	0.930	0,08
0.500	1.005	0.08
0.533	0.899	0.08
0.566	1.000	0.08
0.599	1.086	0.08
0.632	1.038	0.08
0.665	1.234	0.08
0.699	1.145	0.08
0.729	1.158	0.08
0.763	1.220	0.08
0.807	1.258	0.08
0.855	1.155	0.08
0.906	1.102	0.08
0.947	1.181	0.08
1.003	1.352	0.08
1.053	1.228	0.08

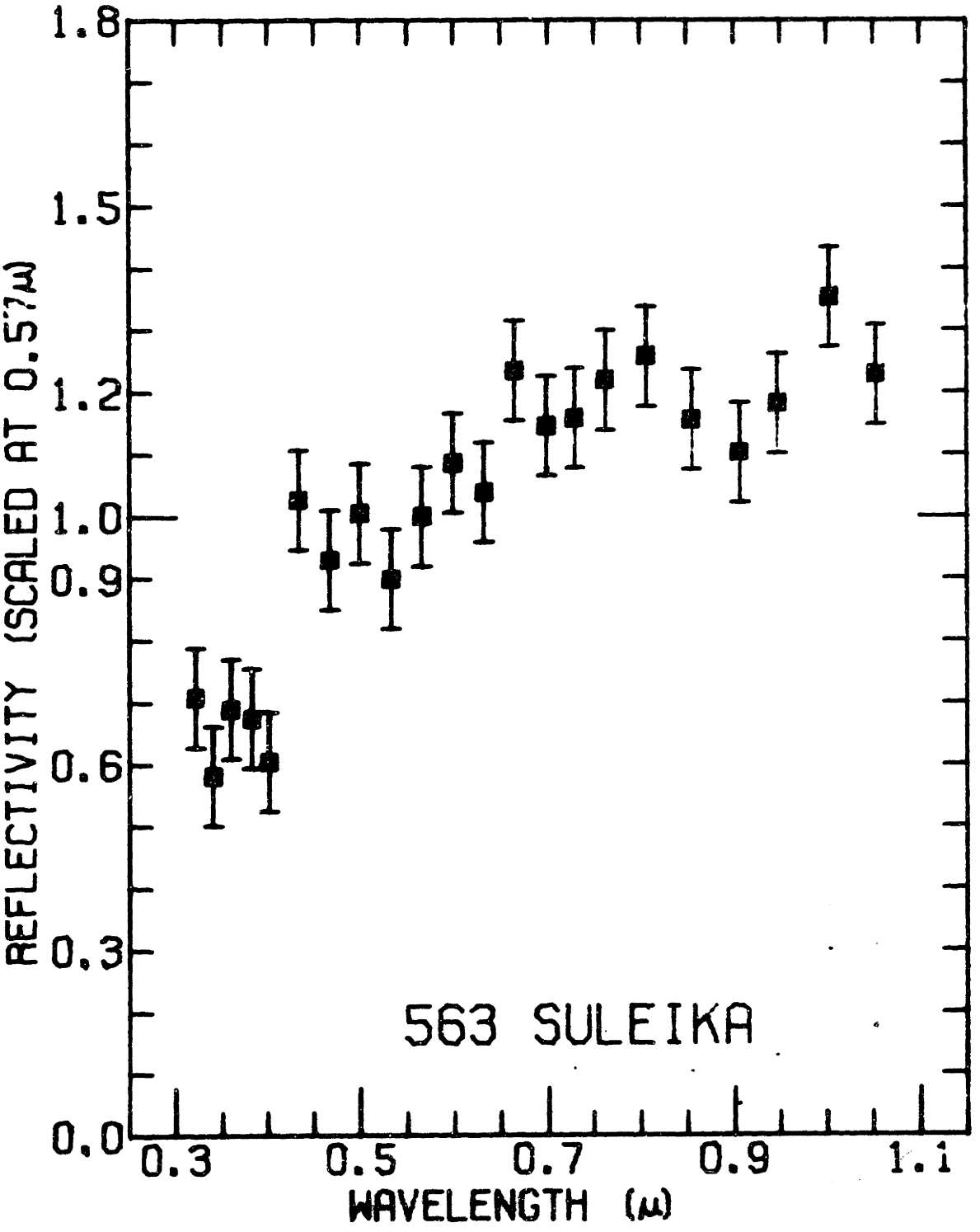
1.8
1.5
1.2
1.0
0.9
0.6
0.3
0.0
REFLECTIVITY (SCALED AT 0.57μ)
563 SULEIKA
0.3
0.5
0.7
0.9
1.1
WAVELENGTH (μ)

704 INTERAMNIA

a = 3.057 AU e = 0.09 sin i = 0.324 Mars dist. = 0.84 AU Doublet

B(1,0) = 7.60 **L. Curve: none (Yang et al, 1965)**

(1) 1/5/71. 1½ runs: 7:23, 9:42 ST ($1^h.05$). i = 10° m = 12.1
Standard: Gamma Gem., sec z = 1.15 - 1.22, good. Counts = 600. ID: "obvious due to motion". Guiding: 11, 13. Second run, fil. 2 - 9 only, stopped due to asteroid's near-occultation of a star. Single weight.

(2) 2/7/71. 1 run: 9:36 ST ($0^h.4$). i = 5° m = 12.0
Standard: Alpha Leo, sec z = 1.16, good. S-20 + ND2. Guiding: 8; star 6, 8. Single weight, multiplied by 1.03.

(3) 2/11/71. 1 run: 7:04 ST ($0^h.8$). i = 6° m = 12.0
Standard: Gamma Gem. and Eta Hya., sec z = 1.18, good. Counts = 970. Guiding: 13. Single weight.

Comments: Taken without regard to possible rotational variations in color, the data show a significant trend toward a bluer color with increasing phase angle (a B-V color change of about 0.1 mag. between 1/5 and 2/7). The dip near 0.65 microns is apparent in all three runs, but shows no phase dependence in strength. Interamnia has one of the flattest spectral reflectivity curves of any asteroid. Group B3.

704 INTERAMNIA

Wavelength	Reflectivity	Mu
0.322	0.878	0.07
0.341	0.879	0.06
0.360	0.947	0.06
0.383	0.841	0.04
0.402	0.901	0.06
0.434	0.925	0.05
0.468	0.929	0.03
0.500	0.931	0.03
0.533	1.018	0.03
0.566	0.998	0.03
0.599	0.973	0.03
0.632	0.911	0.03
0.665	0.923	0.05
0.699	0.988	0.03
0.729	0.998	0.03
0.763	0.957	0.04
0.807	0.974	0.08
0.855	0.987	0.04
0.906	0.906	0.04
0.947	0.913	0.04
1.003	0.940	0.03
1.053	0.906	0.03

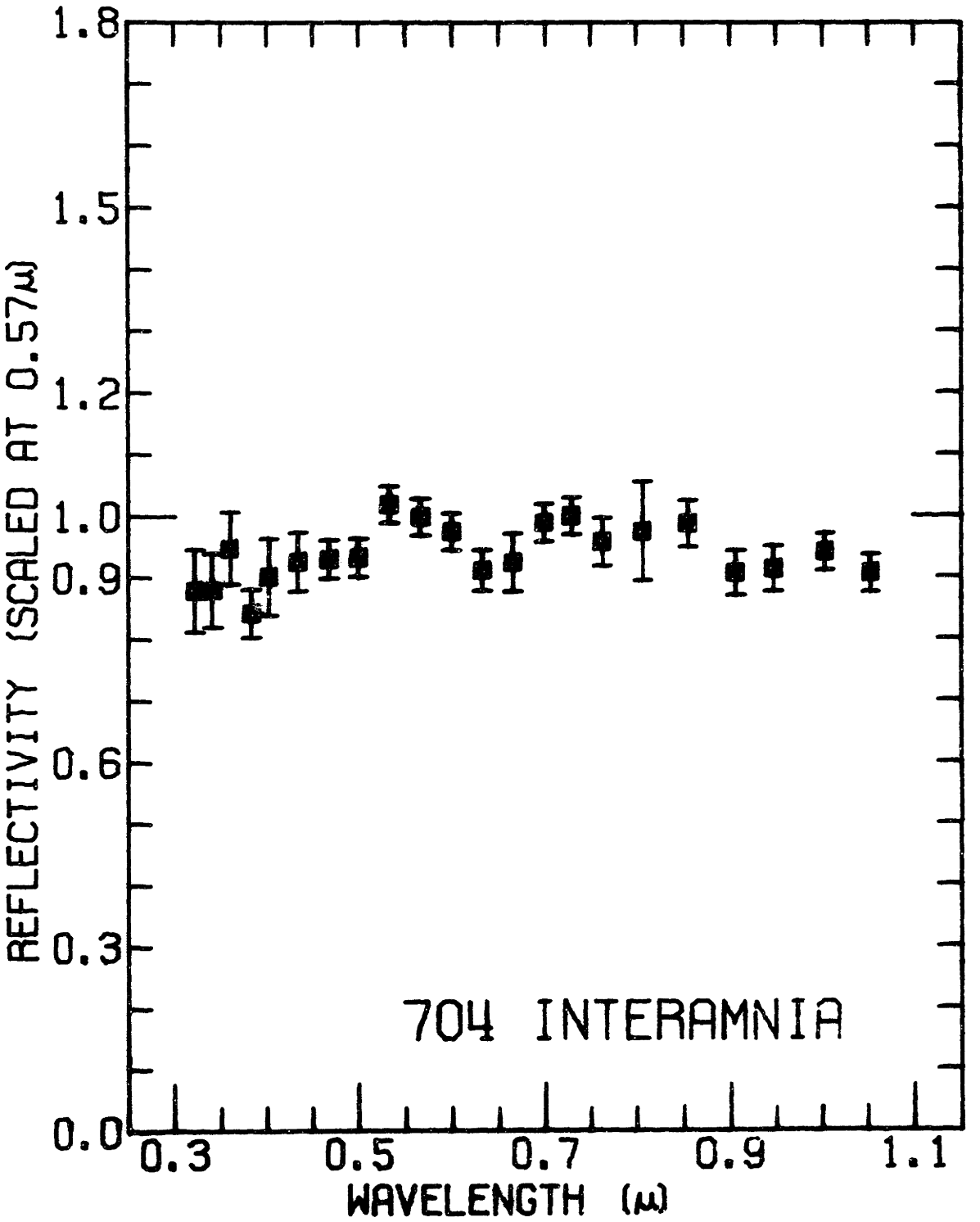
1.8
1.5
1.2
1.0
0.9
0.6
0.3
0.0
REFLECTIVITY (SCALED AT 0.57μ)
704 INTERAMNIA
0.3
0.5
0.7
0.9
1.1
WAVELENGTH (μ)

APPENDIX II

PLANNING AND EXECUTING THE OBSERVING PROGRAM

A. CRITERIA FOR SELECTING ASTEROIDS: PRIORITIES

Prior to each observing run, I listed all asteroids brighter than magnitude 13.0 for which ephemerides existed for the dates of the run. Asteroids were arranged in order of priority by a variety of criteria. Extensive preparations were made for observing the highest ten or twenty asteroids on the priority list, including preparation of finding charts and airmass charts. I describe first the selection criteria and then consider how they might affect statistical interpretations in the thesis.

Visibility Criteria

The 13.0 magnitude cut-off (occasionally a brighter limit, especially for 24-inch telescope runs) is the dominant selection factor. Beyond that, brighter asteroids were given somewhat higher priority than fainter ones. Lower weight was given to asteroids at high negative declinations, especially those south of -20°.

I attempted to observe asteroids near time of transit. For asteroids near opposition, transit occurs near midnight. Away from opposition, most asteroids are too faint to be observed, or ephmerides are not available. Therefore in order to use the hours following twilight or preceding dawn, priority was given to asteroids available then -- generally the brighter asteroids.

Physical Characteristics

The very highest priority was given to pairs of asteroids listed by Arnold (1969) as being members of the same family. There are relatively few asteroids in this category, and some are not in the same family according to Williams (1971, private communication). I attempted to observe asteroids having representative values of several parameters; since average values were common, this meant giving extra weight to those having extreme values. The parameters included: semi-major axis, orbital eccentricity, inclination, absolute magnitude, rotation period, maximum light-curve amplitude, and UBV colors.

Some weight was also given to asteroids about which something else is known. Thus asteroids for which UBV colors are known, or asteroids known to be in a family (from Arnold, 1969), or asteroids whose polarization was discussed by Veverka (1970) received higher weight. Dennis Matson provided lists of asteroids he had either successfully observed in the thermal IR, or was planning to observe.

Selection Bias

The controlling criteria were the availability of ephemerides and the apparent magnitudes. Aside from parameters with strong secondary correlations with those two criteria (B(1,0), perhaps a), the sample is quite representative because of the many selection factors, none of which dominated the final priorities. The sample of 31 asteroids actually observed resembles a subset of any larger sample of brighter asteroids, such as the sample of about 100 asteroids for which good colors are known, discussed in Chap. V. I discuss the characteristics of the final sample at the beginning of Chap. IV.

B. FINDING ASTEROIDS

Ephemerides

The primary source for asteroid locations is the Russian "Ephemerides of Minor Planets" (volumes for 1970 and 1971: Chebotarev, 1969; 1970). Particularly useful in the 1970 volume were the ephemerides of bright minor planets, which gave positions for a six-month period centered on opposition, instead of the usual two-month period. Unfortunately, this section has been discontinued; P. Herget of the Cincinnati Observatory, however, provided lengthy ephemerides for some of the brighter minor planets visible in the first half of 1971.

Finding Charts

Jay Kunin, of the M.I.T. Planetary Astronomy Laboratory, developed a computer program to produce finding charts for asteroids. The basic program (SAOPLOT) was obtained from the M.I.T. X-ray Astronomy Group and was modified to meet the specifications of the asteroid observing project. The input data are the 10-day ephemeris positions. The program interpolates, using third differences, to 0^h U.T. on each day; it prints out positions for both epoch 1950.0 and precessed to current date. The program generates a Calcomp plot of the asteroid positions on a grid to the scale of the Palomar Sky Survey; also symbols (scaled according to magnitude) for the 60 brightest stars in the field, obtained from the Smithsonian Astrophysical Observatory Star Catalog (resident on magnetic tape).

One-to-one photographic copies were made of the red Palomar Sky Survey charts for the dozen-or-so highest priority asteroids. During the day before each observing night, the computer-plotted overlays were used to plot positions and paths of the scheduled asteroids on the Sky Survey copies.

Finding at the Telescope

Using the Sky Survey copy directly at the eyepiece of the finder telescope, I could easily locate the proper star field. Generally a "new star" was easily seen at or very near the predicted location of the asteroid. Occasionally scattered moonlight was too bright, or the asteroid too faint, and it took some while to locate the asteroid. The problem was especially acute with the undersized finder of the Mt. Wilson 60-inch reflector. A few asteroids were too faint to find.

The location of the photometer aperture was well-determined with respect to cross-hairs in the finder, and the asteroid could be placed very nearly in the aperture using the finder alone. The position with respect to field stars was rechecked periodically during the course of observations; usually slight motion could be detected. Occasionally more obvious motion with respect to field stars was noted in the eyepiece of the photometer.

Misidentifications and Failures to Locate

Several asteroids could not be found, probably because they were too faint. Repeated failures to find two asteroids (56 Melete and 679 Pax) suggest they were much fainter than predicted or that their ephemerides were bad. One other asteroid was found a full day behind in its orbit. Asteroid 563 could not be found in February, although it was

observed in January.

In most cases the identifications were certain. No object was observed and subsequently discovered to be a star. There remains a small but finite possibility that one of the observed asteroids is in fact a G-type star, but it is unlikely.

C. ALLOCATION OF TIME DURING A NIGHT

Airmass Charts

I have modified a program originally written by J. Elias, of the M.I.T. Planetary Astronomy Laboratory, which plots out a graph of airmass versus sidereal time for each standard star (from the Oke and Hayes lists, see Appendix V). Charts were made for each observatory. Similar airmass charts were made for priority asteroids, valid for the dates of each observing run. These charts permit easy planning, since one can readily determine the time when the closest standard star will be at the same airmass as an asteroid.

Nightly Observing Schedule

A tentative observing schedule was prepared during each day preceding an observing night. Asteroids were selected from the top of the priority list, with consideration given to their availability at an open time in the schedule, whether or not the same standard star could be used for several asteroids, and similar factors. Time was allotted for other projects, for changing and re-icing the photomultipliers, etc. Alternative asteroids were selected and prepared in the event the first priority could not be located, or was in an unfavorable location with respect to orographic clouds or sources of scattered light.

Periods of cloudiness and equipment problems frequently forced a modification of the planned schedules, but efficiency in the dome was kept to a high level by the careful planning. Fig. A-2-1 shows two representative time-lines of the actual use of telescope time.

D. OBSERVING MODES

Efficient use of the double-beam photometer and its electronics requires two observers -- one observer at the telescope, the second handling the computer and the log.

The first observer, nearly always myself (CRC), performed a variety of tasks at the telescope: (1) locating the asteroid or star in the finder; (2) guiding with the paddle to keep the object in the aperture; (3) switching filters, when not controlled by the computer; (4) watching sky conditions and (5) making verbal comments about guiding problems, sky conditions, etc.

The second observer (sometimes assisted by a third, or an observatory night assistant) usually did the following tasks in a distant part of the dome (or in the downstairs observing room of the 24-inch in August 1970): (1) maintaining the log (recording sidereal times and filter numbers of tape dumps, comments on the quality of the data as it appears on the oscilloscope display, and comments from the telescope observer): (2) pushing control buttons on the computer to start and stop runs and to dump data on the tape: and (3) watching the sky conditions and dome position.

The observing set-up is illustrated schematically in Fig. A-3-1.

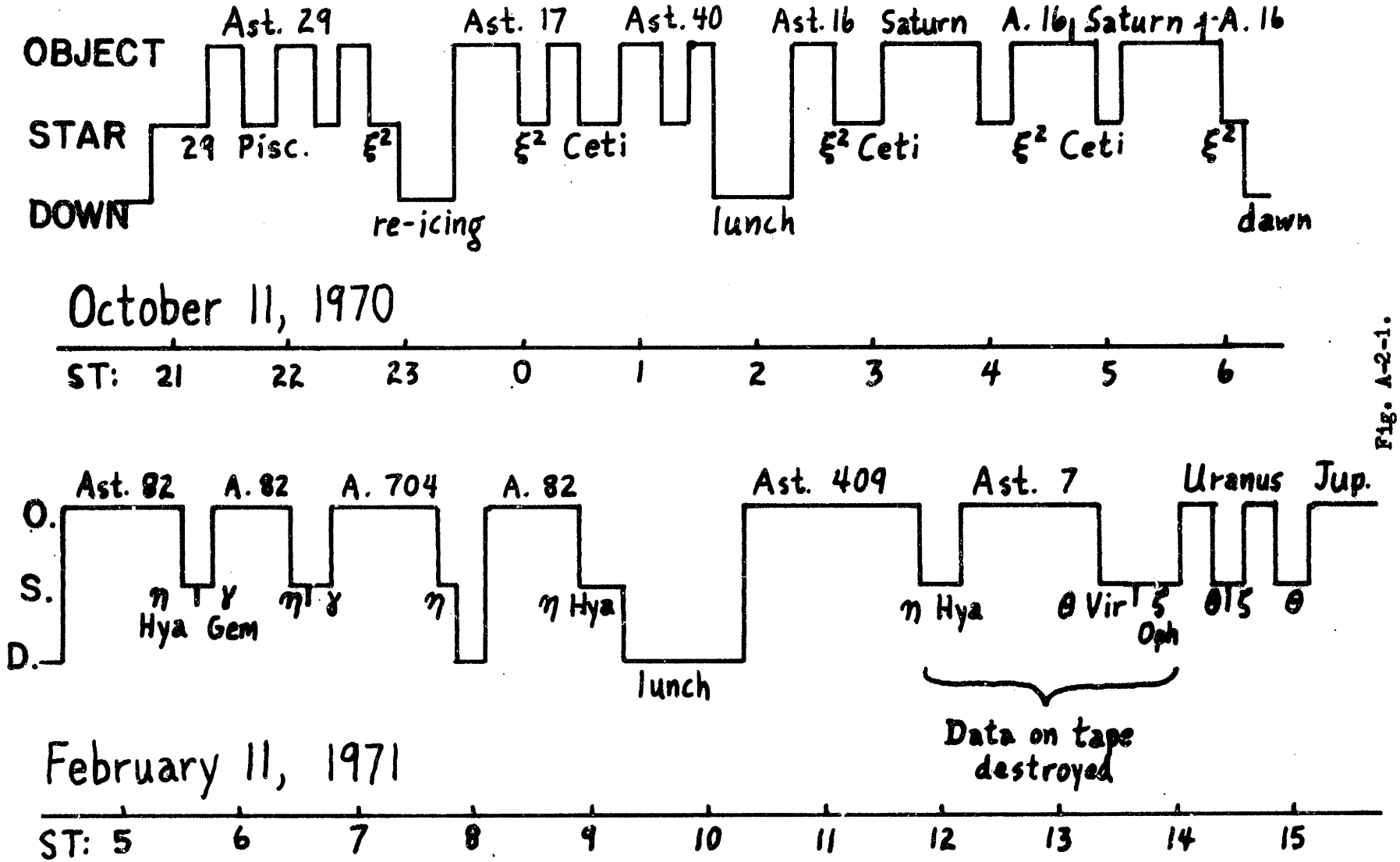
OBJECT
STAR
DOWN
Ast. 29
29 Pisc.
ξ²
re-icing
Ast. 17
ξ² Ceti
Ast. 40
lunch
Ast. 16
ξ² Ceti
Saturn
A. 16
ξ² Ceti
Saturn 1
A. 16
ξ²
dawn
October 11, 1970
ST: 21 22 23 0 1 2 3 4 5 6
O.
S.
D.
Ast. 82
η Hya
A. 82
γ Gem
A. 704
η
γ
η
A. 82
η Hya
lunch
Ast. 409
η Hya
Ast. 7
θ Vir
ζ Oph
Uranus
θ15
Jup.
θ
Data on tape destroyed
February 11, 1971
ST: 5 6 7 8 9 10 11 12 13 14 15

Fig. A-2-1.

APPENDIX III

TELESCOPES, INSTRUMENTATION, OPERATING MODES

A. TELESCOPES

Four telescopes were used for acquiring spectral reflectivity data on asteroids. Characteristics of these telescopes relevant to interpreting the asteroid data are briefly discussed here.

Some data on 1 Ceres, 2 Pallas and 3 Juno were acquired on the Palomar 200-inch reflector. The photometer was mounted in the east arm. Little care was made to shield the instrument from scattered light, which may have affected some data taken during bright twilight and dawn. Complete descriptions of the problems encountered are given in Appendices IV and V.

The Mt. Wilson 24-inch reflector (of the Caltech Division of Geological Sciences) was used on two occasions. The instrument is compact and versatile and is equipped with an especially good finder. However there were occasional problems with the tracking drive, especially when the telescope was well west of the meridian. Scattered light proved to be a considerable potential problem, especially after a layer of white insulation material was sprayed over the inside of the small dome. Special care was taken to shield the photometer from lights on the electronic equipment.

The Mt. Wilson 60-inch reflector is a nearly ideal instrument for the project. However the small finder was barely adequate. Severe radio interference from nearby transmitting stations created intolerable noise until a shielded signal cable was substituted during the first night of the

October run. The photometer was mounted at the Cassegrain focus.

The Kitt Peak no. 2 36-inch reflector was used on two occasions. I understand that it had been recently prepared for minimal light-scattering behavior just prior to the February run. The telescope was very convenient to use and the skies were darker than on Mt. Wilson. The only major problem was occasional failure of the Tucson city power supply (see Appendix IV).

B. PHOTOMETER

The latest version of Prof. McCord's double-beam photometer (see McCord, 1968) was used for the observations. For reasons of experimentation, as well as necessity due to equipment failure, the photometer was operated in a variety of modes. Several minor modifications to the photometer were prompted by my early experience with it. These were the first extended series of observations of faint sources made with the photometer. The general design of the instrument and its set-up on the telescope are shown in Fig. A-3-1.

Photomultipliers

A photomultiplier with an S-1 detector was used for most data throughout its range of sensitivity (0.3 to 1.1 microns). On several occasions a photomultiplier with an S-20 sensor was used over its narrow range. Generally only one photomultiplier was kept on high voltage at a time, generally for an entire night. However, as a result of earlier experience, the advantages of using both more-or-less simultaneously became clear. A mount for holding both cold-boxes, permitting rapid switch-over, was designed by T. Johnson and first used during the May 1971 run. Both photomultipliers were kept on high voltage continuously and the signal cable was switched

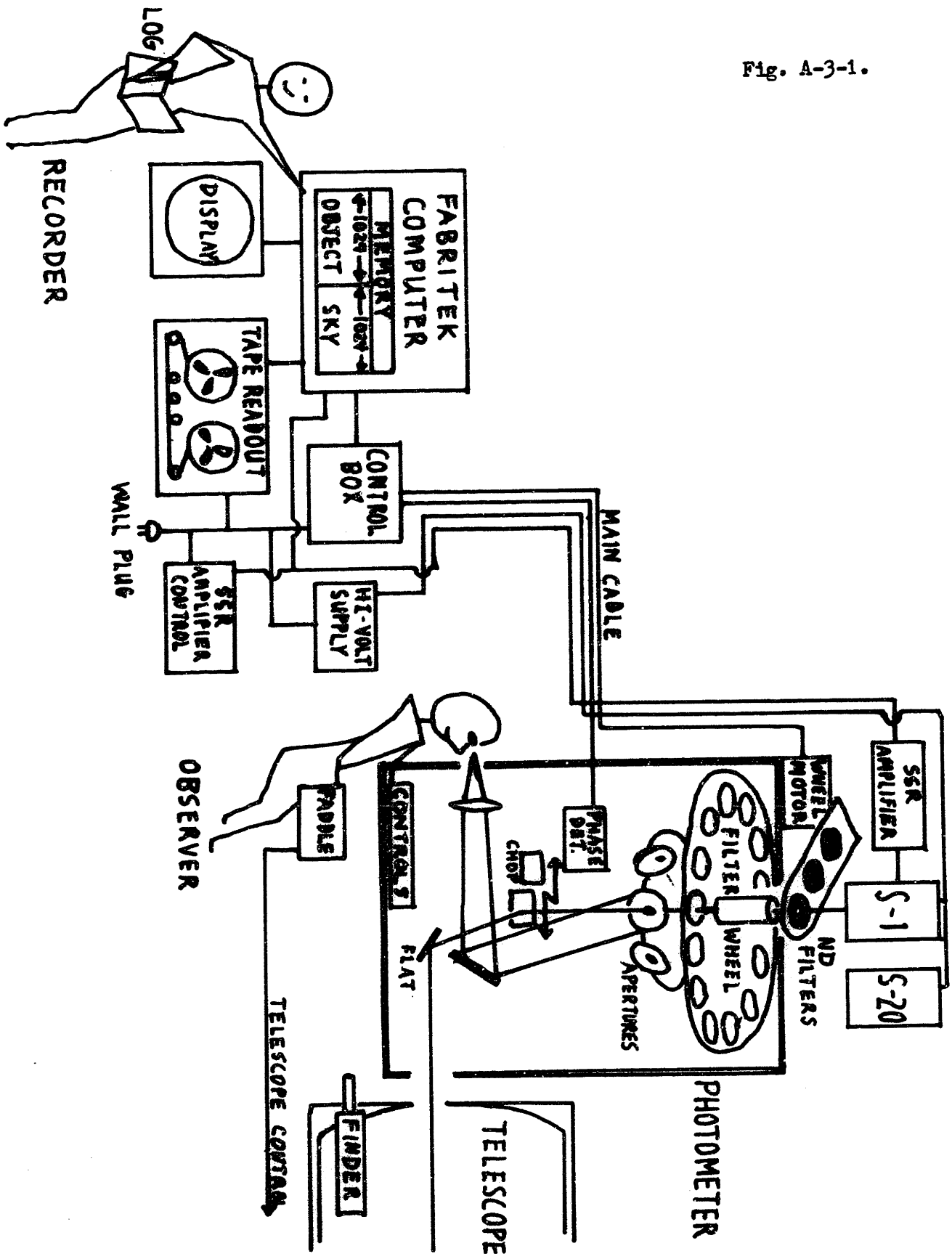
LOG
RECORDER
DISPLAY
FABRITEK COMPUTER
MEMORY
OBJECT
SKY
TAPE READOUT
CONTROL BOX
WALL PLUG
SSR AMPLIFIER CONTROL
HI-VOLT SUPPLY
MAIN CABLE
OBSERVER
PADDLE
CONTROLS
PHASE DET.
CHOP
WHEEL MOTOR
FILTER WHEEL
ND FILTERS
APERTURES
SSR AMPLIFIER
S-1
S-20
FLAT
PHOTOMETER
TELESCOPE
FINDER
TELESCOPE CONTROL

Fig. A-3-1.

when the tube positions were switched.

The tubes were generally run with an applied voltage of between 1800 and 2100 volts (usually 1800 for the S-20, and 1900 or 2000 for the S-1). Use was made of 0 to 10 dB attenuators, as well as direct observation of the change of signal level with voltage, to determine that these were suitable operating voltages. Normal voltage fluctuations did not appreciably affect the signal.

The cold boxes were filled with dry ice at least twice a night; they remained frosty for periods exceeding half a day. The dark current was continually monitored; it remained low and quite constant. There was one exception during the August run when all dry ice evaporated; the data taken for that particular asteroid have been omitted from consideration.

Double-beam Chopper and Aperture Wheel

Two identical mirrors are mounted on a flying shuttle in McCord's photometer. The mirror separation (and hence beam separation) can be adjusted, with some difficulty. The shuttle chops at ten hertz (full cycle), while data is taken for 40 msec first from one beam, then from the second beam, with 10 msec dead time. A rotor attached to the chopper assembly spins between a small light source and a detector, which signals the computer the phase of the chopper. The image is directed from the chopping mirrors upwards to an aperture mirror. A set of half a dozen mirrors, with aperture holes of various dimensions drilled in them, are located on a wheel which can be quickly turned to change apertures. The image of the field of view is reflected off the mirror (except for the small portion admitted through the aperture to the filter and phototube), through an eyepiece, and into the eye of the observer.

The observer perceives a dim field with a small black patch (the aperture). The field flickers as the observer perceives first an empty field (with the image of the object invisible in the aperture), followed by an off-shifted image of the object in the second beam displaced from the aperture, during which time the phototube is sampling the brightness of a spot of sky. A typical beam separation is several aperture diameters, or perhaps 20 arcseconds. The smallest aperture was used that permitted easy guiding and negligible light leakage -- typically 5 arcseconds or somewhat bigger. This is sufficiently large to minimize effects of differential refraction. Guiding was accomplished by three procedures: (1) prior to the start of each integration, the aperture wheel was rotated slightly back and forth so that the object could be accurately centered; (2) any drift could be detected by drift of the flickering second beam image with respect to the aperture; (3) a faint halo which could usually be detected around the aperture -- containing less than a fraction of a percent of the light -- becomes asymmetrical in distribution if the object drifts toward the edge of the aperture. It is perhaps interesting to note that I suffered moderately serious psychological reactions on occasions, particularly when trying to detect the aperture against an unusually dark sky. Typical symptoms were blindness, dizziness, and mild bewilderment. This may be caused by the Alpha-wave frequency of the chopper; other observers reported similar reactions.

Changing the separation of the mirrors proved to be particularly difficult. On several occasions a mirror broke and required some hours, or even days, to be fixed. After such mishaps, the photometer was operated as a single-beam photometer -- first observing the object in the aperture, followed by guiding off onto the sky. The observing efficiency was reduced operating in this mode, but the quality of the data was not impaired.

Although similar when originally mounted, the two mirrors can change their reflectivity characteristics with time. Frequent tests were run to observe standard stars in both beams, generally in the 11th of 16th filters only; occasional tests throughout the 0.3 to 1.1 micron span indicated wavelength-dependent differences. Since the second beam is only used for measuring the faint sky, differences of even several percent in mirror reflectivities have negligible effect on object-minus-sky values. The same beam was always used for asteroids and standards.

Narrowband Interference Filters and Filter-wheel Operating Modes

Twenty-four narrowband interference filters are mounted in a circular filter wheel which can be spun at 3 rpm or advanced incrementally by either computer or switch control. The characteristics of the filters are listed in Table A-3-1 (center wavelengths, approximate bandpasses and peak transmissions, and effective wavelengths when used with the S-20 and S-1 tubes).

The filter bandpasses were measured with a spectrometer in spring of 1971 by J. Elias. The characteristics were essentially unchanged from those determined at the time of purchase. However, the filters collect dirt and fingerprints. Although first-order effects are of no consequence since the brightness of the asteroid is ratioed to the brightness of the standard star (with or without dirt), the effect of a dead insect lying on one filter during an August test run was unmistakable. Also non-uniformities across filters were noticeable in data taken in the spinning-mode in October 1970, but affect both asteroid and standard star data similarly.

Table A-3-1. Interference Filters

No.	Wavelength (μ)	Bandpass (μ)	Peak Transmission	λ_{eff} S-20	λ_{eff} S-1
1*	0.3010	0.019	0.13	--	0.3100 ?
2	0.3196	0.016	0.19	0.3216	0.3229
3	0.3383	0.022	0.14	0.3406	0.3412
4	0.3590	0.014	0.18	0.3598	0.3593
5**	0.3831	0.013	0.23	0.3833	0.3825
6	0.4019	0.028	0.48	0.4021	0.4015
7	0.4344	0.028	0.42	0.4344	0.4340
8	0.4687	0.033	0.49	0.4684	0.4685
9	0.5001	0.029	0.57	0.4998	0.5001
10	0.5336	0.033	0.46	0.5331	0.5336
11***	0.5662	0.029	0.55	0.5658	0.5663
12	0.5993	0.032	0.54	0.5987	0.5994
13	0.6328	0.032	0.56	0.6322	0.6326
14	0.6649	0.027	0.50	0.6645	0.6649
15	0.6991	0.026	0.54	0.6986	0.6992
16	0.7299	0.033	0.51	0.7287	0.7300
17	0.7640	0.031	0.57	0.7628	0.7640
18	0.8078	0.049	0.46	0.8016	0.8072
19	0.8551	0.047	0.48	0.8499	0.8551
20	0.9063	0.048	0.58	--	0.9058
21	0.9475	0.051	0.59	--	0.9469
22	1.0036	0.050	0.53	--	1.0025
23	1.0548	0.050	0.55	--	1.0525
24	1.1033	0.049	0.44	--	1.1009

*Filter 1 destroyed, Nov. 1970.

**Filter 5: data poor due to Balmer discontinuity in standard stars.

***Filter 11: normalizing filter.

There were occasional problems advancing the filter wheel when operating in the filter-by-filter mode, but the filter sequence was rarely lost; in those rare cases, comparison with separate runs of the same object revealed any duplication or omission of filters.

Scattered Light

Observing procedures previously used for lunar and planetary spectrophotometry had to be abandoned for precision photometry of faint asteroids. The 'white-shirt effect" was detected during the first test run in August 1970. Thereafter, increasing care was taken to insure that all holes in the photometer box were patched with black tape and that the dark-cloth securely covered the front of the box. All sources of stray light in the dome were kept well-shielded, and attempts were made to avoid illuminating either the telescope, the photometer, or the observer with direct moonlight. The only two openings left into the box are through the telescope and through the guiding eyepiece. Tests suggest the latter opening was not a significant source for stray light in the box.

The chief extraneous light was reflected moonlight (off the telescope and skylight), and the sky brightening at dawn. Frequent measurements were made of "sky versus sky" (i.e. no object in the aperture) to determine inequalities in the background of the two beams. Scattered light tests were made either through no filter (clear hole) or through an opaque filter. Inequalities between the beams were important only during bright twilight or dawn; all such runs have been excluded well before the point where problems are apparent. Full moonlight caused some problems (mentioned when applicable in Appendix I), but no runs were deemed useless due to moonlight.

Neutral Density Filters

Many standard stars are too bright to be observed with the S-20 tube. For the brighter stars, data were taken in February and May through Oriel ND1 and ND2 filters. They have relatively flat spectral characteristics throughout the wavelength range of interest, unlike Wratten ND filters which have large infrared light leaks. In February, the ND2 filter was mounted behind an aperture mirror (at a 45°angle); calibration difficulties may be due to the angle, although the filters are of the thin-metal-coating variety. For the May run, a neutral density filter holder was built in conjunction with the double tube mount.

C. THE COMPUTER AND OPERATING MODES

Fabritek Computer

A hard-wired Fabritek computer controls the photometer and stores the data taken during each run. It has a memory of 4K, half of which was used for storing or co-adding data being taken (1K for object counts, 1K for sky); the other half was available for auxiliary purposes. The data are displayed in real-time on an oscilloscope. Upon command from the observing recorder, the computer memory is dumped onto magnetic tape. I now describe the several computer-controlled operating modes used most frequently.

Spinning and Co-adding Mode

The computer will record a specified number of chops from each filter when the filter wheel is spun. About six chops can be recorded in each filter without getting too near the edge of the filter; but the time spent between filters reduces efficiency by a factor of two. The computer will

co-add data for a specified number of filter-wheel revolutions (limited to powers of two). The advantages of this method include the benefits of multiplexing -- data are taken in all wavelengths nearly simultaneously. Therefore variable sky conditions, or differences due to asteroid rotation, are minimized. It is more practical to make frequent and rapid standard star observations in this mode. Among the disadvantages are: ((1) inefficiency of data-taking; (2) non-uniformities across filters; (3) problems with vignetting at the edges of filters; and (4) the fact that guiding errors, if any, show up as spectral features and are difficult to detect by inspection of the data. This mode was used for the October 1970 run only.

Incremental Mode with Fixed Number of Chops

A more advantageous alternative mode is one in which the computer advances the filter wheel automatically and integrates for a specified number of chops before advancing again. Unfortunately this mode was not readily available until certain modifications were made in the spring of 1971. The data in May were taken in this manner, while using both photomultipliers. The number of chops were selected so as to just fill memory with either filters 2 - 18 (S-20) or 19 - 24 (S-1). This mode reduces the disadvantages of the spinning-mode, while largely retaining its advantages.

Filter-by-filter Mode

Most data were taken in this fashion. The computer is set so as to record data continuously after the start button is pushed and until the stop button is pushed or until memory is filled. The observer advances the filter wheel by a switch located in the photometer box, checks the guiding, and notifies the recorder to start observations. On some

occasions all of memory was filled with data from a single filter; on other occasions the stop button was pushed after a quarter or half of the available memory was filled. The data acquisition is efficient in this mode, but a complete cycle of 24 filters can take more than one hour; standard stars can be observed less frequently and it is riskier to work in marginal weather.

A variation of this mode was used to speed up standard star runs. There is no need to integrate for long on bright stars, so the filter wheel is advanced periodically by switch while the data fills up memory. Later examination of the data clearly reveals dips to zero during the intervals when the filter wheel advanced.

APPENDIX IV

THE OBSERVING RUNS

I obtained spectral reflectivity data on asteroids during seven observing runs with four telescopes from June 1970 to May 1971. Different problems were encountered during each run, and different observing procedures were used as dictated by both circumstance and hindsight. A full appreciation of the accuracies of the final results requires some discussion of these special circumstances.

Mt. Palomar 200-inch: June 1970

Twilight time was granted to Prof. McCord during the month of June for a variety of solar system observing projects. I was present during the last week in June, during which time morning observations of Ceres, Pallas, and Juno were made. Torrence Johnson also assisted. There was much high cloudiness during this period, although some mornings were reasonably clear. The abbreviated telescope time available each morning permitted us to take only barely adequate standard star data. Several runs suffered from the brightness of the dawn sky. Data were taken on the mornings of June 24, 26, 27, 28, and 29. The only data salvable were observations of Pallas on the 24th, Ceres on the 28th, and Juno on the 29th. The star Eta Piscium was used as a standard for Pallas and Juno; it is a G-type star which has been only poorly poorly calibrated against other Oke standards and not calibrated at all short of 0.4 microns. Wratten neutral density filters were used for the standard star observations. Coincidence corrections and ND filter calibrations are discussed

in Appendix V. The reduced reflectivities, also presented in Appendix V, show the major differences between the three asteroids, but are omitted from general discussion in this thesis because of the many problems peculiar to the June run.

Mt. Wilson 24-inch: August 1970

The first week and a half of August provided the first lengthy asteroid observing run. Clouds hampered, and largely prohibited, observations until the night of August 5/6; however, there was sufficient opportunity during the first nights to devise efficient observing procedures and to correct the severe scattered light problem caused by absence of a dark-cloth. Scattered light from various sources (especially the moon and the lights from the Los Angeles Basin) remained a potential problem. Due to sky brightness, the signal-to-noise ratio was too poor to salvage observations of the fainter asteroids (numbers 584 and 230); observations of the latter were further ruined by clouds and a failure to keep the cold-box filled with dry ice.

The nights of August 6 - 12 were generally clear, with occasional well-defined patchy clouds at medium altitudes. A Santa Ana condition was in effect causing high winds and fairly poor seeing; the guiding was not impaired, however. The top of the mountain was usually not entirely free of smog and haze from the Basin.

Only a single asteroid (plus standard star) could be run adequately during the course of a short summer night. An attempt on August 12 to observe the moon, the faint asteroid 19 Fortuna, and Ceres did not seem particularly successful, although no attempt has been made yet to reduce those two runs.

An examination of preliminary asteroid spectral reflectivities reduced from the August data, as well as some tests (sky versus sky), suggest that there was a small additive constant difference between the two beams. The August reflectivities presented in this thesis were reduced by subtracting 0.07 counts/chop from each object-minus-sky difference.

The photometer was operated in the filter-by-filter mode, resulting in lengthy runs and relatively few standard star observations during the course of a night. Despite all the problems, and the relatively low signal-to-noise ratio, the data for asteroids 2 and 192, and to some extent 11, should be satisfactory at about the 5% level. Larry Lebofsky assisted with the observations.

Mt. Wilson 60-inch: October 1970

Four nights were assigned to Torrence Johnson for observing asteroids, Saturn, and Saturn's satellites. About two-thirds of each night was spent on asteroids. The weather was nearly perfect; skies were completely clear all four nights and the seeing conditions ranged from fairly good to truly excellent (on October 12 Ceres showed a beautiful disk, estimated at 3/4 of the apparent diameter of Titan, and fully 2½ to 3 times the apparent Airy disks of stars). We were forced to close down an hour early on the night of October 10 due to blowing ash from recent forest fires.

The evening of October 9 was not successfully used due to difficulties in getting the electronics working, including a serious RF noise problem on the signal cable. Considerable time also was spent patching holes in the photometer to minimize scattered light. Great care was taken throughout the four nights minimizing scattered light, especially from the moon which was approaching full. The front end of the telescope was

usually shielded from direct moonlight by the windscreen. A chopper mirror broke and was hastily replaced just prior to the October 12th runs on 17 Thetis; this change should not affect the data, despite no calibration of the mirror, because it was the sky-beam mirror. There were no other problems.

All runs were made in the spinning-filter wheel mode with the S-1 tube (see Appendix III). These data are probably of a consistently higher quality than those obtained during any other observing run.

Mt. Wilson 24-inch: December 1970

Five nights were scheduled at the end of the year on the 24-inch telescope. Asteroids were the first priority, but attempts were made to observe Saturn's rings early in the night. The Saturn observations were rendered impossible by image-motion approaching 5 seconds of arc. The asteroid observing run was about 50% successful; two nights were mostly cloudy, one night was completely clear, and two nights were clear in the evening only. The data probably are not affected at all by clouds, though clouds could occasionally be seen to the south, except shortly before skies became overcast. Sufficiently large apertures were used so that the bad seeing was not a problem.

Care was taken to minimize scattered light. The electronic equipment was so positioned in the dome that little light was emitted in the direction of the photometer. The only serious problem was the failure of the beam-adjuster, resulting in a broken mirror. The mirror could not be replaced for two nights, so data on Dec. 29 and 30 were taken in the filter-by-filter single-beam mode. No sky measurements were made for standard stars because the sky generally amounted to far less than a percent of the

signal. The observations of 40 Harmonia were made in the normal double-beam filter-by-filter mode. Larry Lebofsky assisted with the observations.

Mt. Wilson 60-inch: January 1971

Five nights were assigned to Prof. McCord, primarily for the purpose of observing asteroids. Cancellation of his airplane reservations due to weather and holiday traffic kept McCord from arriving until the night of January 5/6. Larry Lebofsky assisted until then. Carle Pieters, of the M.I.T. Planetary Astronomy Laboratory, and Jim Dittmar (60-inch night assistant) served as recorders on the last night.

The run was mostly successful despite bad seeing conditions. No observations could be made on January 3 because of 30 arcsecond seeing and gale-force winds (gusts were recorded exceeding hurricane force). The next two nights were perfectly clear, though cold temperatures hindered perfect efficiency in the dome. The seeing on January 4 started at 5 - 10" but improved to 4". Seeing of 2" worsened to 10" on January 5. There were some problems guiding with 10 arcsecond seeing. On one occasion a minor earthquake jolted Asteroid 704 out of the aperture. January 6 was clear until it suddenly clouded up around 11 PM Standard Time. The final night was generally clear, with occasional thin clouds which were mostly of the stationary lee-wave type; the seeing was bad. Moonlight posed some potential problems during evening hours on all nights.

The data are believed to be generally sound at the couple percent level, despite the seeing conditions (15 arcsecond seeing would have badly impaired the data). The photometer was operated in the double-beam filter-by-filter mode with the S-1 photomultiplier. There were no equipment failures.

Kitt Peak No. 2 36-inch: February 1971

This eight-night run was assigned for two non-conflicting projects: asteroids and Venus air-glow. I was assisted in the asteroid observations by Prof. McCord and Andy Lazarewicz. There were occasional spells of cloudiness conveniently near the time of midnight lunch, but every night was usable to some extent. Most clouds were orographic and did not affect the data. The three main periods of cloudiness were: evening of Feb. 5/6, morning of Feb. 8, and around midnight of Feb. 12. It was fairly breezy but the seeing was moderately good. Moonlight was occasionally a hindrance, especially during observations of 10 Hygiea on Feb. 9. The period of darkness during the total lunar eclipse on Feb. 10 was used to great advantage for observing asteroids near the moon.

The first night of the observing run could not be used because of a failure of American Airlines to ship the equipment to Tucson from O'Hare. Difficulties with the electronics forced operation in the single-beam mode during the nights of Feb. 6 and 7. Otherwise the filter-by-filter double-beam mode was used. Observing time was divided about equally between the S-1 and S-20 photomultipliers. There were no other equipment problems.

Kitt Peak No. 2 36 inch: May 1971

Observing time was assigned to Torrence Johnson and myself primarily for a project involving Jupiter's satellites. During free time, other objects were observed, including four asteroids. The observing conditions were good. There are some uncertainties in the results, however, due to the new double-tube operating mode (incremental with fixed number of chops -- see Appendix III). Problems in calibrating the ND1 filter, used for some S-20 standard star runs, are discussed in Appendix V; they may

account for discontinuities in reflectivities for Asteroids 12 and 51 near 0.85 microns. However no filter was used for Asteroids 7 and 93 and there are some peculiarities (quite possibly real) in their reflectivities. I can think of no additional sources of error and am inclined to accept the results at face value.

APPENDIX V

DATA REDUCTION TECHNIQUES

A. INTRODUCTION

The task of converting the numbers on magnetic tape into a set of reliable spectral reflectivities is never easy. It was complicated by the numerous observing modes and problems encountered. There were dozens of different ways in which asteroid reflectivities were reduced, though there were fundamental similarities.

There were three chief parts to the reduction. The first consisted of the preliminary sorting, examination and correction of the raw data. The second part -- the actual calculation of the reflectivities -- was handled by a lengthy Fortran computer program which I wrote. Finally the computer results were carefully checked for errors and other problems; superior reductions were selected for interpretation.

I must emphasize that the details are described in this Appendix for the sake of completeness; not for the purpose of emphasizing problems. In most cases, the raw asteroid numbers could have been ratioed to the raw star numbers, and the old star-sun ratios which our Laboratory has previously used could have been employed with results showing no qualitative and little quantitative difference from the more sophisticated reductions. However, by performing these elaborate and more accurate reductions, I am able to determine the accuracy and reliability of the data to a degree not otherwise possible. Jonathan Elias, with my encouragement, completed a detailed reanalysis of the stellar standardizations in time for me to apply his results to the asteroid reductions (see Part D below).

B. PRELIMINARY DATA HANDLING

The raw data were first plotted out in strip-chart format: counts versus Fabritek memory location (each memory location equals one 40 msec chop). These records were examined for "glitches" (occasional bad points), slight wiggles indicative of imperfect guiding, etc. Data containing glitches, guiding errors, or other anomalies were omitted in calculating the average number of counts per chop for the filter in question.

For each run on an object, a number for each filter (counts per chop) was computed for both object and sky. These numbers, and similar numbers for various tests, were examined for possible systematic errors. The tests included the following: (1) Dark current was examined for stability as well as systematic differences between the object and sky channels. The dark current was nearly always stable at a small fraction of a count per chop (about 1 count per second) and no systematic object/sky differences were detected. (2) Stars were observed with the object first in one beam, then the other. Reflectivity differences between the two chopper mirrors were never greater than about 4% in UV filters and generally not detectable in the IR. The implied corrections were too small to be important and were not applied. (3) Measurements were made periodically with both beams on sky. Systematic differences can be due to mirror reflectivity differences, gradients in sky brightness, differing intensities of scattered light (originating from skylight, moonlight, and artificial lights), and other problems. Systematic differences were rarely noticeable except during dawn or twilight when rapid changes prohibit accurate calibration so runs made under such conditions are ignored. (4) Scattered light measurements of two kinds (through an open filter hole and through -- actually around -- an opaque filter) showed no systematic

differences between the two beams and demonstrated that scattered light in the box was rarely measurable above the dark current. (5) Neutral density filter calibrations and coincidence corrections are discussed in Part E below.

For each acceptable run on an object or star, 24 values for the quantity object-minus-sky were determined and associated with a sidereal time, accurate to several minutes, obtained from the observing log. These 48 numbers are the chief input data to the master reflectivity reduction program.

C. REFLECTIVITY REDUCTION PROGRAM: AIRMASS CORRECTIONS

A major part of the reduction program consists of corrections for differences in airmass (secant of the zenith angle). There are standard methods of performing airmass reductions (Hardie, 1962). Differences in my observing procedures, contrasted with standard UBV photoelectric photometry, require -- or permit -- different reduction techniques.

In general the extinction coefficient k relating a linear change in stellar magnitude to an increment in airmass is not constant but varies with time (as sky conditions change during a night), azimuth (particularly at Mt. Wilson where sky conditions differ in the direction of Los Angeles), and wavelength (extinction being far greater in the UV). Additionally, the extinction may not even be linear, especially if there is considerable stratification, such as near Los Angeles. Usual astronomical practices range from simply adopting standard extinction coefficients (as a function of wavelength) for a particular observatory to much more elaborate procedures. Frequently extinction measurements are made on a set of standard stars only at the beginning and end of a night and are assumed valid for

the entire sky throughout the night. Much of the problem, in normal astronomical practice, centers about determining "color corrections" in order to appropriately determine an extinction coefficient for objects of certain UBV colors.

Two factors make airmass reductions much simpler in the case of asteroid spectrophotometry. First, I make observations of standard stars chosen to be at nearly the same airmass as the asteroid observed; hence corrections for differences in airmass between object and standard are usually very small. (Note that the standard is observed not only for purposes of making airmass corrections, but more fundamentally to calibrate the photometry.) Secondly, observations are made at twenty-four wavelengths, so the functional relationship between k and wavelength is much better determined than for traditional cases. In what follows the reader should remember that extinction corrections are at most second-order corrections to asteroid reflectivities; what I present below is the framework for a much more accurate airmass reduction than has been necessary for the current program. It will suffice to point out that the final reflectivities for several asteroids differ almost not at all from earlier results produced when the program erroneously took the declination of the standard star to be the absolute value of the correct declination! The reduction routine primarily served the asteroid project as a time-saver.

The reduction procedures to be described were performed for each of the twenty-four wavelengths. All observations of a standard star made within an interval of $0^h.1$ were averaged since no estimate of extinction could be made in such a brief time (this is applicable to spinning-filter-wheel observations only). In the case of only a single standard star observation during a night (observations cut short by clouds), I adopted the

standard extinction coefficients shown in Table A-5-1. They have the same functional relationship to wavelength as those in Fig. 3 of Hardie's (1962) article, but have been normalized to newer values determined at several wavelengths by Hodge (1971) for Mt. Wilson. Comparison of these extinction coefficients with those I determined independently show good overall agreement, although it is clear from nightly fluctuations that the use of standard extinction coefficients is a very suspect procedure if there is much extrapolation at all in airmass between object and standard.

Table A-5-1. Extinction Coefficient k.

Filter	k	Filter	k	Filter	k	Filter	k
1	2.25	7	.38	13	.143	19	.064
2	1.42	8	.30	14	.127	20	.054
3	1.05	9	.255	15	.109	21	.049
4	.76	10	.220	16	.098	22	.045
5	.60	11	.190	17	.084	23	.042
6	.51	12	.165	18	.074	24	.038

For multiple observations of a star, successive measurements are compared to determine the possible significance of the extinction derived from each pair of observations. On the standard log-intensity versus airmass plot, where k is the (negative) slope (see Fig. A-5-1), error-bars are assigned to each intensity based on the counting statistics. Depending on the error-bars and the separation in airmass, the two observations are found to yield either a very significant, partly significant, or not significant determination of extinction. If not significant, the two points are averaged and compared with the next point in the same fashion. This procedure results in a series of "significant" segments on the log-I vs sec z plane. If the number of "significant"

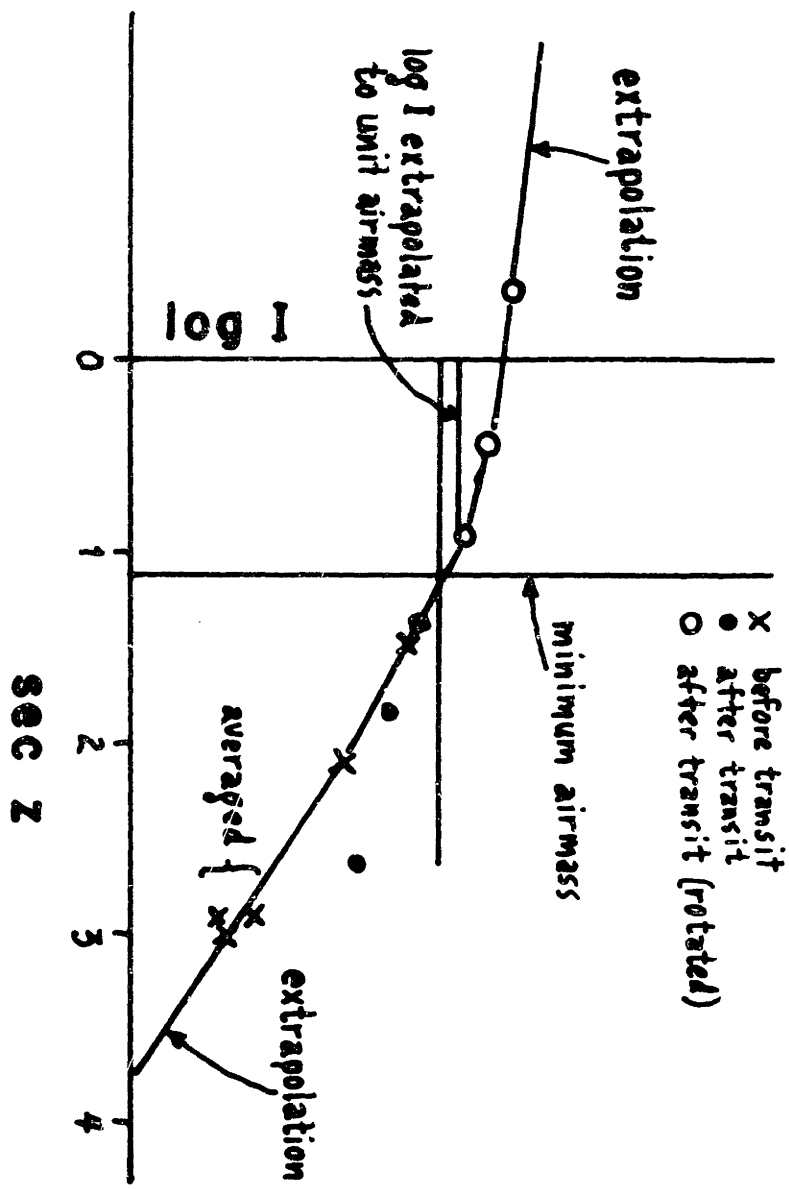
log I
0
1
2
3
4
sec z
extrapolation
log I extrapolated to unit airmass
minimum airmass
averaged
extrapolation
x before transit
• after transit
o after transit (rotated)

Fig. A-5-1.

observations is reduced to one, the standard extinction coefficient (Table A-5-1) is used. If the number of significant observations is reduced to two, then the following procedures are used: very significant determinations are accepted; for partly significant determinations, the standard $\underline{k}$ is used if it is within the error bars, otherwise for $\underline{k}$ outside the error bars the extreme value in the direction of $\underline{k}$ consistent with the error bars is used. Similar criteria are used for extrapolating the extinction coefficient to airmasses beyond the range covered by the star data, using the extreme two significant observations at both the high and low airmass ends.

For observations (and segments as determined above) made after transit, the data are rotated 180° about the point of minimum airmass; see Fig. A-5-1. Then, for purposes of smoothing, sample points are read off along the segments and extrapolations, provided they are reasonably consistent. Otherwise the segments are ignored and a smooth curve (low-order polynomial) is fit to the observed points plus extrapolations. Finally, these samples are mapped onto an intensity-vs-sidereal-time plane and are fitted by a tenth-order polynomial. This curve is intended to be, and usually is, a good fit to the measured intensities of the star plotted against sidereal time (see Fig. A-5-2). The master program then ratios asteroid intensities to standard star intensities, obtained from the polynomial coefficients, for the time at which the star had the same airmass as the asteroid, (either pre- or post- transit, whichever is best). For observations of an object at an airmass less than that ever attained by the standard, the extrapolated extinction coefficient is used.

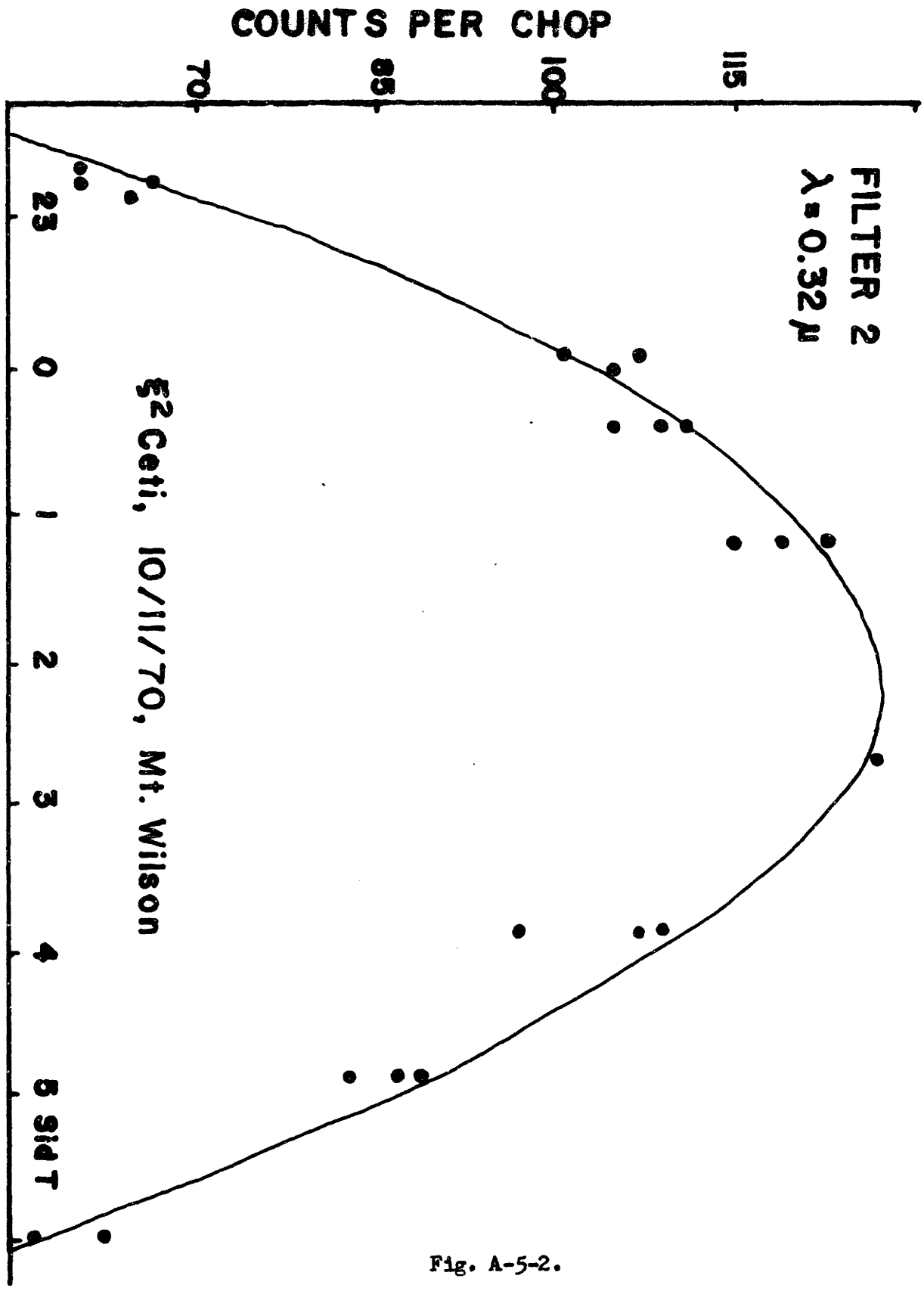
COUNTS PER CHOP
70
85
100
115
FILTER 2
λ=0.32μ
23
0
1
2
3
4
5 SID T
ξ² Ceti, 10/11/70, Mt. Wilson

Fig. A-5-2.

It is often desirable to use several <u>different</u> stars for determining the extinction properties of the sky. The program reduces other stars to the brightness-versus-time curve for one star (that which reaches lowest minimum airmass) using the accurately-known ratios of brightnesses of the stars. Thus observations of several stars can be treated as observations of a single star. Through judicious selection of observations of stars near the same azimuth as the object, or at the same sidereal time, one can to some degree make allowances for differences between sky quadrants or changing sky conditions.

The intent of the above detailed procedures is to produce, by machine computation alone, a brightness-versus-time extinction curve which not only is a good fit to the data in a statistical sense, but which is also physically and logically realistic. I have largely achieved this goal, although the polynomial curve-fitting routine is less than ideal for this purpose. All star curves were examined and hand corrections were made for the relatively rare cases in which the computed curves deviated by more than a percent from what appeared to the eye as the best fit.

D. STANDARD STARS

The reflectivity of an asteroid, illuminated by the sun, is determined by the formula

$$\frac{\text{Ast.}}{\text{Sun}} = \left(\frac{\text{Ast.}_{ob}}{\text{Star}_{ob}}\right)\left(\frac{\text{Star}}{\text{Vega}}\right)\left(\frac{\text{Vega}}{\text{Sun}}\right) \qquad \text{(A-5-1)}$$

for each filter. Since I scale all reflectivities to that in the 11th filter, absolute values of the component fluxes in the formula are unimportant; the accuracy of those quantities relative to similar quantities at different wavelengths <u>is</u> important.

The first term is formed by ratioing the two observables, corrected to the same airmass. The second term is obtained by interpolation in tables published by Oke (1964) and Hayes (1970). The final term is obtained from an absolute spectrum for Alpha Lyrae (Vega) published by Schild et al (1971) and a solar spectrum by Arvesen et al (1969). The final two terms can be combined into a star/sun ratio. Such ratios are listed in Table A-5-2 for the standard stars used in this thesis.

Previous spectral reflectivity reductions published by members of the M.I.T. Planetary Astronomy Laboratory were made using the following assumptions and sources: (1) The same Oke standard star calibrations; (2) an observationally-based determination of the absolute spectrum of Alpha Lyrae (Oke and Schild, 1970); (3) a solar spectrum due to Labs and Neckle (1968); (4) an assumed square-wave response for the interference filters; and (5) no consideration of shifts in the effective wavelength of observations due to the spectral responses of the photomultipliers, mirrors, or atmosphere. "Smoothing factors" were sometimes employed for reasons discussed in Part F. The errors introduced by some of the latter assumptions were known to be small; the errors introduced by the imprecision of stellar and solar calibrations were harder to evaluate, but it was hoped that they were small and in any case no better calibrations were available.

Now there are better sources for some of the calibrations. The spectrum of Alpha Lyrae used here is a theoretical model; it agrees well with the earlier Vega spectrum in gross characteristics but now permits stellar lines to be taken into account. The new solar spectrum of Arvesan et al, obtained at an altitude of 12 km in a NASA jet, seems distinctly superior to the spectrum of Labs and Neckle, obtained at the Jungfraujoch. At wavelengths short of 0.5 microns the earlier spectrum is 5% too low. The new

TABLE A-5-2. STAR/SUN RATIOS

STAR	X2 CET	E ORI	G GEM	ETA HYA
MAG., TYPE	4.3 A0	1.7 B0	1.9 A0	4.3 B3
R.A.	02 26	05 34	06 36	08 41
DEC.	+08 19	-01 13	+16 25	+03 30
SOURCE	OKE	OKE	HAYES	HAYES
FILTER				
1	4.1091	16.9409	2.9566	13.5018
2	3.0589	12.0292	2.2577	9.3936
3	2.3733	8.7788	1.7857	6.5875
4	2.1826	7.4397	1.7309	5.5840
5	3.1819	6.0479	2.6119	4.2062
6	2.8168	3.1652	2.7368	3.2381
7	2.1028	2.2671	2.0804	2.3450
8	1.5450	1.6316	1.5600	1.6940
9	1.2952	1.3463	1.3134	1.3780
10	1.1723	1.1918	1.1798	1.2137
11	1.0000	1.0000	1.0000	1.0000
12	0.8581	0.8527	0.8764	0.8537
13	0.7705	0.7523	0.7857	0.7423
14	0.6766	0.6551	0.6869	0.6330
15	0.6412	0.6186	0.6589	0.5961
16	0.6073	0.5837	0.6365	0.5628
17	0.5703	0.5401	0.6040	0.5229
18	0.5301	0.5020	0.5643	0.4779
19	0.5249	0.4716	0.5700	0.4545
20	0.5069	0.4188	0.5581	0.4184
21	0.4672	0.3730	0.5214	0.3786
22	0.4522	0.3554	0.5253	0.3525
23	0.4235	0.3306	0.4858	0.3221
24	0.3930	0.3069	0.0	0.0

TABLE A-5-2 (CONTINUED).

STAR	A LEO	TH CRT	TH VIR	109 VIR
MAG., TYPE	1.3 B8	4.8 B9	4.5 A0	3.8 A0
R.A.	10 06	11 35	13 08	14 44
DEC.	+12 06	-09 38	-05 23	+02 00
SOURCE	OKE	HAYES	HAYES	OKE
FILTER				
1	6.5361	4.7573	3.1123	3.3166
2	4.7492	3.4845	2.3730	2.5119
3	3.5739	2.6176	1.8767	1.9898
4	3.1560	2.4153	1.7974	1.8770
5	3.8260	3.0509	2.6705	3.0250
6	2.9860	2.8942	2.7099	2.7249
7	2.2112	2.1567	2.0534	2.0481
8	1.6043	1.5934	1.5340	1.5114
9	1.3402	1.3387	1.2974	1.2985
10	1.1876	1.1911	1.1646	1.1666
11	1.0000	1.0000	1.0000	1.0000
12	0.8666	0.8719	0.8764	0.8723
13	0.7673	0.7635	0.7759	0.7845
14	0.6719	0.6584	0.6772	0.6928
15	0.6403	0.6295	0.6527	0.6626
16	0.6064	0.6025	0.6269	0.6323
17	0.5629	0.5649	0.5915	0.5970
18	0.5265	0.5255	0.5569	0.5654
19	0.5165	0.5229	0.5578	0.5651
20	0.4987	0.5032	0.5432	0.5556
21	0.4597	0.4673	0.5106	0.5121
22	0.4242	0.4439	0.4975	0.5003
23	0.3933	0.3988	0.4489	0.4729
24	0.3605	0.0	0.0	0.4389

TABLE A-5-2 (CONTINUED).

STAR	Z OPH	E AQR	29 PSC	ETA PSC
MAG., TYPE	2.7 B0	3.8 A0	5.1 B8	3.7 G5
R.A.	16 35	20 46	00 00	1 29
DEC.	-10 30	-09 36	- 3 11	+15 11
SOURCE	OKE	OKE	OKE	MCCORD
FILTER				
1	11.3804	2.8594	8.2523	0.0
2	8.2044	2.1889	5.9600	0.0
3	6.1108	1.7557	4.4496	0.0
4	5.3404	1.6883	3.9207	0.0
5	4.5017	2.8915	4.2664	0.0
6	2.4902	2.6960	3.0879	0.5958
7	1.8682	2.0388	2.2433	0.7100
8	1.4128	1.5036	1.6226	0.8227
9	1.2332	1.2876	1.3389	0.8557
10	1.1534	1.1621	1.1858	0.9712
11	1.0000	1.0000	1.0000	1.0000
12	0.8775	0.8750	0.8582	0.9988
13	0.8043	0.7821	0.7585	1.0629
14	0.7162	0.6897	0.6607	1.0524
15	0.6992	0.6670	0.6308	1.1220
16	0.6746	0.6411	0.5995	1.1518
17	0.6389	0.6073	0.5601	1.1614
18	0.6089	0.5681	0.5207	1.1709
19	0.5854	0.5678	0.5103	1.2225
20	0.5310	0.5594	0.4800	1.2465
21	0.4811	0.5178	0.4348	1.1992
22	0.4647	0.5073	0.4162	1.2245
23	0.4392	0.4820	0.4003	1.2313
24	0.4078	0.4586	0.3856	1.2319

spectrum's estimated accuracy is 1%. Additionally, the resolution is better and the tabulation is convenient for digitization so that solar lines can be taken into account accurately.

J. Elias has digitized the responses of our filters (except filter 1). Using the digitized spectra of Vega and the sun, and taking into account photomultiplier and mirror responses, he has calculated Vega/sun ratios appropriate to each filter as well as the "effective wavelength" for each filter. Interpolations are made in the Oke and Hayes star calibrations at these effective wavelengths to obtain the star/sun ratios given in Table A-5-2. The effect of atmospheric absorptions in altering the effective wavelengths was not taken into account explicitly, but Mr. Elias has estimated the sign and magnitude of the effect for each filter. All modifications are of the order of 1% or less, except for filter 2 (and presumably filter 1), and possibly in the IR.

It is clear that the chief remaining source of uncertainty is in the Oke and Hayes relative star calibrations. Since most of the standard stars are of a spectral type similar to Alpha Lyrae, there should be little difficulty due to failure to take into account differences in the fine structure of stellar spectra relative to that of Vega. The precision of the calibrations of Oke and Hayes has recently been studied by Breger (1971). I list below conservative estimates of the accuracies of these calibrations relative to Vega, obtained from a figure published by Breger:

Wavelength (microns):	0.3-0.4	0.4-0.5	0.5-0.6	0.6-0.9	0.9-1.1
Error:	3%	1%	2%	3%	4%

The errors seem chiefly due to scatter, although there is a component of slope error. Breger believes that Xi^2 Ceti is the best secondary calibration standard in the sky (except for Vega itself). Fortunately, this

is the star used most frequently in the asteroid program; the errors for Xi^2 Ceti may be half those listed above. The interpolation between the bandpasses measured by Oke and Hayes is somewhat uncertain; they avoided stellar lines while our filters do not necessarily do so. The effects are small, except for filter 5 which straddles the Balmer jump and for which errors may be in the 5% - 10% range.

Planetary astronomers have commonly calibrated solar system photometry against G-type stars which have a "solar" spectrum. Many flinch at the thought of using A and B-type stars for calibration, as I have done. This prejudice is not justified. There are three chief criteria for selecting standard star sequences: (1) the reliability of the absolute calibration; (2) the accuracies of the relative secondary calibrations; and (3) the accuracy of interpolations in the standard sequence to one's own effective wavelengths. The standardization I adopt is probably superior on the first two counts, and certainly is on the third due to the weakness of stellar lines in the Oke-Hayes standards compared with solar-type stars. Ideally we should use standards calibrated against an absolute standard in our own filters, but we have not yet done that. If we do, then use of G-type stars would be preferable and would lessen uncertainties near the Balmer discontinuity, for example.

E. NEUTRAL DENSITY FILTER CALIBRATION AND COINCIDENCE CORRECTION

June 1970 Run

A Wratten ND3 filter was used for standard star observations during the June Palomar run. Calibration measurements were made of several stars both with and without the filter. I discovered, when calculating the filter function from these data, that there were large effects dependent on

the absolute count-level. Fig. A-5-3 shows a plot of part of the filter function as well as a plot of the absolute count level for three stars. The results can be understood easily in terms of a saturation or "coincidence" effect, despite the fact that the count-rate was orders of magnitude below the specifications of the photomultiplier. It was subsequently discovered than an unsuspected characteristic of the Fabritek computer counter was the source of the problem.

An empirical coincidence correction as a function of count-rate was calculated and applied to the Palomar observations. A reasonably accurate filter function was also computed. Finally, I applied some smoothing to the reflectivities for Pallas and Juno in an attempt to remove several single-filter bumps or dips common to both but absent in the spectrum of Ceres. I attribute these bumps to poor calibration of our tertiary standard Eta Piscium, which was used as a standard for Pallas and Juno but not for Ceres; there is no firm proof that the star calibration is at fault, however. Reflectivities are presented in Fig. A-5-4 for the three asteroids, with Vesta shown for comparison. These data were reduced with the earlier stellar and solar calibrations. The major differences in reflectivity between the four main asteroids are clear in the Palomar results and have been subsequently confirmed. However, the errors due to Eta Piscium, the coincidence correction, and the ND filter calibration are sufficiently large that I attach little quantitative significance to the results and have omitted them from further consideration in the thesis.

February 1971 Run

The counter limitation in the computer was supposedly fixed by a Laboratory technician following the Palomar run. However, it turns out to have been a misunderstanding. I once again discovered a saturation

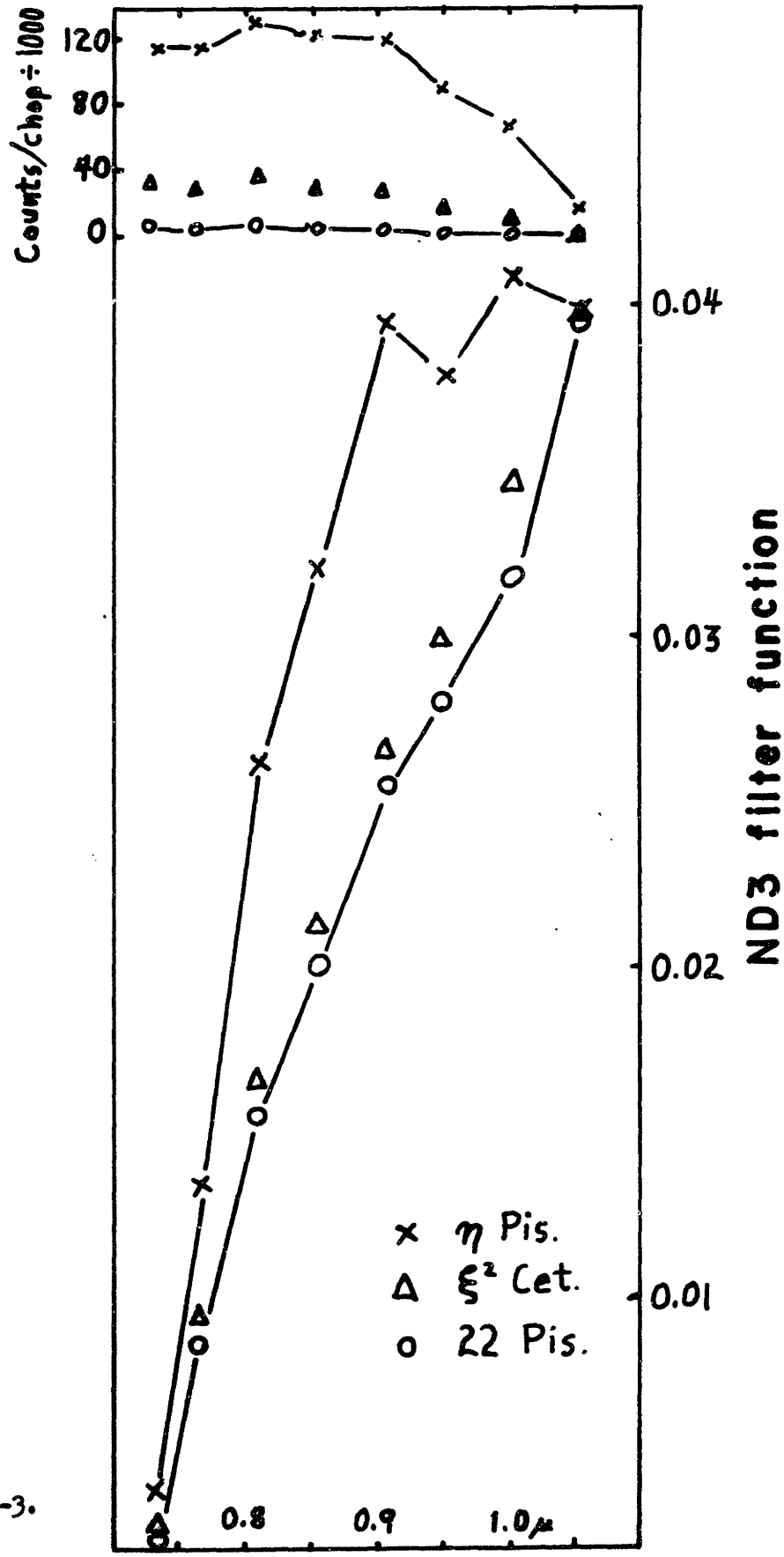
Counts/chop÷1000
120
80
40
0
0.04
0.03
0.02
0.01
ND3 filter function
× η Pis.
Δ ξ² Cet.
o 22 Pis.
0.8
0.9
1.0μ

Fig. A-5-3.

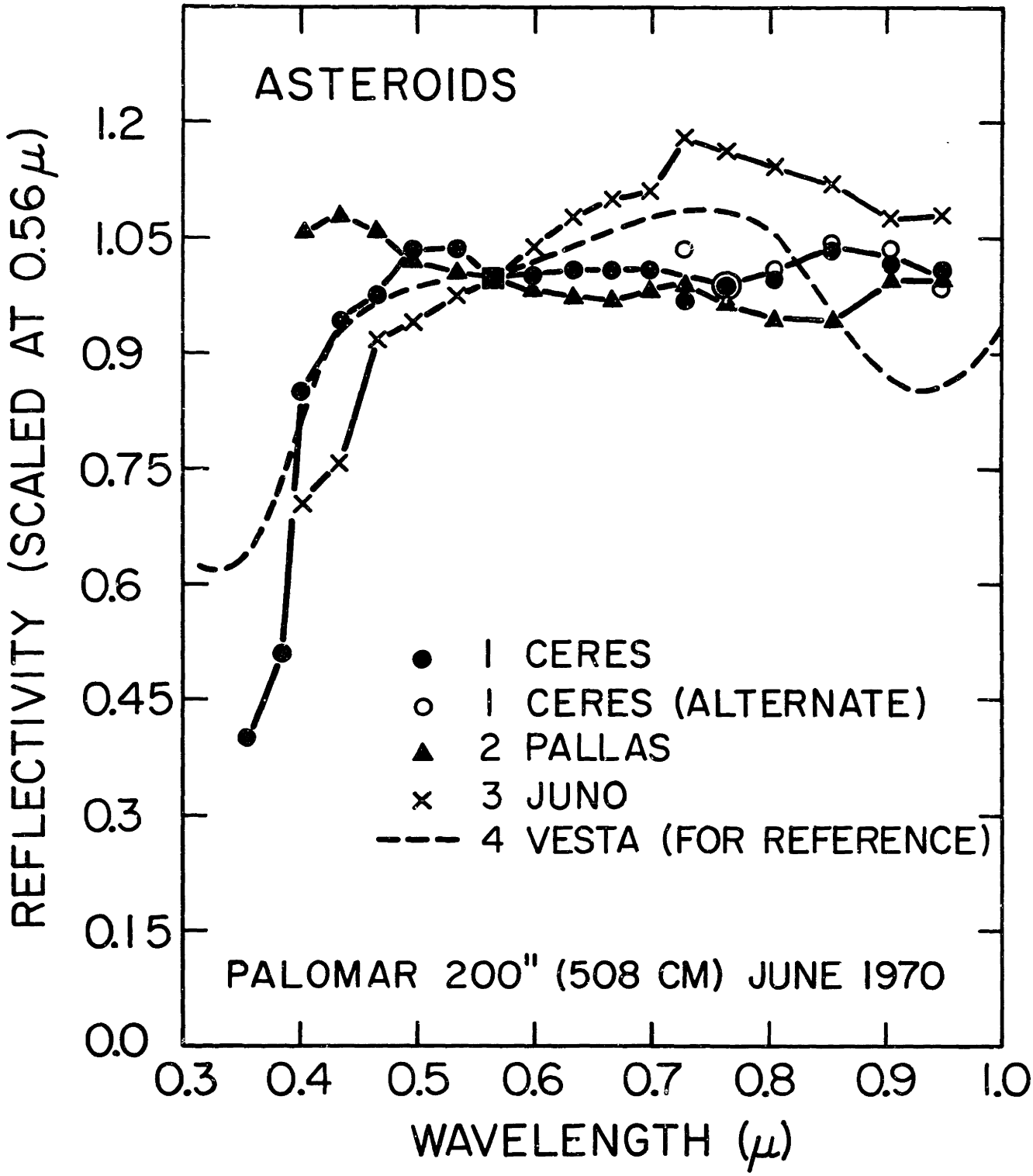
ASTEROIDS
REFLECTIVITY (SCALED AT 0.56μ)
1.2
1.05
0.9
0.75
0.6
0.45
0.3
0.15
0.0
0.3
0.4
0.5
0.6
0.7
0.8
0.9
1.0
WAVELENGTH (μ)
1 CERES
1 CERES (ALTERNATE)
2 PALLAS
3 JUNO
4 VESTA (FOR REFERENCE)
PALOMAR 200" (508 CM) JUNE 1970

Fig. A-5-4.

problem of similar magnitude while calculating the response function for the Oriel ND2 filter used for some S-20 star observations in February. Sufficient data were taken to permit me to derive a coincidence correction accurate to about 20%. Since the correction is never itself larger than about 15% for the star data used in the calibration, errors in that calibration from this cause should be less than 3%. Fig. A-5-5 shows that the empirical coincidence correction is similar to that of a theoretical 4 Mhz counter. The effect is about 10% at 30,000 counts per chop (0.7 Mhz) and is 2% at 6,000 counts per chop. Corrections were made to all star and asteroid data prior to final reduction, although the effect was usually negligible.

Less easy to understand were discrepancies in the ND2 filter calibration itself. Fig. A-5-6 shows four independent calibrations of the filter function, as well as the function finally adopted. The function determined from Xi^2 Ceti and Theta Virgo (observed with and without the filter) are in good agreement. Somewhat different is the function implied by comparison of asteroid runs reduced against stars observed without the filter (Xi^2 Ceti and Eta Hya.) and against stars observed with the filter. Even more different is the function measured with a spectrometer by J. Elias after the filter was returned to Cambridge. The differences in absolute level, though not fully understood, are less important than the color differences which remain after normalization. I have considered many possible explanations for the discrepancies, but have reached no conclusion. Apparently the filter was mounted in the photometer in a haphazard manner at a 45° tilt; there are indications this may be part of the problem but it is not certain. I have adopted the asteroid calibrations. (Consistency suggests that this was the proper procedure, but there remains an outside

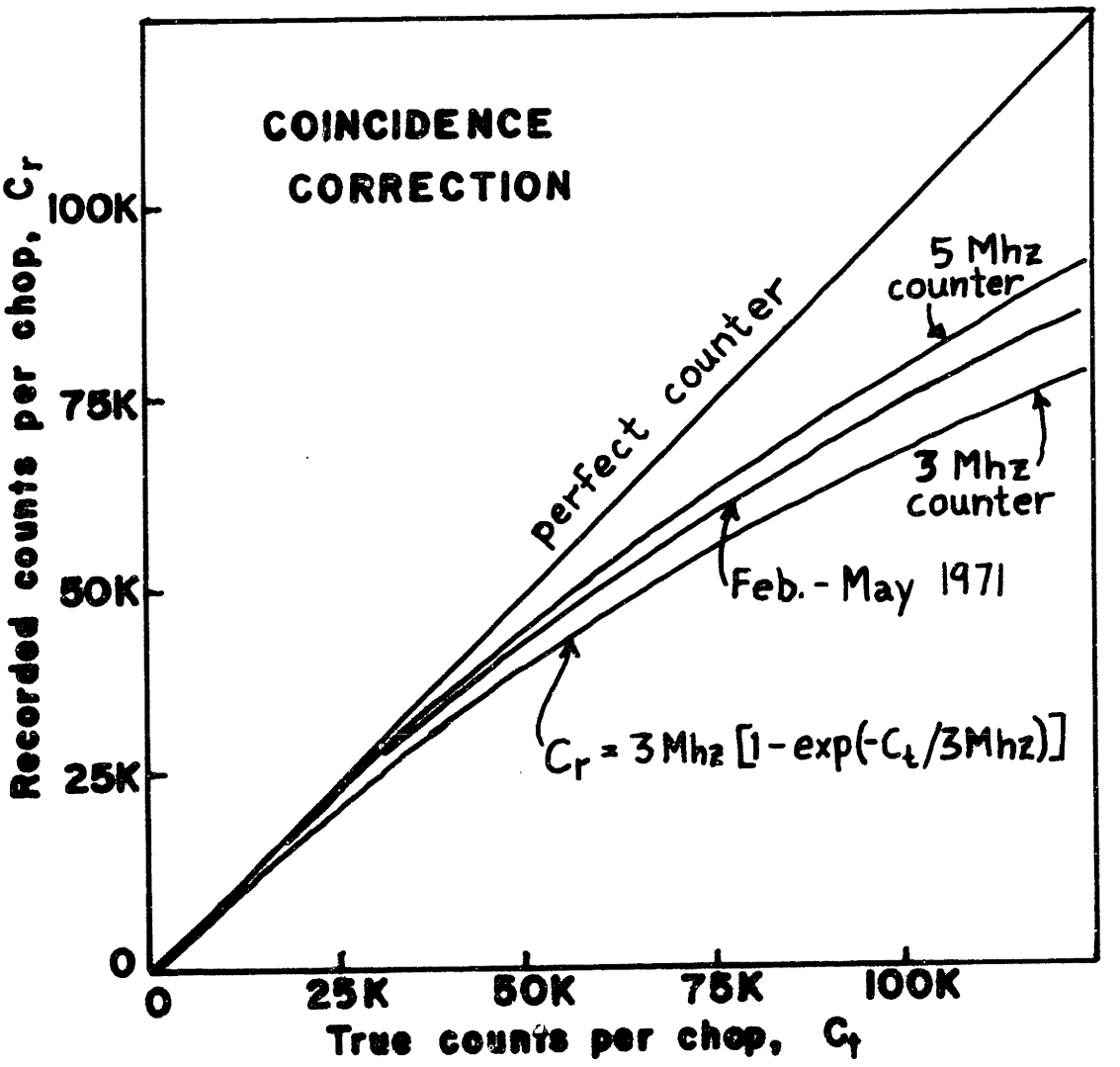
COINCIDENCE
CORRECTION
Recorded counts per chop, C_r
100K
75K
50K
25K
0
0
25K
50K
75K
100K
True counts per chop, C_t
perfect counter
5 Mhz
counter
3 Mhz
counter
Feb. - May 1971
$C_r = 3\,Mhz\,[1 - exp(-C_t/3Mhz)]$

Fig. A-5-5.

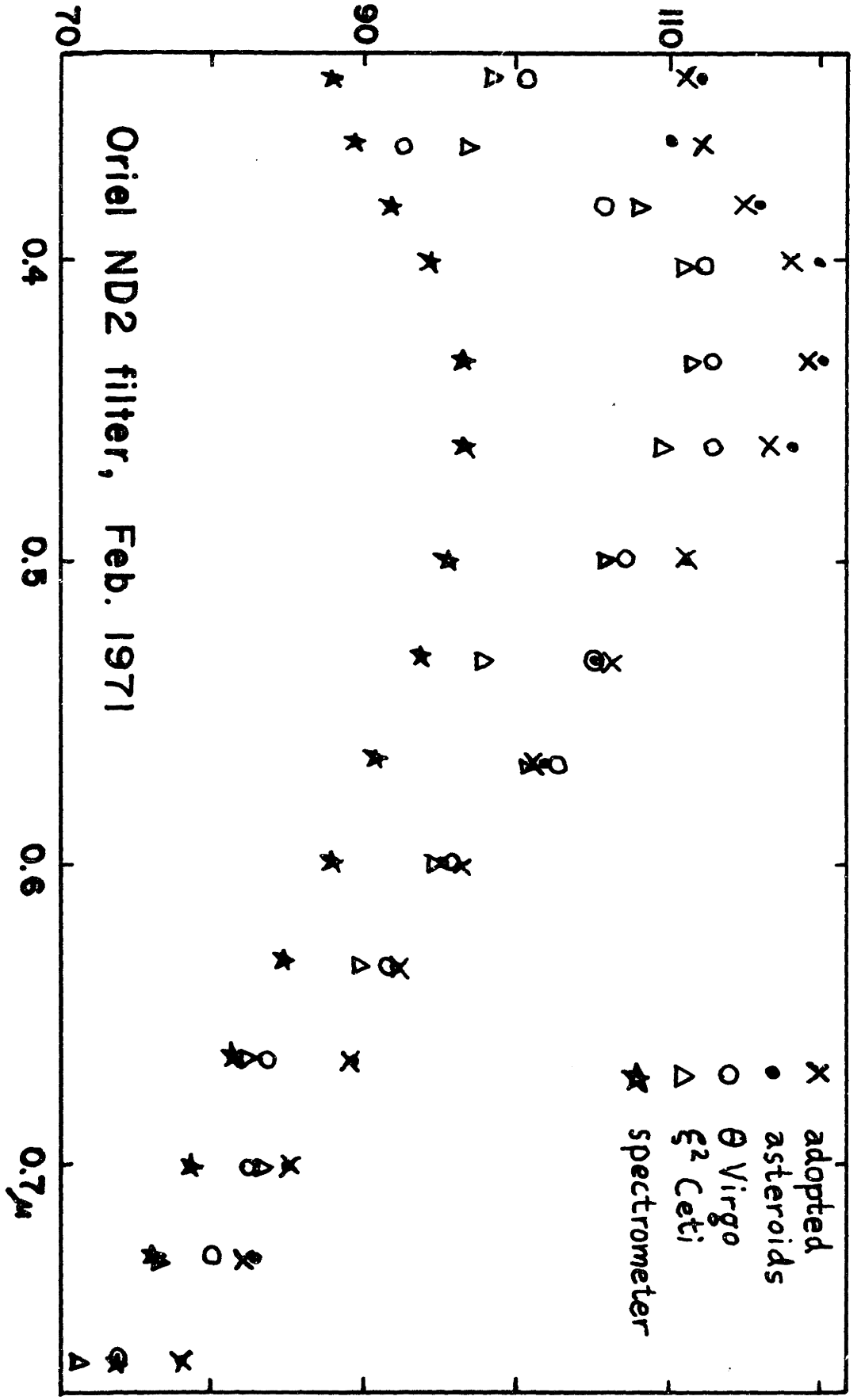
70
90
110
0.4
0.5
0.6
0.7μ
Oriel ND2 filter, Feb. 1971
adopted
asteroids
θ Virgo
ξ² Ceti
spectrometer

Fig. A-5-6.

possibility that data reduced using the ND2 filter function shown in Fig. A-5-6 may be in error by 5 to 10%, or more.

May 1971 Run

Star observations indicate that the same kind of coincidence error exists in the May data as in the February data, as expected since no changes were made to the Fabritek counter in the interim. Calibrations of the Oriel ND1 filter -- used for some S-20 observations of stars -- are shown in Fig. A-5-7. Calibrations obtained from Jupiter data are in general agreement with those shown for Theta Crt., but both differ once again from a laboratory calibration. The color discrepancy is less than for the ND2 filter, and I am reasonably confident (at the 5% level, anyway) of the reflectivity reductions. However, because of the dual-tube operating mode used in May the absolute density of the filter near 0.57 microns must be known in order to scale the S-1 infrared observations (made without a filter) to the S-20 data in the visible (reduced against stars observed with the filter in several cases). A 10% error is certainly a possibility; hence structure in reflectivity curves for Asteroids 12 and 51 near 0.85 microns should be viewed with considerable suspicion.

F. REDUCTION ERRORS: SUMMARY

There are special problems with data taken using the S-20 photomultiplier and reduced by stars observed through ND filters. But aside from that, what can be confidently said about errors in the data? Random errors due to counting statistics, minor guiding problems, scattered clouds, and the like can be rather easily guaged from the consistency of successive runs (error bars on graphs in Appendix VII).

It is harder to guage systematic errors in slope, due to variable sky

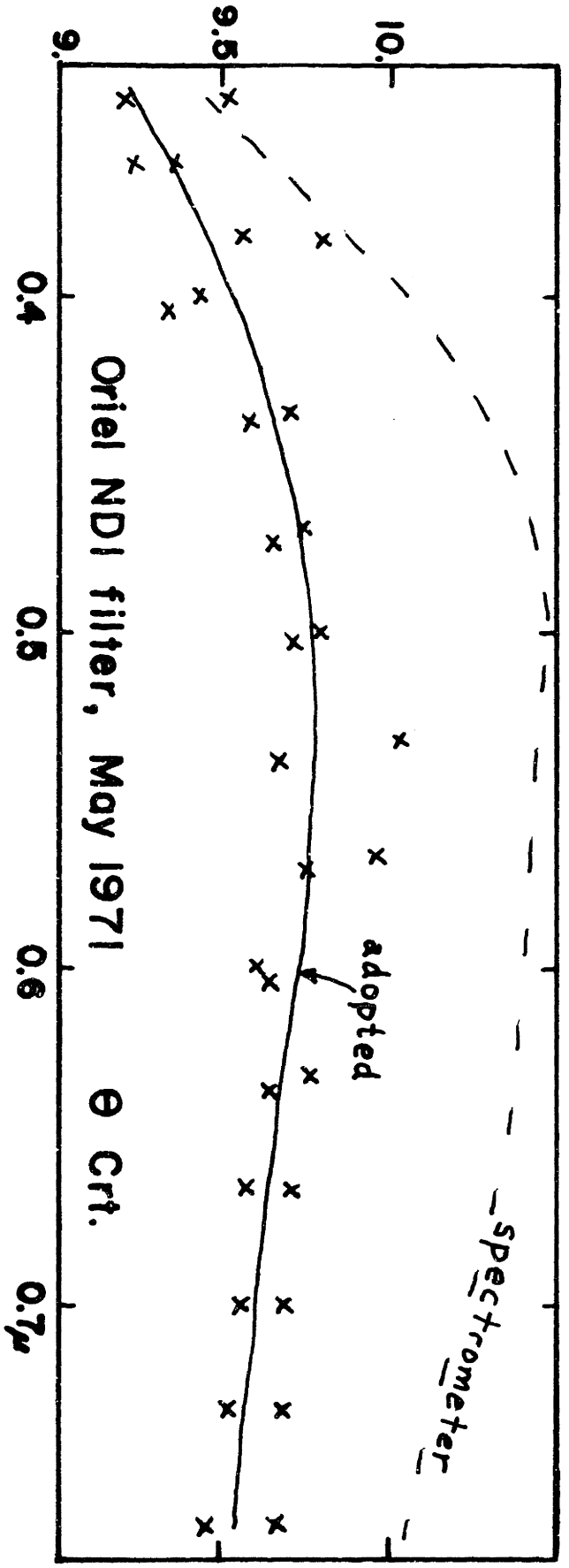
9.
9.5
10.
0.4
0.5
0.6
0.7μ
Oriel NDI filter, May 1971 θ Crt.
adopted
Spectrometer

Fig. A-5-7.

conditions, too-infrequent stellar calibrations, etc. Difficulties at the several percent level are certainly possible, particularly in the UV and IR. From the consistency of the results, I am inclined to believe such effects are small. One could, of course, argue that the differences I ascribe to correlations with phase angle or rotational phase are in fact evidence of inconsistency in the data. However, some of the clearest cases of rotational or phase angle variations are for asteroids observed under the best observing conditions, while some asteroids observed under poorer conditions show less evidence for such variations. Also because of correlations with other evidence (known phase effects for asteroids and known lightcurve components due to albedo differences) I am inclined to believe my interpretations are correct, although verification is desirable.

It appears, therefore, that the asteroid reflectivity curves can be compared with each other with little risk of overinterpretation. However, what about the absolute characteristics of the curves, so important, for instance, in mineralogical identification? The calibration procedures described in Part D involve a lengthy chain; a single weak link may affect my interpretations.

In order to clarify this problem, I will summarize previous procedures used in the Planetary Astronomy Laboratory. During the past two years, the star/sun standardization has been performed incompletely, using inferior sources and assumptions described in Part D. Spectral reflectivities derived for many diverse solar system objects showed some identical "unnatural" characteristics which suggested imperfect standardization. When laboratory reflectivities of Apollo 11 soil samples (Adams and Jones, 1970) were compared with telescopic reflectivities of the 15-km spot centered on the landing site, it was found that some structure in the astronomical

data was not evident in the soil, despite an overall similarity in slope (McCord and Johnson, 1970). Accordingly, and with some misgivings, approximate "smoothing factors" were devised to correct the telescope data by removing unnatural features in solar system spectra and features not confirmed by the "ground truth" soil measurements. These smoothing factors (see Table A-5-3) have been generally applied to our solar system reflectivities for the last year.

It can be argued, however, that not enough is known about the mineralogical homogeniety of the lunar surface on a scale of kilometers to assert that soil samples from one locality are representative of a vast area. Despite a widespread belief that the lunar surface is subject to considerable lateral mixing due to impact ejecta, there remains the incontrovertible fact that many color boundaries, even within the maria, are sharp on the scale of a kilometer. Also, another uncertainty is the strongbias against Apollo landing sites being located in boulder-strewn areas (for reasons of safety); although boulders probably cover a limited percentage of any lunar region, it must be remembered that they are heavily weighted in reflectivity spectra due to their high albedo. Perhaps more important are substantial compositional differences as a function of particle size (e.g. see LSPET, 1971). Between 5% and 30% of Apollo 14 soil consists of particles larger than 1 mm diameter -- sizes excluded from Adams' laboratory measurements. The fraction of soil smaller than 1 mm contains nearly all the dark glass, shown by Adams and McCord (1970) to yield a smooth and very red reflectivity; however 70% to 100% of the 1 to 2-mm fraction consists of lithic fragments -- just the kind of high albedo material expected to produce strong ansorption bands. According to the Preliminary Examination Team (LSPET, 1971) there is a variation in plagioclase

Table A-5-3. Smoothing Factors and New Calibrations

Filter No.	Smoothing Factor	New Calibration
1	0.9728	0.8
2	0.9728	0.884
3	0.9728	0.909
4	0.9728	1.023
5	0.9728	1.048
6	0.9728	0.911
7	0.9728	0.915
8	0.9728	0.969
9	0.9728	0.955
10	1.0170	0.985
11	1.0000	1.000
12	1.0130	0.984
13	1.0210	0.976
14	0.9689	0.970
15	0.9796	1.000
16	0.9728	1.013
17	0.9767	1.017
18	0.9728	1.028
19	0.9698	1.029
20	0.9728	1.002
21	0.9728	0.954
22	0.9728	0.968
23	0.9728	0.945
24	0.9728	0.955

Explanation: Most spectral reflectivity curves published by the M.I.T. Planetary Astronomy Laboratory prior to mid-1970 can be multiplied by both factors listed above to convert approximately to the calibrations used in this thesis. Those calculated since mid-1970 should be multiplied by the new calibration factor, only.

to clinopyroxene ratio as a function of particle size. A final uncertainty in relating telescopic observations to laboratory measurements is the possibility of special color characteristics of the uppermost layer of the lunar surface in situ which are destroyed upon removal to earth; although there is no evidence for such a color effect, albedo differences in the uppermost layers have been observed.

My doubts about the validity of the lunar "ground-truth smoothing factors" were increased by the substantial discrepancy between laboratory reflectivities for the Apollo 12 soil samples and telescopic observations of the landing site; this discrepancy has been ascribed by Adams and McCord (1971) to the presence of a bright ray in the vicinity. In defense of the smoothing factors, it can be mentioned that some of the "unnatural" features removed are not characteristic of measured lunar rocks, nor can they all be produced by simple mixtures of several known soil components. But while the possibility of an unmeasured rock-type being an appreciable component of the soil may seem remote, Adams (1971, private communication) finds preliminary indications for Apollo 14 soil samples to show bands different from those of Apollo 14 rocks.

In the absence of good star/sun calibrations, use of the "smoothing factors" may well have been the best procedure in the past. It is proper, however, now that we have a much-improved star/sun calibration, to address ourselves again to the question of whether the "smoothing factors" are still preferable. I believe the answer is probably no, and have not used the "smoothing factors" in this thesis. However, there remain some wiggles in the reflectivities of some solar system bodies such as the moon, Mercury, Europa, Ganymede, Callisto, but not Io (see Part B of Appendix VII; ignore lunar points at wavelengths less than 0.4 microns).

Many of the asteroids show peculiar wiggles and dips that appear to be statistically real. In an attempt to ascertain whether or not these reflectivities could be "improved" in a subjective sense, I have ratioed all reflectivities to the mean reflectivity of four well-observed blue asteroids; they have reasonably flat spectra which one might expect to be truly flat if due to dominance of opaques. The asteroids whose mean was taken as the standard are numbers 2, 10, 1, and 704. Some of the ratios of other asteroids to this mean are shown in Figs. A-5-8 to A-5-10. (The standard is not flat in the UV so these ratios should not be considered to be alternative reflectivities in any sense.) About a third of the asteroids had a subjectively improved appearance as a result of applying these "smoothing factors" but an equal number were worsened to a similar degree. Others might choose differently, but I am inclined to believe that at least some of the wiggles and peculiar dips observed in asteroid reflectivities are real and that there is no justification for applying a smoothing factor of this kind.

I believe that the errors listed near the end of Part D constitute the best estimate of the accuracy of the absolute calibration of the asteroid spectral reflectivities. I have adopted 3% as a lower limit to errors tabulated in Appendix I; there may be random errors approaching 5% and systematic slope errors approaching 3%. The effect of such errors on measuring band positions can be large. An unlucky relative shift between two neighboring points of 5% can change the estimated center of a Vesta-type band by as much as 0.03 microns (and did -- see Chap. VII), and of a band like that of 79 Eurynome by as much as 0.05 microns.

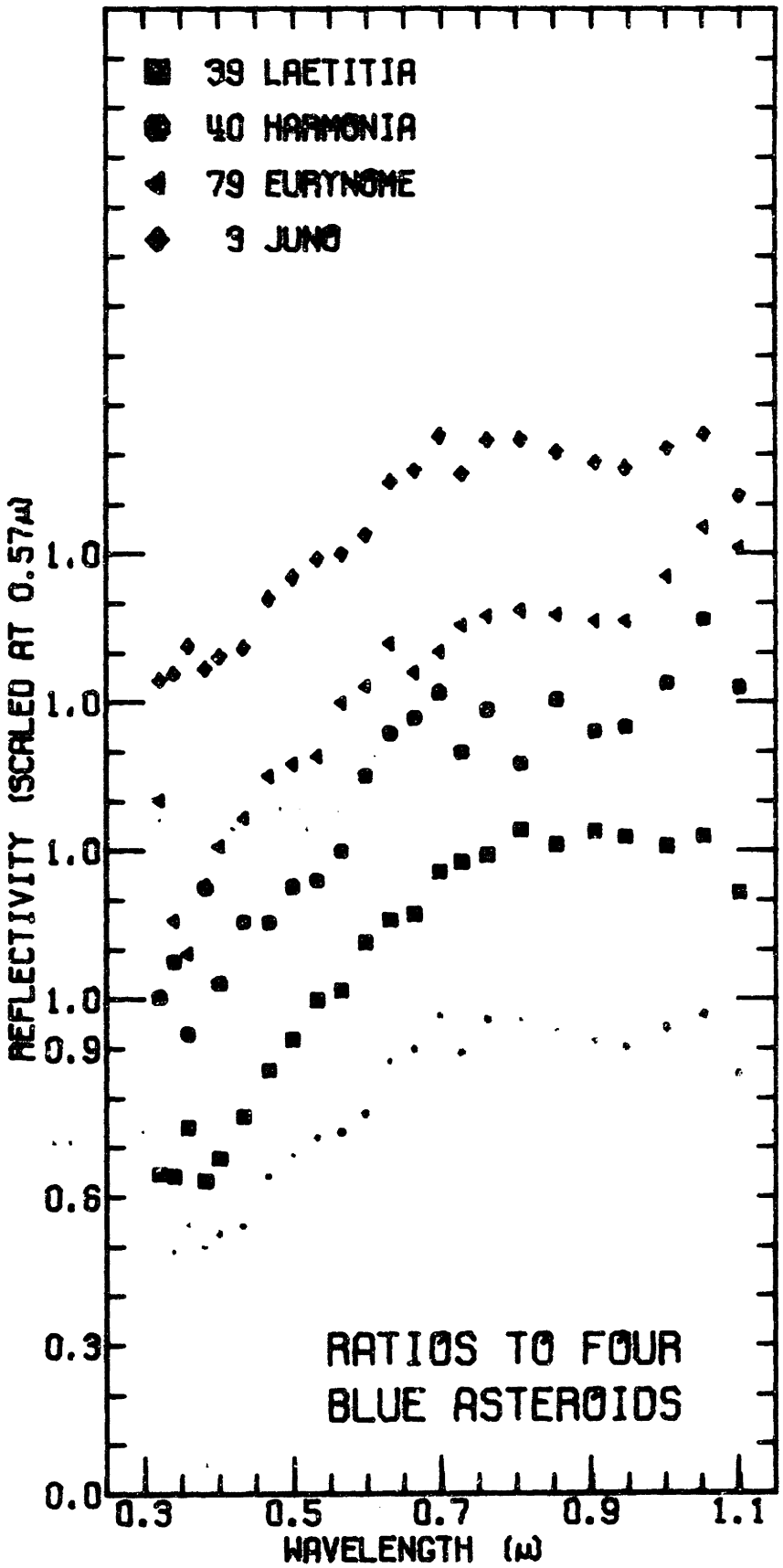
39 LAETITIA
40 HARMONIA
79 EURYNOME
3 JUNO
REFLECTIVITY (SCALED AT 0.57μ)
1.0
1.0
1.0
1.0
0.9
0.6
0.3
0.0
0.3
0.5
0.7
0.9
1.1
WAVELENGTH (μ)
RATIOS TO FOUR
BLUE ASTEROIDS

Fig. A-5-8.

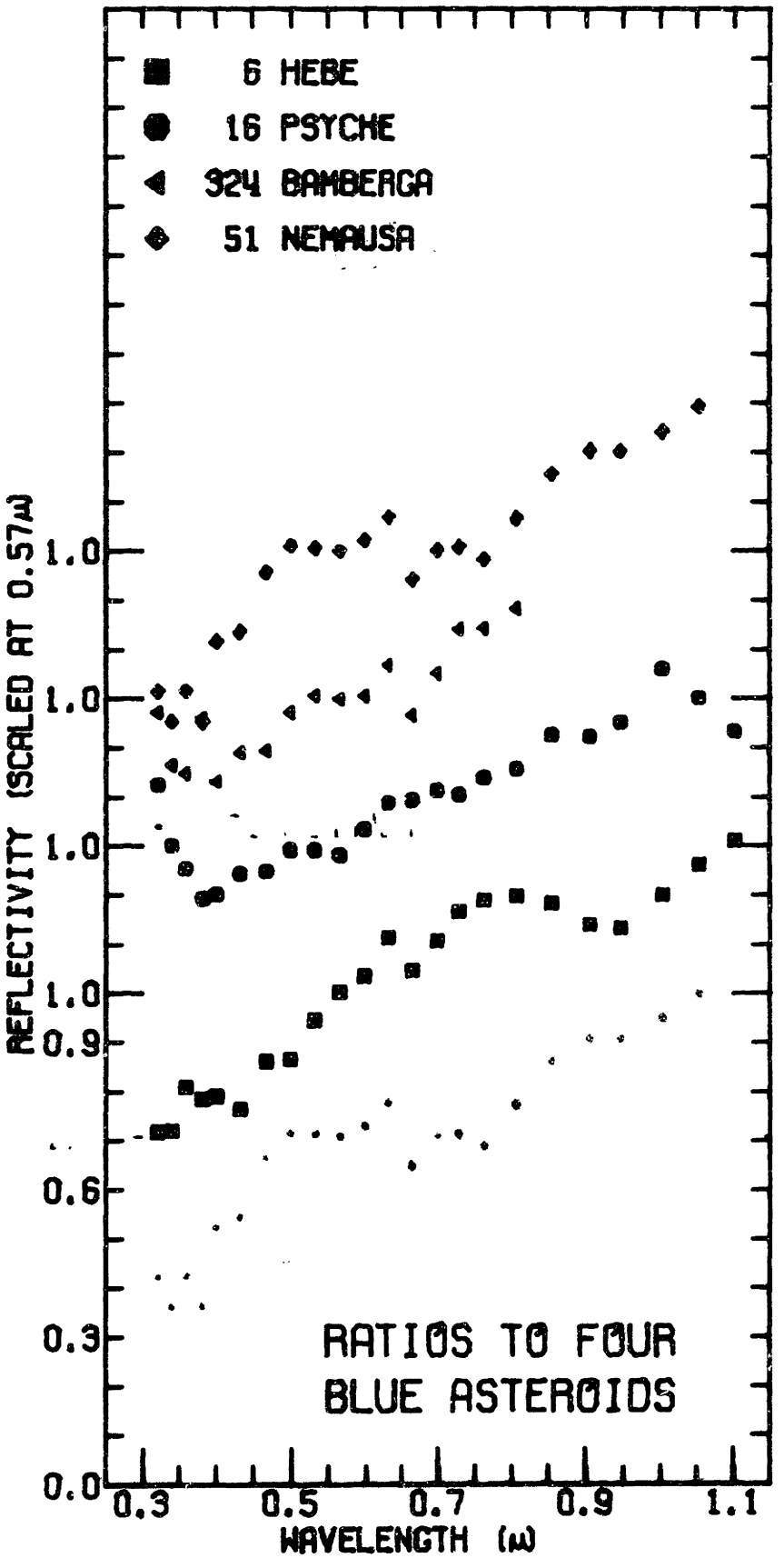
6 HEBE
16 PSYCHE
324 BAMBERGA
51 NEMAUSA
REFLECTIVITY (SCALED AT 0.57μ)
1.0
1.0
1.0
1.0
0.9
0.6
0.3
0.0
0.3
0.5
0.7
0.9
1.1
WAVELENGTH (μ)
RATIOS TO FOUR
BLUE ASTEROIDS

Fig. A-5-9.

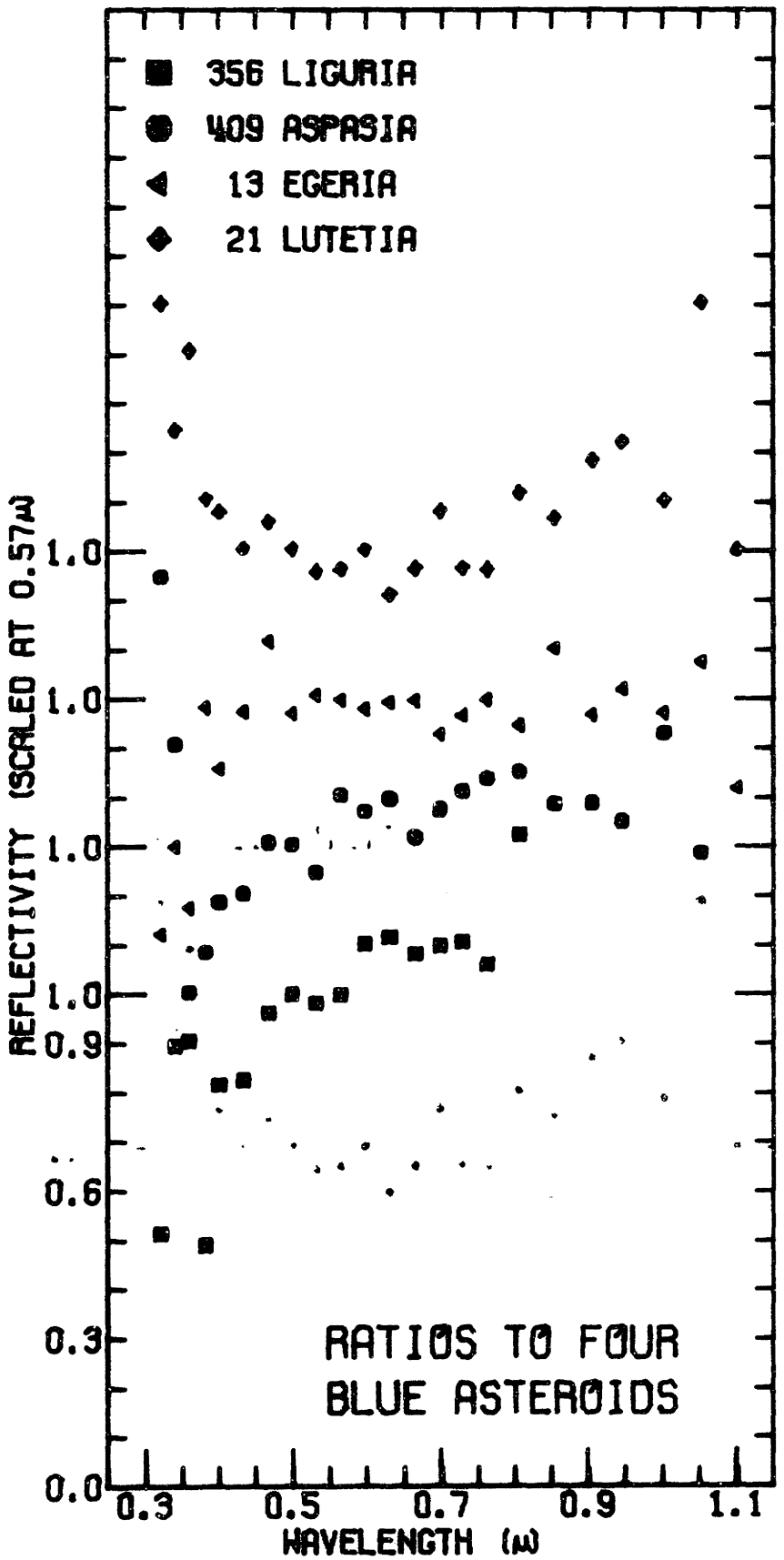
356 LIGURIA
409 ASPASIA
13 EGERIA
21 LUTETIA
REFLECTIVITY (SCALED AT 0.57μ)
1.0
1.0
1.0
1.0
0.9
0.6
0.3
0.0
RATIOS TO FOUR
BLUE ASTEROIDS
0.3
0.5
0.7
0.9
1.1
WAVELENGTH (μ)

Fig. A-5-10.

APPENDIX VI

PASSAGE OF ASTEROIDS NEAR STARS

A. SPECTRAL CONTAMINATION BY UNSEEN STARS

Asteroids are faint objects. During periods of bad seeing, such as encountered at Mt. Wilson in January, it is hard to detect stars more than a couple magnitudes dimmer than the fainter asteroids while guiding through the photometer eyepiece. On more than one occasion, asteroid observations were suspended because the asteroid passed uncomfortably close to recognizable stars. What is the probability that some spectral reflectivity runs are affected to a significant degree by starlight contamination?

Allen (1963) lists typical frequencies for stars per deg^2 brighter than a given magnitude. A typical aperture diameter is 7 seconds of arc and during a typical run the asteroid moves causing the aperture to sweep an area equal to about two aperture areas. The chances of an asteroid run being contaminated by a star two magnitudes fainter (6% contribution) or five magnitudes fainter (1% contribution) are given in Table A-6-1.

Table A-6-1. Chances of Starlight Contamination

Asteroid Magnitude	6% Error	1% Error
10	0.002	0.02
12	0.02	0.1
14	0.1	0.4

Clearly there is only a small chance that any of my data have been affected by stars to a significant degree. However observation of

asteroids even one magnitude fainter becomes more risky. One can perhaps go a magnitude or two fainter by reducing the aperture size and guiding more carefully. But the prospects for observing asteroids or other objects fainter than 15th magnitude are poor, without adopting much more complicated procedures (e.g. photographing the star field ahead-of-time). Further refinements can be made to this analysis, but it serves to demonstrate the magnitude of the problem.

B. DETERMINING ASTEROID DIAMETERS BY STELLAR OCCULTATIONS

A clearly related matter is the possibility of observing an occultation of a star by an asteroid. The two successful observations of occultations to date were of a single chord, which only yields lower limits to diameters (Taylor, 1962). The technique has been tried on only the four brightest asteroids. However, occultations are much more common than usually is assumed.

I will suppose that it is feasible to observe occultations of stars as faint as 14th magnitude by asteroids no more than $2\frac{1}{2}$ magnitudes brighter, using a relatively simple "portable" telescope-photometer system. I will consider the chances for observing star occultations from locations in or near the United States and populated areas of Canada.

The probability of a tiny asteroid occulting a star visible from some place in America is geometrically equivalent to the probability of a hypothetical asteroid with the dimensions of America occulting a star as viewed from a specified location on earth. At a typical asteroidal distance from earth (weighted toward opposition distances) America would subtend about 3 arcseconds. At any given time there is the order of 50 asteroids visible in the sky with apparent magnitudes brighter than magnitude

12.5. Fifty "Americas" in the sky would cover about 2.5×10^{-5} deg^2. Allen's (1963) tables show that there are about 200 stars/deg^2 brighter than magnitude 14. Hence at any time there is probability $(200)(2.5 \times 10^{-5}) = 0.005$ that an observable occultation is visible from someplace in America. Asteroids typically move at the rate of 600 arcsec per day so an America-sized asteroid would cover a new portion of the sky every 0.1 hour. Given ten hours of observing time per night, there would appear to be about a 50% chance of an observable occultation occuring each night! This is a slight overestimate for several reasons; for instance, a few of the asteroids brighter than magnitude 12.5 are in fact much brighter, and they would be unlikely to occult stars equally brighter than the 14th magnitude star limit. However, an observable occultation once every week or two is certainly a reasonable expectation.

A few comments about the feasibility of such a project are in order. First, the skies ahead of each of the fifty asteroids would have to be monitored, presumably photographically, to permit reasonably accurate predictions of occultations. The diameters of asteroids of apparent magnitude 12.5 could be as small as 50 km. Since the "shadow" cast on the earth by an asteroid has a width nearly equal to the asteroid diameter, and occultations must be observed across two chords in order to estimate the diameter, observers should be spaced no farther apart than every 50 km (along an approximately north-south line, or its equivalent). For N observers with the requisite portable equipment, we require position predictions for the asteroid accurate to about N/30 second of arc. It is clear that such an asteroid diameter project would have to be fairly elaborate in terms of personnel and equipment, but the prospects for obtaining several asteroid diameters per month are good. These results could be

quite important. A more detailed feasibility study of such a project is warranted.

APPENDIX VII

SPECTRAL REFLECTIVITY CURVES FOR ASTEROIDS AND OTHER OBJECTS

A. NIGHTLY AVERAGES FOR ASTEROIDS

The average reflectivity curve obtained from each night's observations of each asteroid are presented in graphical form in this appendix. In the case of a single run for several or all filters, no error bars are shown. Otherwise error bars are derived from the internal consistency of the data. The standard stars used in the reduction are listed on the graphs, using English-letter abbreviations for the Greek letters. "Multiple" refers to more than two standard stars.

These data are arranged according to the observing run and mode of data reduction. This arrangement will serve to emphasize the different magnitudes and types of errors peculiar to each mode of data acquisition.

Data pertaining to the individual runs which comprise the nightly means shown here may be found in Appendix I, which also presents the mean asteroid reflectivity curve.

B. SOLAR SYSTEM COMPARISONS

At the end of the appendix are several figures showing spectral reflectivities for other solar system objects which might be interesting to compare with the asteroids. The data were obtained from files in the M.I.T. Planetary Astronomy Laboratory. The new Vega-sun ratio has been employed in calculating these reflectivities, so they should be directly comparable with the asteroid results (except for lunar data short of 0.4 microns).

August 1970 run.

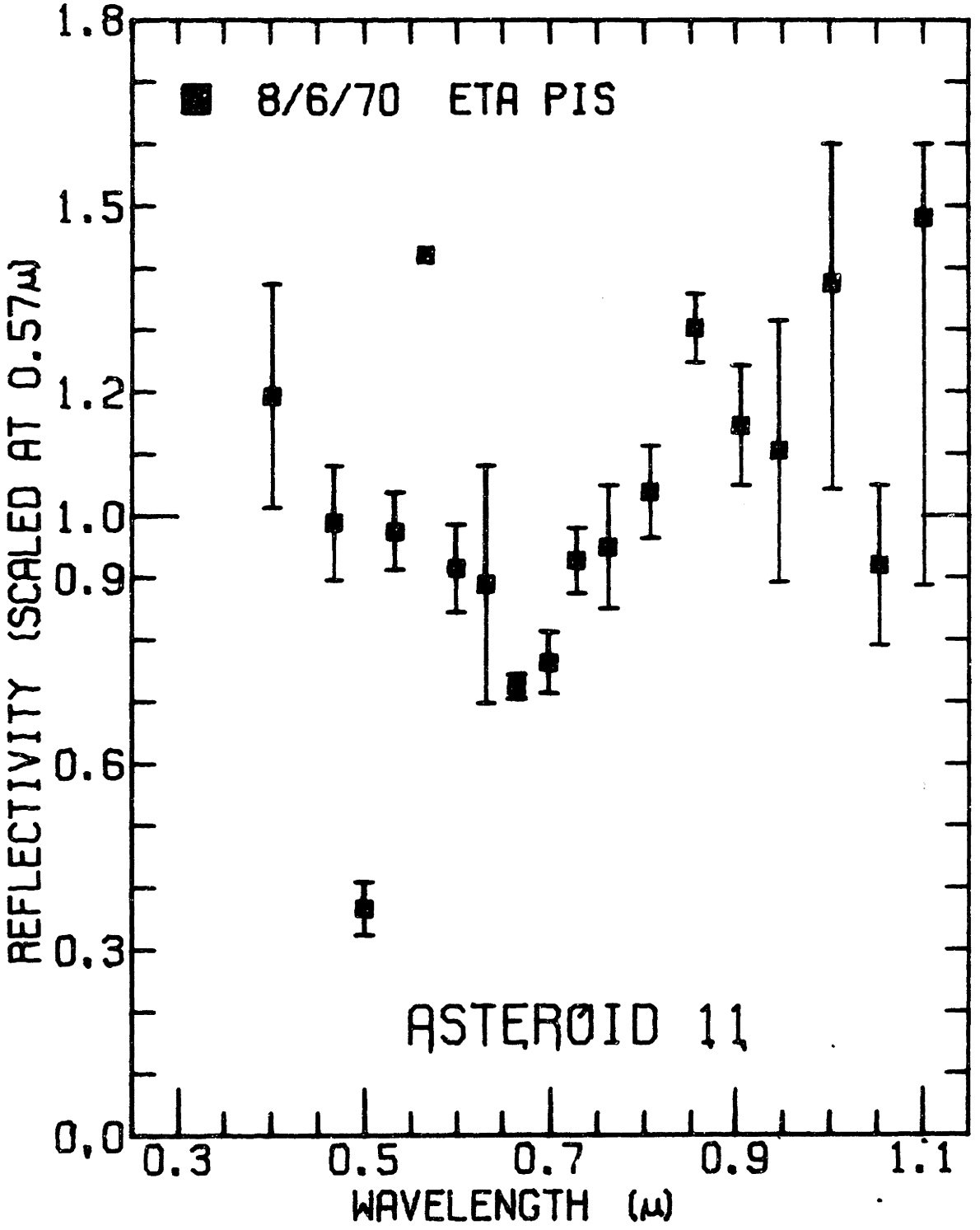
8/6/70 ETA PIS
ASTEROID 11
REFLECTIVITY (SCALED AT 0.57μ)
WAVELENGTH (μ)
1.8
1.5
1.2
1.0
0.9
0.6
0.3
0.0
0.3
0.5
0.7
0.9
1.1

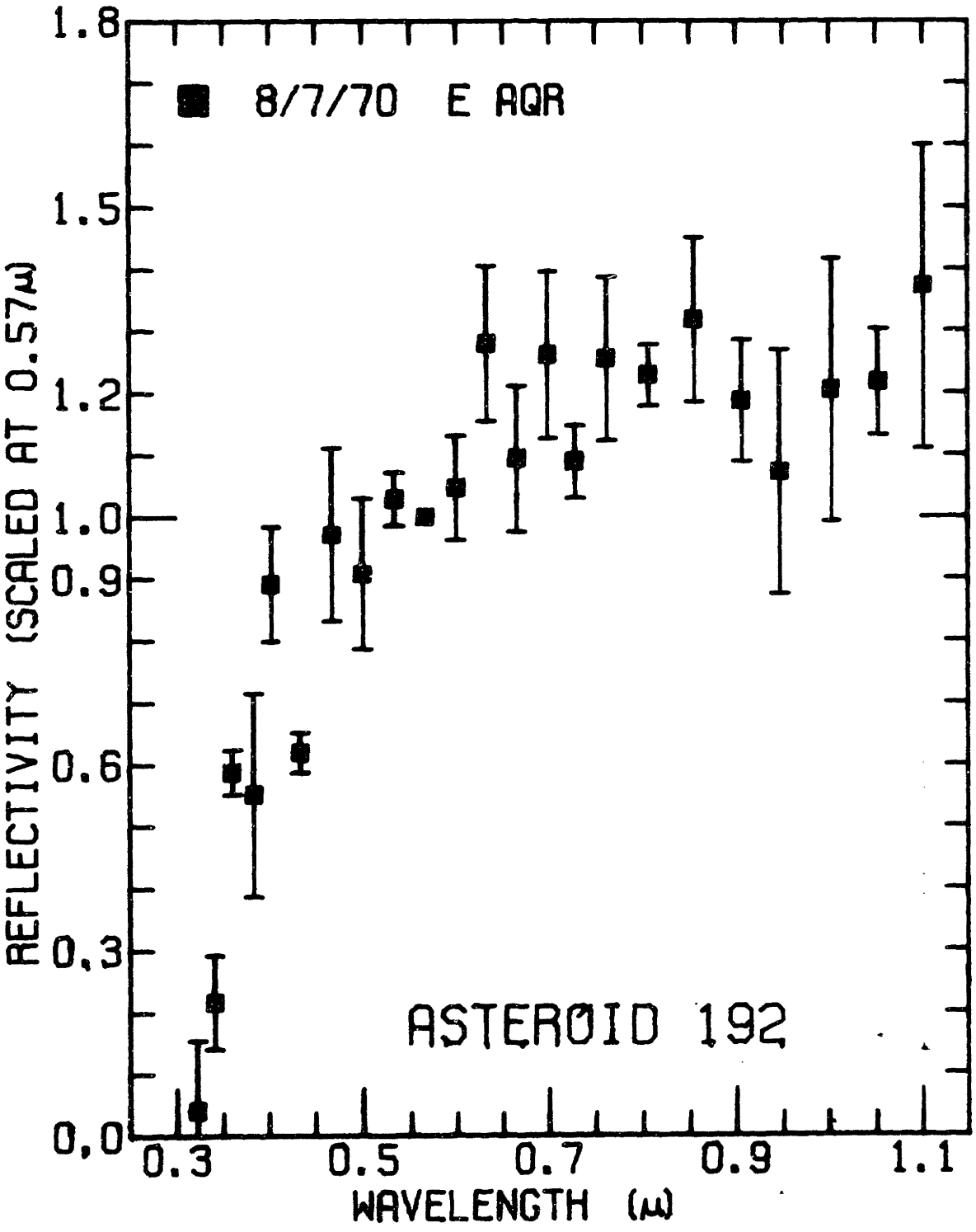
8/7/70 E AQR
ASTEROID 192
REFLECTIVITY (SCALED AT 0.57μ)
WAVELENGTH (μ)
1.8
1.5
1.2
1.0
0.9
0.6
0.3
0.0
0.3
0.5
0.7
0.9
1.1

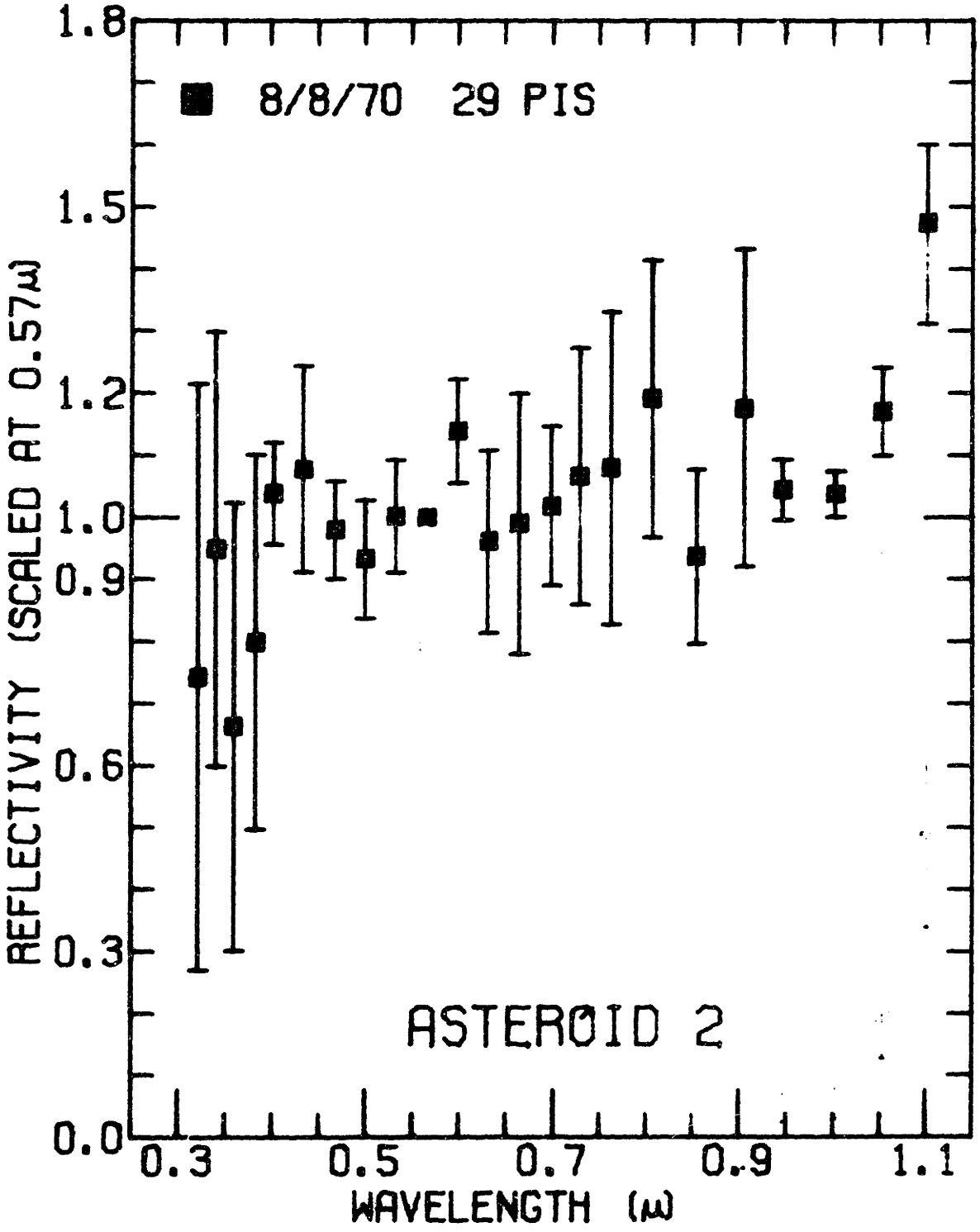
8/8/70 29 PIS
ASTEROID 2
REFLECTIVITY (SCALED AT 0.57μ)
WAVELENGTH (μ)
1.8
1.5
1.2
1.0
0.9
0.6
0.3
0.0
0.3
0.5
0.7
0.9
1.1

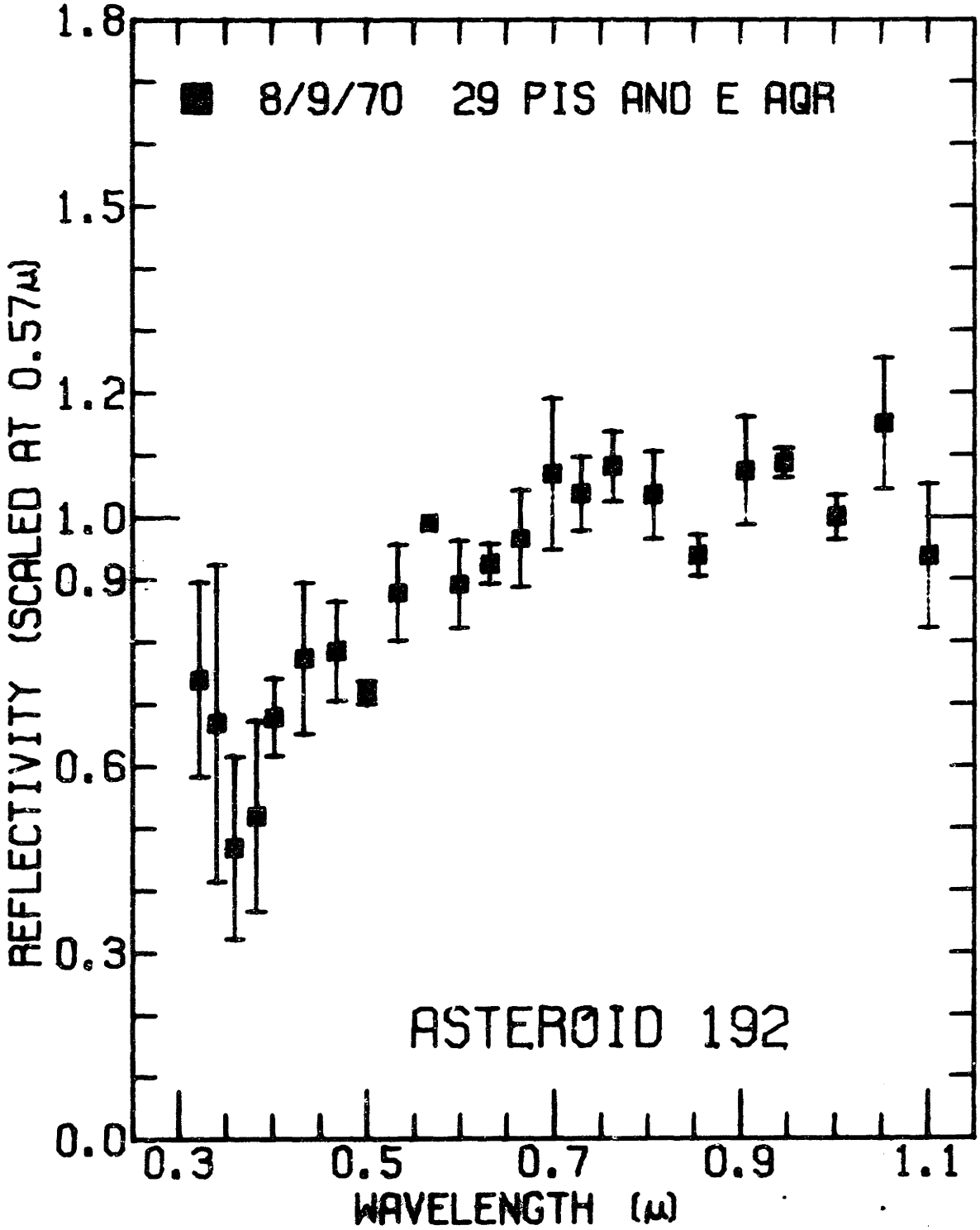
8/9/70 29 PIS AND E AQR
ASTEROID 192
REFLECTIVITY (SCALED AT 0.57μ)
WAVELENGTH (μ)
1.8
1.5
1.2
1.0
0.9
0.6
0.3
0.0
0.3
0.5
0.7
0.9
1.1

October 1970 run.

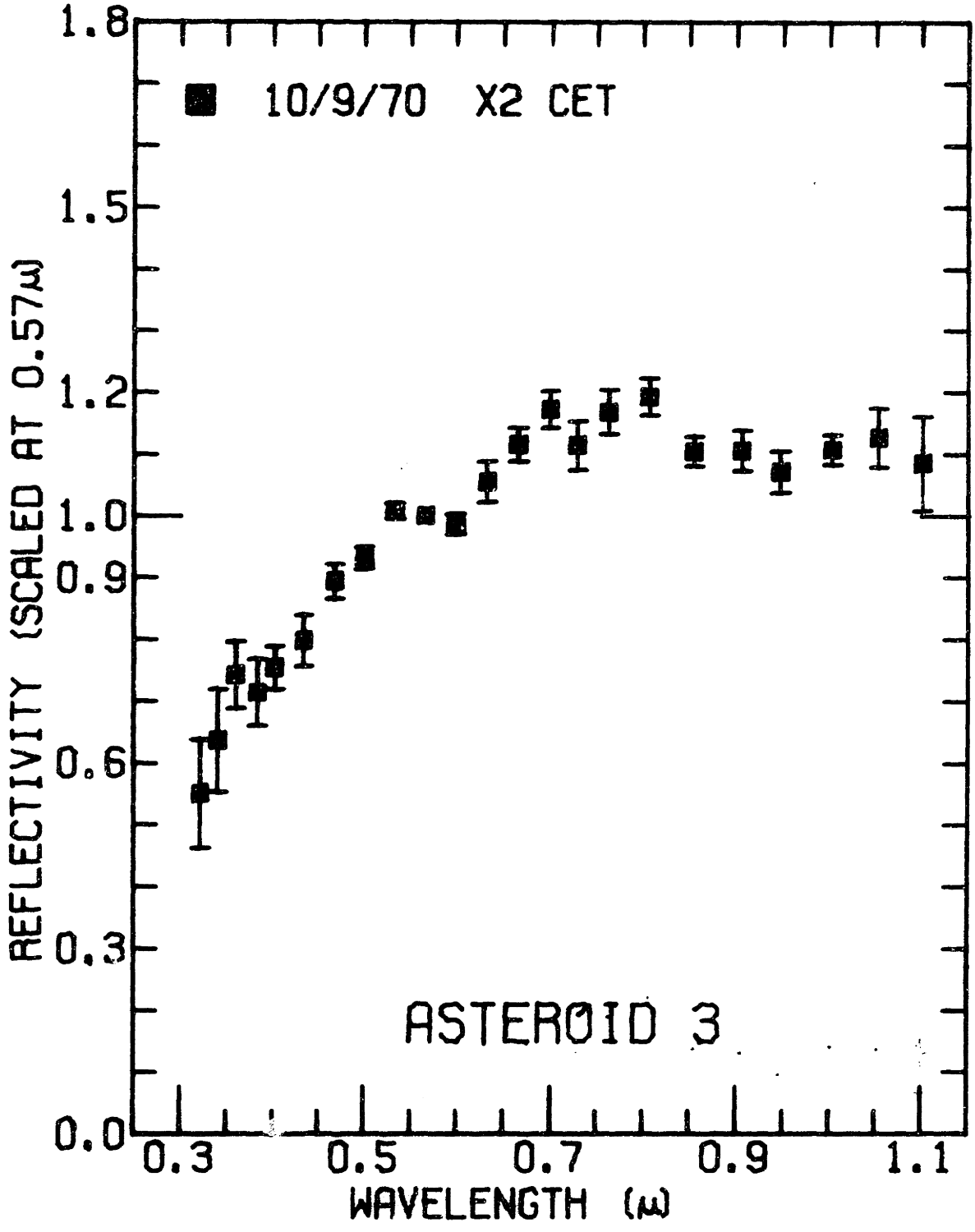
10/9/70 X2 CET
ASTEROID 3
REFLECTIVITY (SCALED AT 0.57μ)
WAVELENGTH (μ)
1.8
1.5
1.2
1.0
0.9
0.6
0.3
0.0
0.3
0.5
0.7
0.9
1.1

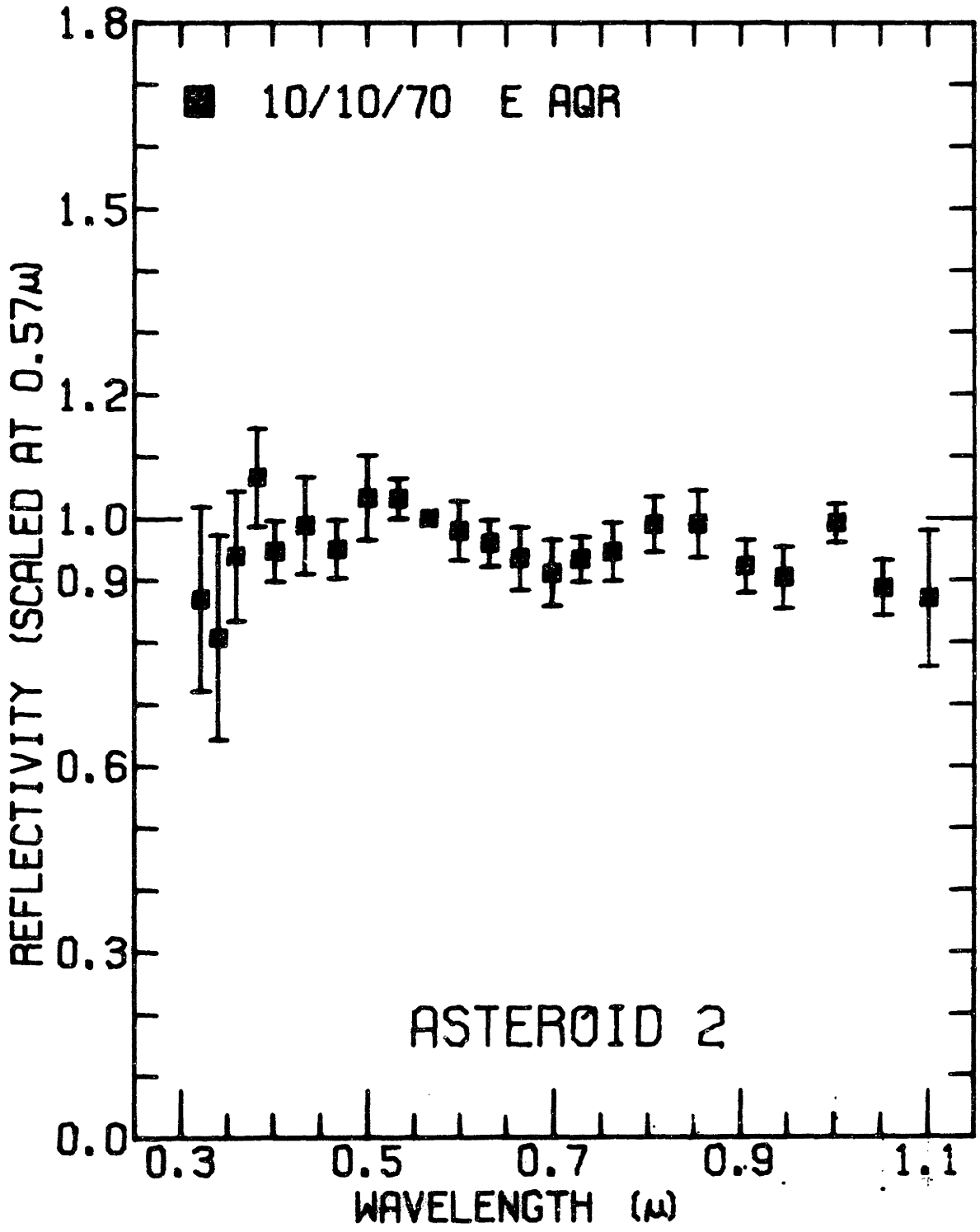
10/10/70 E AQR
ASTEROID 2
REFLECTIVITY (SCALED AT 0.57μ)
WAVELENGTH (μ)
1.8
1.5
1.2
1.0
0.9
0.6
0.3
0.0
0.3
0.5
0.7
0.9
1.1

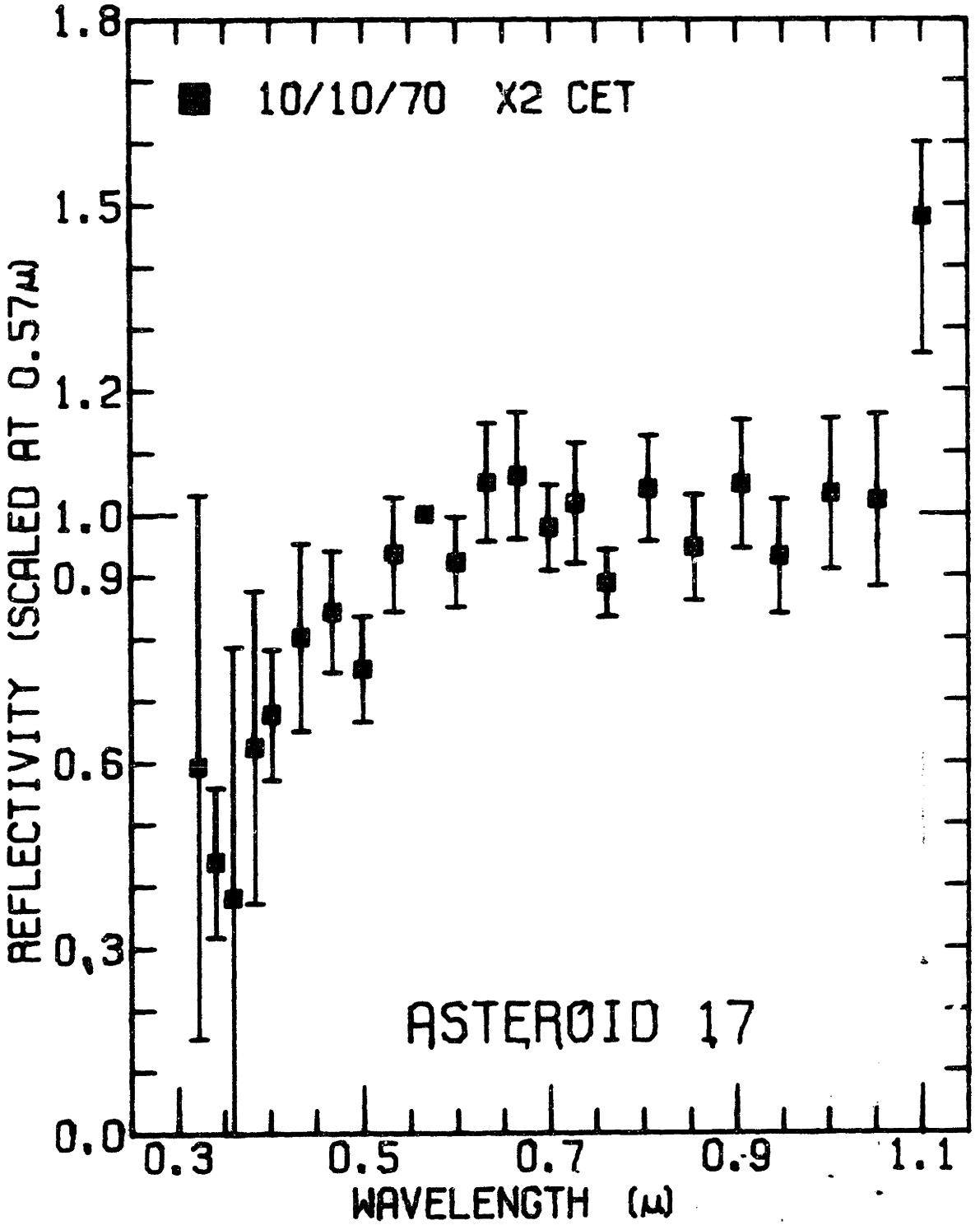
10/10/70 X2 CET
ASTEROID 17
REFLECTIVITY (SCALED AT 0.57μ)
WAVELENGTH (μ)
1.8
1.5
1.2
1.0
0.9
0.6
0,3
0.0
0.3
0.5
0.7
0.9
1.1

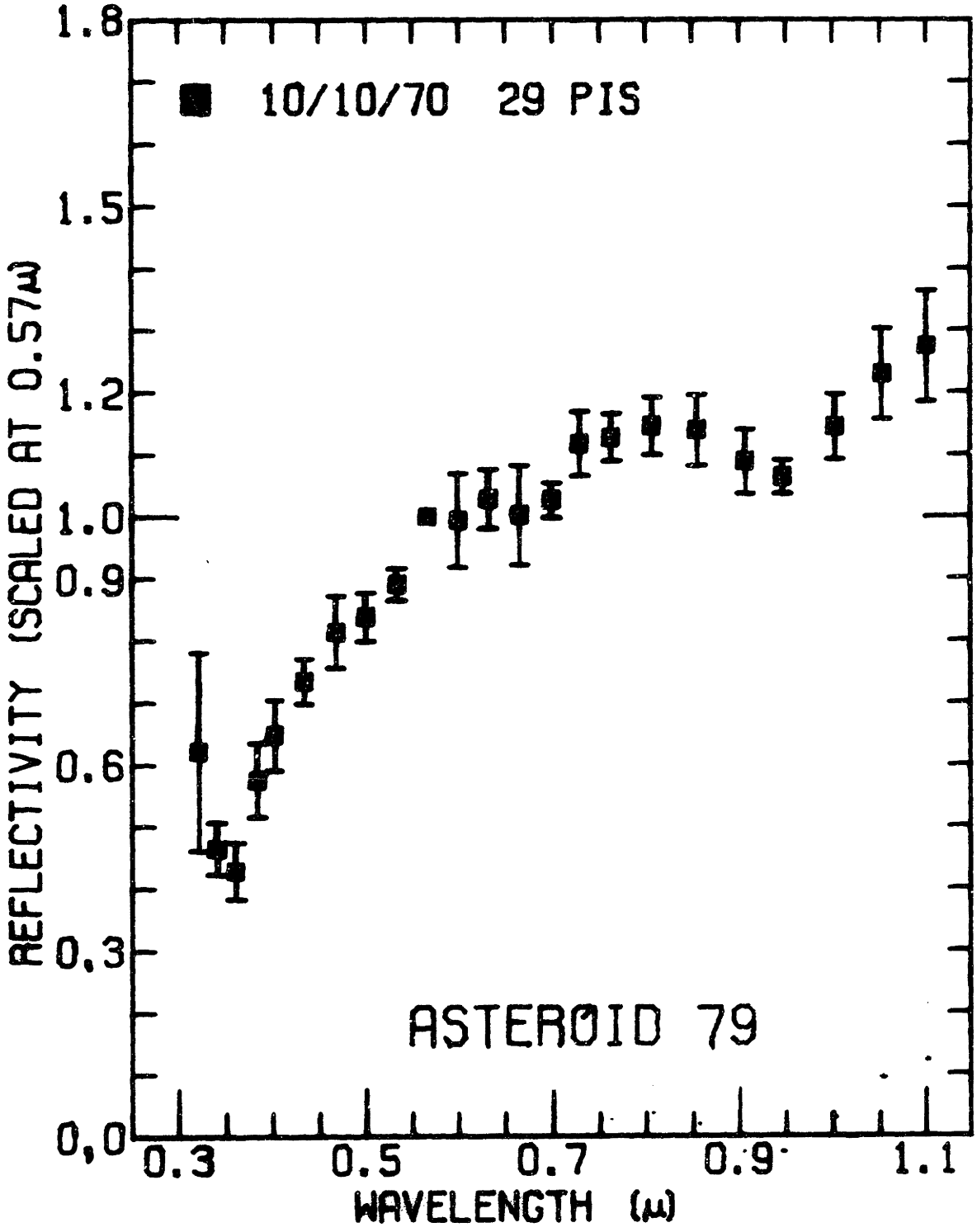
10/10/70 29 PIS
ASTEROID 79
REFLECTIVITY (SCALED AT 0.57μ)
WAVELENGTH (μ)
1.8
1.5
1.2
1.0
0.9
0.6
0.3
0.0
0.3
0.5
0.7
0.9
1.1

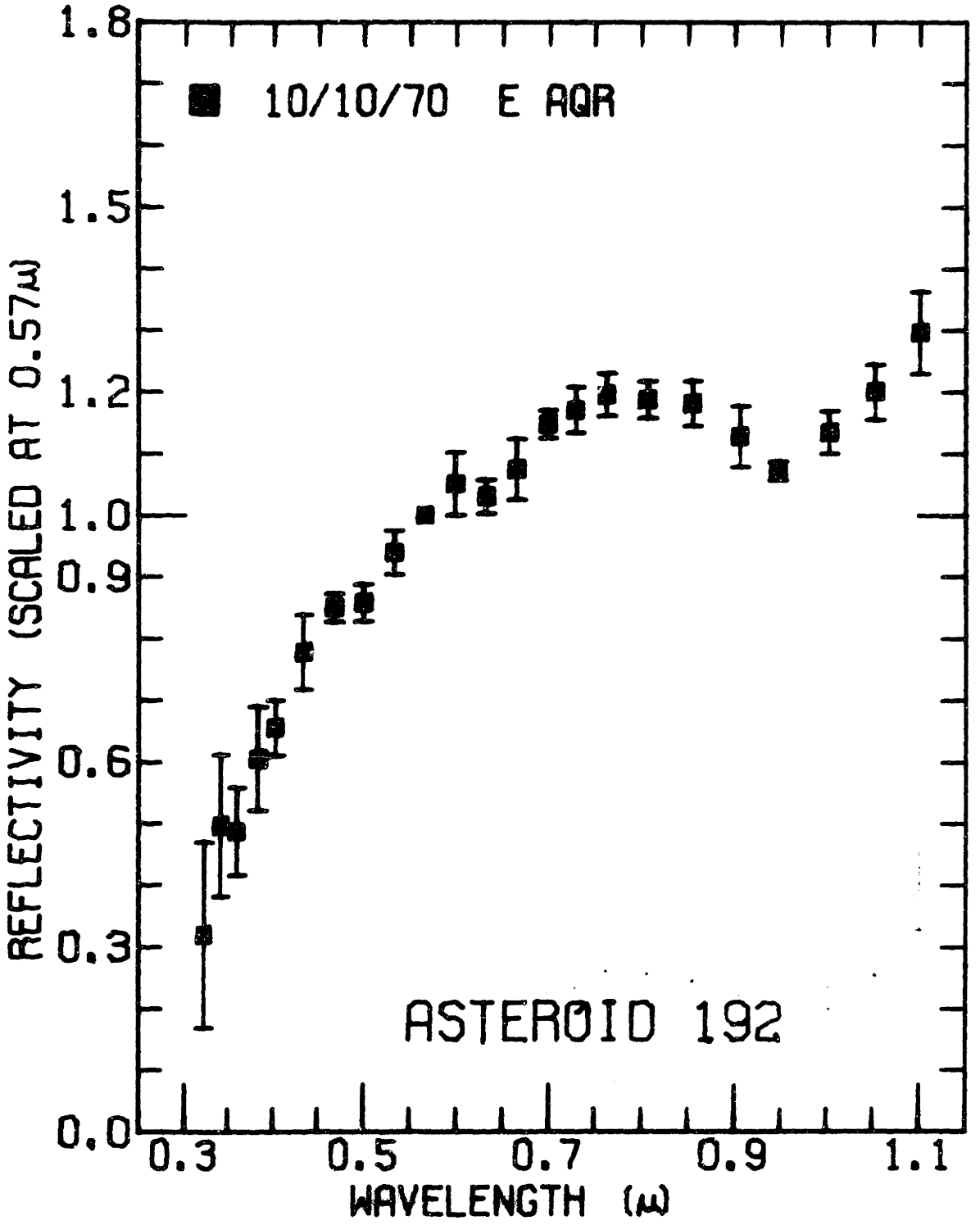
10/10/70 E AQR
ASTEROID 192
REFLECTIVITY (SCALED AT 0.57μ)
WAVELENGTH (μ)
1.8
1.5
1.2
1.0
0.9
0.6
0.3
0.0
0.3
0.5
0.7
0.9
1.1

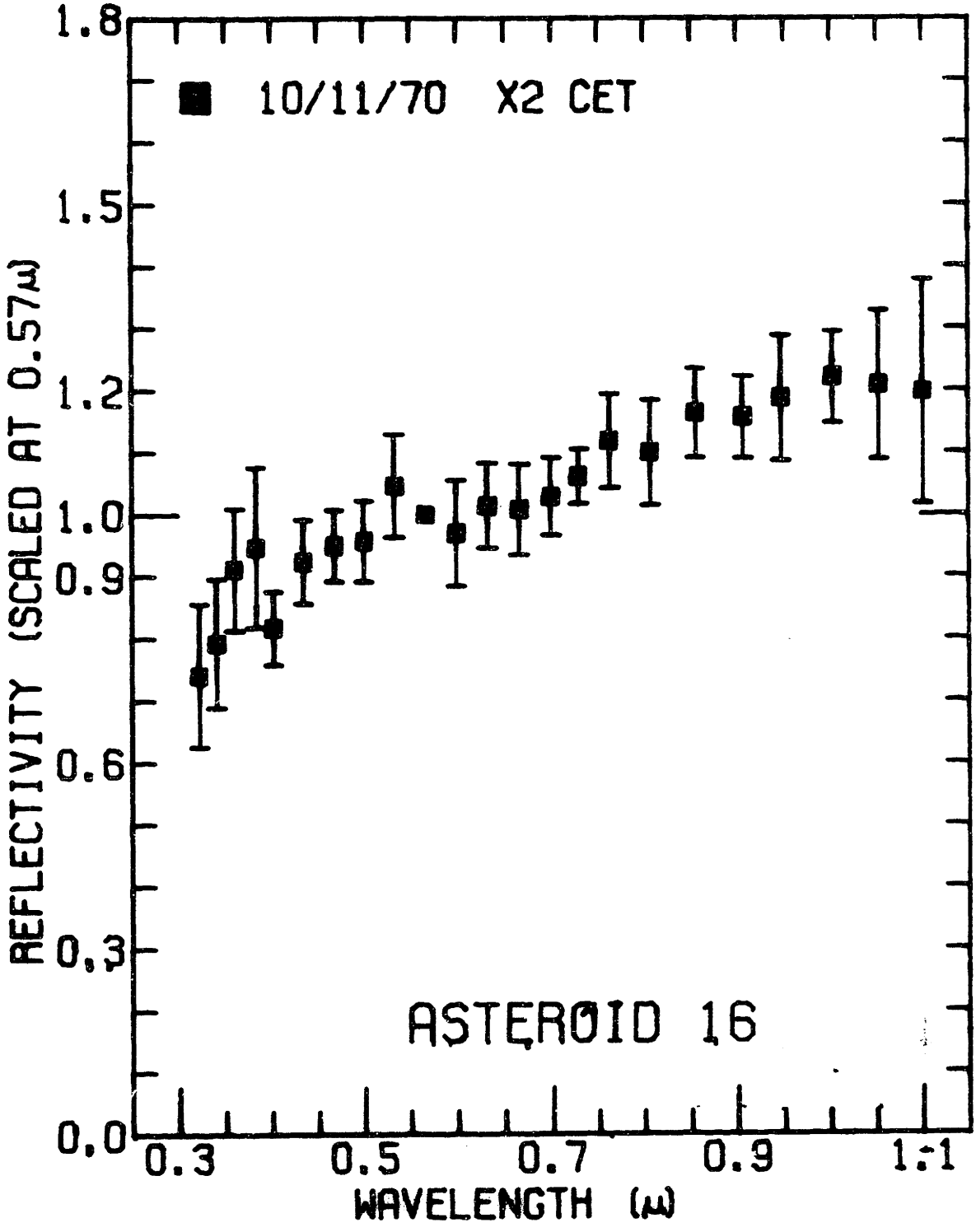
10/11/70 X2 CET
ASTEROID 16
REFLECTIVITY (SCALED AT 0.57μ)
WAVELENGTH (μ)
1.8
1.5
1.2
1.0
0.9
0.6
0.3
0.0
0.3
0.5
0.7
0.9
1.1

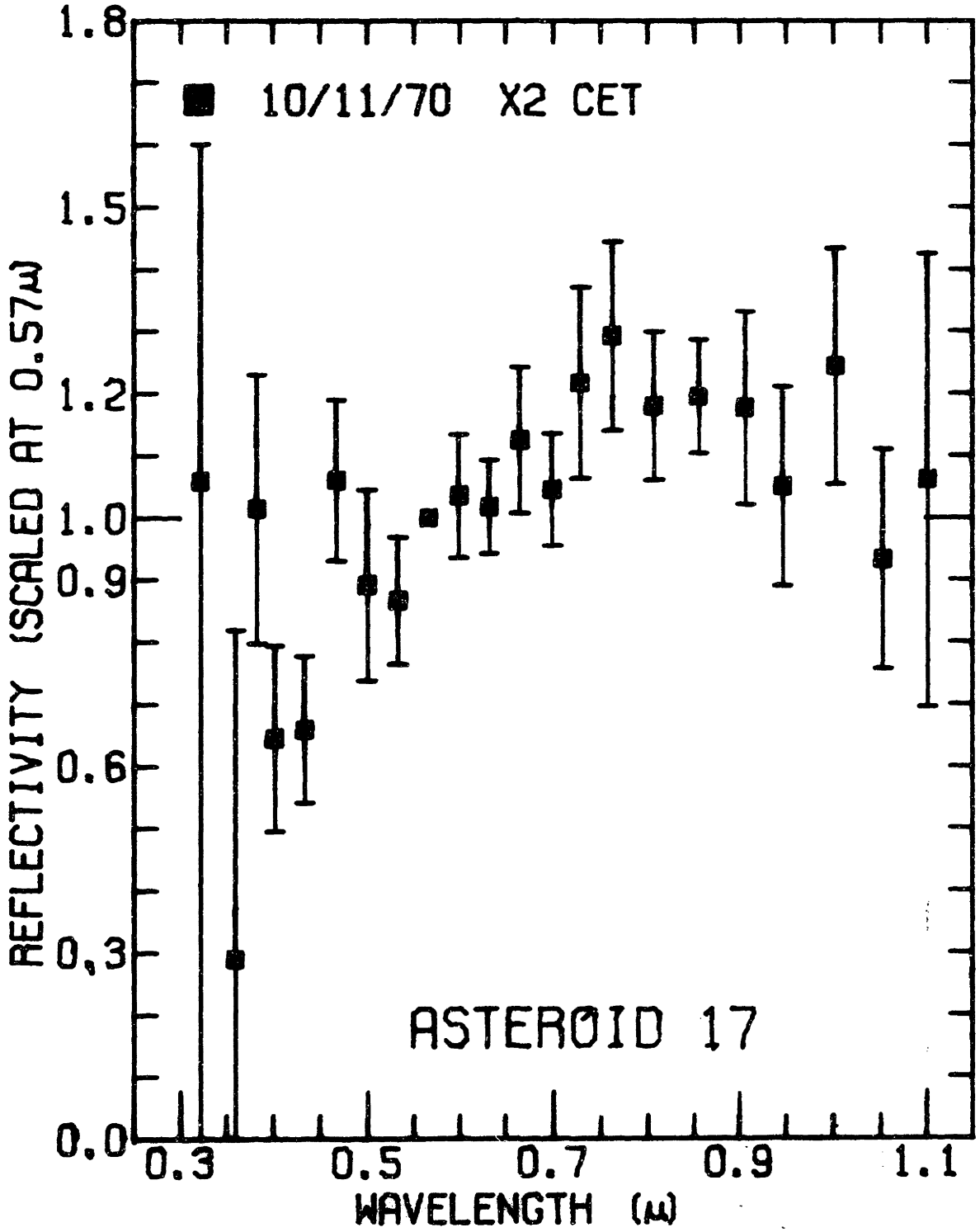
10/11/70 X2 CET
ASTEROID 17
REFLECTIVITY (SCALED AT 0.57μ)
WAVELENGTH (μ)
1.8
1.5
1.2
1.0
0.9
0.6
0.3
0.0
0.3
0.5
0.7
0.9
1.1

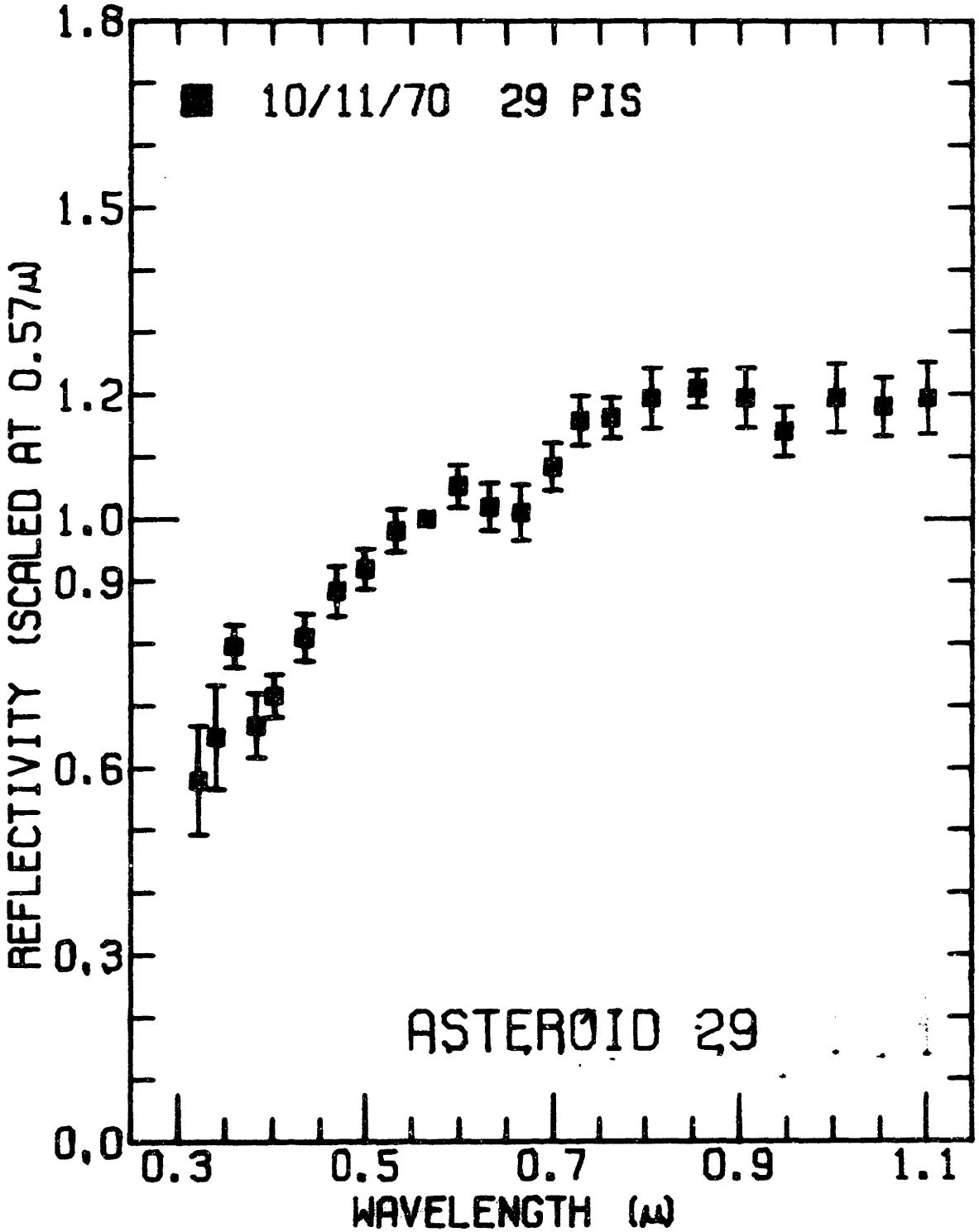
10/11/70 29 PIS
ASTEROID 29
REFLECTIVITY (SCALED AT 0.57μ)
WAVELENGTH (μ)
1.8
1.5
1.2
1.0
0.9
0.6
0.3
0.0
0.3
0.5
0.7
0.9
1.1

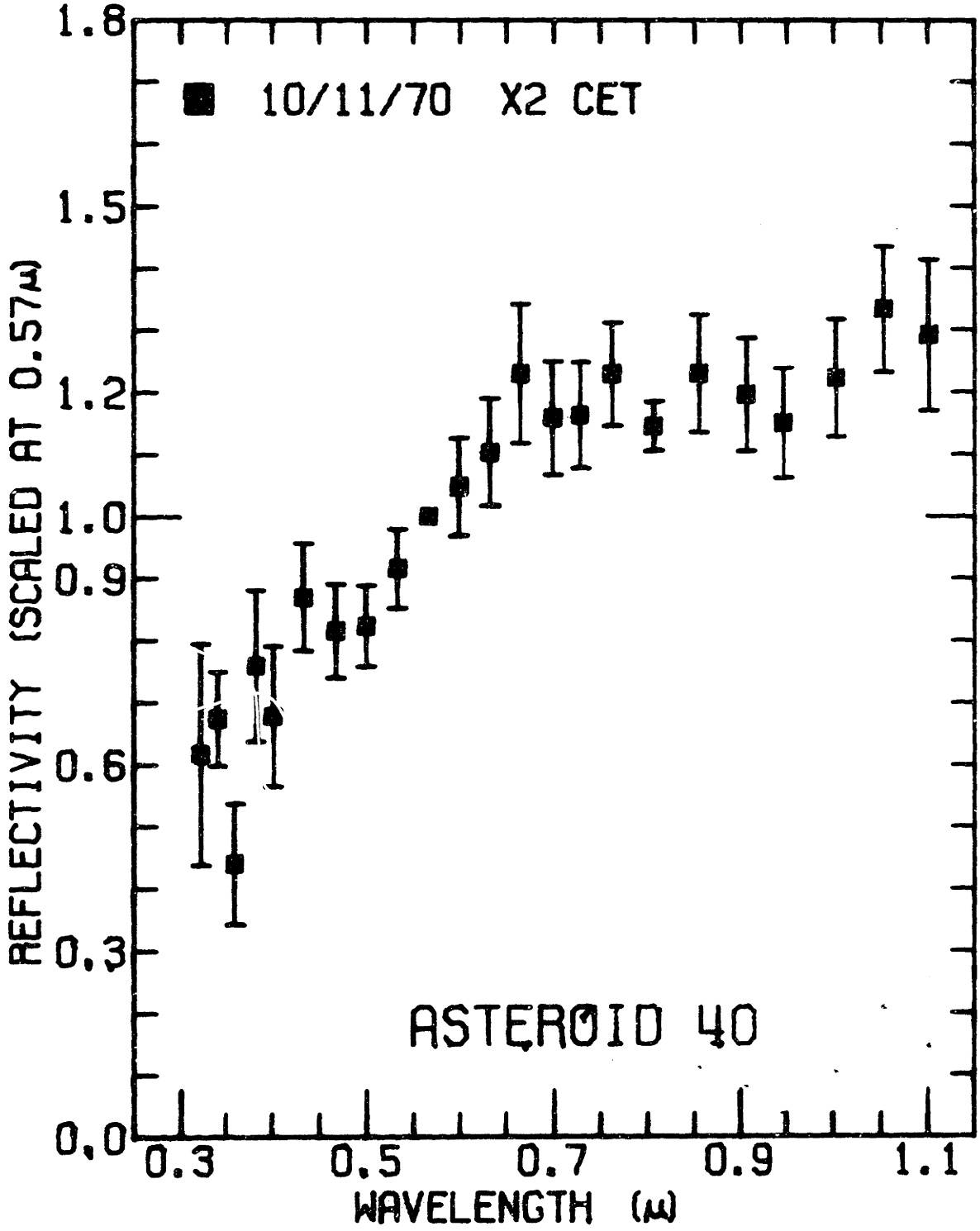
10/11/70 X2 CET
ASTEROID 40
REFLECTIVITY (SCALED AT 0.57μ)
WAVELENGTH (μ)
1.8
1.5
1.2
1.0
0.9
0.6
0.3
0.0
0.3
0.5
0.7
0.9
1.1

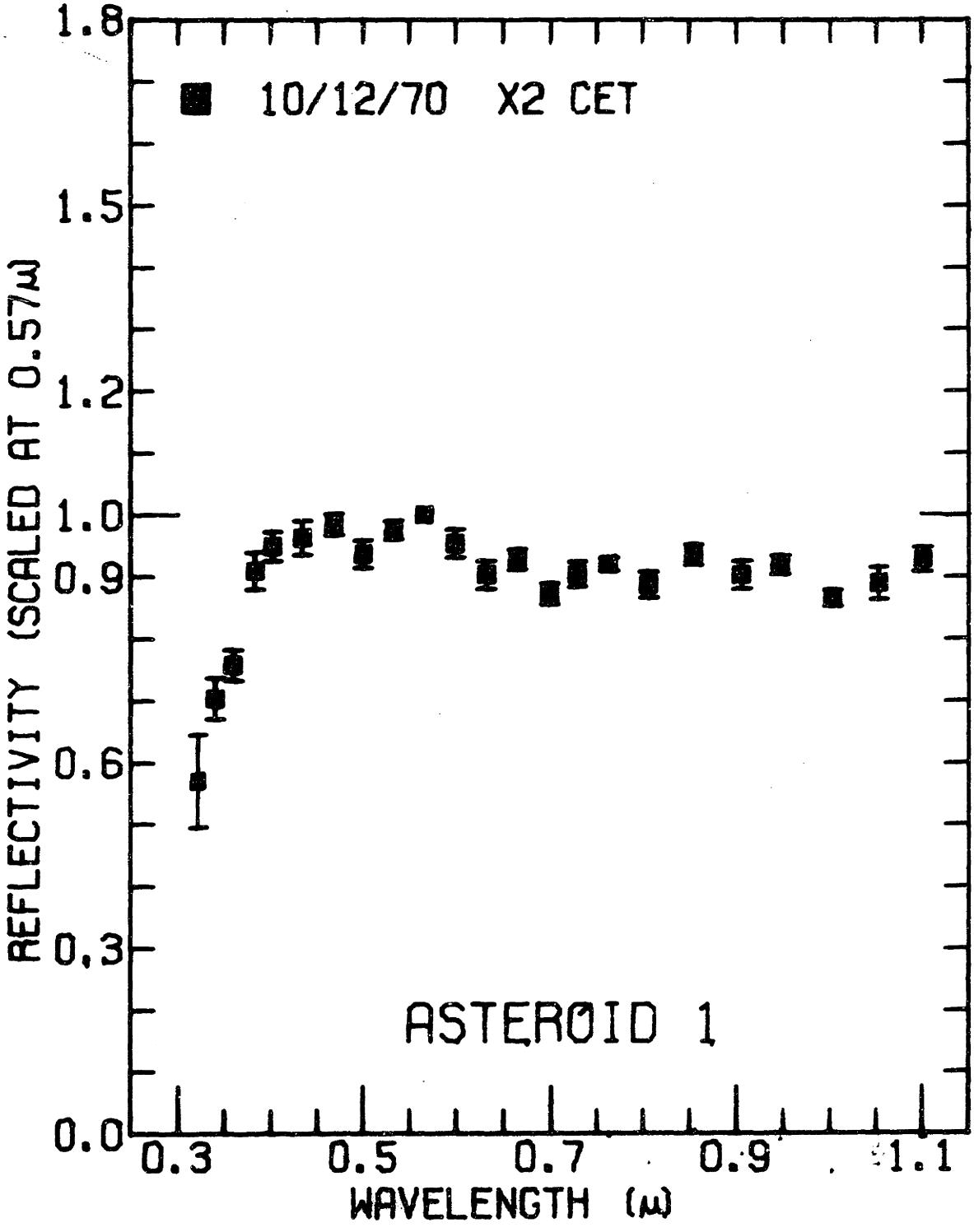
10/12/70 X2 CET
ASTEROID 1
REFLECTIVITY (SCALED AT 0.57μ)
WAVELENGTH (μ)
1.8
1.5
1.2
1.0
0.9
0.6
0.3
0.0
0.3
0.5
0.7
0.9
1.1

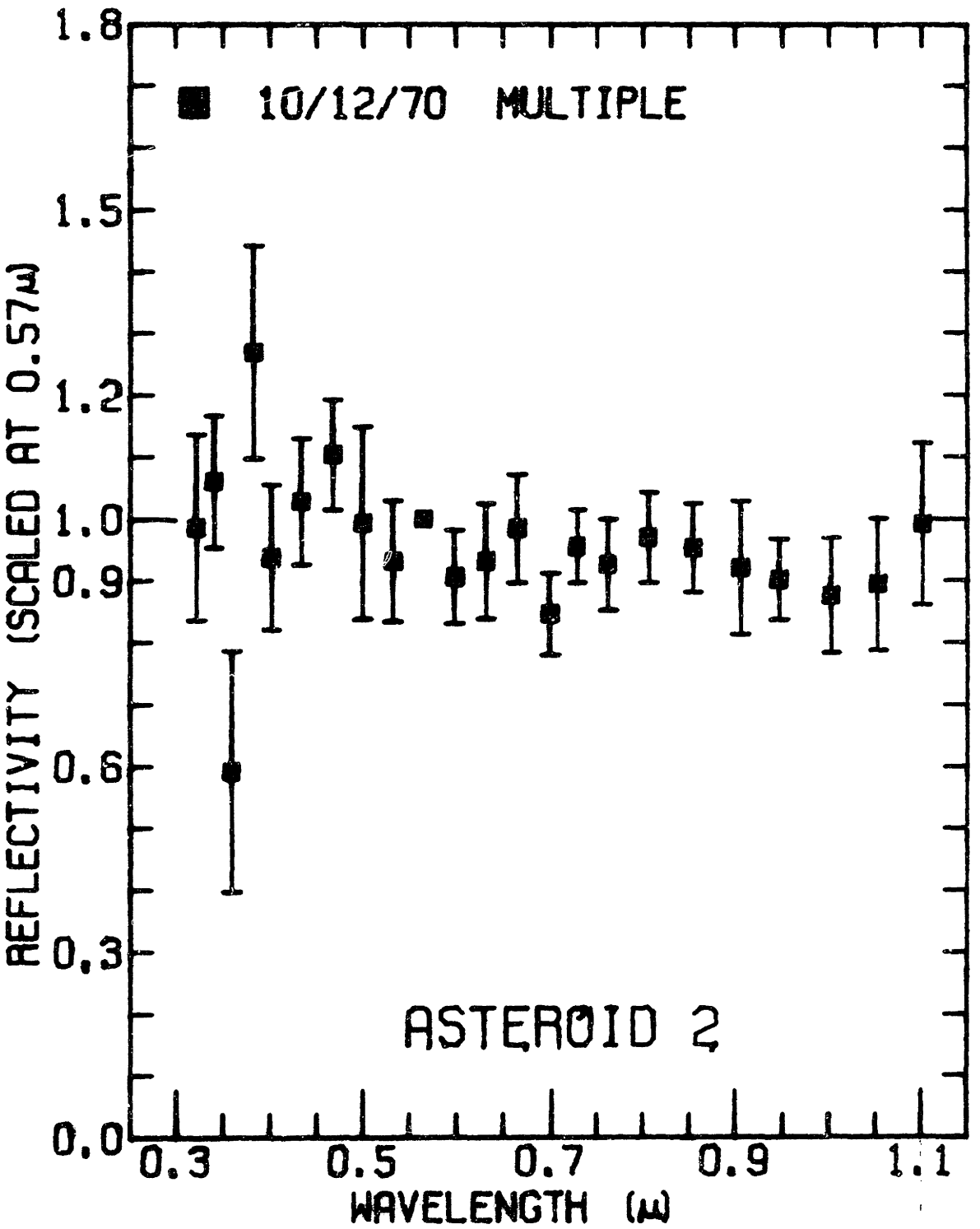
10/12/70 MULTIPLE
ASTEROID 2
REFLECTIVITY (SCALED AT 0.57μ)
WAVELENGTH (μ)
1.8
1.5
1.2
1.0
0.9
0.6
0.3
0.0
0.3
0.5
0.7
0.9
1.1

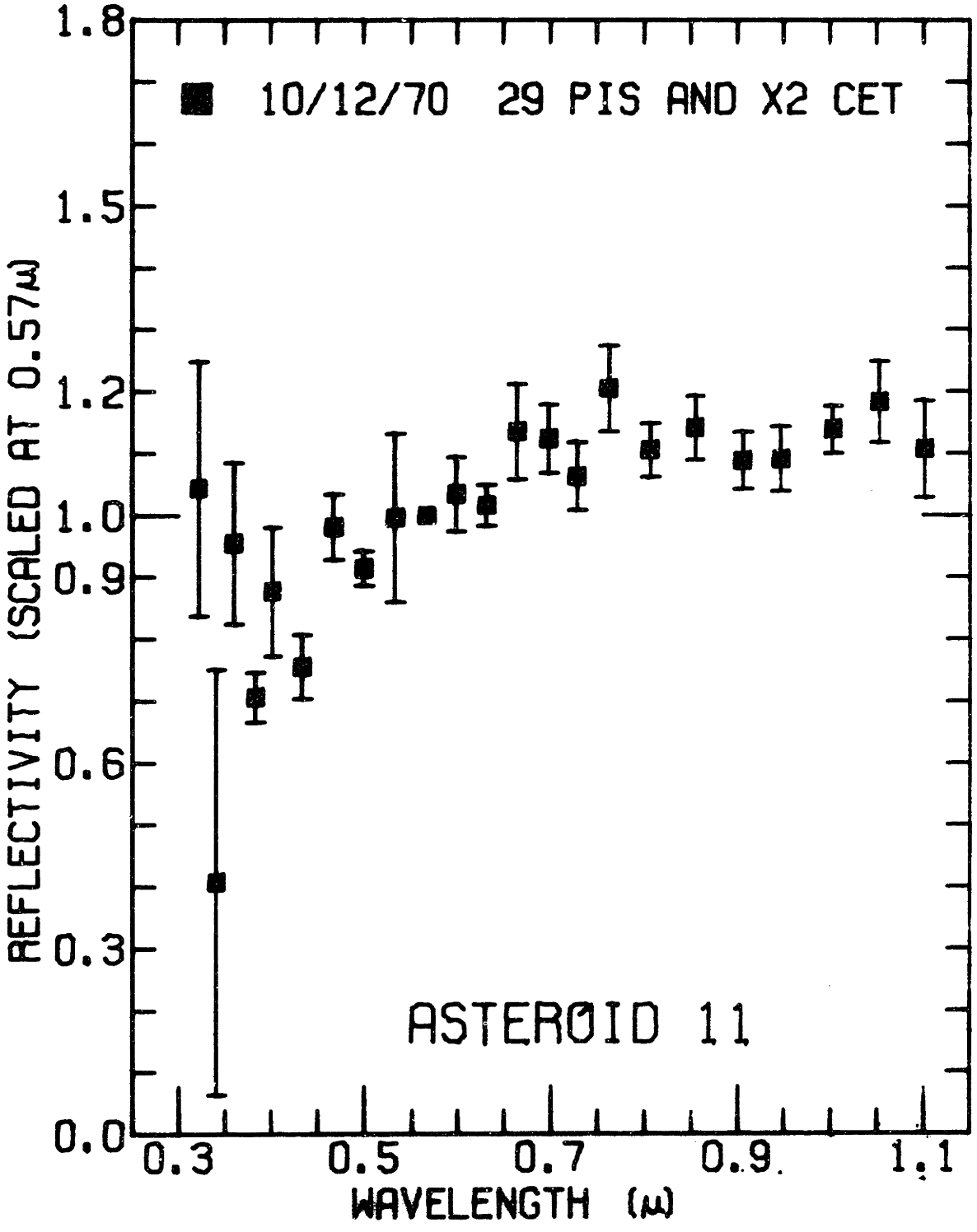
10/12/70 29 PIS AND X2 CET
ASTEROID 11
REFLECTIVITY (SCALED AT 0.57μ)
WAVELENGTH (μ)
1.8
1.5
1.2
1.0
0.9
0.6
0.3
0.0
0.3
0.5
0.7
0.9
1.1

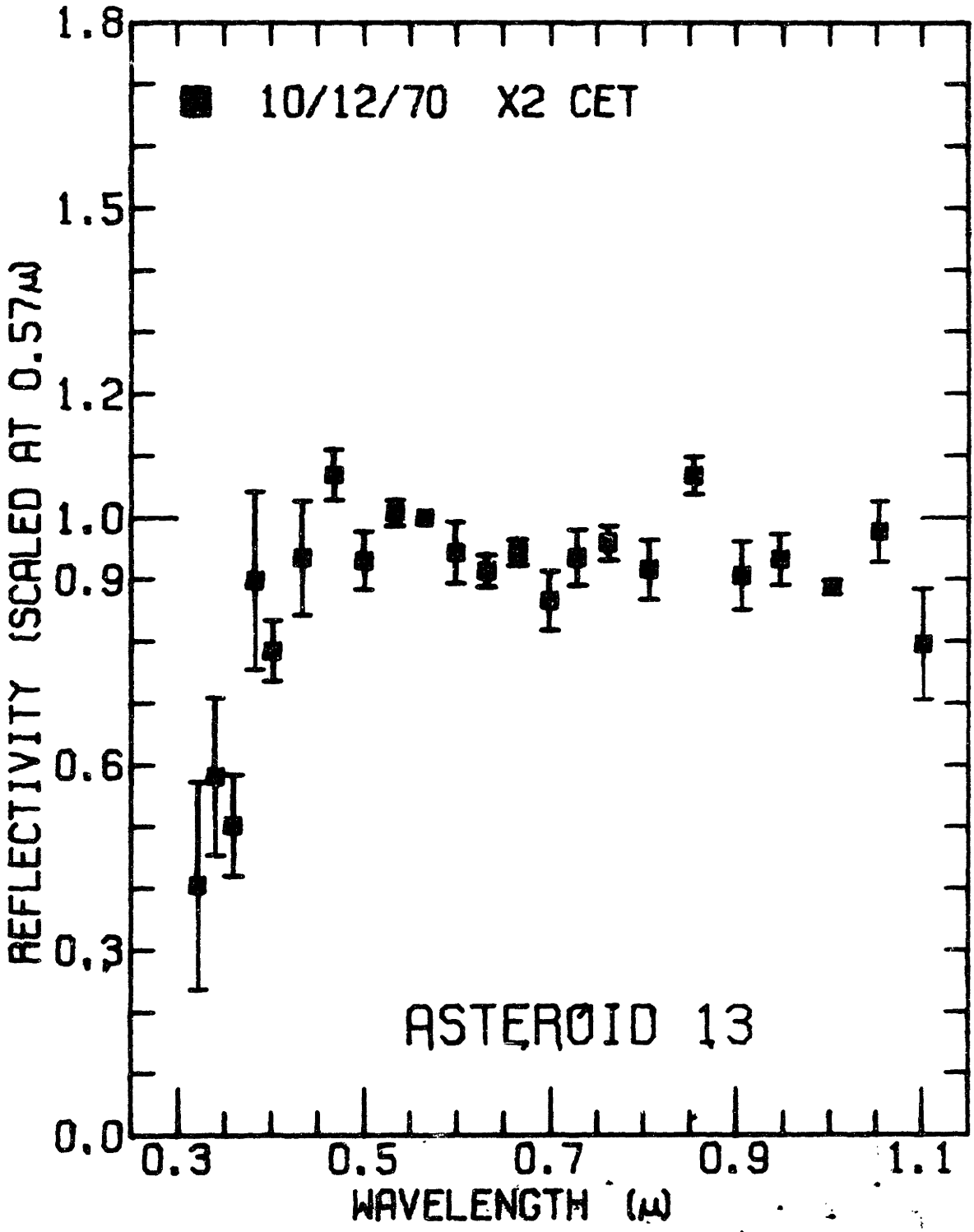
10/12/70 X2 CET
ASTEROID 13
REFLECTIVITY (SCALED AT 0.57μ)
WAVELENGTH (μ)
1.8
1.5
1.2
1.0
0.9
0.6
0.3
0.0
0.3
0.5
0.7
0.9
1.1

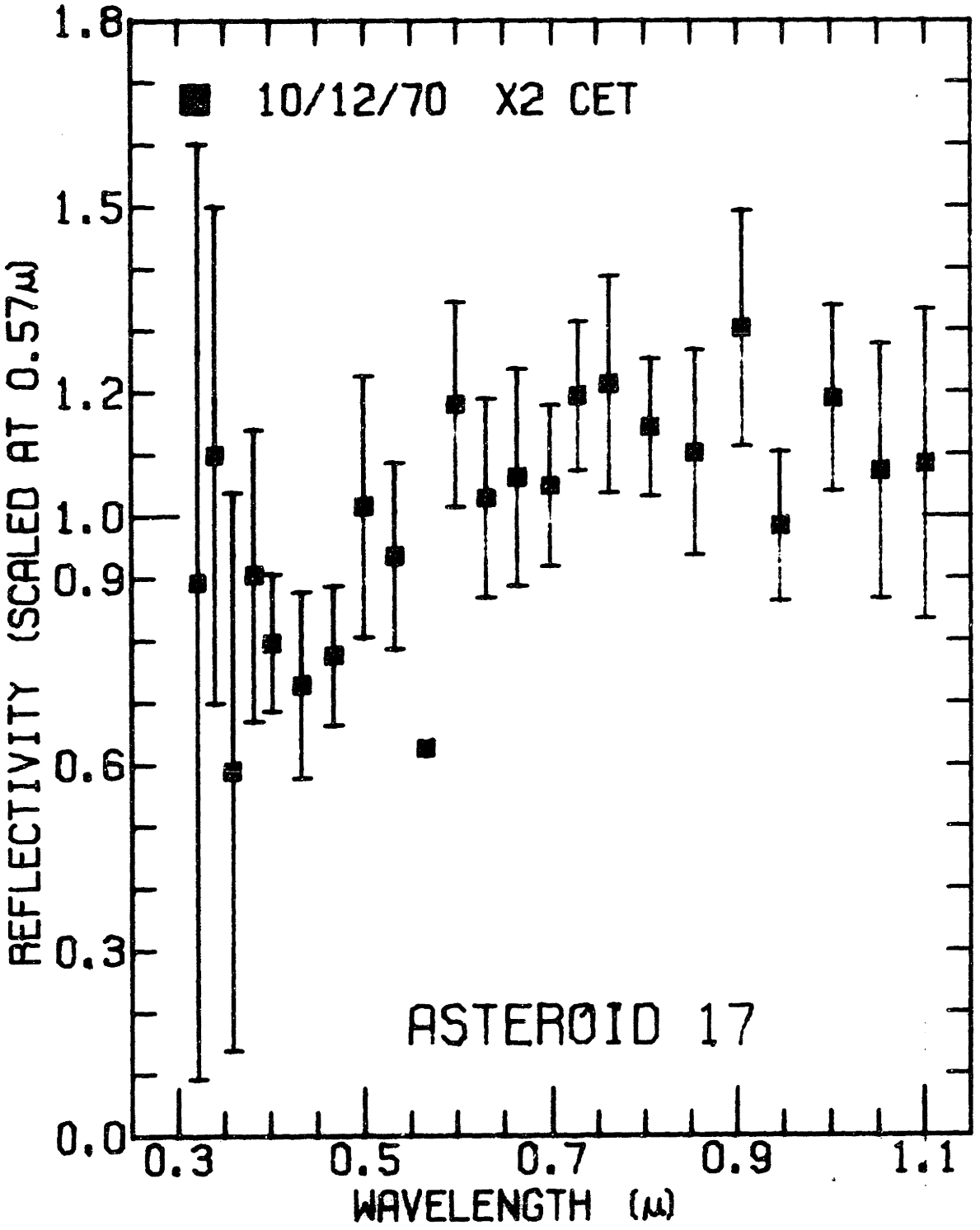
10/12/70 X2 CET
ASTEROID 17
REFLECTIVITY (SCALED AT 0.57μ)
WAVELENGTH (μ)
1.8
1.5
1.2
1.0
0.9
0.6
0.3
0.0
0.3
0.5
0.7
0.9
1.1

December-January 70/71 24-inch run.

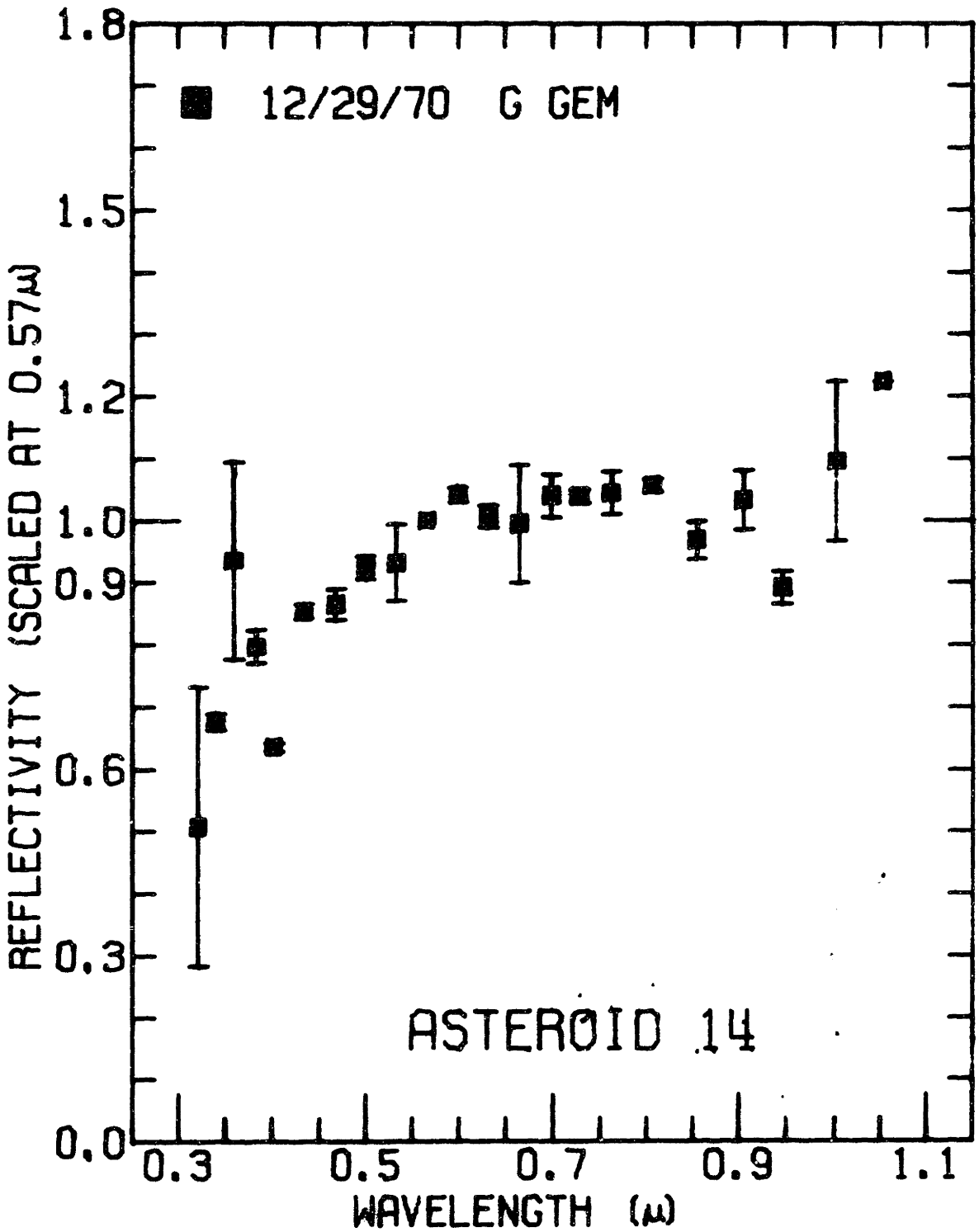
12/29/70 G GEM
ASTEROID 14
REFLECTIVITY (SCALED AT 0.57μ)
WAVELENGTH (μ)
1.8
1.5
1.2
1.0
0.9
0.6
0.3
0.0
0.3
0.5
0.7
0.9
1.1

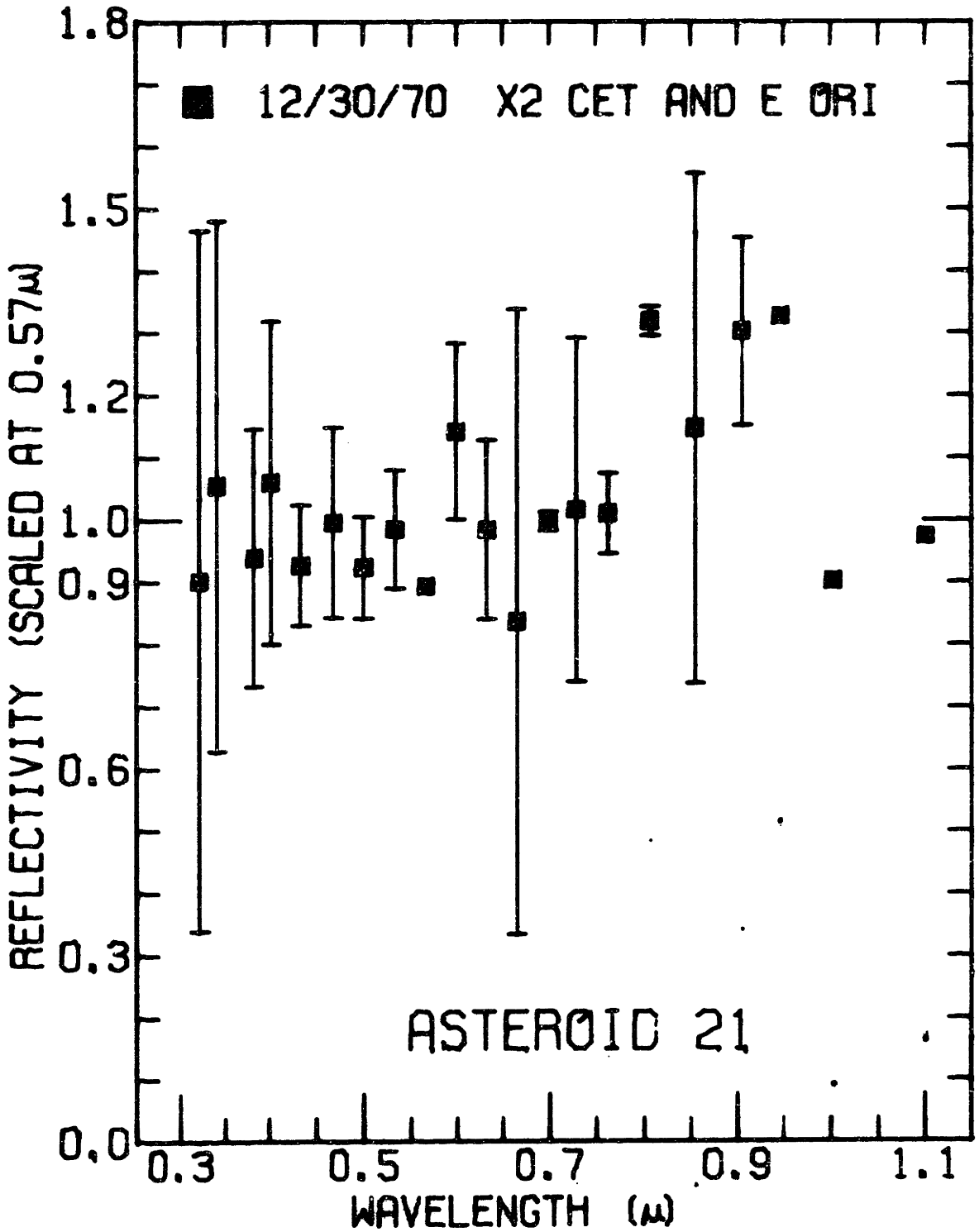
12/30/70 X2 CET AND E ORI
ASTEROID 21
REFLECTIVITY (SCALED AT 0.57μ)
WAVELENGTH (μ)
1.8
1.5
1.2
1.0
0.9
0.6
0.3
0.0
0.3
0.5
0.7
0.9
1.1

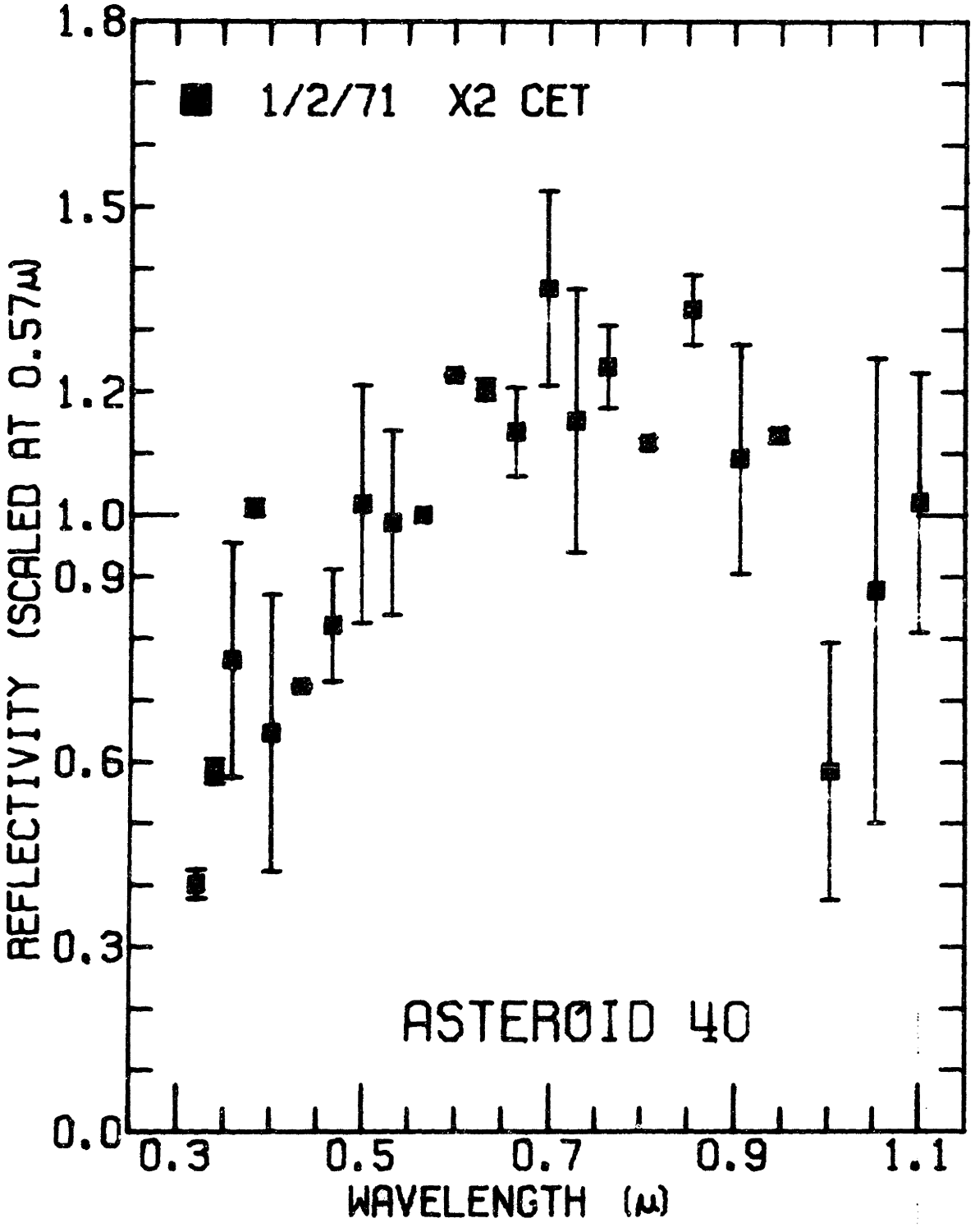
1/2/71 X2 CET
ASTEROID 40
REFLECTIVITY (SCALED AT 0.57μ)
WAVELENGTH (μ)
1.8
1.5
1.2
1.0
0.9
0.6
0.3
0.0
0.3
0.5
0.7
0.9
1.1

January 1971 60-inch run.

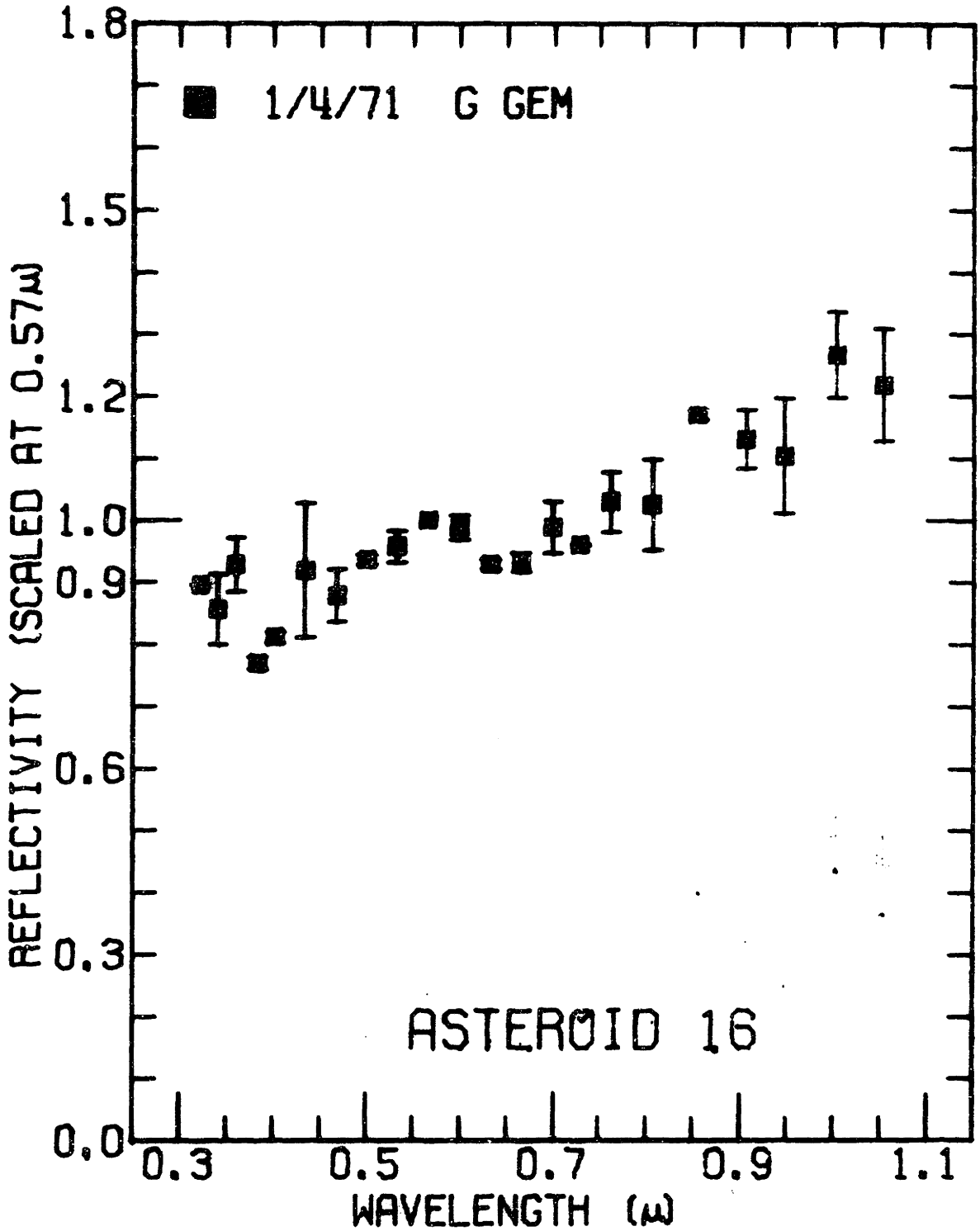
1/4/71 G GEM
ASTEROID 16
REFLECTIVITY (SCALED AT 0.57μ)
WAVELENGTH (μ)
1.8
1.5
1.2
1.0
0.9
0.6
0.3
0.0
0.3
0.5
0.7
0.9
1.1

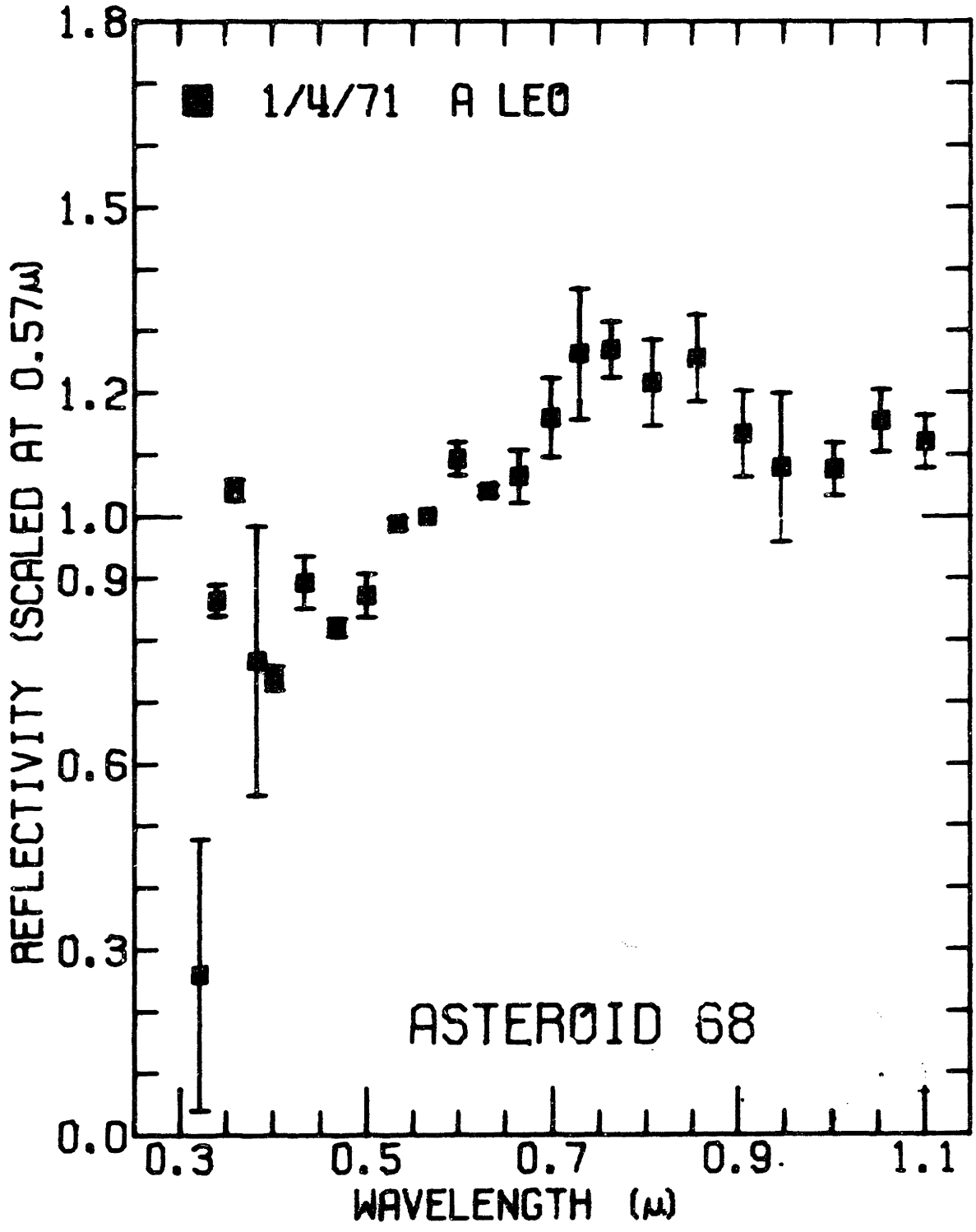
1/4/71 A LEO
ASTEROID 68
REFLECTIVITY (SCALED AT 0.57μ)
WAVELENGTH (μ)
1.8
1.5
1.2
1.0
0.9
0.6
0.3
0.0
0.3
0.5
0.7
0.9
1.1

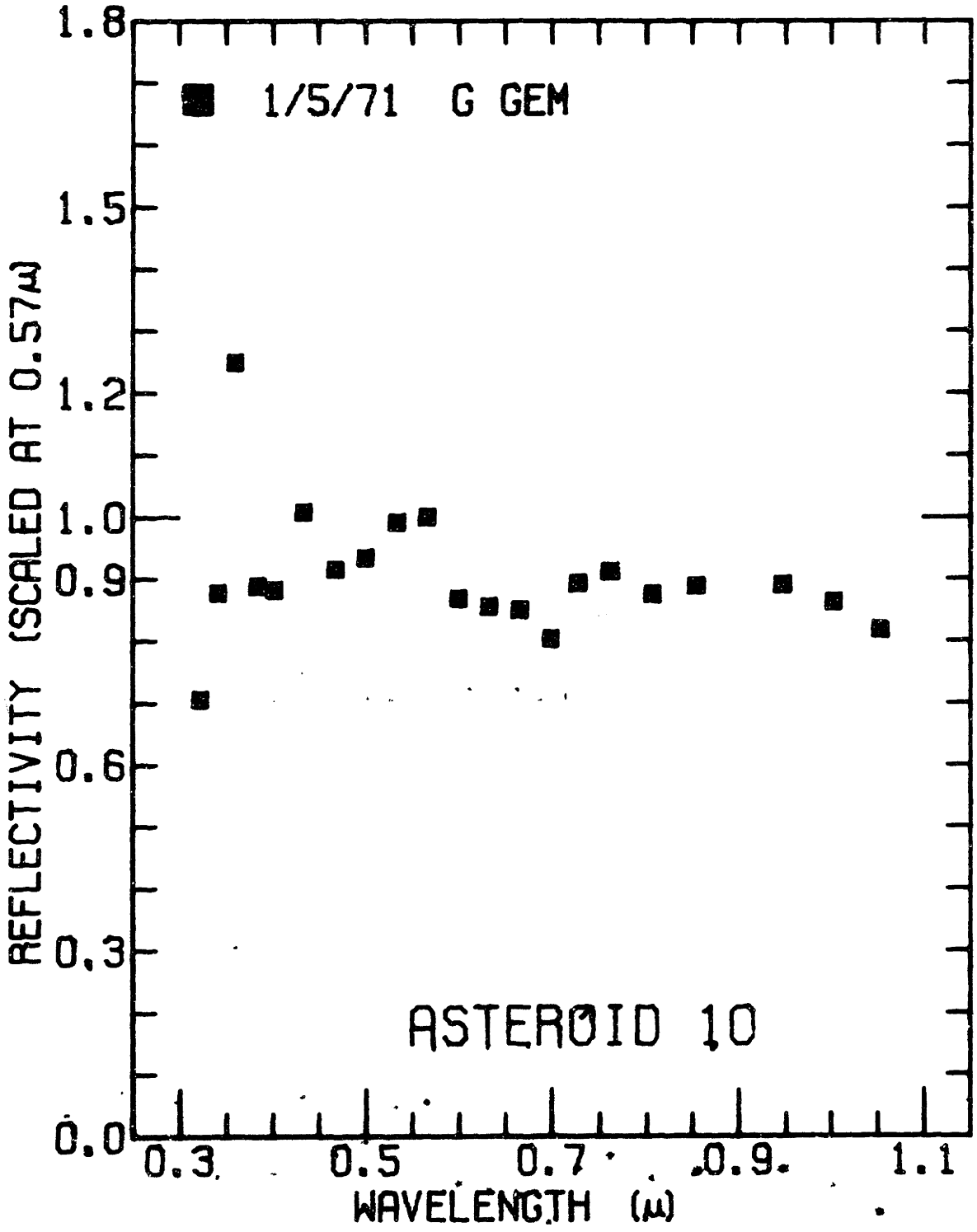
1/5/71 G GEM
ASTEROID 10
REFLECTIVITY (SCALED AT 0.57μ)
WAVELENGTH (μ)
1.8
1.5
1.2
1.0
0.9
0.6
0.3
0.0
0.3
0.5
0.7
0.9
1.1

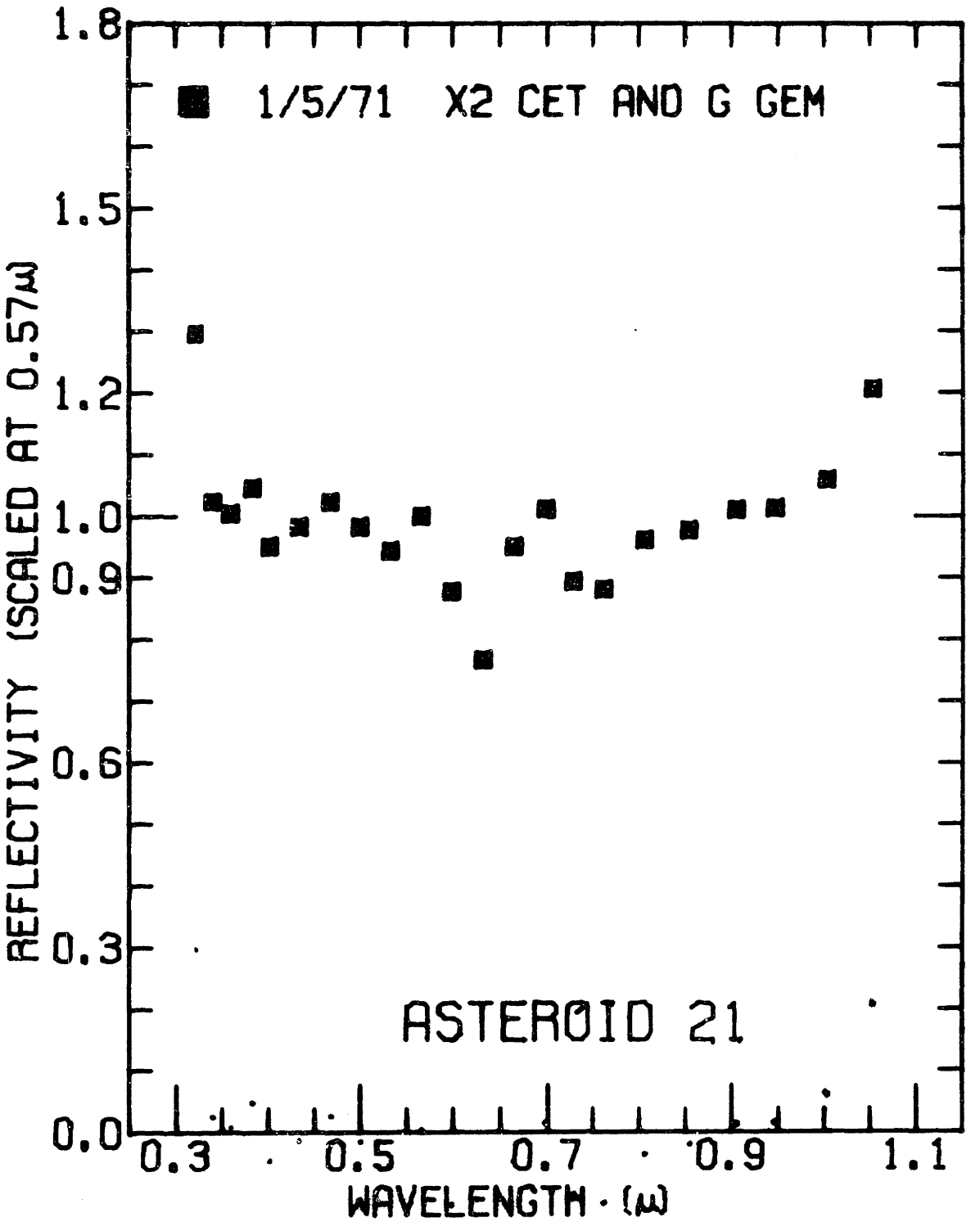
1/5/71 X2 CET AND G GEM
ASTEROID 21
REFLECTIVITY (SCALED AT 0.57μ)
WAVELENGTH · (μ)
1.8
1.5
1.2
1.0
0.9
0.6
0.3
0.0
0.3
0.5
0.7
0.9
1.1

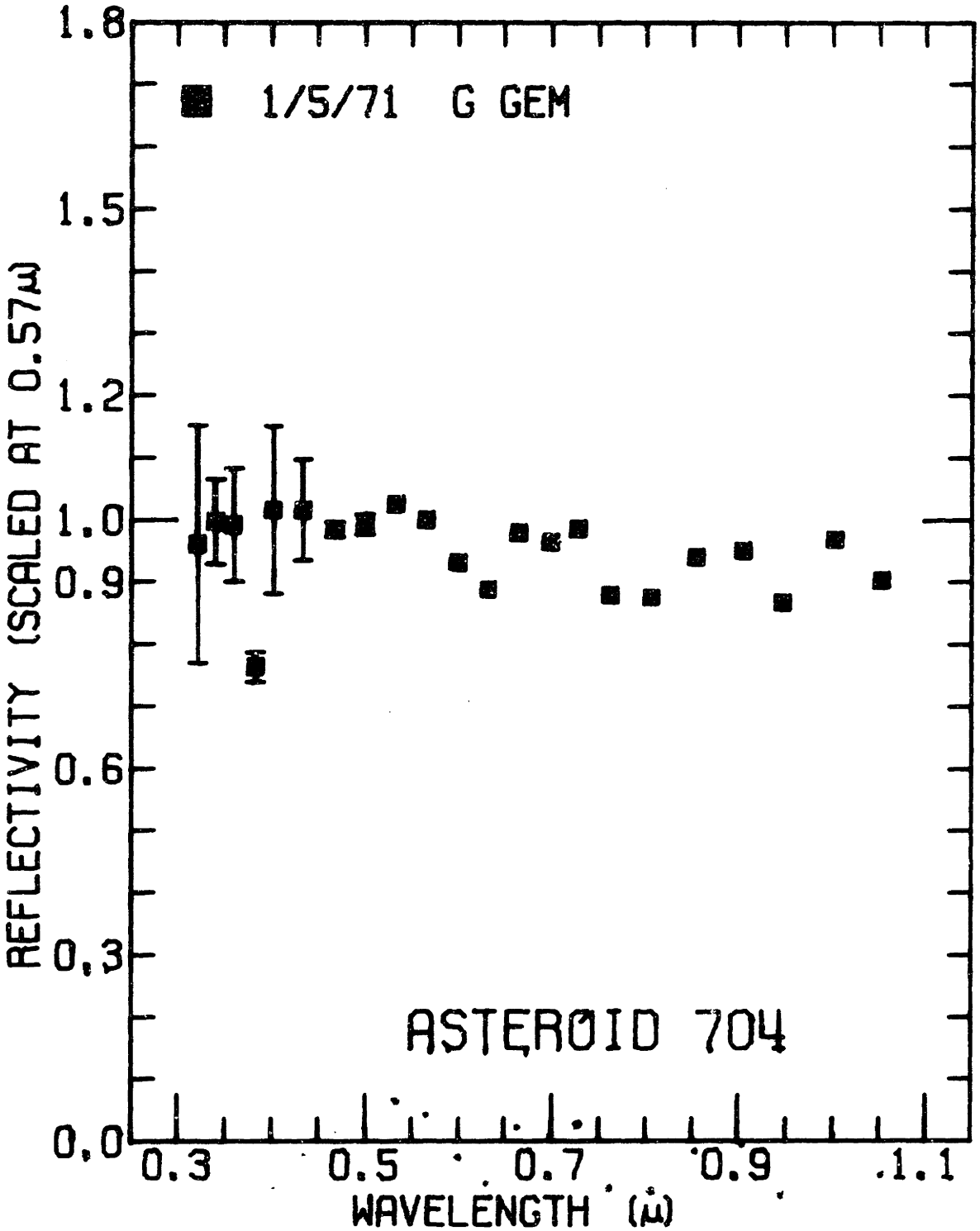
1/5/71 G GEM
ASTEROID 704
REFLECTIVITY (SCALED AT 0.57μ)
WAVELENGTH (μ)
1.8
1.5
1.2
1.0
0.9
0.6
0.3
0.0
0.3
0.5
0.7
0.9
1.1

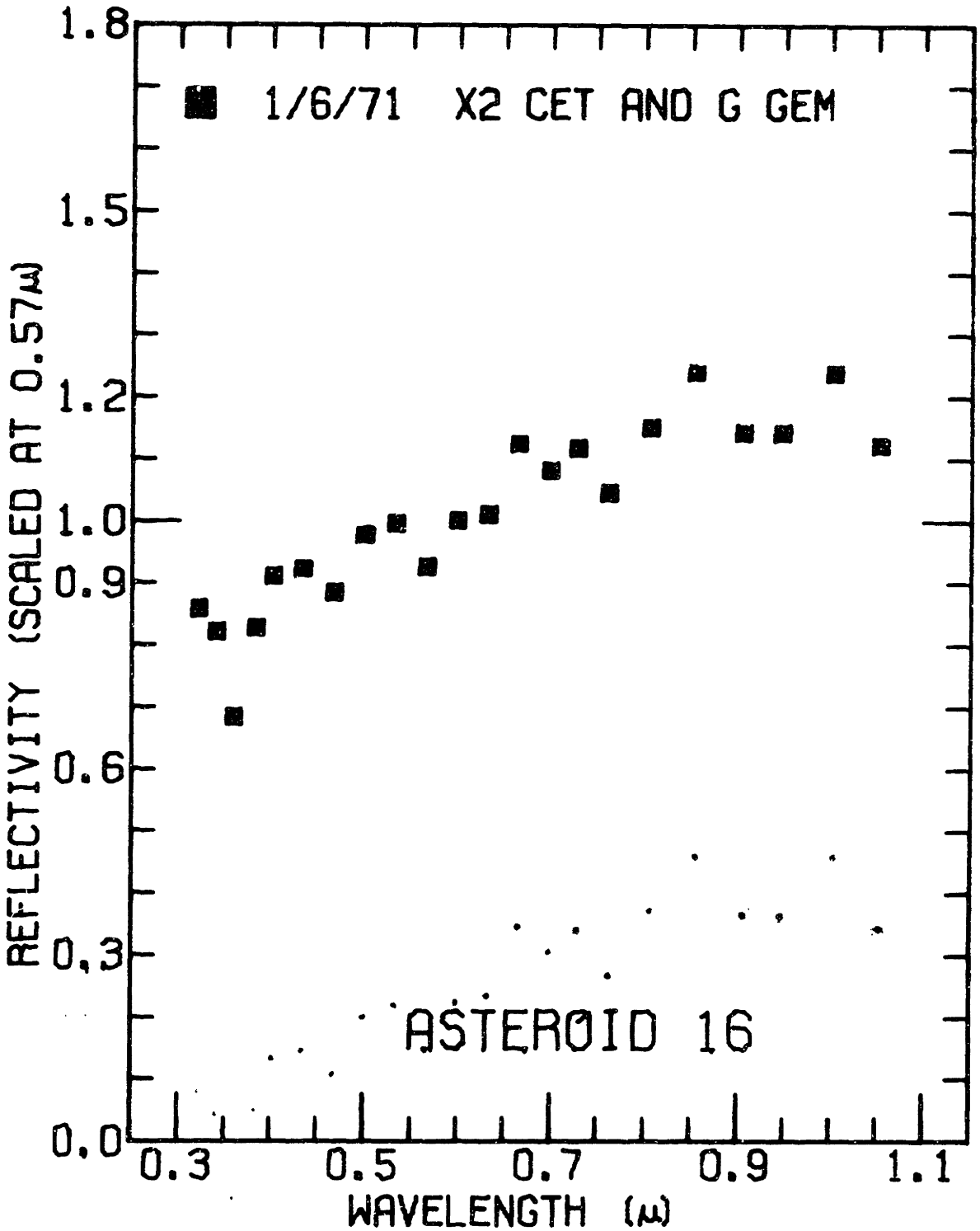
1/6/71 X2 CET AND G GEM
ASTEROID 16
REFLECTIVITY (SCALED AT 0.57μ)
WAVELENGTH (μ)
1.8
1.5
1.2
1.0
0.9
0.6
0.3
0.0
0.3
0.5
0.7
0.9
1.1

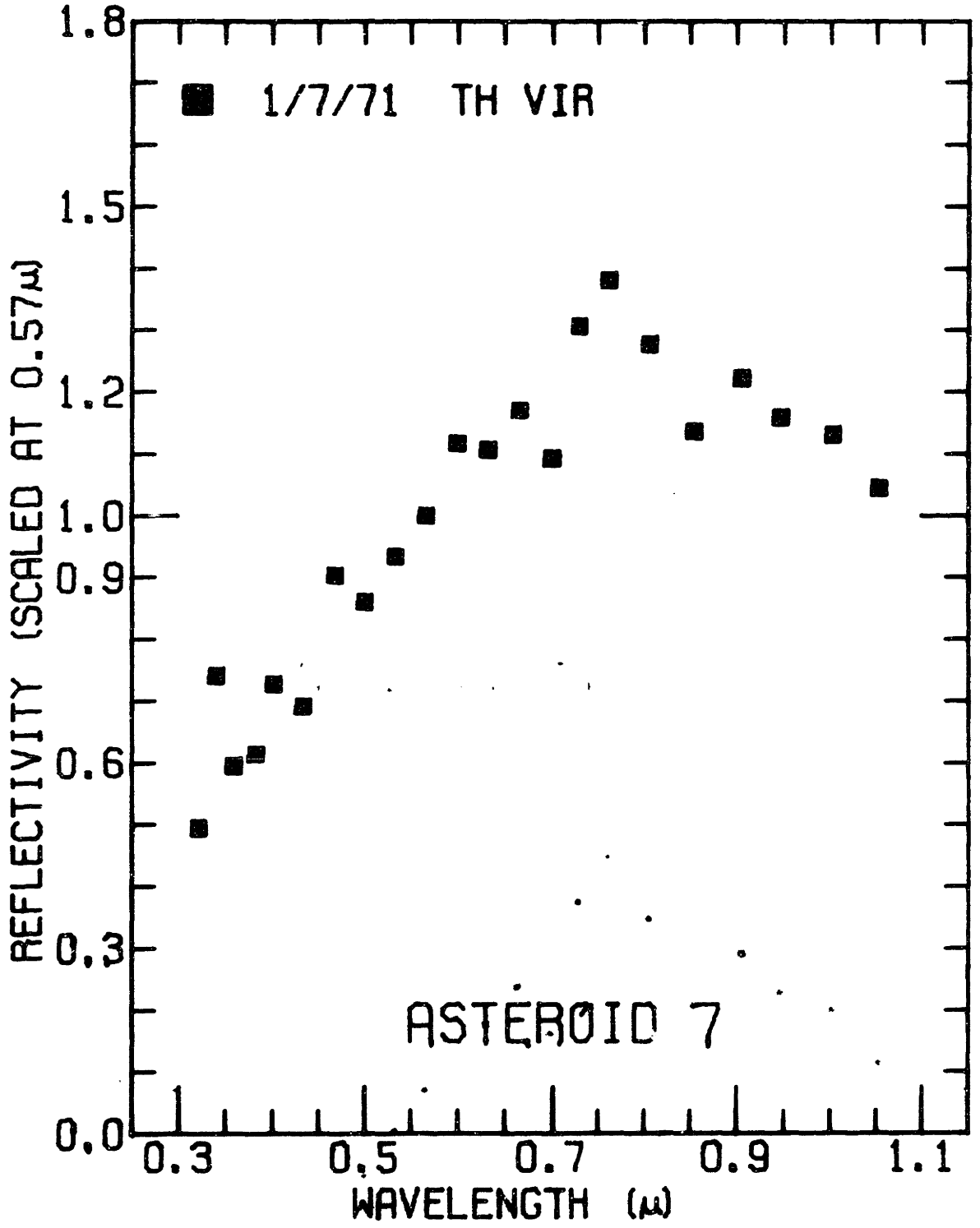
1/7/71 TH VIR
ASTEROID 7
REFLECTIVITY (SCALED AT 0.57μ)
WAVELENGTH (μ)
1.8
1.5
1.2
1.0
0.9
0.6
0.3
0.0
0.3
0.5
0.7
0.9
1.1

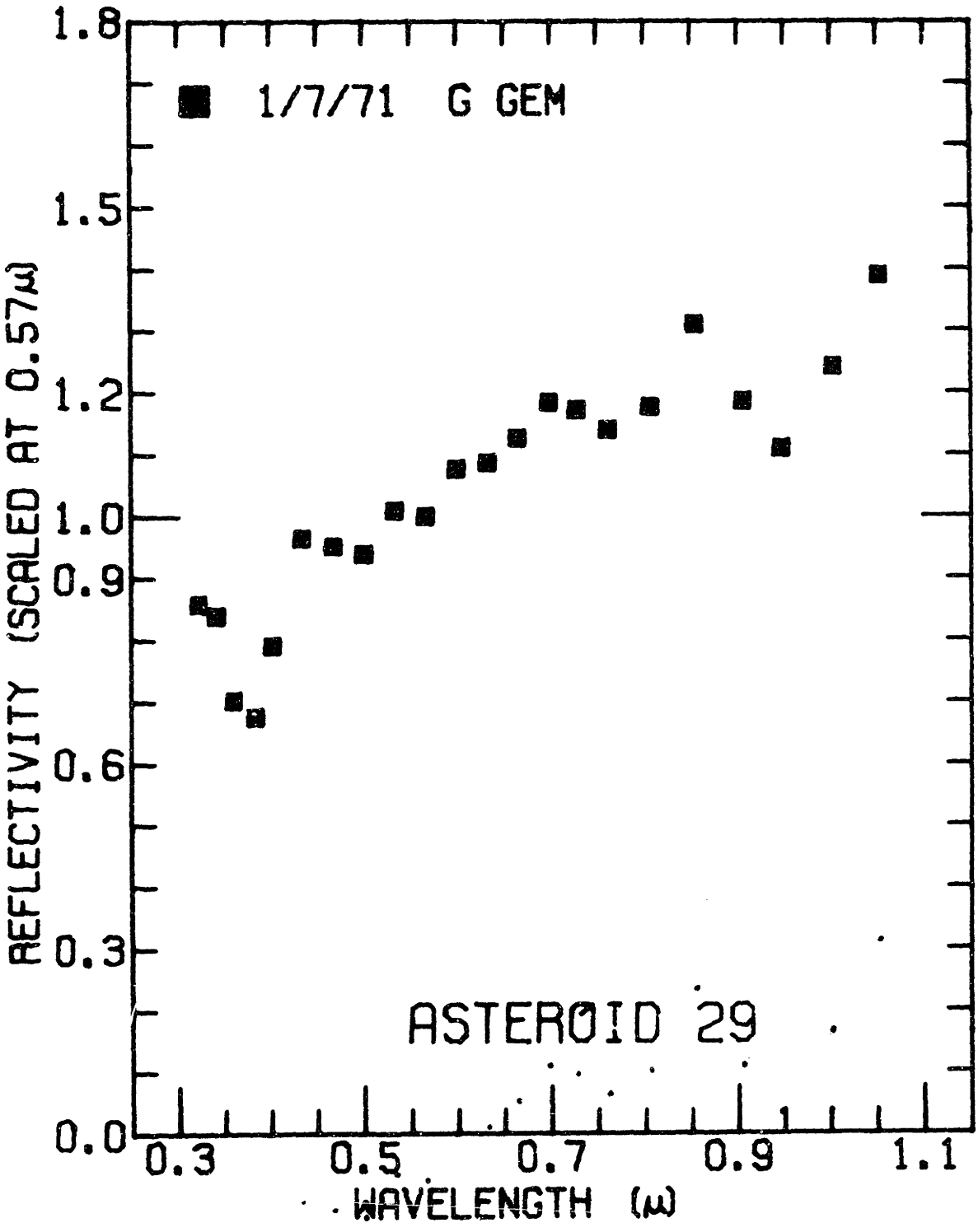
1/7/71 G GEM
ASTEROID 29
REFLECTIVITY (SCALED AT 0.57μ)
WAVELENGTH (μ)
1.8
1.5
1.2
1.0
0.9
0.6
0.3
0.0
0.3
0.5
0.7
0.9
1.1

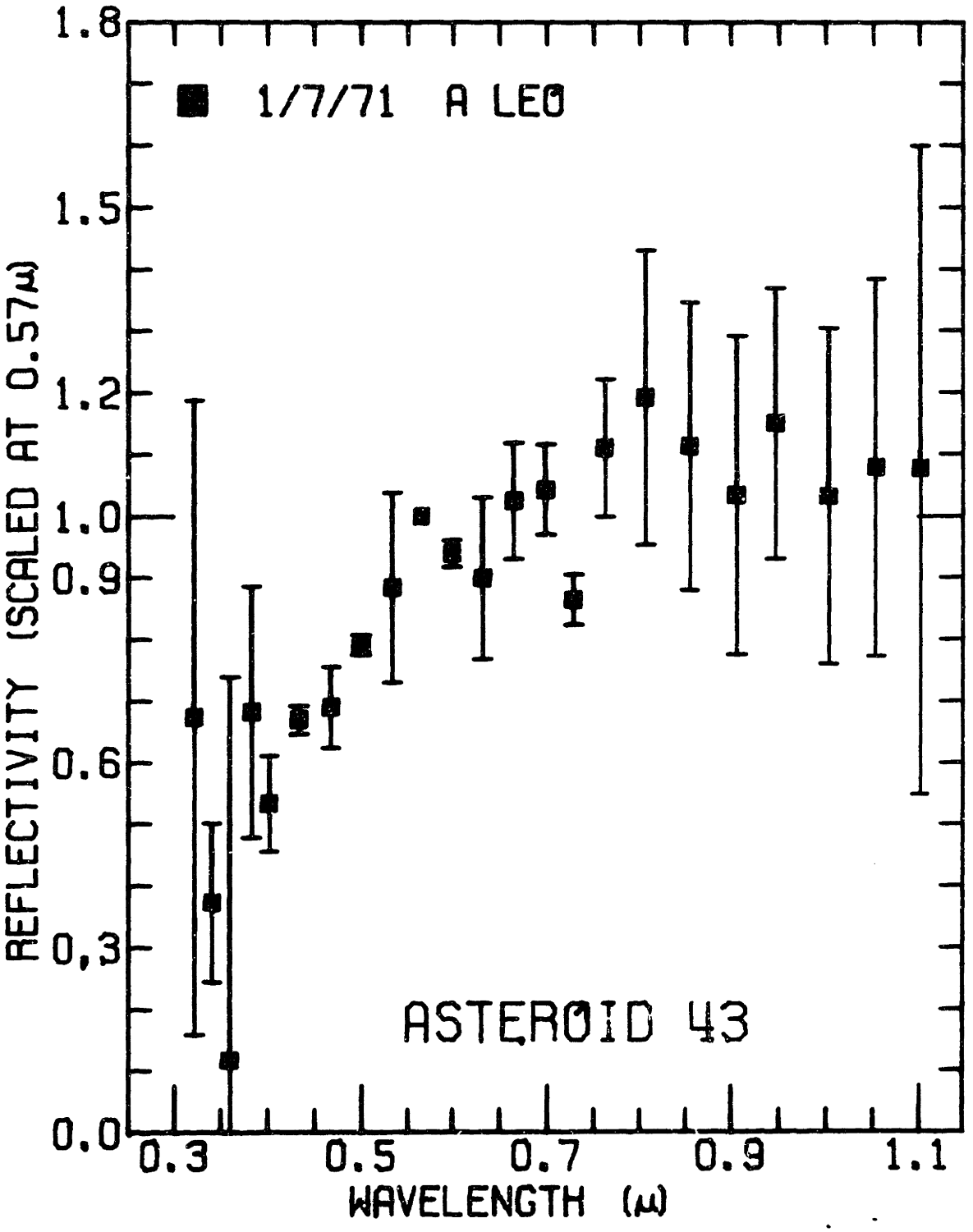
1/7/71 A LEO
ASTEROID 43
REFLECTIVITY (SCALED AT 0.57μ)
WAVELENGTH (μ)
1.8
1.5
1.2
1.0
0.9
0.6
0.3
0.0
0.3
0.5
0.7
0.9
1.1

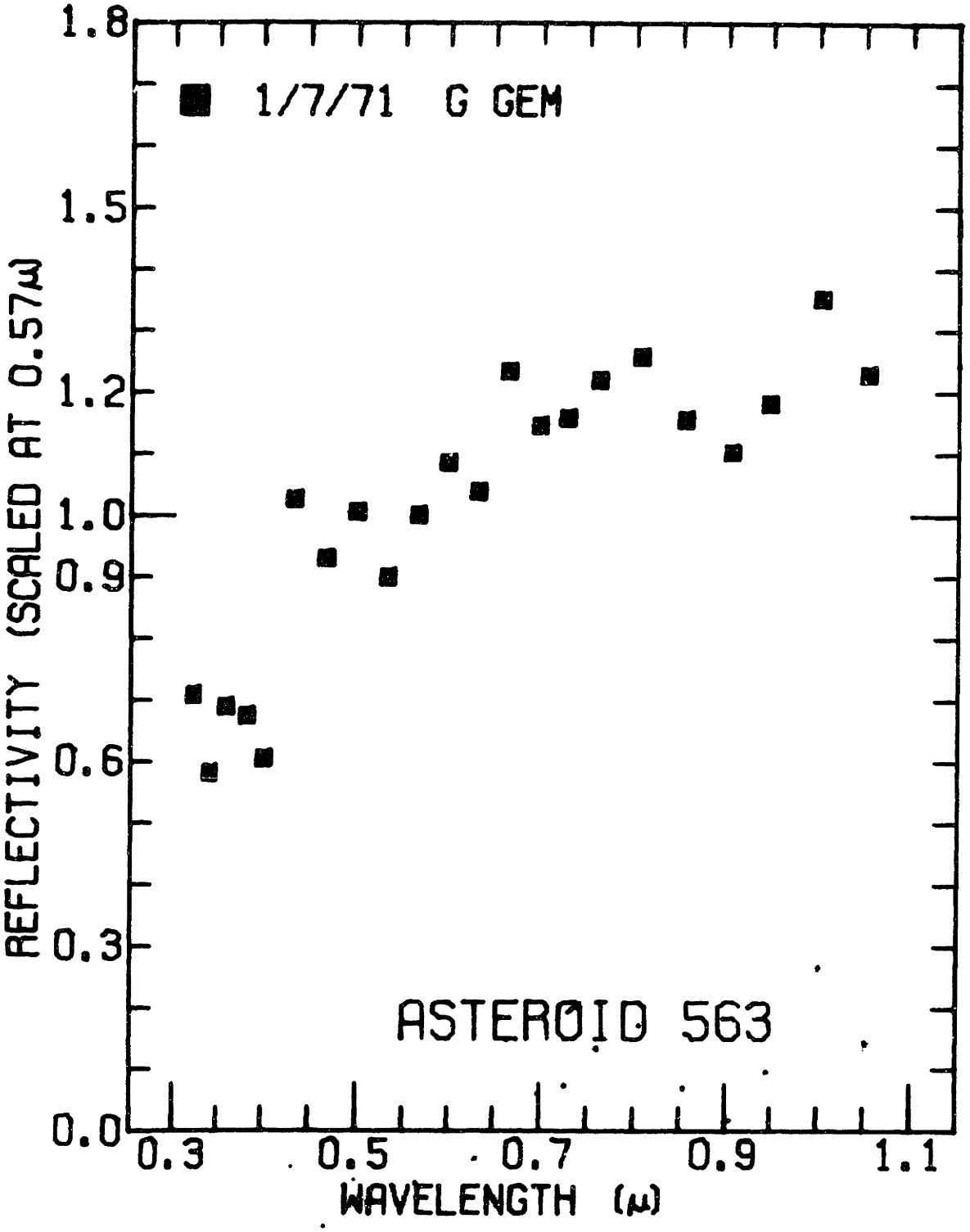
1/7/71 G GEM
ASTEROID 563
REFLECTIVITY (SCALED AT 0.57μ)
WAVELENGTH (μ)
1.8
1.5
1.2
1.0
0.9
0.6
0.3
0.0
0.3
0.5
0.7
0.9
1.1

February 1971 run.

(1) S-1 photomultiplier

(2) S-20 photomultiplier, no ND filter

(3) S-20 photomultiplier, ND filter

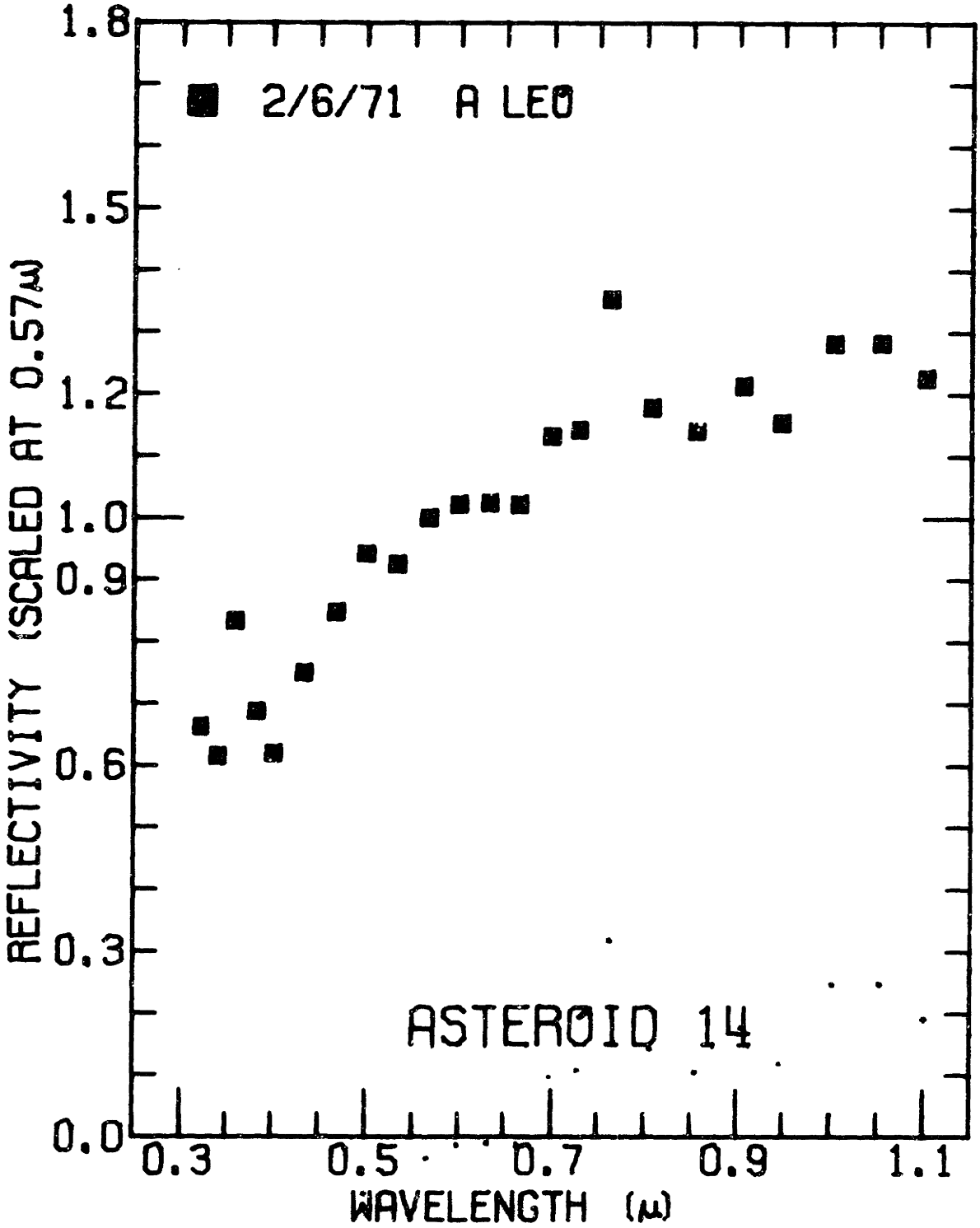
2/6/71 A LEO
ASTEROID 14
REFLECTIVITY (SCALED AT 0.57μ)
WAVELENGTH (μ)
1.8
1.5
1.2
1.0
0.9
0.6
0.3
0.0
0.3
0.5
0.7
0.9
1.1

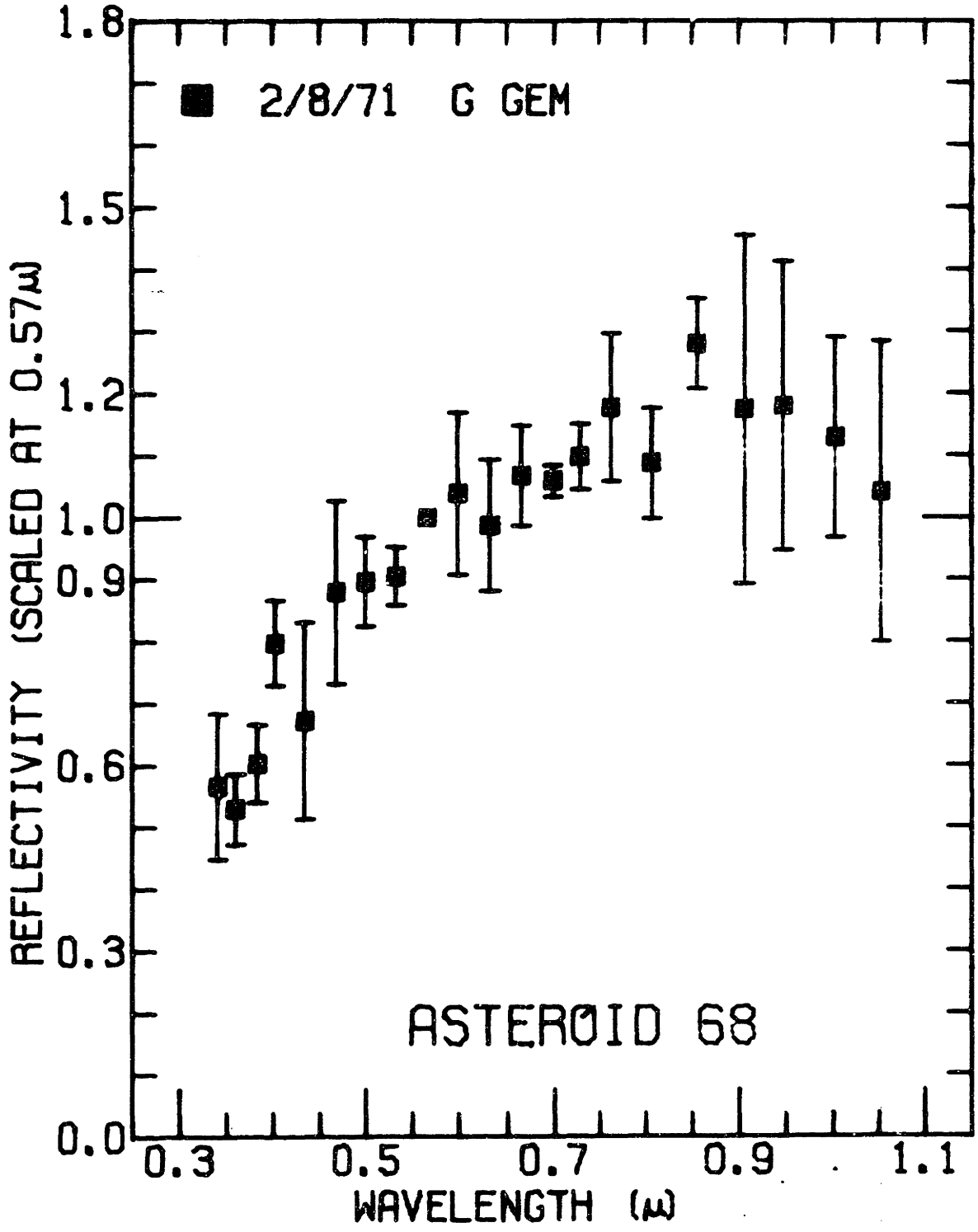
2/8/71 G GEM
ASTEROID 68
REFLECTIVITY (SCALED AT 0.57μ)
WAVELENGTH (μ)
1.8
1.5
1.2
1.0
0.9
0.6
0.3
0.0
0.3
0.5
0.7
0.9
1.1

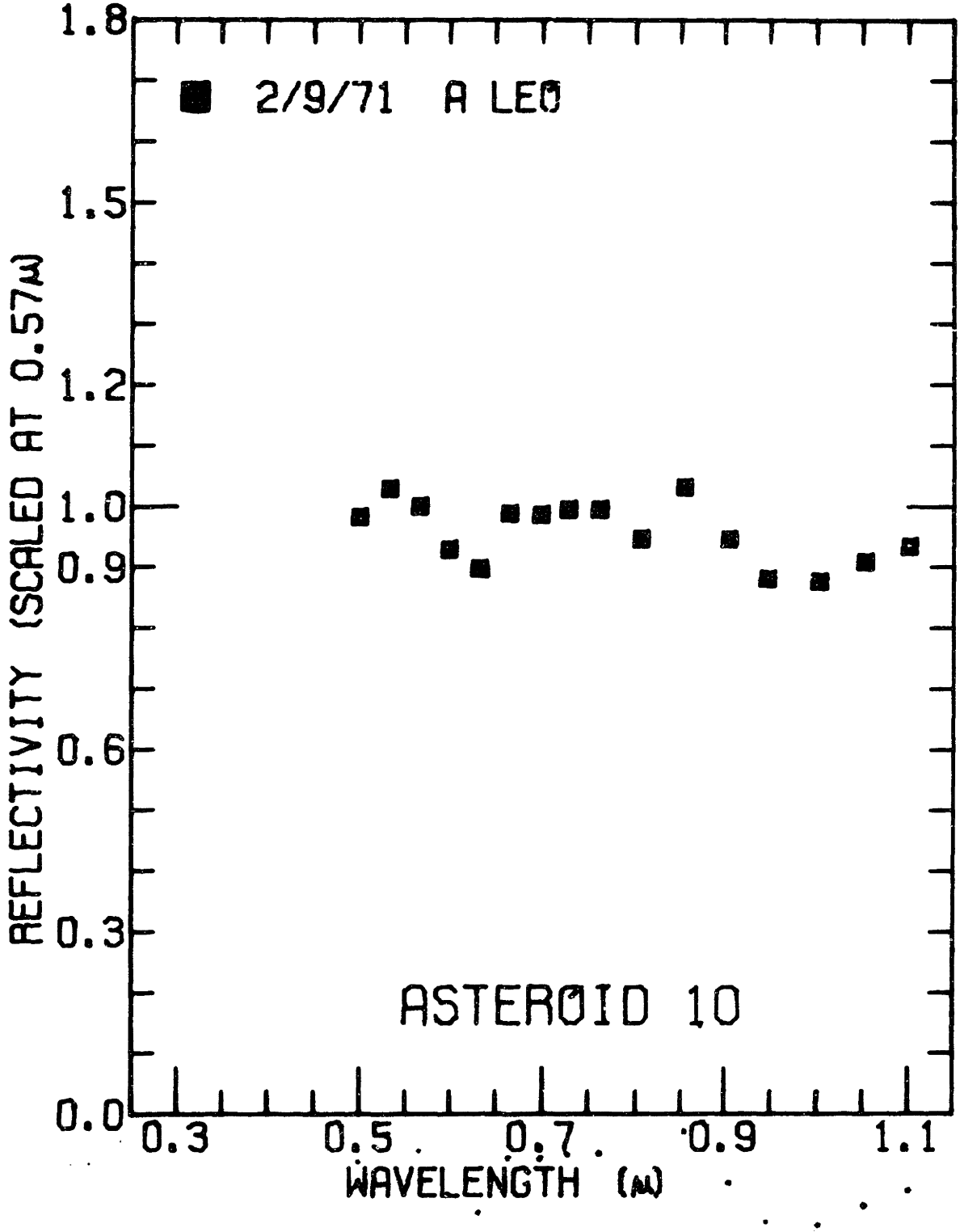
2/9/71 A LEO
ASTEROID 10
REFLECTIVITY (SCALED AT 0.57μ)
WAVELENGTH (μ)
1.8
1.5
1.2
1.0
0.9
0.6
0.3
0.0
0.3
0.5
0.7
0.9
1.1

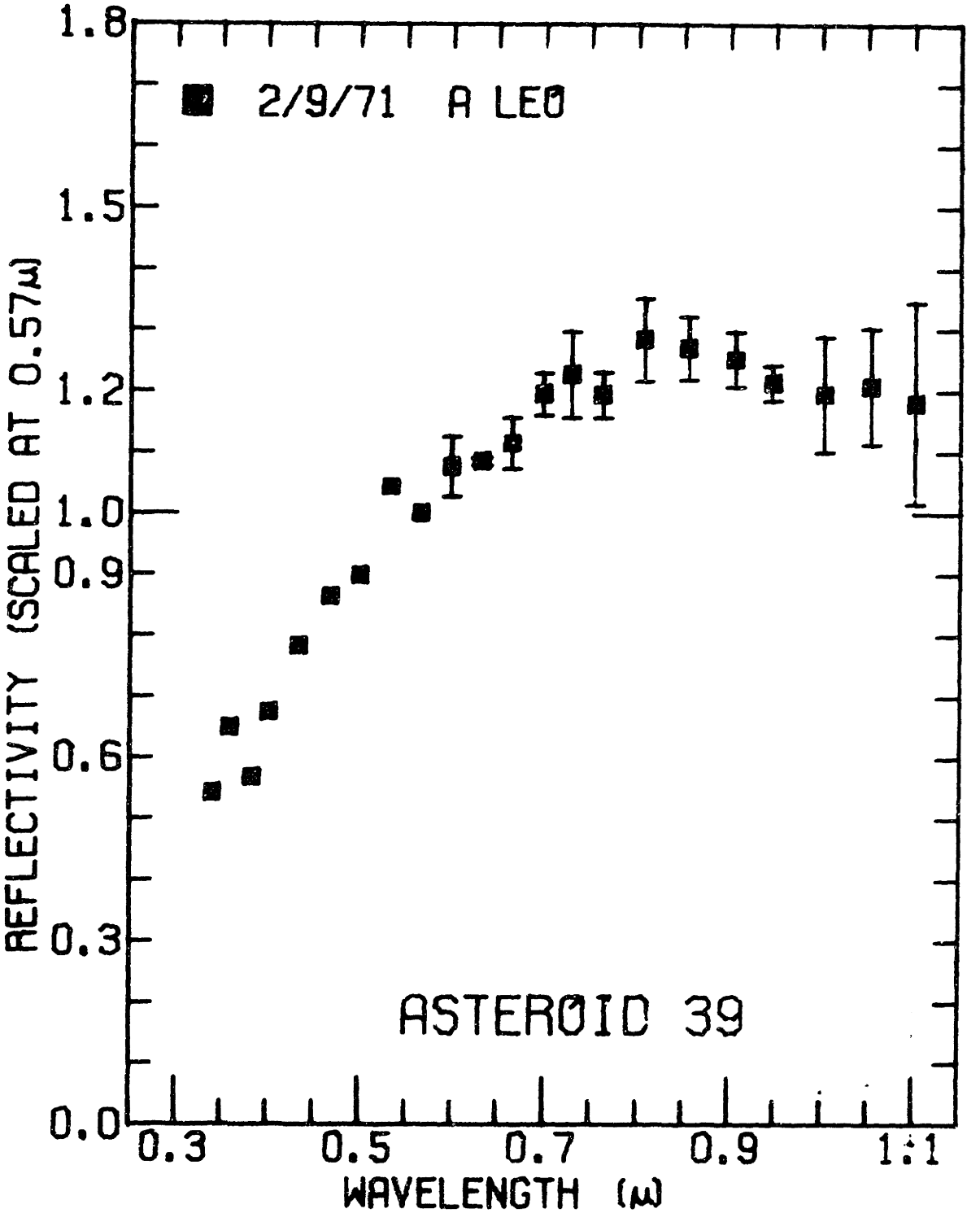
2/9/71 A LEO
ASTEROID 39
REFLECTIVITY (SCALED AT 0.57μ)
WAVELENGTH (μ)
1.8
1.5
1.2
1.0
0.9
0.6
0.3
0.0
0.3
0.5
0.7
0.9
1.1

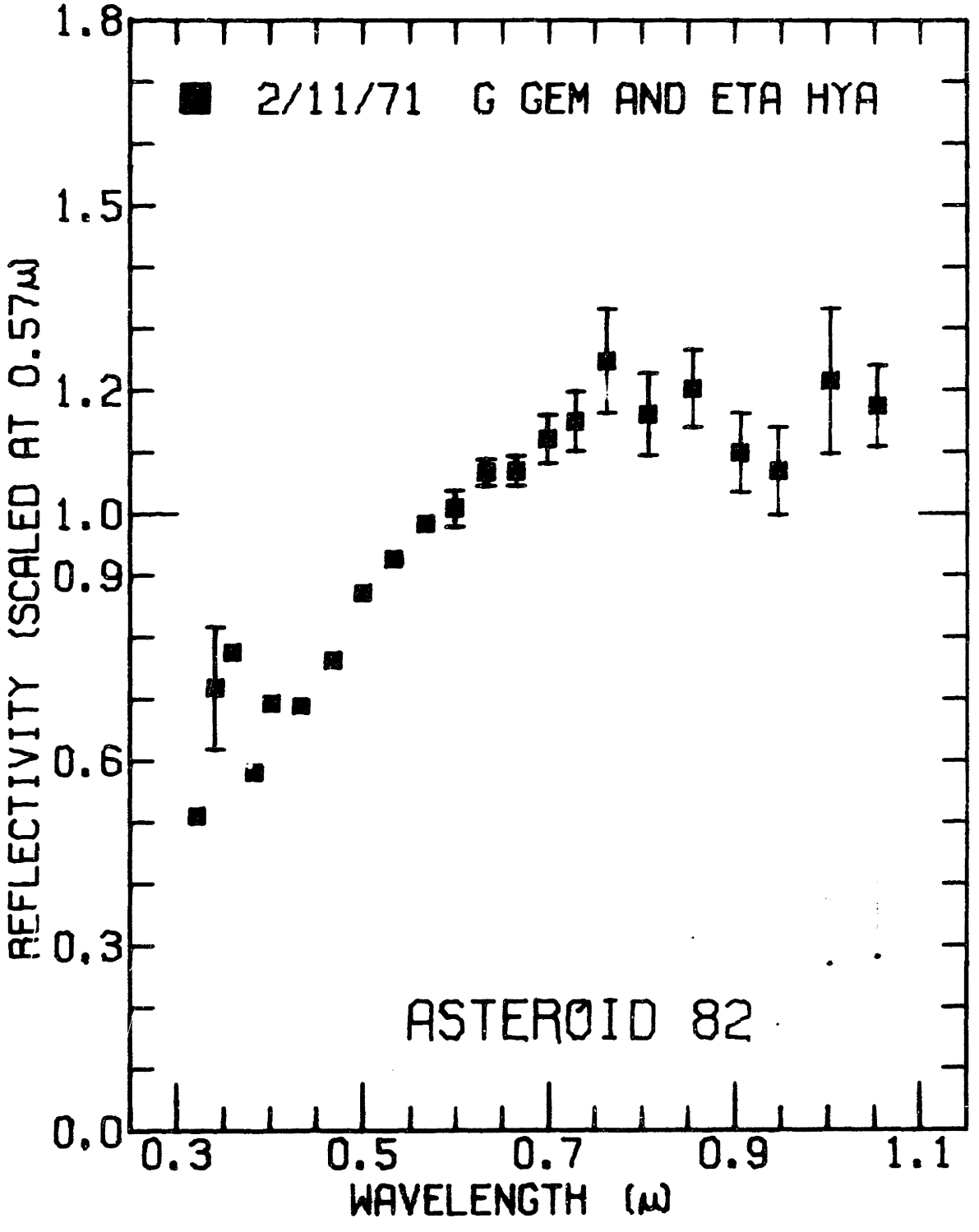
2/11/71 G GEM AND ETA HYA
ASTEROID 82
REFLECTIVITY (SCALED AT 0.57μ)
WAVELENGTH (μ)
1.8
1.5
1.2
1.0
0.9
0.6
0.3
0.0
0.3
0.5
0.7
0.9
1.1

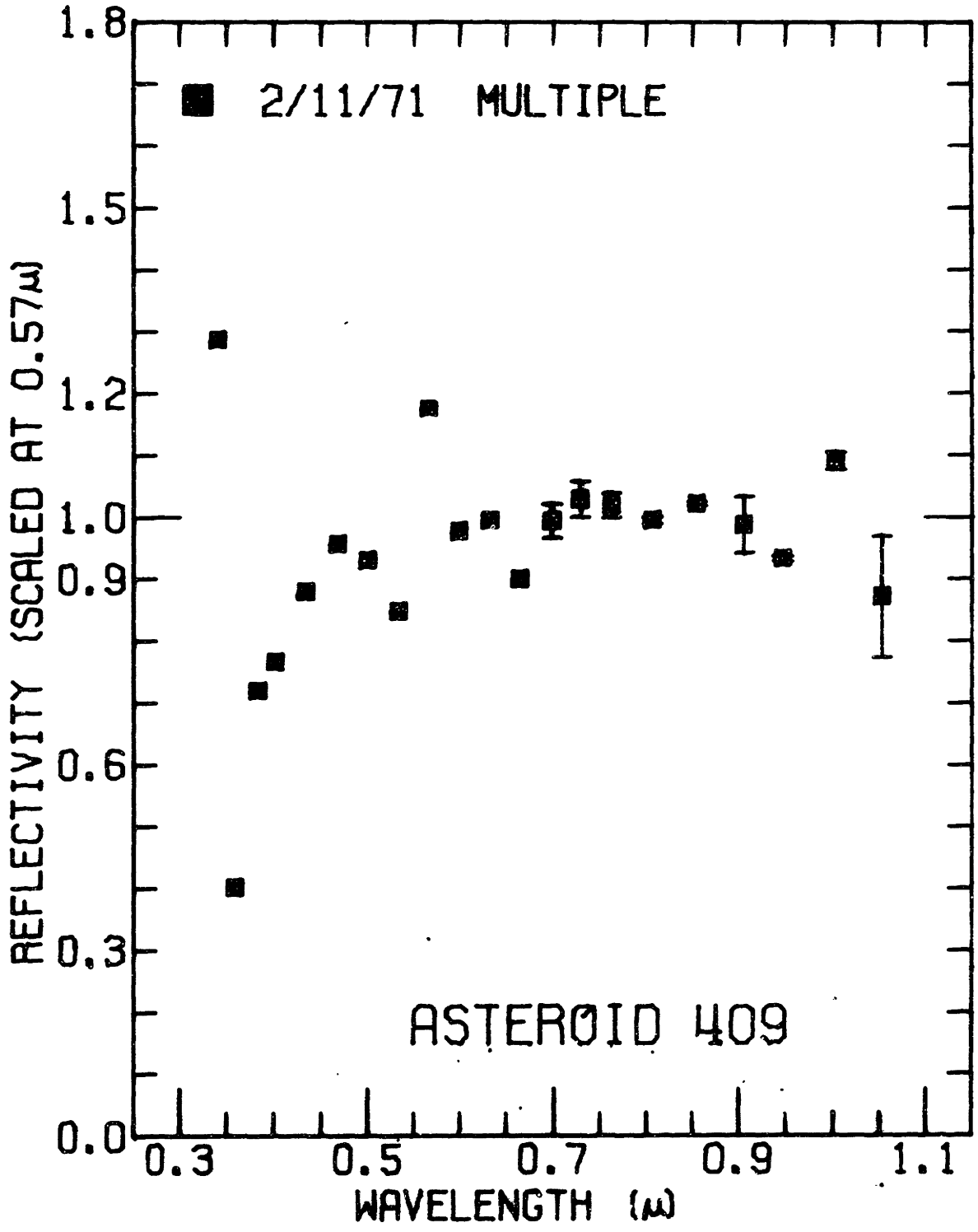
2/11/71 MULTIPLE
ASTEROID 409
REFLECTIVITY (SCALED AT 0.57μ)
WAVELENGTH (μ)
1.8
1.5
1.2
1.0
0.9
0.6
0.3
0.0
0.3
0.5
0.7
0.9
1.1

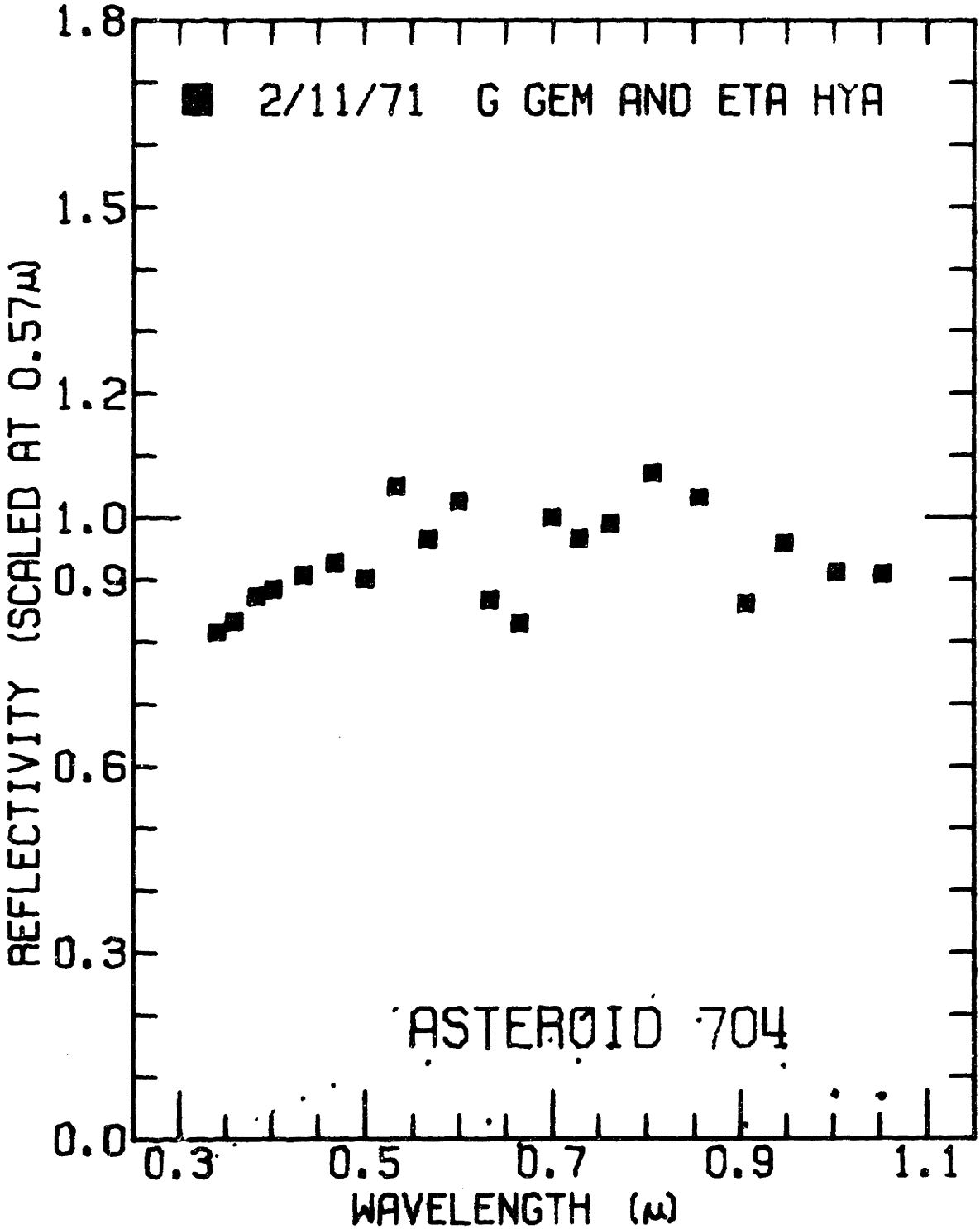
2/11/71 G GEM AND ETA HYA
ASTEROID 704
REFLECTIVITY (SCALED AT 0.57μ)
WAVELENGTH (μ)
1.8
1.5
1.2
1.0
0.9
0.6
0.3
0.0
0.3
0.5
0.7
0.9
1.1

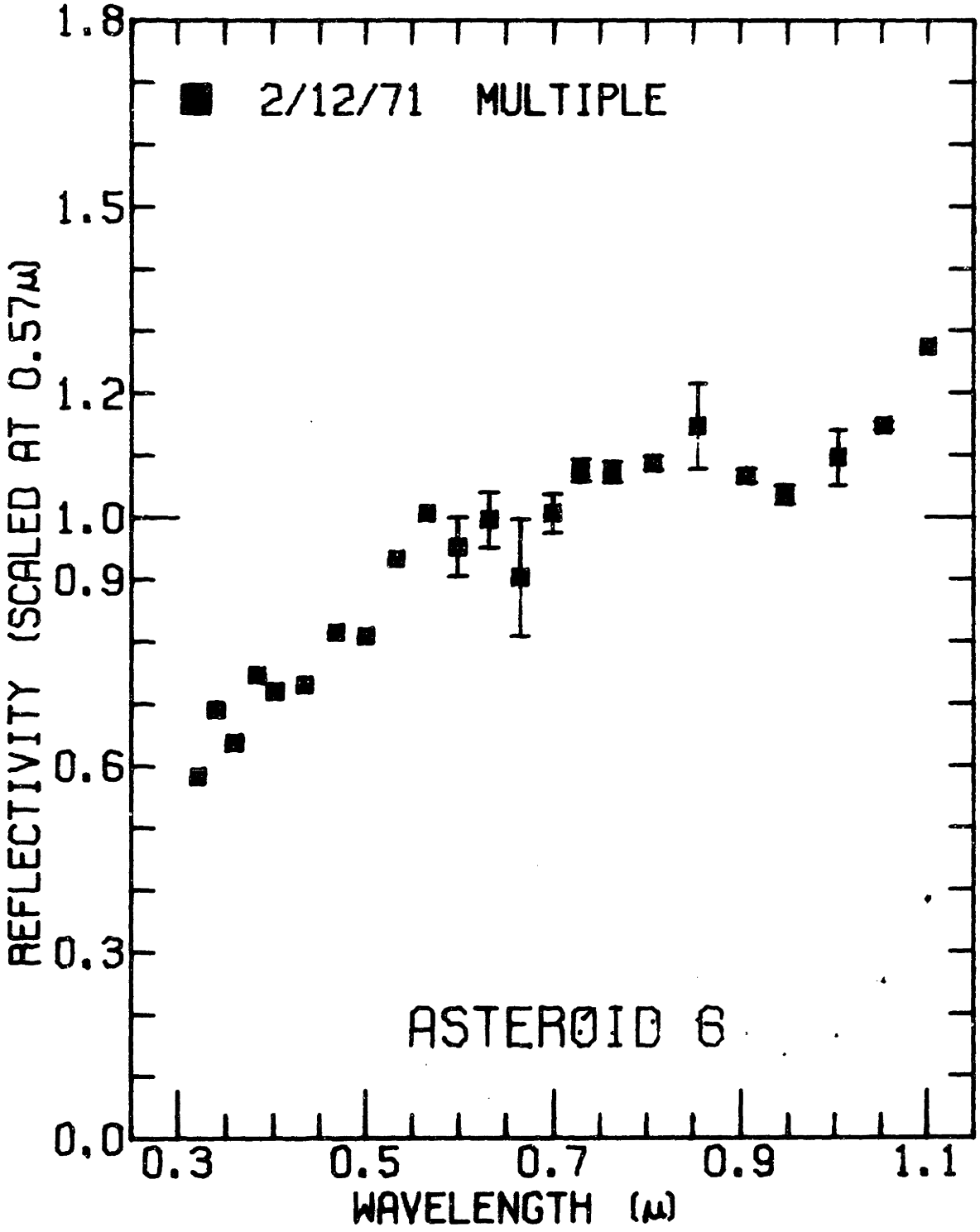
2/12/71 MULTIPLE
ASTEROID 6
REFLECTIVITY (SCALED AT 0.57μ)
WAVELENGTH (μ)
1.8
1.5
1.2
1.0
0.9
0.6
0.3
0.0
0.3
0.5
0.7
0.9
1.1

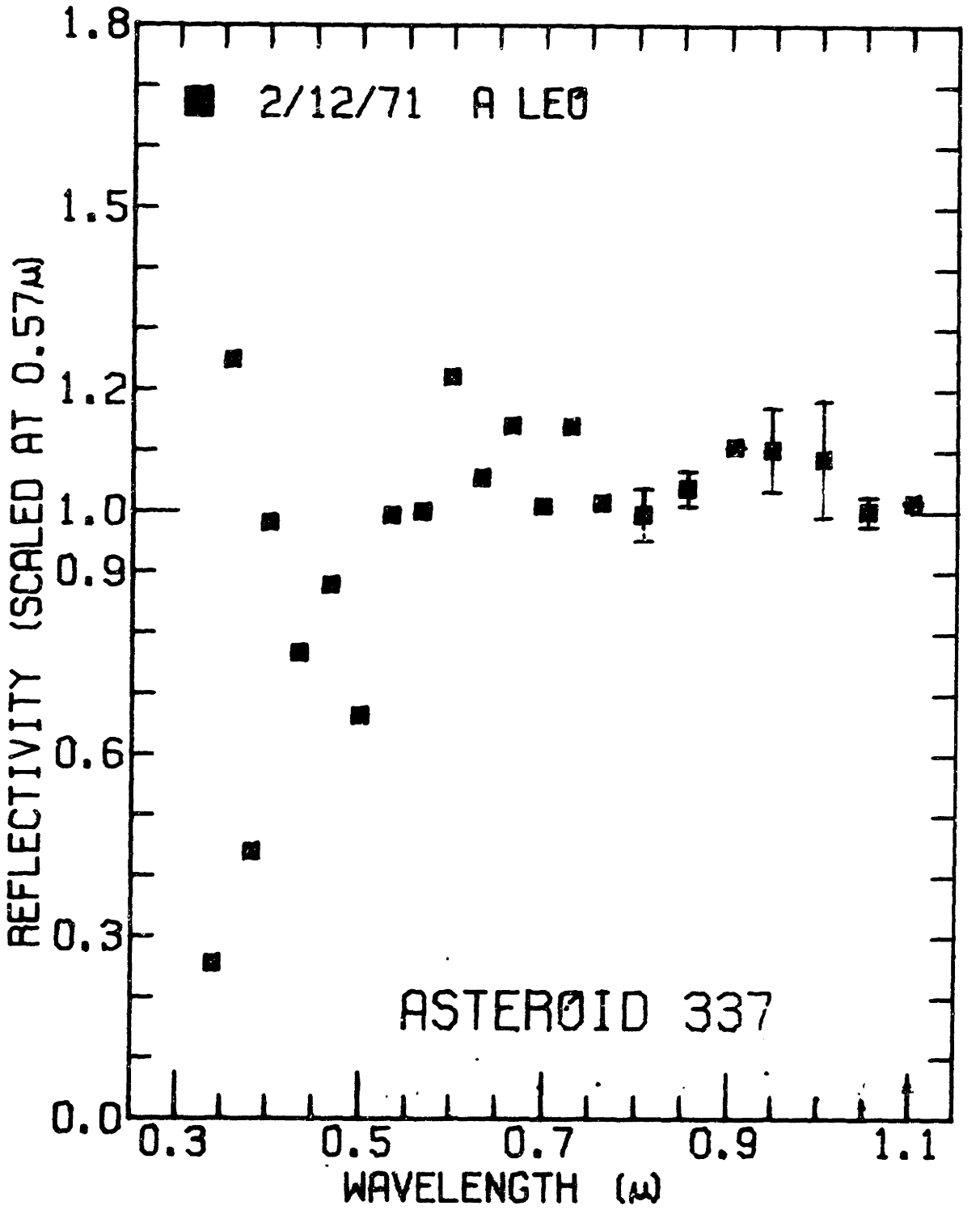
2/12/71 A LEO
ASTEROID 337
REFLECTIVITY (SCALED AT 0.57μ)
WAVELENGTH (μ)
1.8
1.5
1.2
1.0
0.9
0.6
0.3
0.0
0.3
0.5
0.7
0.9
1.1

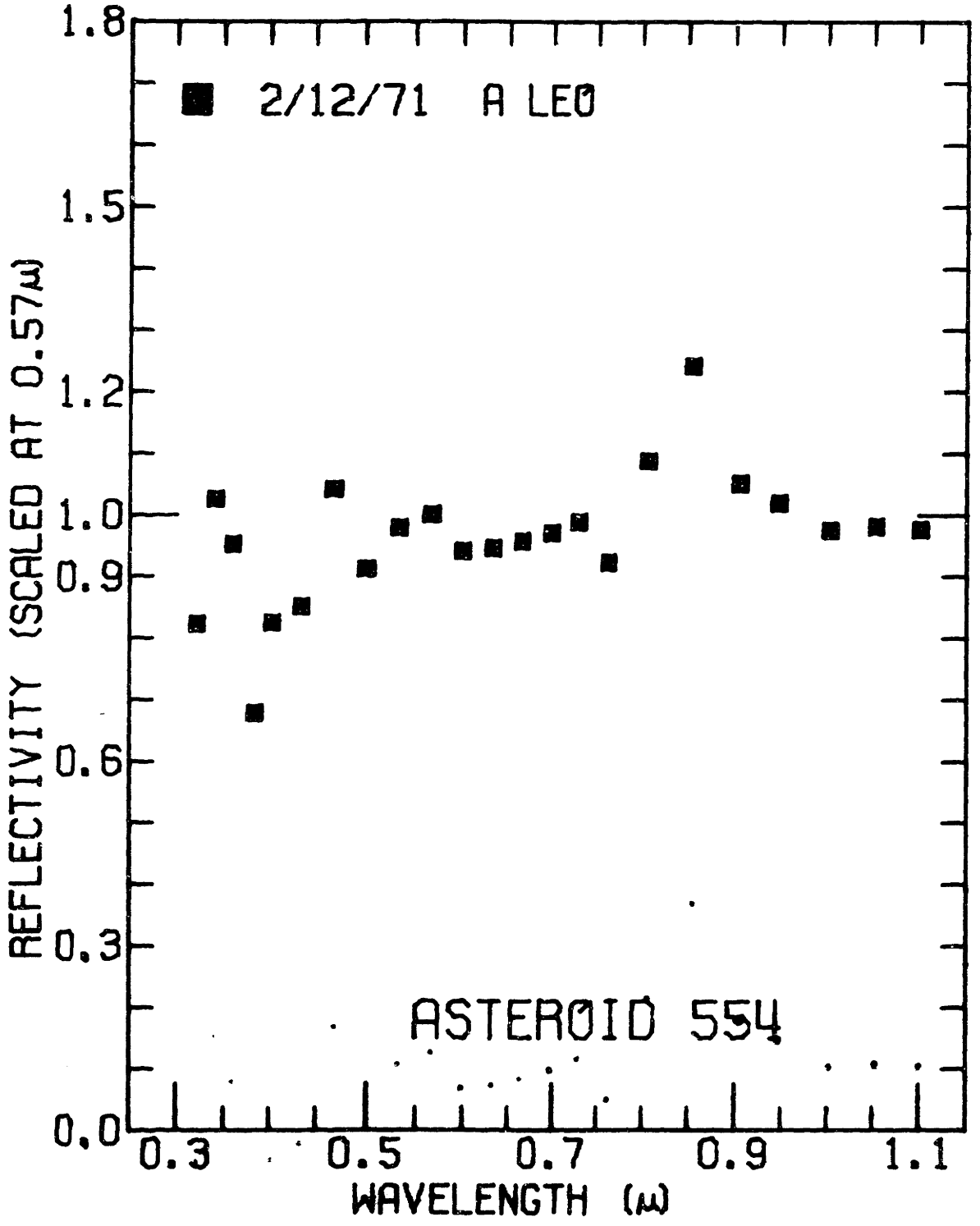
2/12/71 A LEO
ASTEROID 554
REFLECTIVITY (SCALED AT 0.57μ)
WAVELENGTH (μ)
1.8
1.5
1.2
1.0
0.9
0.6
0.3
0.0
0.3
0.5
0.7
0.9
1.1

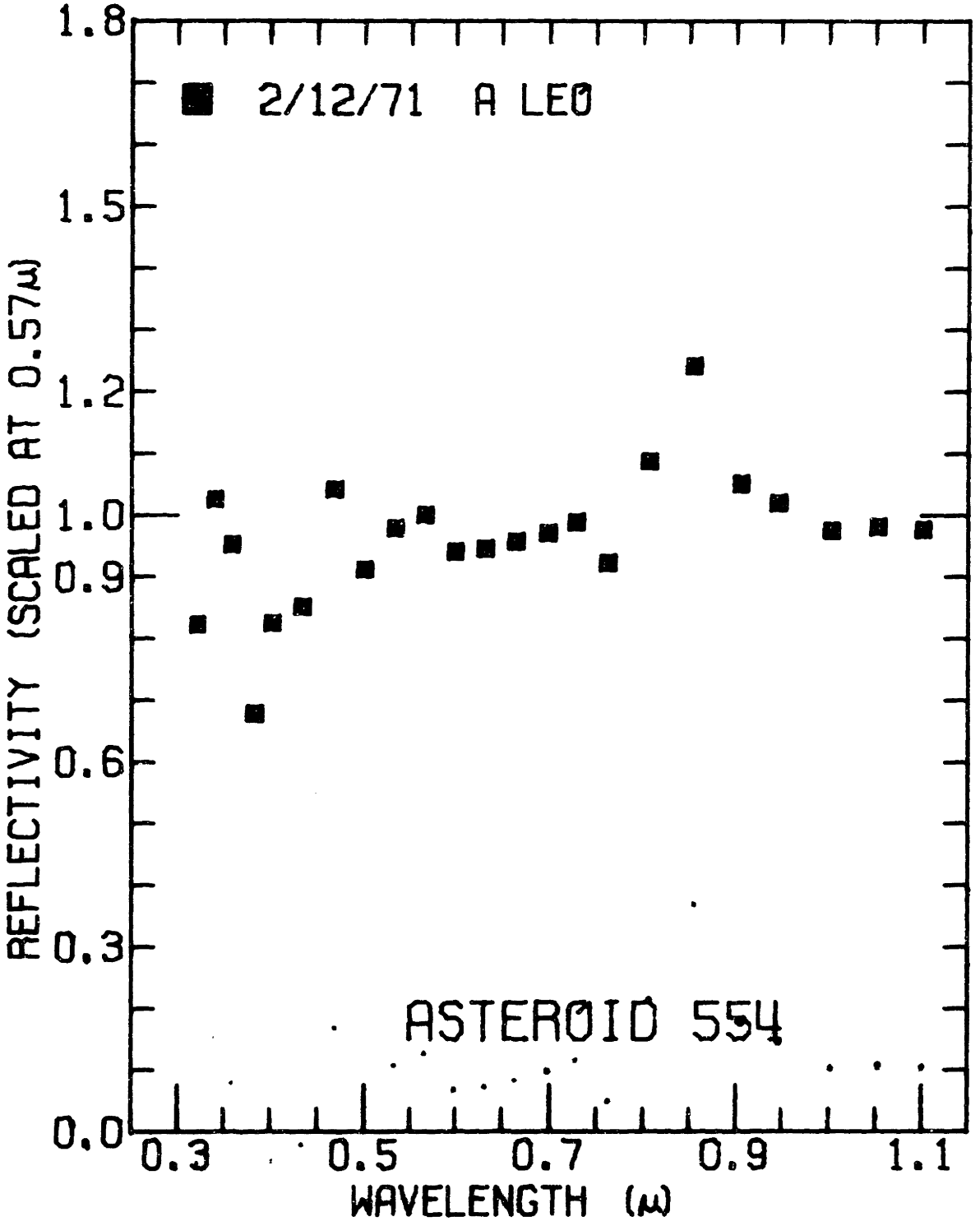
2/12/71 A LEO
ASTEROID 554
REFLECTIVITY (SCALED AT 0.57μ)
WAVELENGTH (μ)
1.8
1.5
1.2
1.0
0.9
0.6
0.3
0.0
0.3
0.5
0.7
0.9
1.1

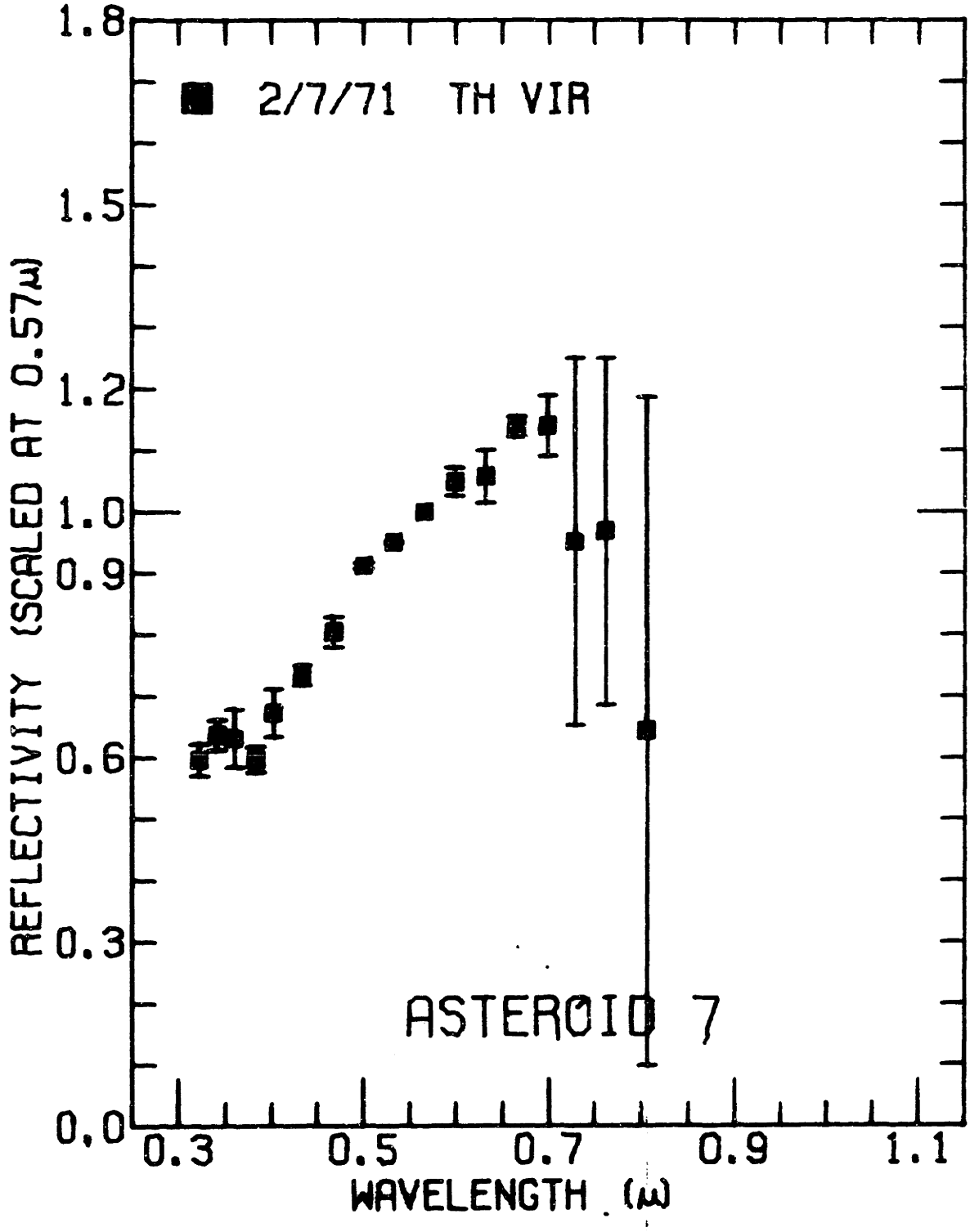
2/7/71 TH VIR
ASTEROID 7
REFLECTIVITY (SCALED AT 0.57μ)
WAVELENGTH (μ)
1.8
1.5
1.2
1.0
0.9
0.6
0.3
0.0
0.3
0.5
0.7
0.9
1.1

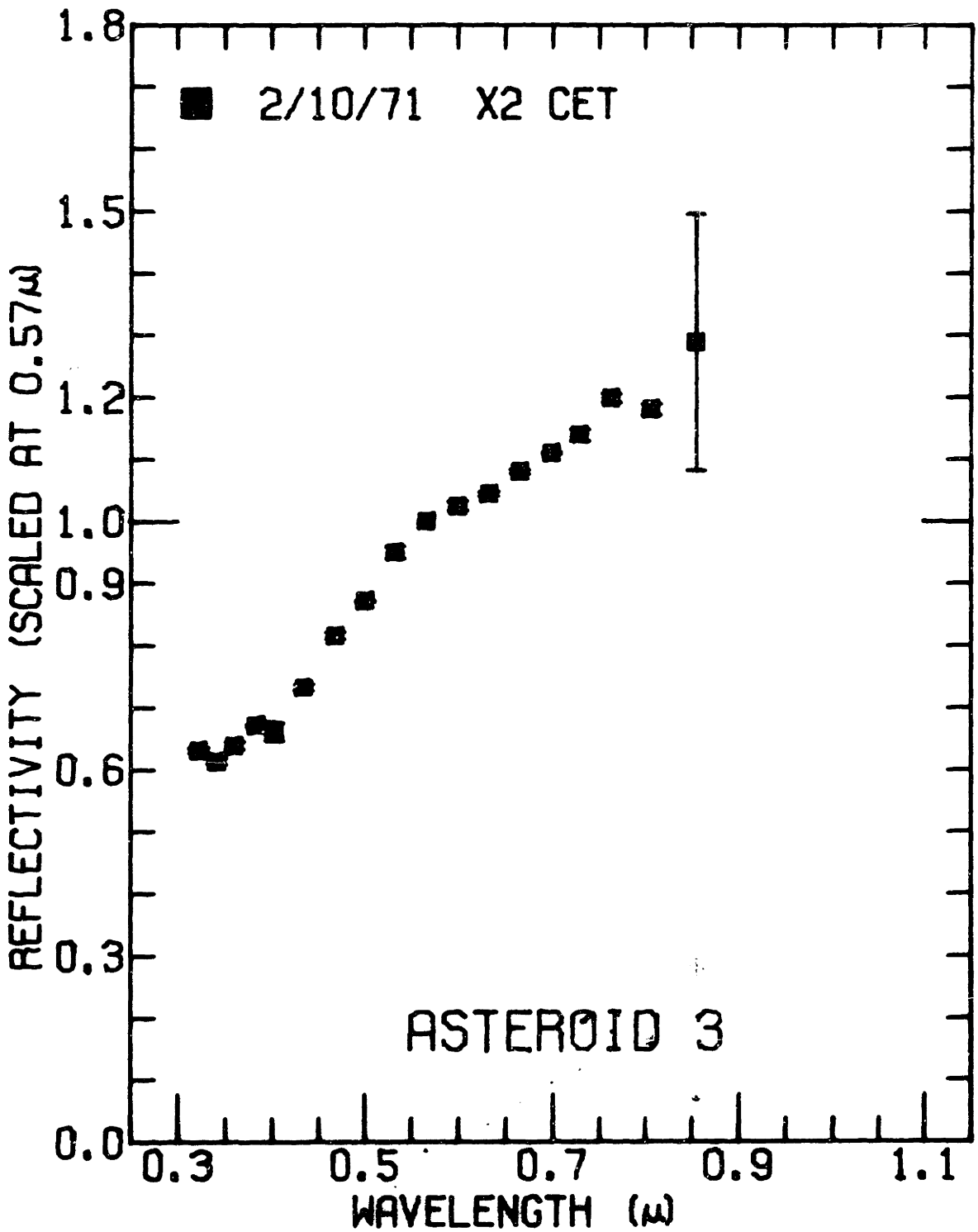
2/10/71 X2 CET
ASTEROID 3
REFLECTIVITY (SCALED AT 0.57μ)
WAVELENGTH (μ)
1.8
1.5
1.2
1.0
0.9
0.6
0.3
0.0
0.3
0.5
0.7
0.9
1.1

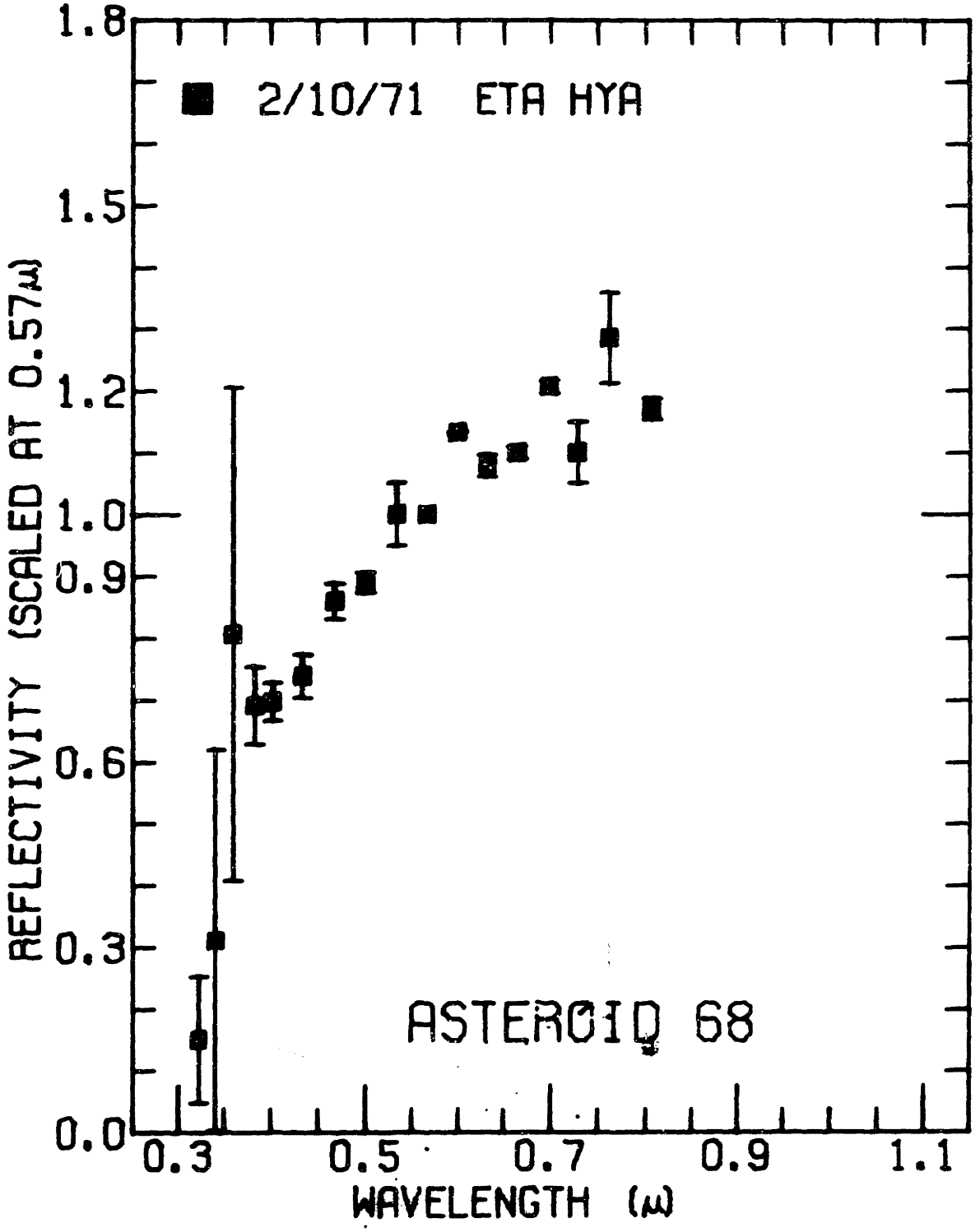
2/10/71 ETA HYA
ASTEROID 68
REFLECTIVITY (SCALED AT 0.57μ)
WAVELENGTH (μ)
1.8
1.5
1.2
1.0
0.9
0.6
0.3
0.0
0.3
0.5
0.7
0.9
1.1

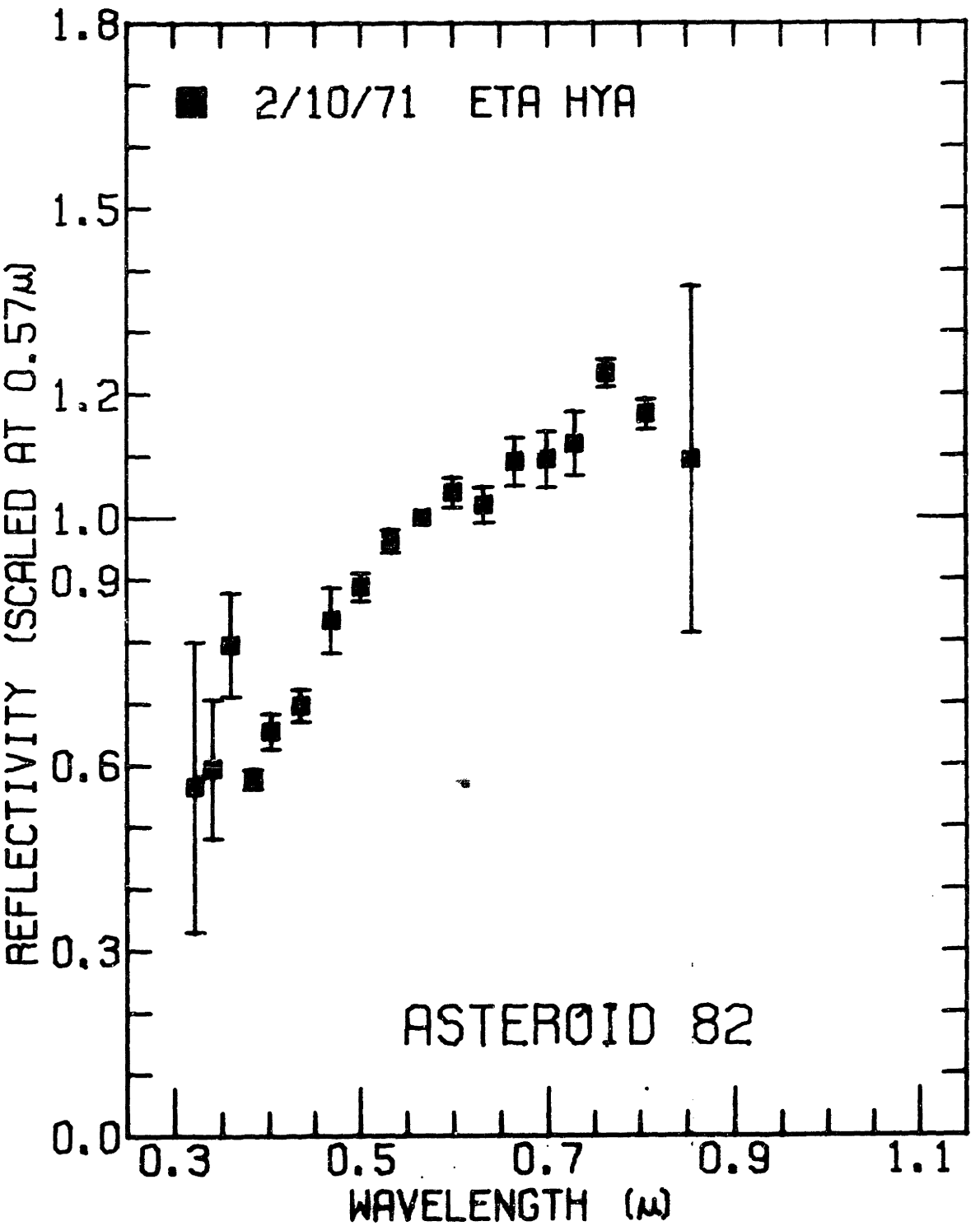
2/10/71 ETA HYA
ASTEROID 82
REFLECTIVITY (SCALED AT 0.57μ)
WAVELENGTH (μ)
1.8
1.5
1.2
1.0
0.9
0.6
0.3
0.0
0.3
0.5
0.7
0.9
1.1

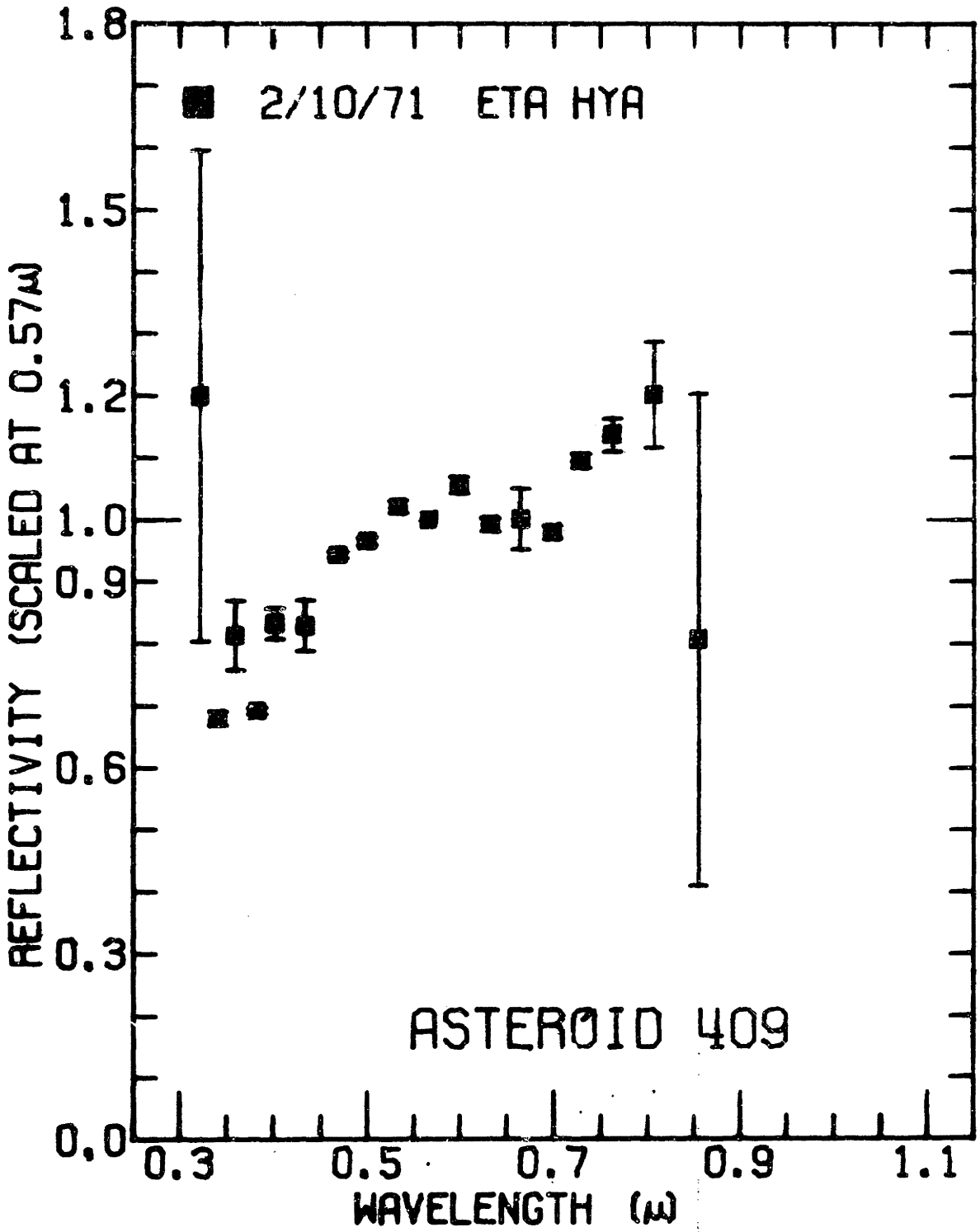
2/10/71 ETA HYA
ASTEROID 409
REFLECTIVITY (SCALED AT 0.57μ)
WAVELENGTH (μ)
1.8
1.5
1.2
1.0
0.9
0.6
0.3
0.0
0.3
0.5
0.7
0.9
1.1

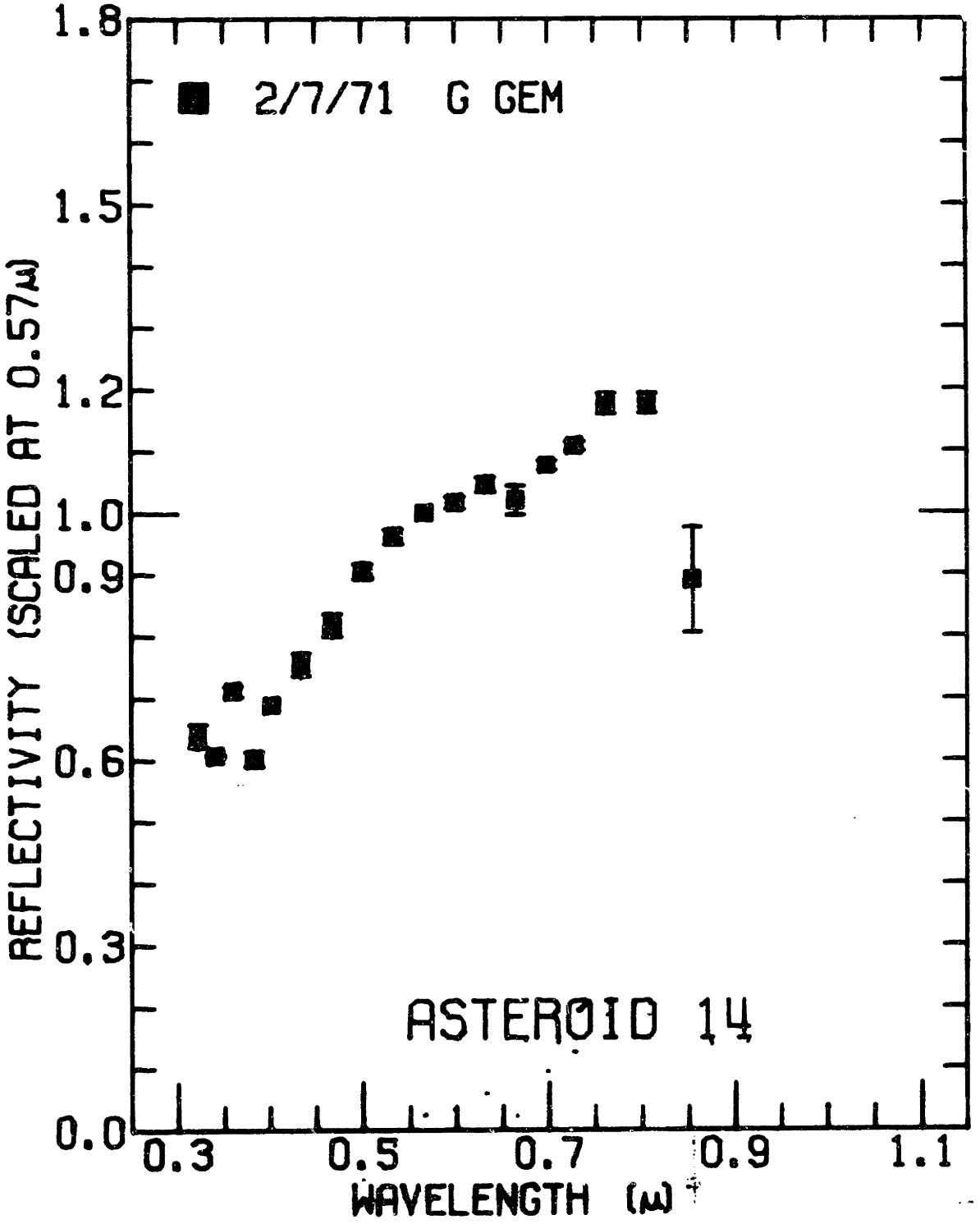
2/7/71 G GEM
ASTEROID 14
REFLECTIVITY (SCALED AT 0.57μ)
WAVELENGTH (μ)
1.8
1.5
1.2
1.0
0.9
0.6
0.3
0.0
0.3
0.5
0.7
0.9
1.1

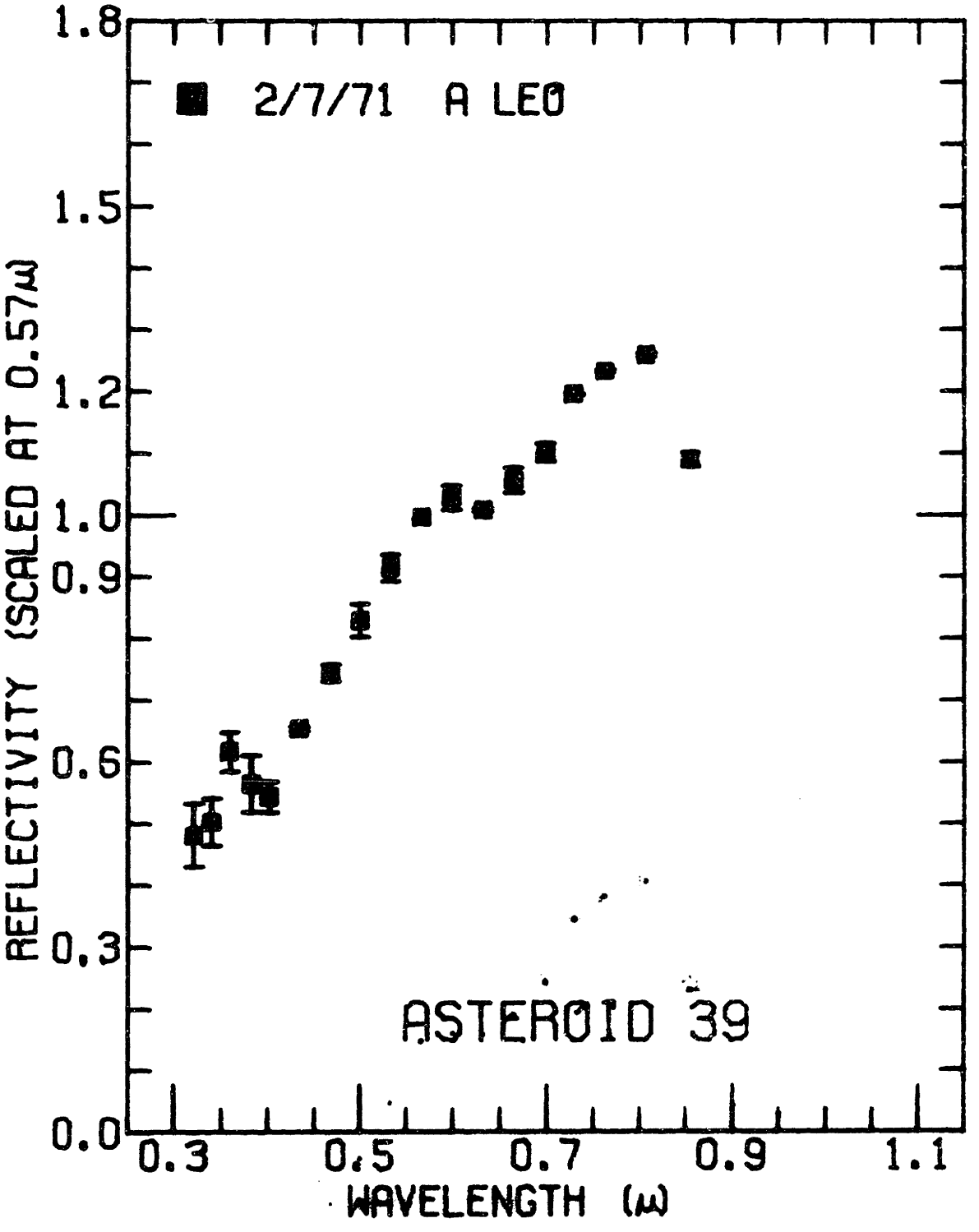
2/7/71 A LE0
ASTEROID 39
REFLECTIVITY (SCALED AT 0.57μ)
WAVELENGTH (μ)
1.8
1.5
1.2
1.0
0.9
0.6
0.3
0.0
0.3
0.5
0.7
0.9
1.1

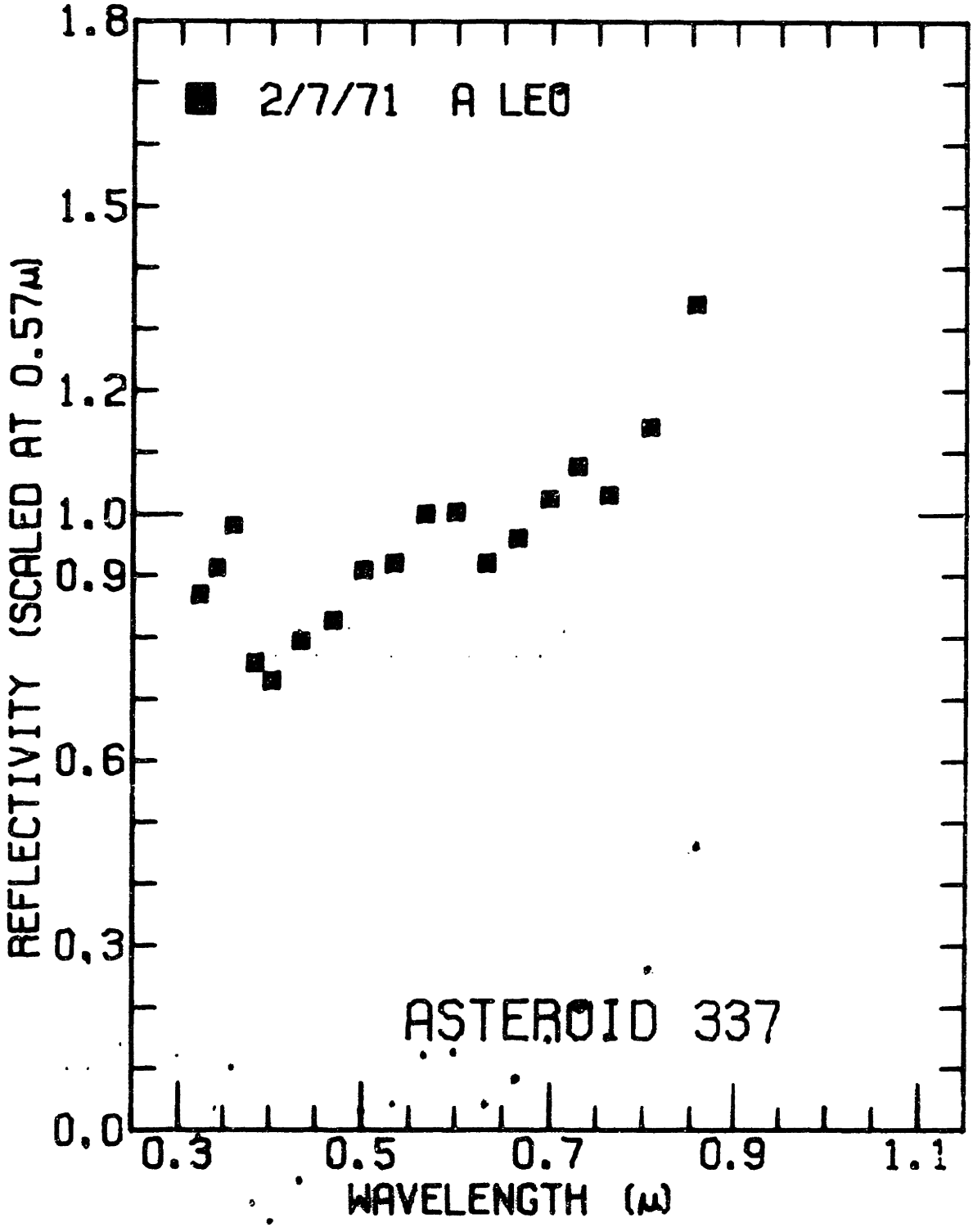
2/7/71 A LEO
ASTEROID 337
REFLECTIVITY (SCALED AT 0.57μ)
WAVELENGTH (μ)
1.8
1.5
1.2
1.0
0.9
0.6
0.3
0.0
0.3
0.5
0.7
0.9
1.1

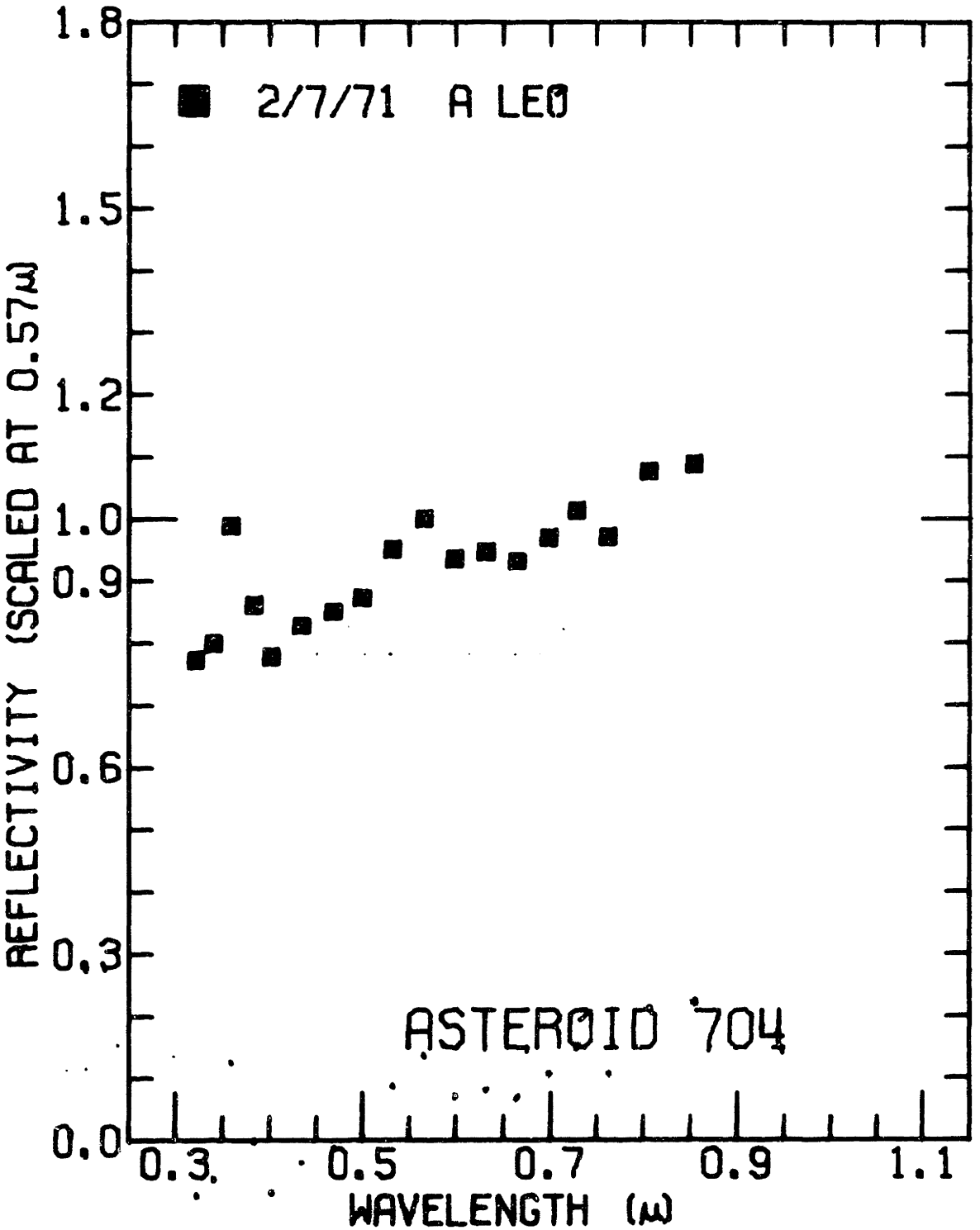
2/7/71 A LEO
ASTEROID 704
REFLECTIVITY (SCALED AT 0.57μ)
WAVELENGTH (μ)
1.8
1.5
1.2
1.0
0.9
0.6
0.3
0.0
0.3
0.5
0.7
0.9
1.1

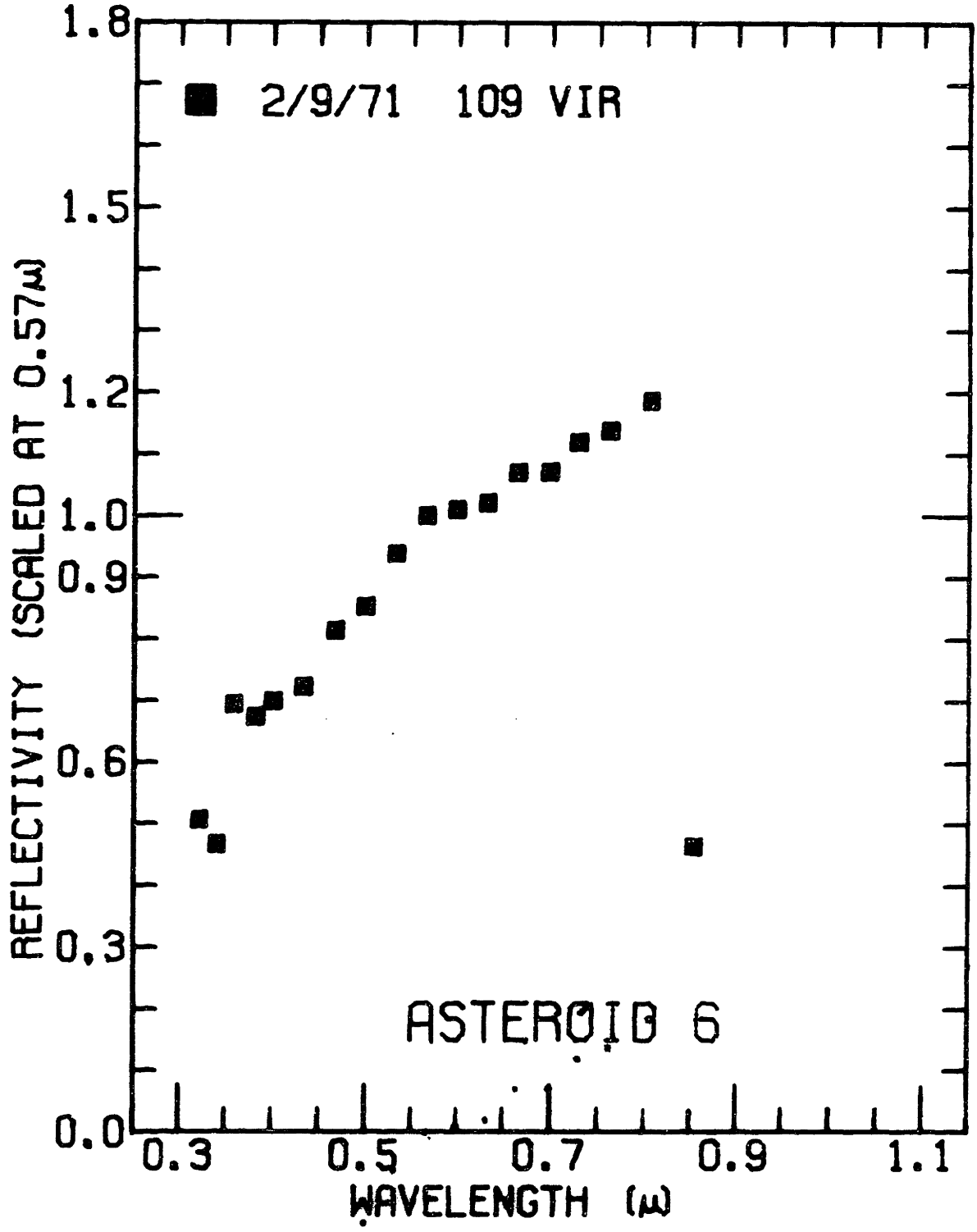
2/9/71 109 VIR
ASTEROID 6
REFLECTIVITY (SCALED AT 0.57μ)
WAVELENGTH (μ)
1.8
1.5
1.2
1.0
0.9
0.6
0.3
0.0
0.3
0.5
0.7
0.9
1.1

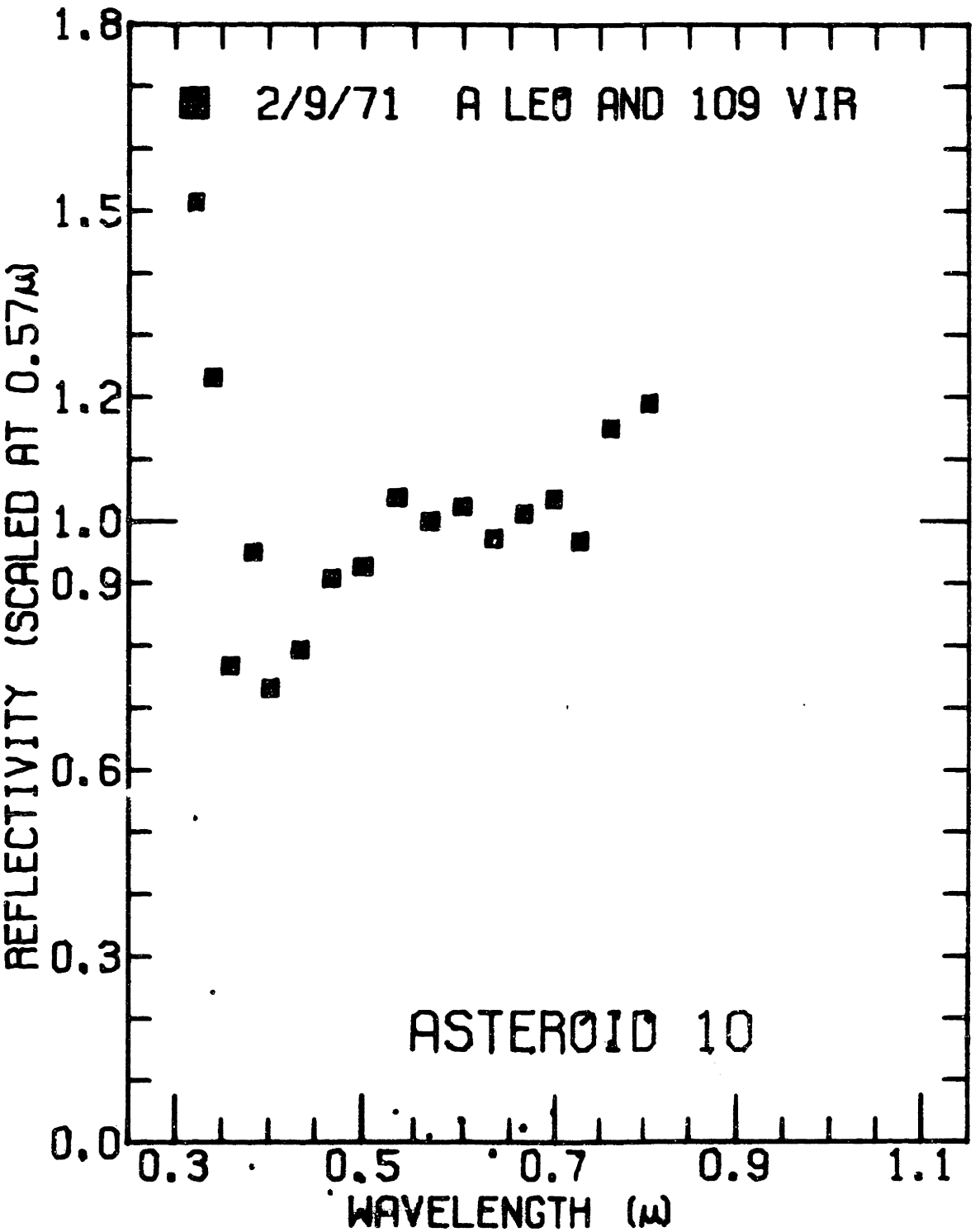
2/9/71 A LEO AND 109 VIR
ASTEROID 10
REFLECTIVITY (SCALED AT 0.57μ)
WAVELENGTH (μ)
1.8
1.5
1.2
1.0
0.9
0.6
0.3
0.0
0.3
0.5
0.7
0.9
1.1

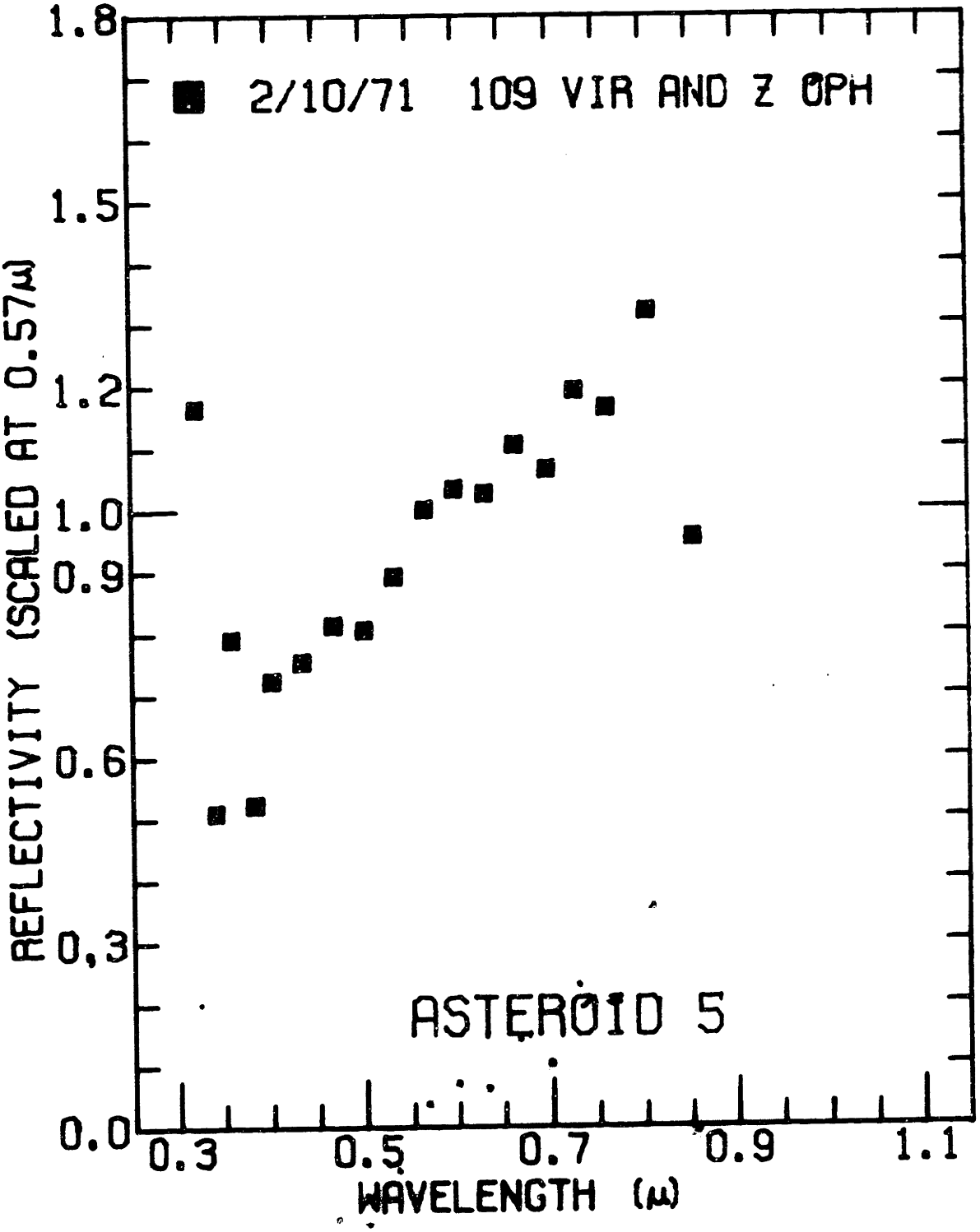
2/10/71 109 VIR AND Z 0PH
ASTEROID 5
REFLECTIVITY (SCALED AT 0.57μ)
WAVELENGTH (μ)
1.8
1.5
1.2
1.0
0.9
0.6
0,3
0.0
0.3
0.5
0.7
0.9
1.1

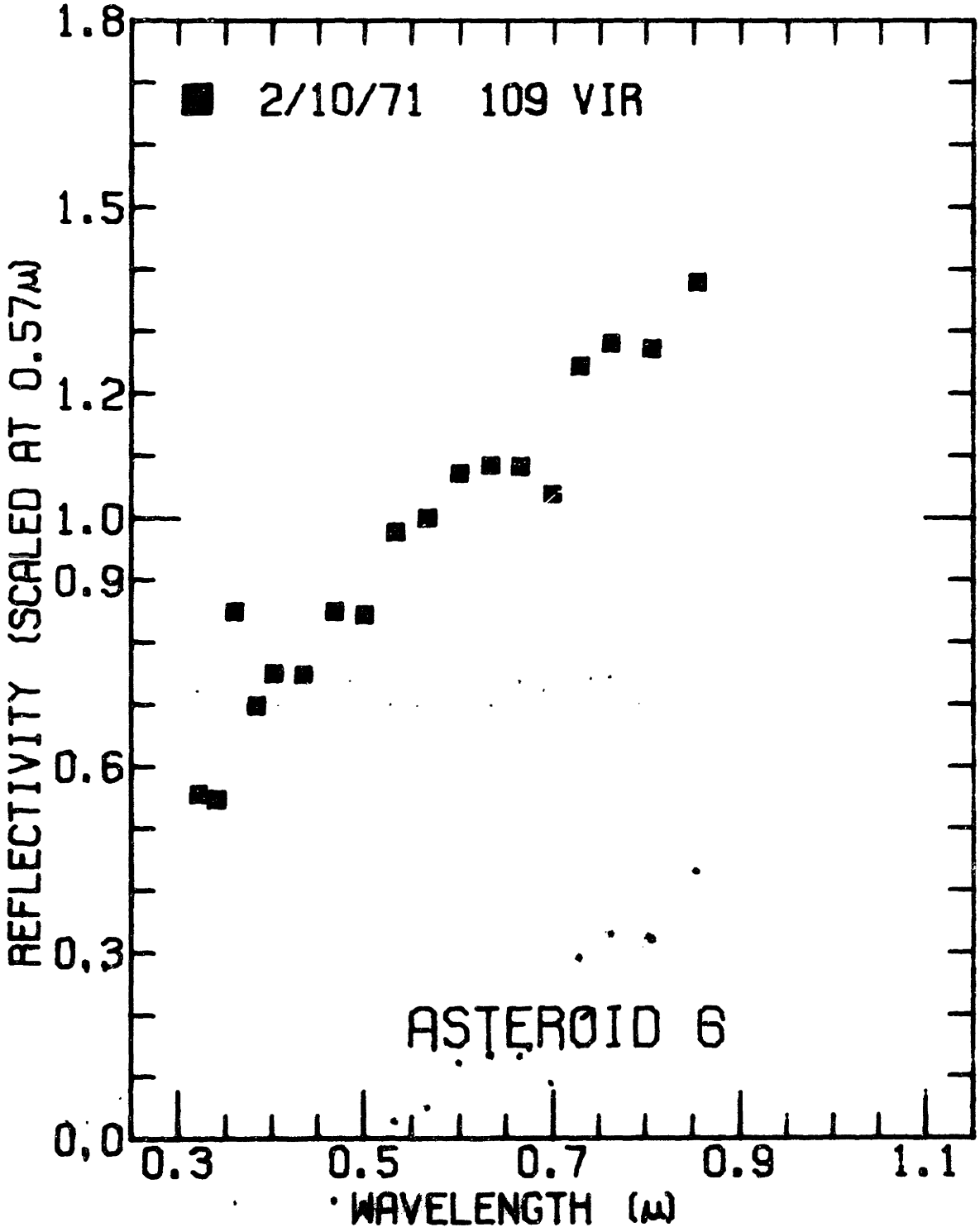
2/10/71 109 VIR
ASTEROID 6
REFLECTIVITY (SCALED AT 0.57μ)
WAVELENGTH (μ)
1.8
1.5
1.2
1.0
0.9
0.6
0.3
0.0
0.3
0.5
0.7
0.9
1.1

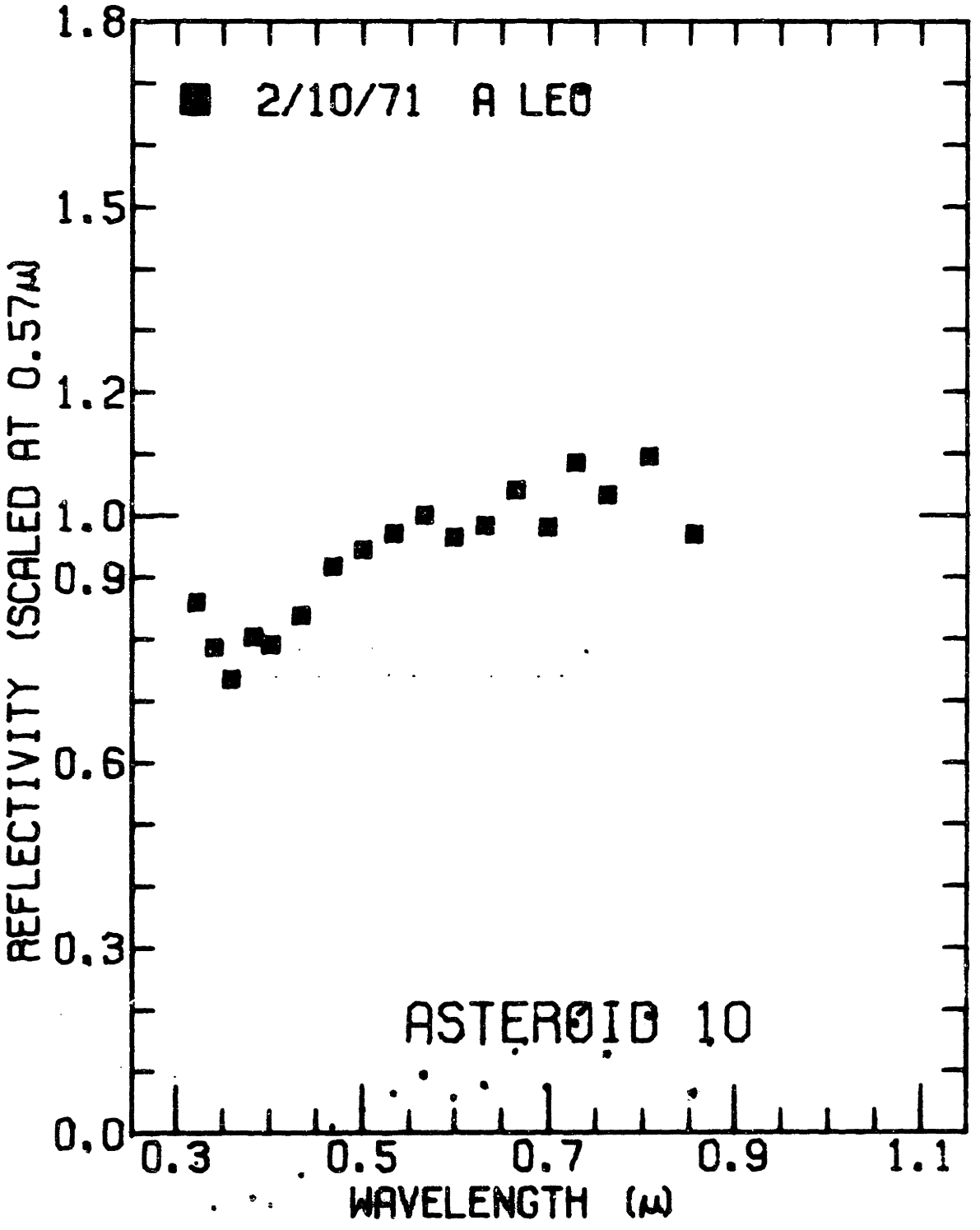
2/10/71 A LEO
ASTEROID 10
REFLECTIVITY (SCALED AT 0.57μ)
WAVELENGTH (μ)
1.8
1.5
1.2
1.0
0.9
0.6
0.3
0.0
0.3
0.5
0.7
0.9
1.1

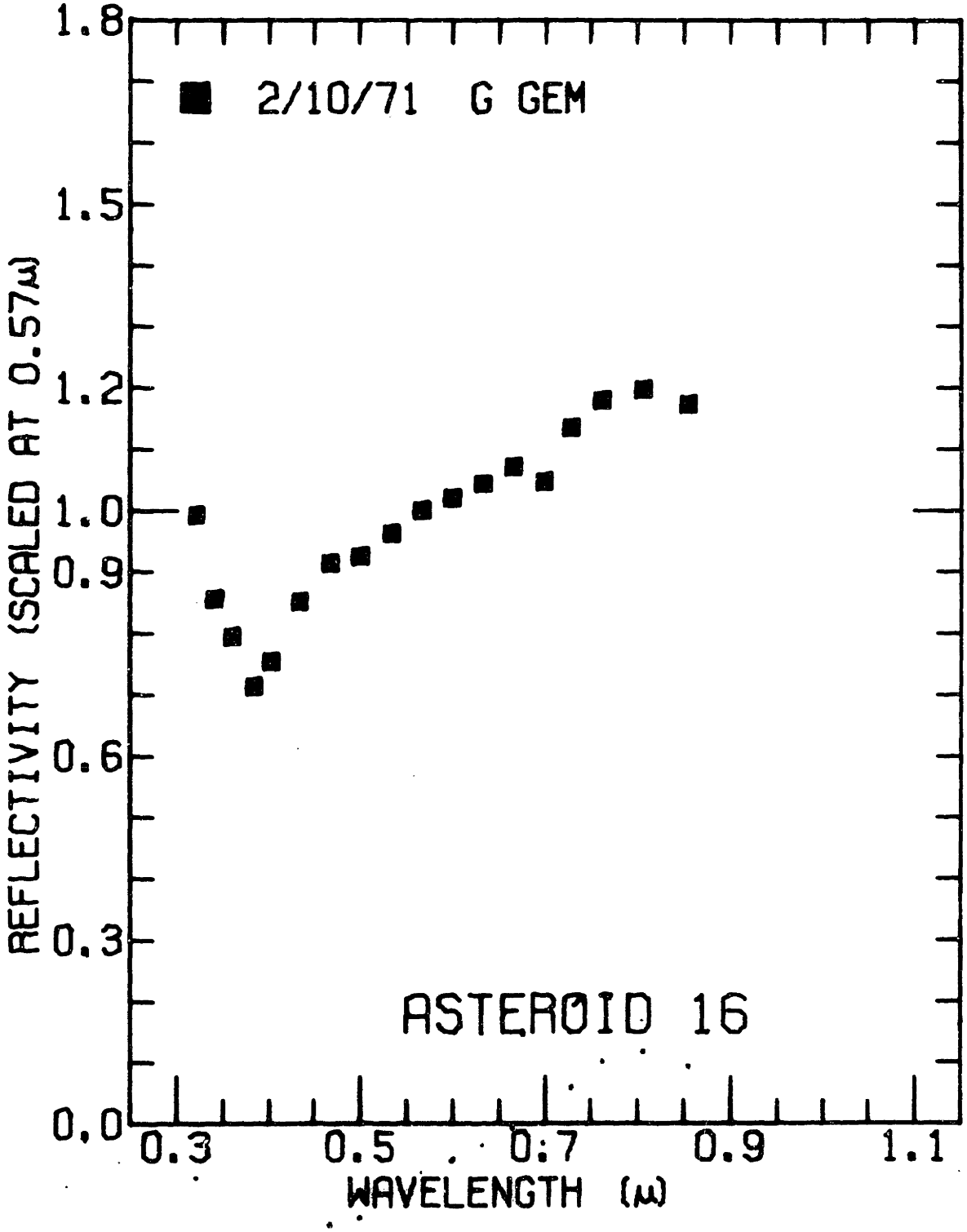
2/10/71 G GEM
ASTEROID 16
REFLECTIVITY (SCALED AT 0.57μ)
WAVELENGTH (μ)
1.8
1.5
1.2
1.0
0.9
0.6
0.3
0.0
0.3
0.5
0.7
0.9
1.1

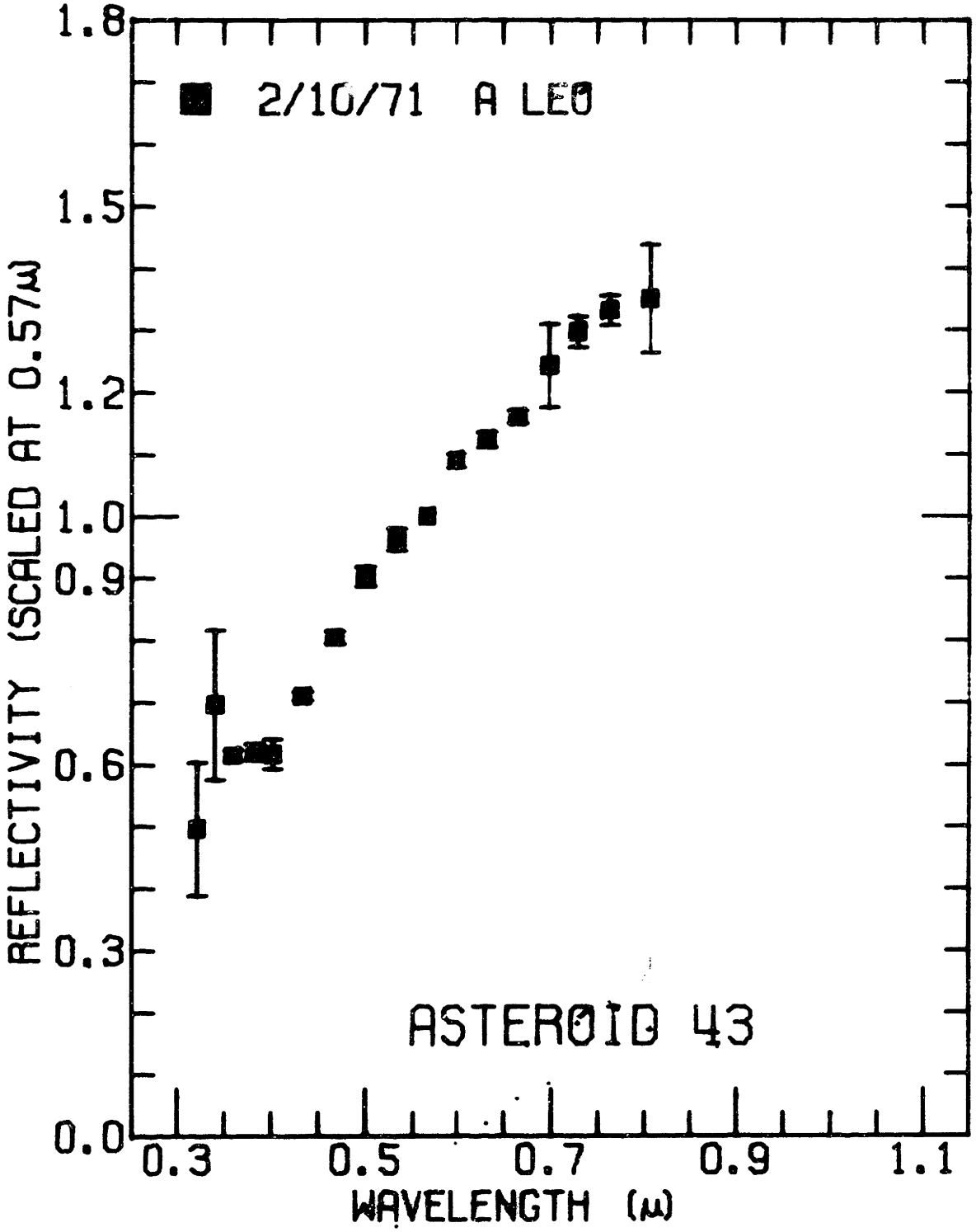
2/10/71 A LEO
ASTEROID 43
REFLECTIVITY (SCALED AT 0.57μ)
WAVELENGTH (μ)
1.8
1.5
1.2
1.0
0.9
0.6
0.3
0.0
0.3
0.5
0.7
0.9
1.1

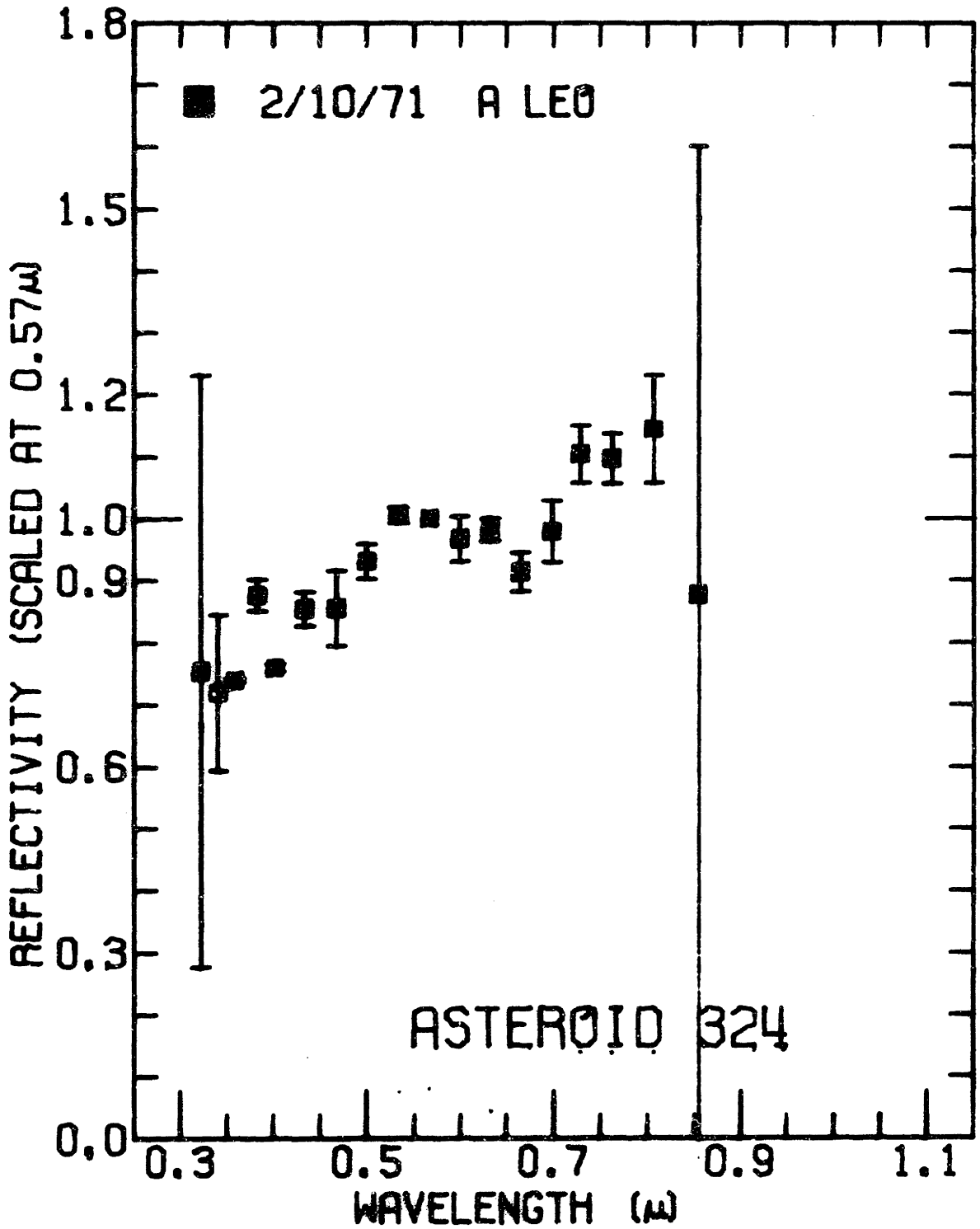
2/10/71 A LE0
ASTEROID 324
REFLECTIVITY (SCALED AT 0.57μ)
WAVELENGTH (μ)
1.8
1.5
1.2
1.0
0.9
0.6
0.3
0.0
0.3
0.5
0.7
0.9
1.1

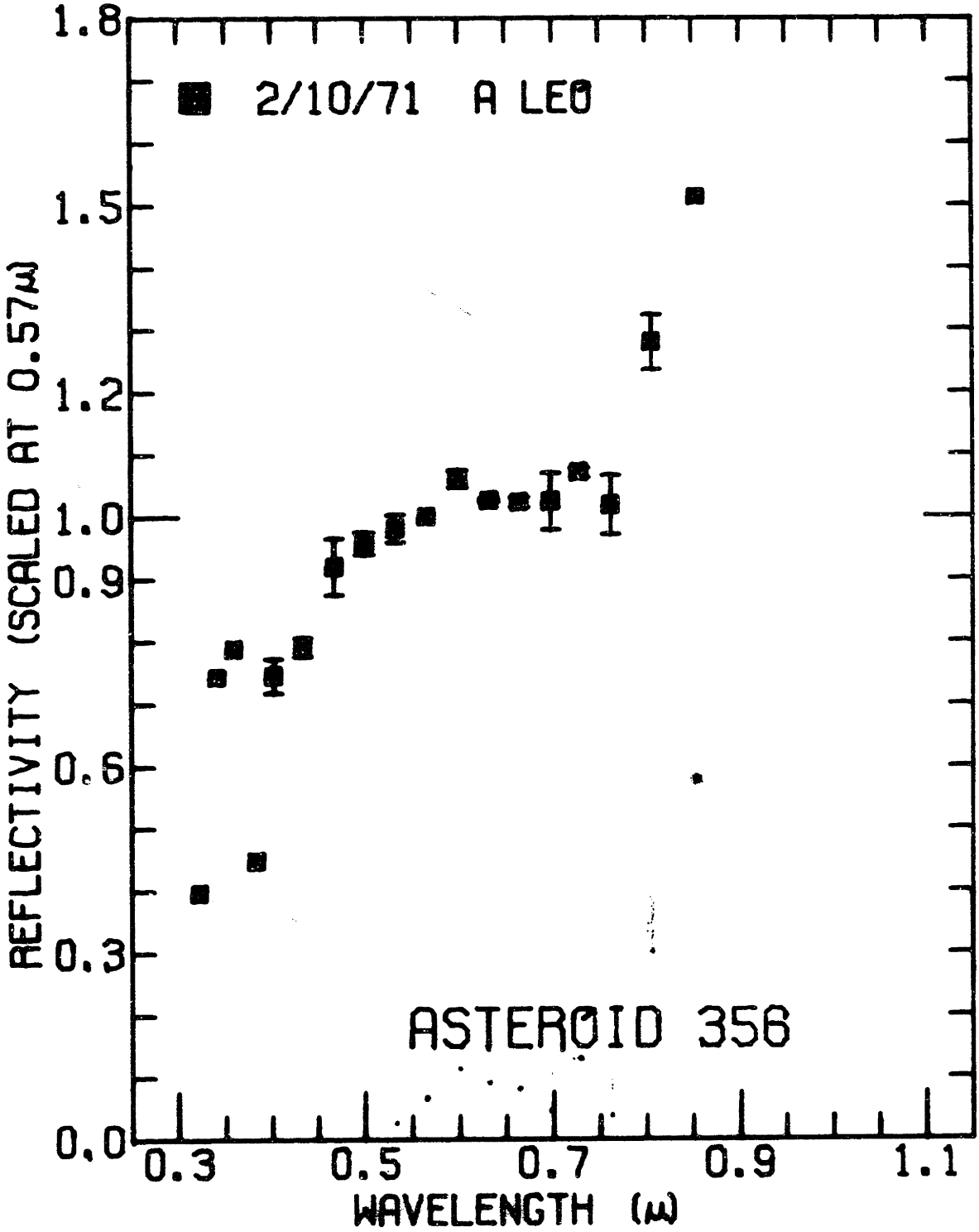
2/10/71 A LE0
ASTEROID 356
REFLECTIVITY (SCALED AT 0.57μ)
WAVELENGTH (μ)
1.8
1.5
1.2
1.0
0.9
0.6
0.3
0.0
0.3
0.5
0.7
0.9
1.1

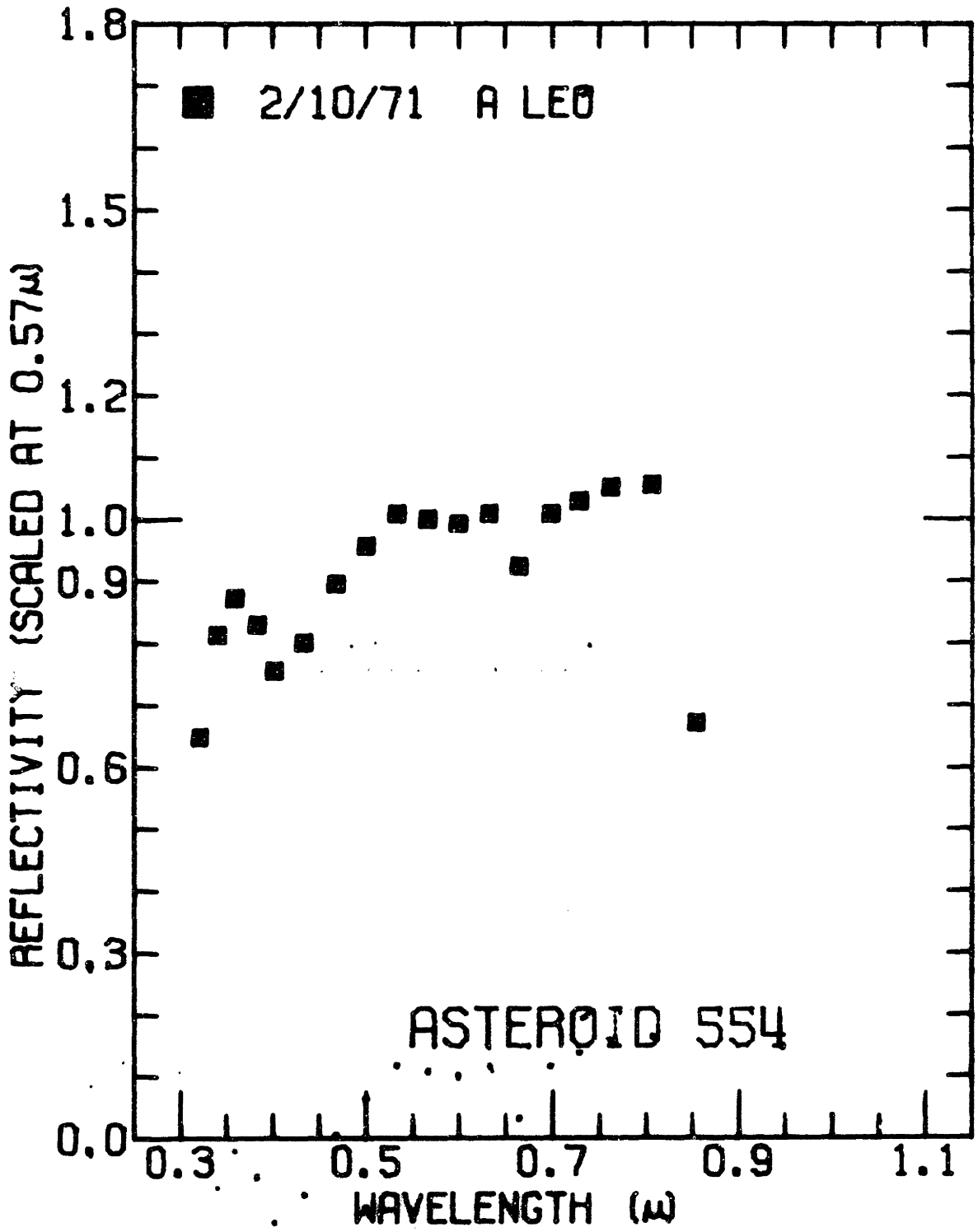
2/10/71 A LEO
ASTEROID 554
REFLECTIVITY (SCALED AT 0.57μ)
WAVELENGTH (μ)
1.8
1.5
1.2
1.0
0.9
0.6
0.3
0.0
0.3
0.5
0.7
0.9
1.1

May 1971 run.

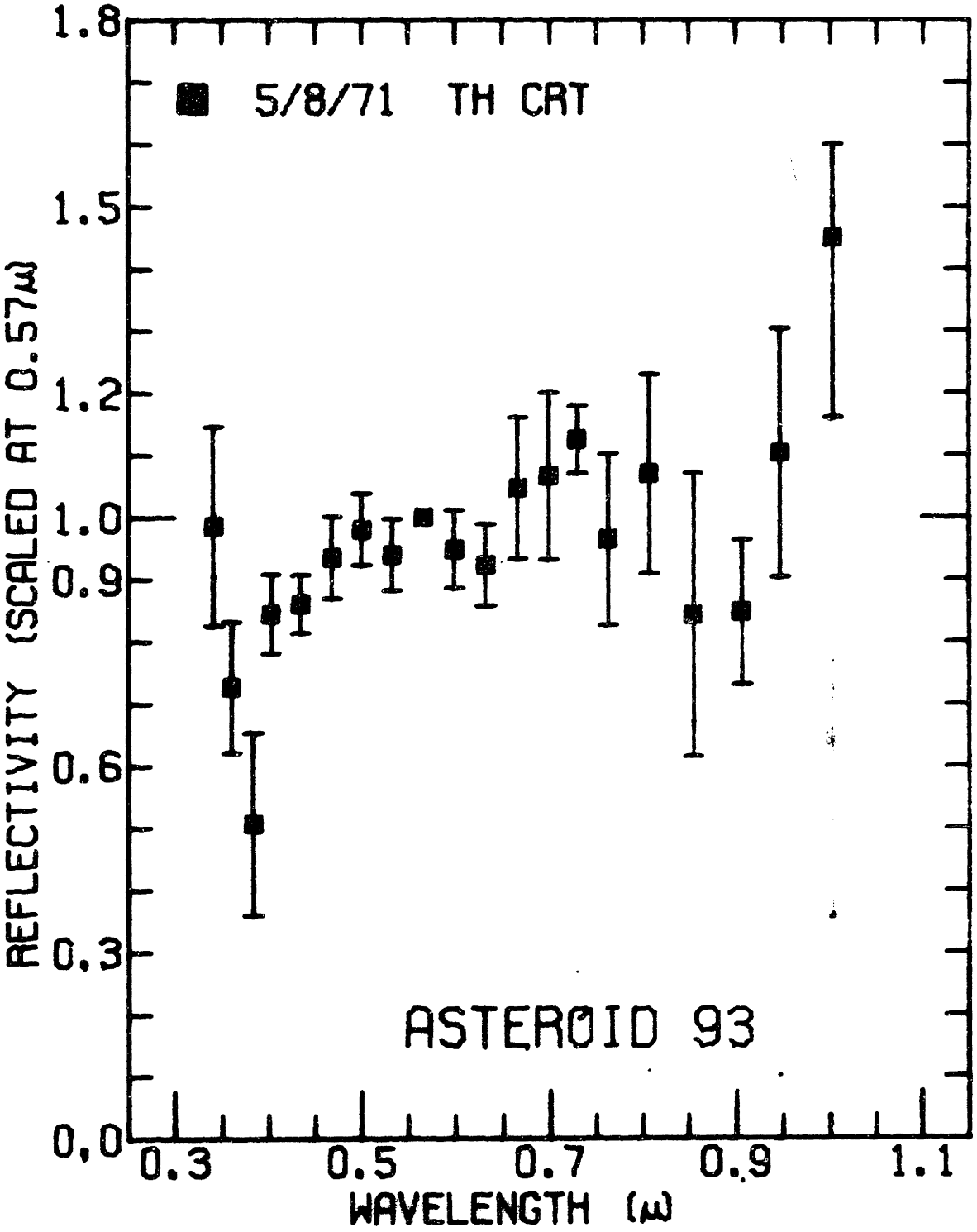
5/8/71 TH CRT
ASTEROID 93
REFLECTIVITY (SCALED AT 0.57μ)
WAVELENGTH (μ)
1.8
1.5
1.2
1.0
0.9
0.6
0.3
0.0
0.3
0.5
0.7
0.9
1.1

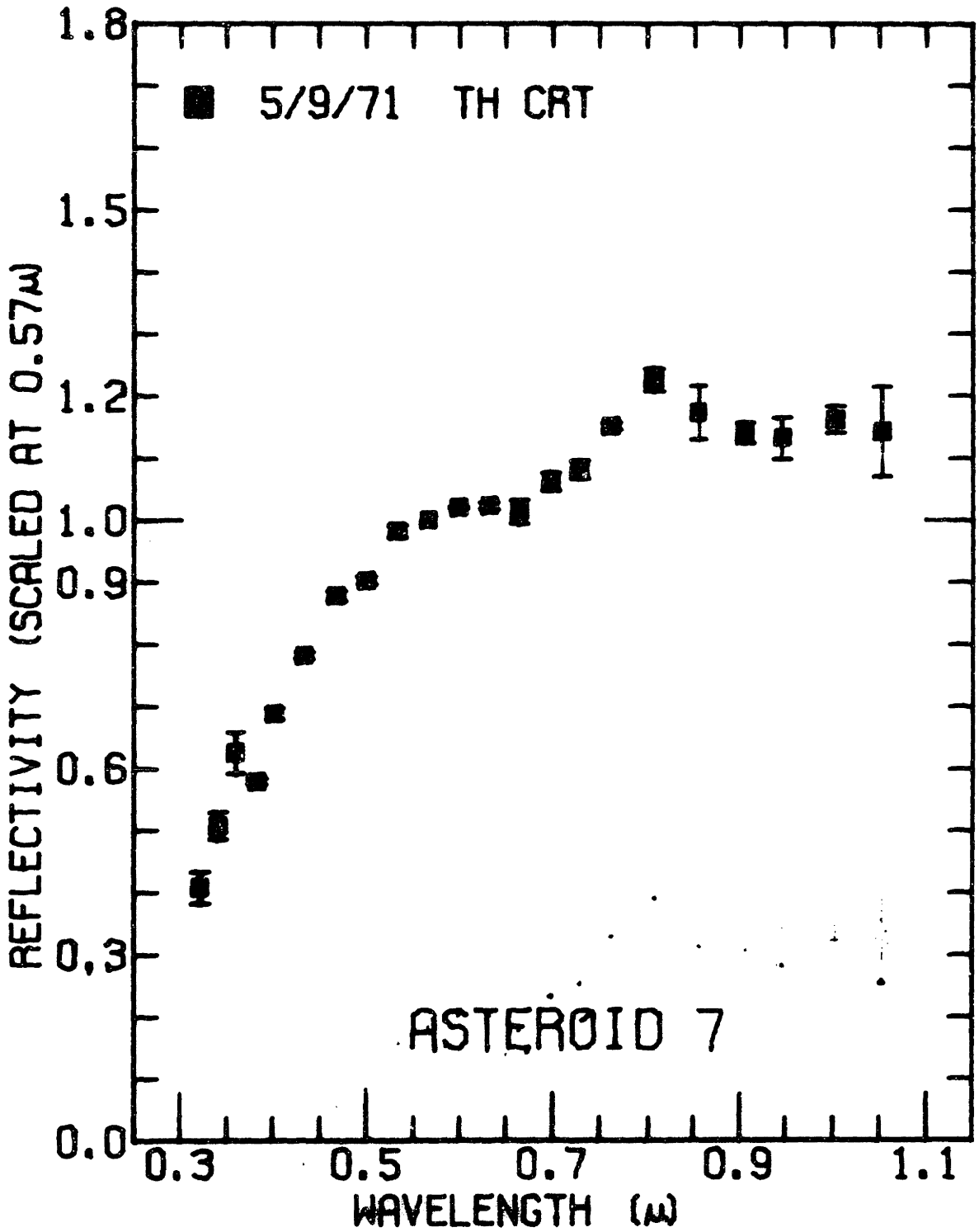
5/9/71 TH CRT
ASTEROID 7
REFLECTIVITY (SCALED AT 0.57μ)
WAVELENGTH (μ)
1.8
1.5
1.2
1.0
0.9
0.6
0.3
0.0
0.3
0.5
0.7
0.9
1.1

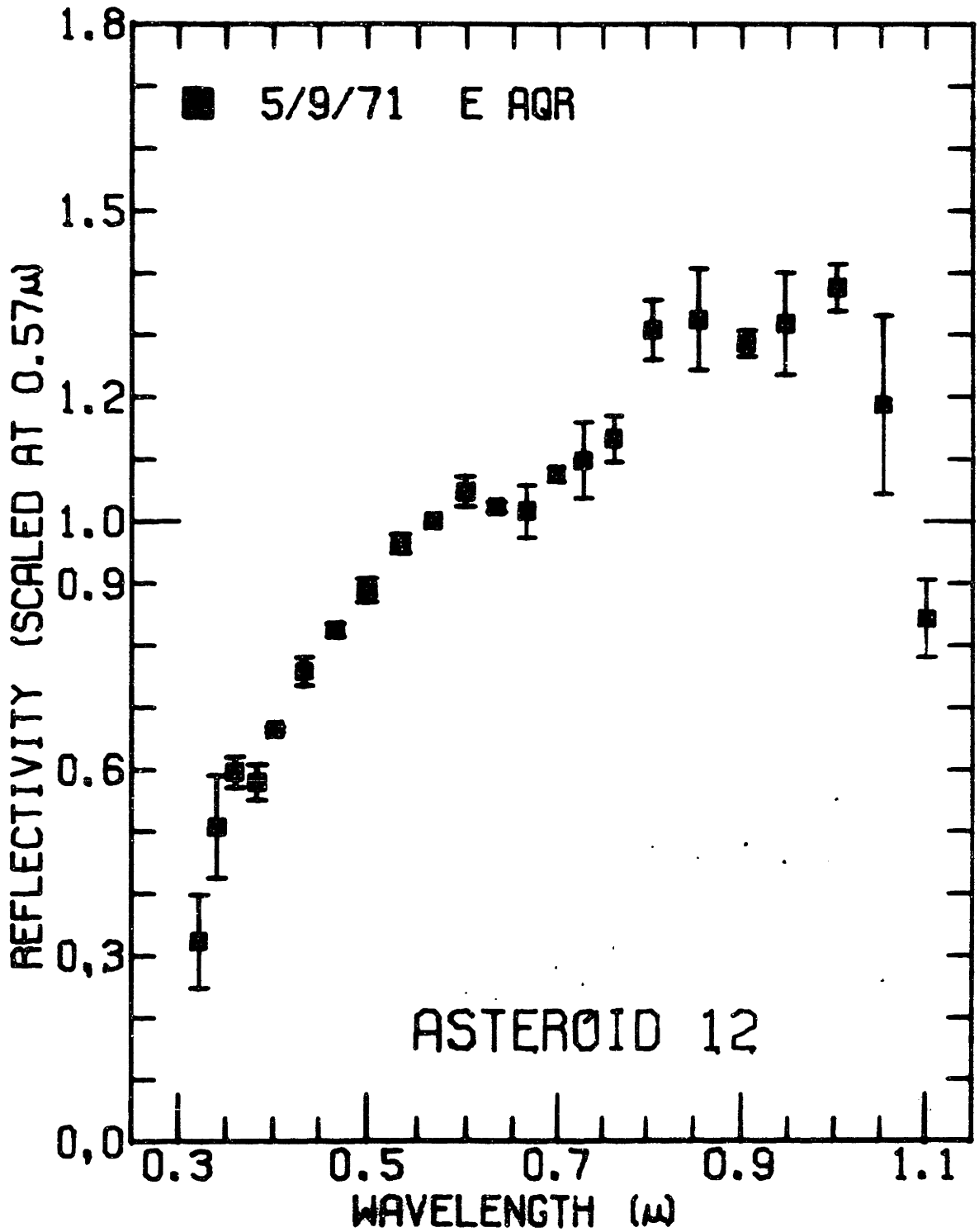
5/9/71 E AQR
ASTEROID 12
REFLECTIVITY (SCALED AT 0.57μ)
WAVELENGTH (μ)
1.8
1.5
1.2
1.0
0.9
0.6
0,3
0,0
0.3
0.5
0.7
0.9
1.1

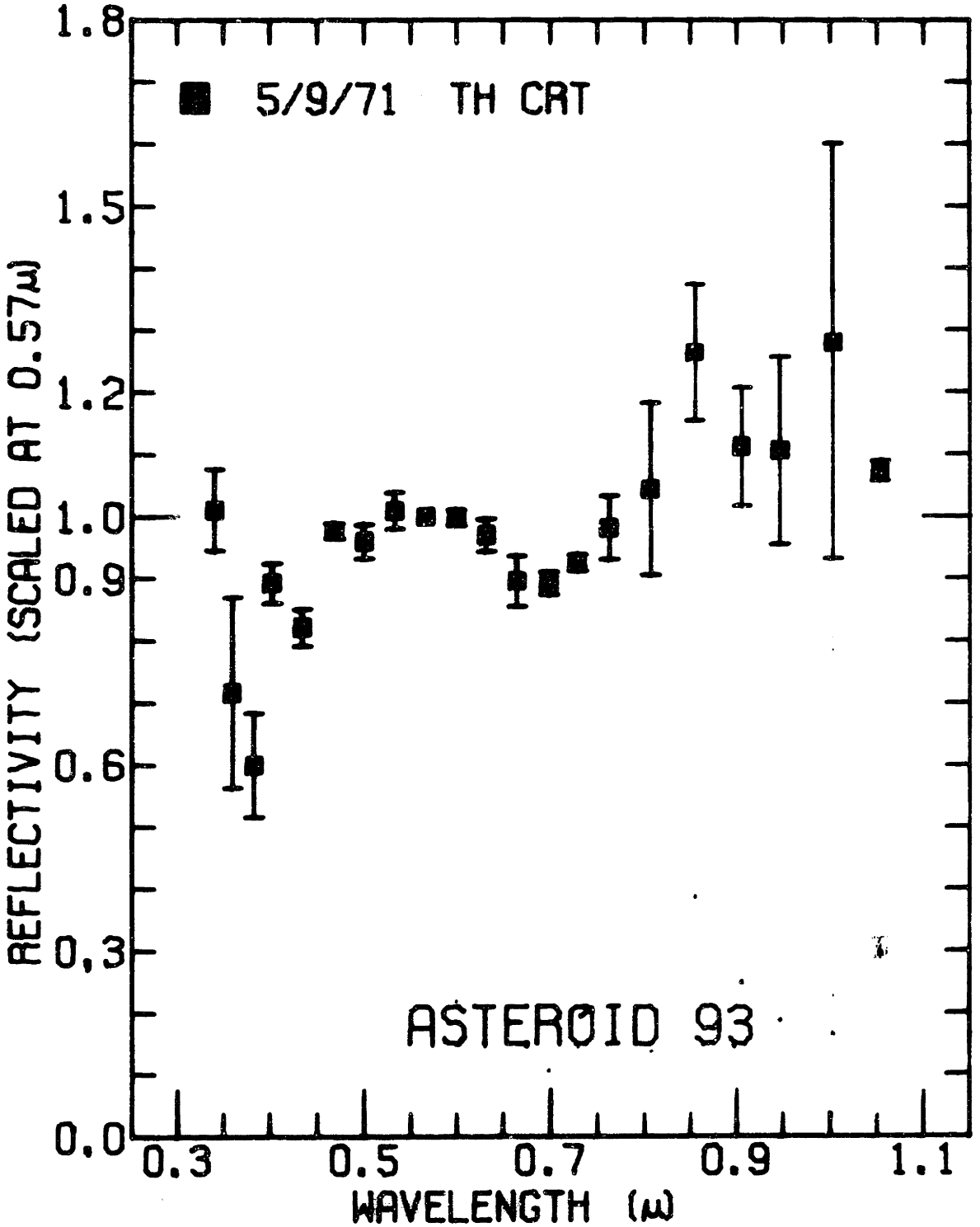
5/9/71 TH CRT
ASTEROID 93
REFLECTIVITY (SCALED AT 0.57μ)
WAVELENGTH (μ)
1.8
1.5
1.2
1.0
0.9
0.6
0.3
0.0
0.3
0.5
0.7
0.9
1.1

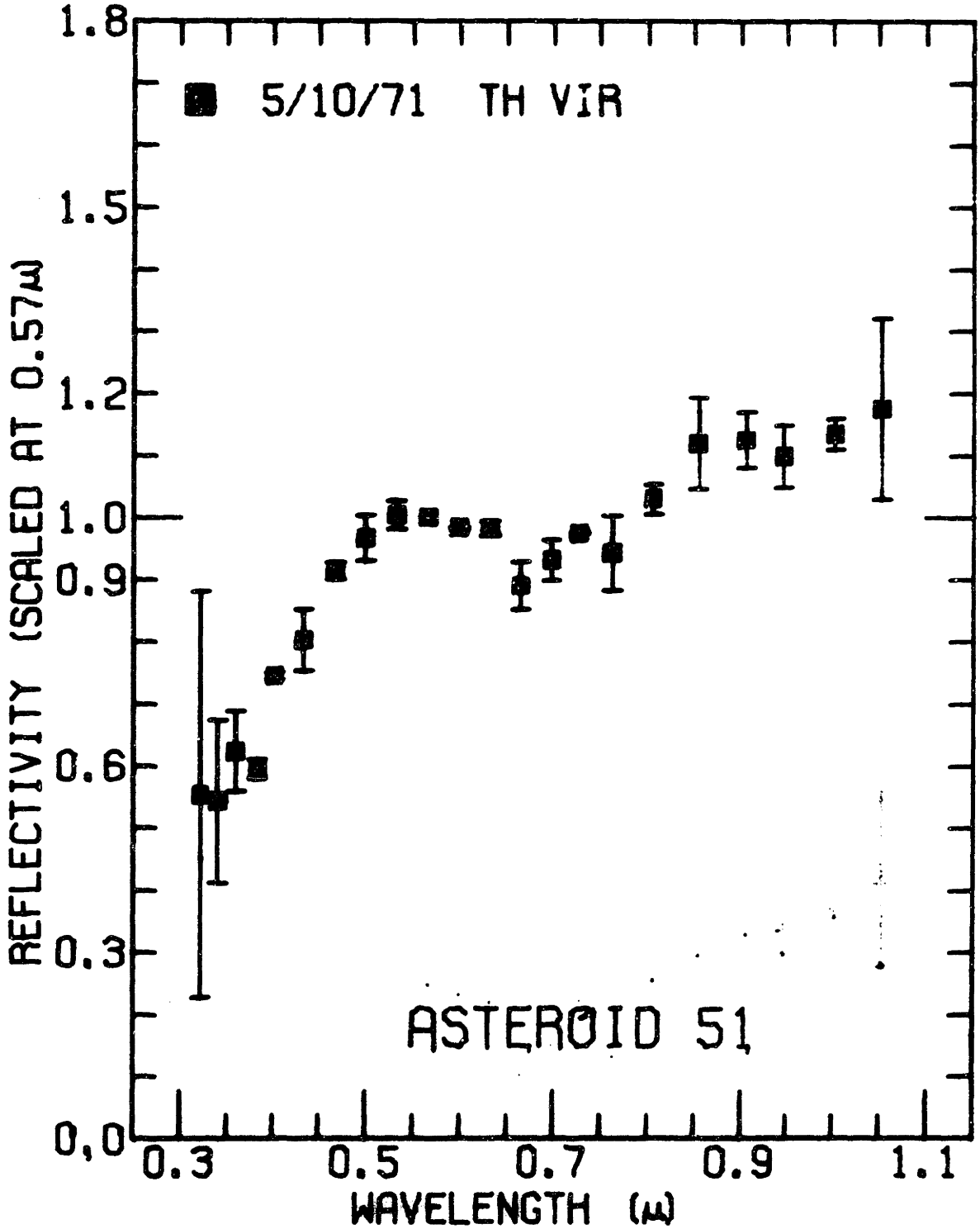
5/10/71 TH VIR
ASTEROID 51
REFLECTIVITY (SCALED AT 0.57μ)
WAVELENGTH (μ)
1.8
1.5
1.2
1.0
0.9
0.6
0.3
0,0
0.3
0.5
0.7
0.9
1.1

Solar System Comparisons

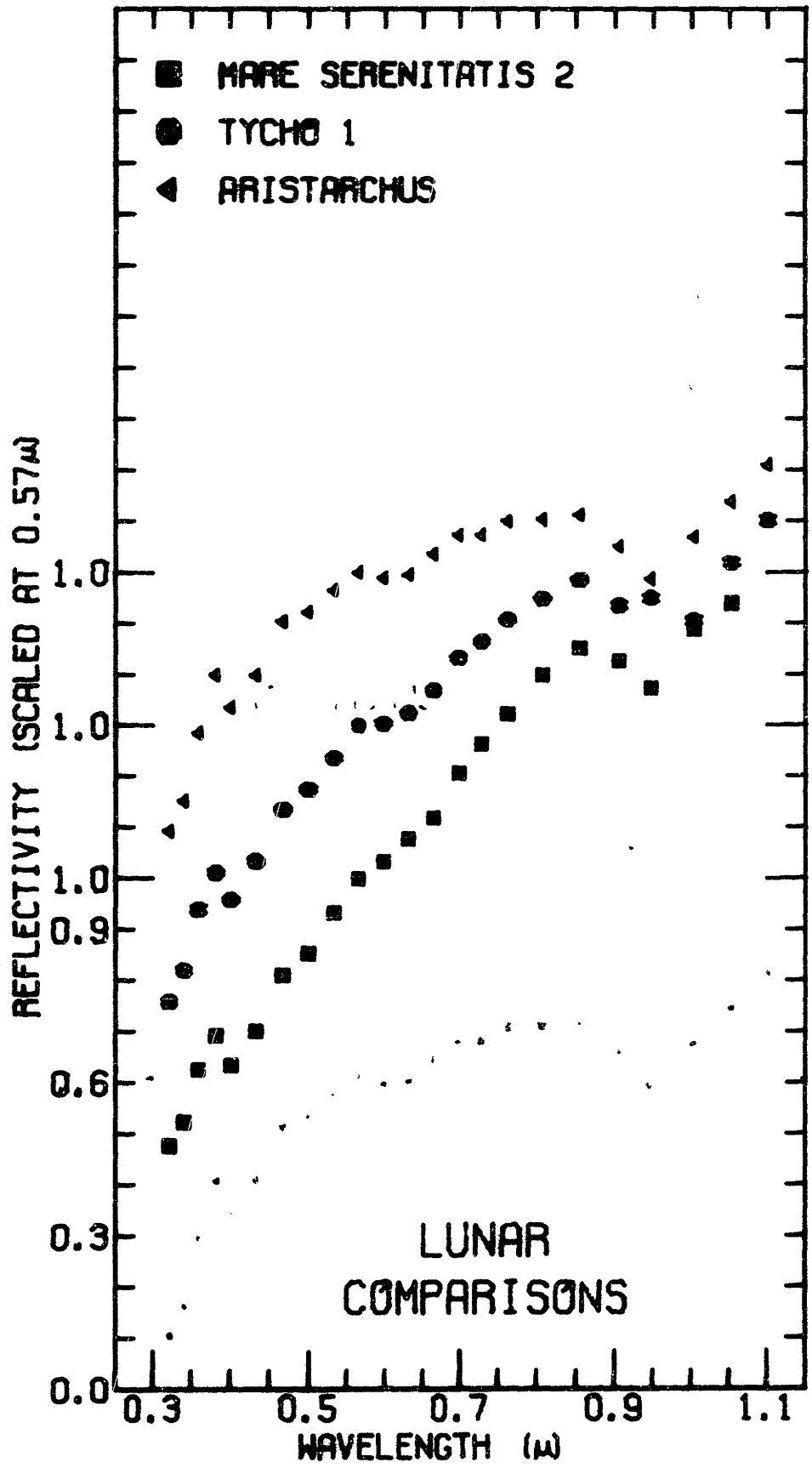
MARE SERENITATIS 2
TYCHO 1
ARISTARCHUS
REFLECTIVITY (SCALED AT 0.57μ)
1.0
1.0
1.0
0.9
0.6
0.3
0.0
0.3
0.5
0.7
0.9
1.1
WAVELENGTH (μ)
LUNAR
COMPARISONS

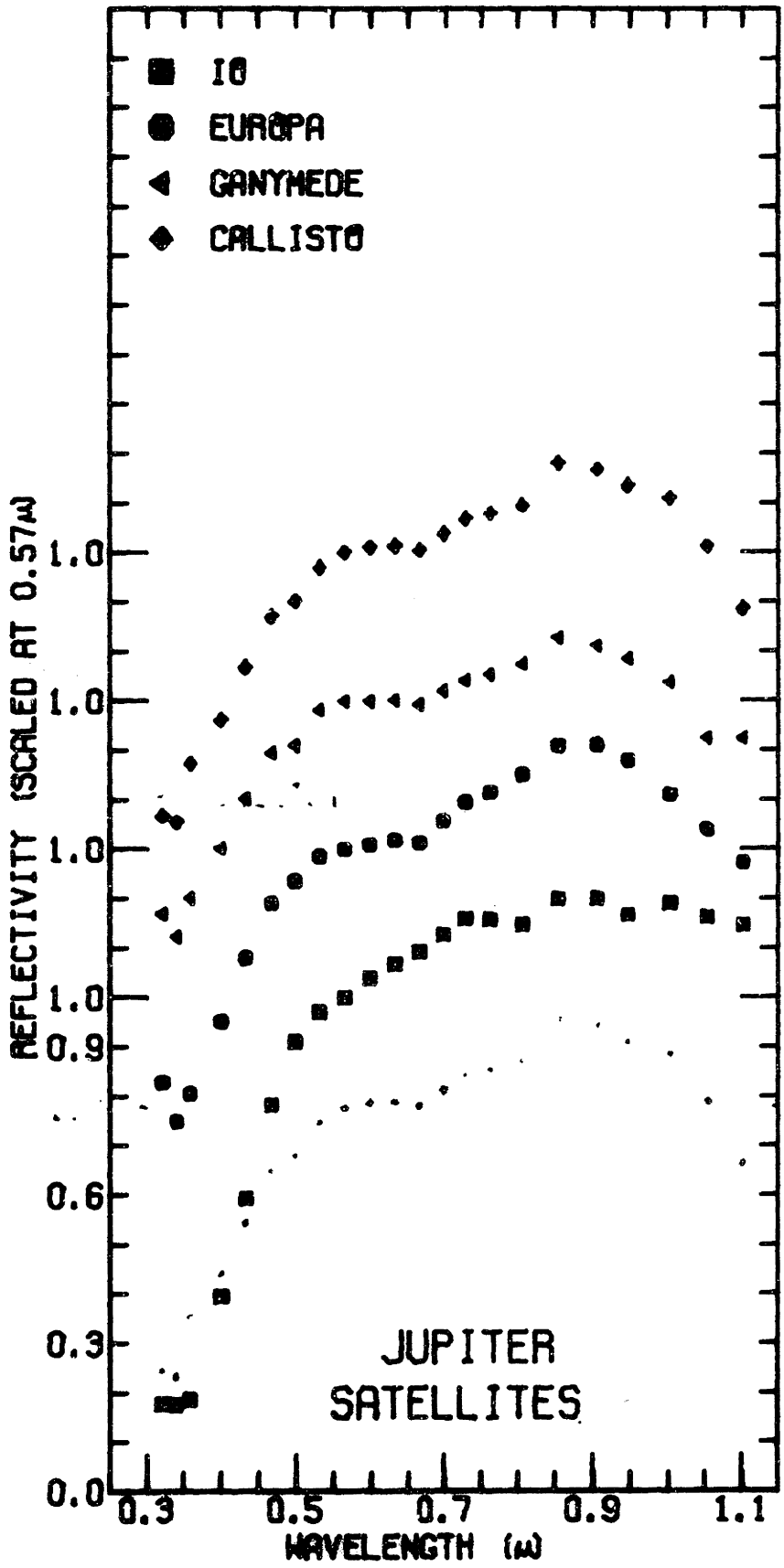
IO
EUROPA
GANYMEDE
CALLISTO
JUPITER
SATELLITES
REFLECTIVITY (SCALED AT 0.57μ)
1.0
1.0
1.0
1.0
0.9
0.6
0.3
0.0
0.3
0.5
0.7
0.9
1.1
WAVELENGTH (μ)

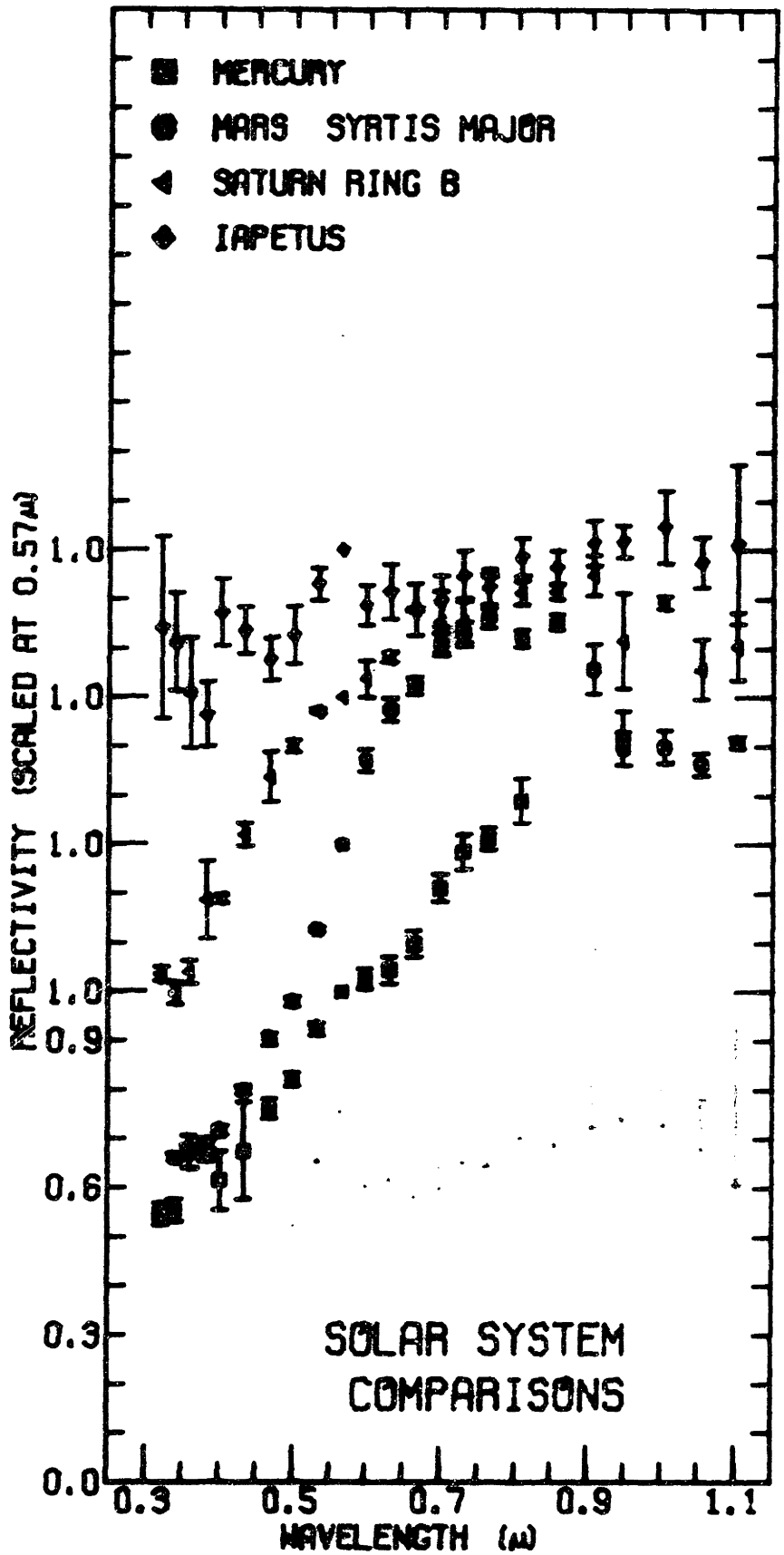
MERCURY
MARS SYRTIS MAJOR
SATURN RING B
IAPETUS
SOLAR SYSTEM
COMPARISONS
REFLECTIVITY (SCALED AT 0.57μ)
1.0
1.0
1.0
1.0
0.9
0.6
0.3
0.0
0.3
0.5
0.7
0.9
1.1
WAVELENGTH (μ)

BIOGRAPHY

Clark R. Chapman, a Californian by birth, attended public schools near Buffalo, N.Y. He studied astronomy at Harvard College (A.B., June 1967). He began graduate study in the Meteorology Department at M.I.T. (S.M., September 1968) before entering the Earth and Planetary Sciences Department. He has worked in planetary studies at the Lunar and Planetary Laboratory (Tucson), The Smithsonian Astrophysical Observatory, the Haystack Radar Facility of M.I.T. Lincoln Laboratory, and in the two departments at M.I.T. He is a member of the American Astronomical Society, the American Geophysical Union, and the American Association for the Advancement of Science. He is author or co-author of about 20 publications on such subjects as lunar and Martian cratering, cartography of Mercury, Jupiter's atmosphere, asteroid spectrophotometry, and composition of Saturn's rings. Some of these are listed below:

1967, A critique of methods for analysis of the diameter-frequency relation for craters with special application to the moon. J. Geophys. Res., 72, 549-557 (with R.R. Haefner).

1968, Interpretation of the diameter-frequency relation for lunar craters photographed by Rangers 7, 8, and 9. Icarus, 8, 1 - 22.

1968, Optical evidence on the rotation of Mercury. Earth and Planet. Sci. Lett., 3, 381 - 385.

1968, A test of the uniformly-rotating source hypothesis for the South Equatorial Belt distrubances on Jupiter. Icarus, 9, 326 - 335 (with E.J. Reese).

1969, Jupiter's zonal winds: variation with latitude. J. Atmos. Sci., 26 986 - 990.

1969, An analysis of the Mariner-4 cratering statistics. Astron. J., 74, 1039 - 1051 (with J.B. Pollack and C. Sagan).

1970, Lunar cratering and erosion from Orbiter 5 photographs, J. Geophys. Res., 75, 1445 - 1466 (with J.A. Mosher and G. Simmons).

1970, Saturn's rings: identification of water frost, Science, 167, 1372 - 1373. (with C.B. Pilcher, L.A. Lebofsky, and H.H. Kieffer).

1971, A review of spectrophotometric studies of asteroids. In "Physical studies of minor planets," (T. Gehrels, ed). NASA SP-267.